

From Pathophysiology to Treatment of Diabetic Retinopathy

Lead Guest Editor: Irimi Chatziralli

Guest Editors: Maria Vittoria Cicinelli, Dominika Pohlmann, and Sara Touhami





From Pathophysiology to Treatment of Diabetic Retinopathy

Journal of Diabetes Research

From Pathophysiology to Treatment of Diabetic Retinopathy

Lead Guest Editor: Irimi Chatziralli

Guest Editors: Maria Vittoria Cicinelli, Dominika
Pohlmann, and Sara Touhami




Copyright © 2021 Hindawi Limited. All rights reserved.

This is a special issue published in "Journal of Diabetes Research." All articles are open access articles distributed under the Creative Commons Attribution License, which permits unrestricted use, distribution, and reproduction in any medium, provided the original work is properly cited.

Chief Editor

Mark Yorek , USA

Associate Editors


Bright Starling Emerald , United Arab Emirates

Christian S. Goebel , Austria

Andrea Scaramuzza , Italy

Akira Sugawara , Japan


Academic Editors

E. Adeghate , United Arab Emirates

Abdelaziz Amrani , Canada


Michaela Angela Barbieri , Italy


Virginia Boccardi, Italy


Antonio Brunetti , Italy


Riccardo Calafiore , Italy

Stefania Camastra, Italy

Ilaria Campesi , Italy


Claudia Cardoso , Brazil


Sergiu Catrina , Sweden

Subrata Chakrabarti , Canada


Munmun Chattopadhyay , USA

Eusebio Chiefari, Italy

Mayank Choubey , USA

Secundino Cigarran , Spain


Huantian Cui, China

Rosa Fernandes , Portugal


Andrea Flex, Italy


Daniela Foti , Italy

Georgia Fousteri , Italy


Maria Pia Francescato , Italy

Pedro M. Geraldes, Canada

Almudena Gómez-Hernández , Spain


Eric Hajduch , France

Gianluca Iacobellis , USA

Carla Iacobini , Italy

Marco Infante , USA

Sundararajan Jayaraman, USA

Guanghong Jia , USA

Niki Katsiki , United Kingdom


Daisuke Koya, Japan

Olga Kozłowska, United Kingdom

Manishekhar Kumar, USA

Lucy Marzban, Canada


Takayuki Masaki , Japan

Raffaella Mastrocola , Italy

Maria Mirabelli , Italy


Ramkumar Mohan, USA

Pasquale Mone , USA

Craig S. Nunemaker , USA

Emmanuel K Ofori, Ghana

Hiroshi Okamoto, Japan

Ike S. Okosun , USA

Driss Ousaaid , Morocco

Dario Pitocco, Italy

Balamurugan Ramatchandirin, USA

Asirvatham Alwin Robert, Saudi Arabia

Saheed Sabiu , South Africa

Toshiyasu Sasaoka, Japan

Adérito Seixas , Portugal

Viral Shah , India

Ali Sharif , Pakistan

Ali Sheikhy, Iran

Md. Hasanuzzaman Shohag, Bangladesh


Daniele Sola , Italy

Marco Songini, Italy

Janet H. Southerland, USA

Vincenza Spallone , Italy

David Strain, United Kingdom

Bernd Stratmann , Germany

Farook Thameem, USA



Kazuya Yamagata, Japan

Liping Yu , USA

Burak Yulug, Turkey


Contents

Optical Coherence Tomography Angiography of Macular Perfusion Changes after Anti-VEGF Therapy for Diabetic Macular Edema: A Systematic Review

Ayman G. Elnahry  and Gehad A. Elnahry 



Review Article (14 pages), Article ID 6634637, Volume 2021 (2021)

Behavior of SD-OCT Detectable Hyperreflective Foci in Diabetic Macular Edema Patients after Therapy with Anti-VEGF Agents and Dexamethasone Implants

Anne RübSam , Laura Wernecke, Saskia Rau, Dominika Pohlmann, Bert Müller, Oliver Zeitz, and Antonia M. Joussem








Research Article (13 pages), Article ID 8820216, Volume 2021 (2021)

Atg16L1 as a Novel Biomarker and Autophagy Gene for Diabetic Retinopathy

Xinxiao Gao , Yunhui Du, Wayne Bond Lau, Yu Li, Siquan Zhu, and Xin-Liang Ma 

Research Article (11 pages), Article ID 5398645, Volume 2021 (2021)

Diabetic Macular Edema Treatment with Bevacizumab Does Not Depend on the Retinal Nonperfusion Presence

Bogumiła Sędziak-Marcinek , Sławomir Teper , Elżbieta Chelmecka , Adam Wylęgała , Mateusz Marcinek , Mateusz Bas , and Edward Wylęgała 



Research Article (15 pages), Article ID 6620122, Volume 2021 (2021)

miR-126 Mimic Counteracts the Increased Secretion of VEGF-A Induced by High Glucose in ARPE-19 Cells

Roberta Sanguineti , Alessandra Puddu , Massimo Nicolò , Carlo Enrico Traverso, Renzo Cordera , Giorgio L. Viviani , and Davide Maggi 



Research Article (7 pages), Article ID 6649222, Volume 2021 (2021)

Multifocal Electroretinogram Can Detect the Abnormal Retinal Change in Early Stage of type2 DM Patients without Apparent Diabetic Retinopathy

Jiang Huang , Yi Li, Yao Chen, Yuhong You, Tongtong Niu, Weijie Zou, and Weifeng Luo 


Research Article (7 pages), Article ID 6644691, Volume 2021 (2021)

The Risk Factors for Diabetic Retinopathy in a Chinese Population: A Cross-Sectional Study

Qingmin Sun, Yali Jing, Bingjie Zhang, Tianwei Gu, Ran Meng, Jie Sun, Dalong Zhu , and Yaping Wang 







Research Article (7 pages), Article ID 5340453, Volume 2021 (2021)

Tangeretin Inhibition of High-Glucose-Induced IL-1 β , IL-6, TGF- β 1, and VEGF Expression in Human RPE Cells

Dong Qin  and Yan-rong Jiang

Research Article (8 pages), Article ID 9490642, Volume 2020 (2020)

Widefield Optical Coherence Tomography Angiography in Diabetic Retinopathy

Alessia Amato , Francesco Nadin , Federico Borghesan , Maria Vittoria Cicinelli , Irini Chatziralli , Saena Sadiq, Rukhsana Mirza, and Francesco Bandello 


Review Article (10 pages), Article ID 8855709, Volume 2020 (2020)

Influence of Metabolic Parameters and Treatment Method on OCT Angiography Results in Children with Type 1 Diabetes

Marta Wysocka-Mincewicz , Marta Baszyńska-Wilk , Joanna Gołębiewska , Andrzej Olechowski , Aleksandra Byczyńska , Wojciech Hautz , and Mieczysław Szalecki 

Research Article (6 pages), Article ID 4742952, Volume 2020 (2020)

Quantitative Analysis of Retinal Microvascular Perfusion and Novel Biomarkers of the Treatment Response in Diabetic Macular Edema

Young Gun Park and Young-Hoon Park 

Research Article (8 pages), Article ID 2132037, Volume 2020 (2020)

The Role of SGLT2 Inhibitor on the Treatment of Diabetic Retinopathy

Wenjun Sha, Song Wen, Lin Chen, Bilin Xu, Tao Lei , and Ligang Zhou 

Review Article (6 pages), Article ID 8867875, Volume 2020 (2020)

Review Article

Optical Coherence Tomography Angiography of Macular Perfusion Changes after Anti-VEGF Therapy for Diabetic Macular Edema: A Systematic Review

Ayman G. Elnahry ^{1,2} and Gehad A. Elnahry ^{1,2}

¹Department of Ophthalmology, Faculty of Medicine, Cairo University, Cairo, Egypt

²Elnahry Eye Clinics, Giza, Egypt

Correspondence should be addressed to Ayman G. Elnahry; ayman_elnahri@hotmail.com

Received 13 December 2020; Revised 14 January 2021; Accepted 20 April 2021; Published 25 May 2021

Academic Editor: Maria Vittoria Cicinelli

Copyright © 2021 Ayman G. Elnahry and Gehad A. Elnahry. This is an open access article distributed under the Creative Commons Attribution License, which permits unrestricted use, distribution, and reproduction in any medium, provided the original work is properly cited.

Background. Diabetic macular edema (DME) is a major cause of vision loss in diabetics that is currently mainly treated by antivascular endothelial growth factor (VEGF) agents. The effect of these agents on macular perfusion (MP) is a current concern. Optical coherence tomography angiography (OCTA) is an imaging modality that allows noninvasive high-resolution retinal microvasculature imaging. Several recent studies evaluated the effect of anti-VEGF agents on the MP of DME patients using OCTA. Our aim is to provide a systematic review of these studies. **Methods.** Multiple databases were searched including PubMed, Ovid Medline, EMBASE, and Google Scholar for relevant studies published between January 2016 and November 2020 which were included in this review. Studies were compared regarding their design, the number of included patients, the machine and scanning protocol used, the inclusion and exclusion criteria, the number of injections given, the type of anti-VEGF agent used, the outcome measures assessed, and the effect of injections on different MP parameters. **Results.** A total of 16 studies were included. The studies assessed various OCTA parameters that define MP including the foveal avascular zone area and superficial and deep vascular density and yielded conflicting results. Seven studies showed stable or improved MP following treatment, while 7 studies showed worsening MP following treatment, and 2 studies showed inconclusive results. This could have been due to differences in study design, inclusion criteria, type of anti-VEGF agents used, treatment duration, and methods of image analysis and vascular density quantification. All identified studies were noncomparative case series, and 14 of them (87.5%) used the RTVue XR Avanti OCTA machine. Only one study compared OCTA to fluorescein angiography findings. **Conclusion.** Analysis of MP changes following VEGF inhibition for DME could benefit from a unified scanning protocol and analysis approach that uses similar study designs to eliminate potential sources of bias. This may provide more definitive conclusions regarding the effect of treatment on MP.

1. Introduction

Diabetic macular edema (DME) is the most common cause of loss of vision in diabetic patients, affecting around 21 million people globally [1]. The treatment of macular edema associated with various retinal diseases, including DME (Figure 1), is currently dependent on the repeated intravitreal injection of different anti-vascular endothelial growth factor (anti-VEGF) agents [2–6]. Other treatment modalities for DME include steroid injections and macular laser photocoagulation [2].

VEGF-A is one of the members of the VEGF family and is currently the most implicated in the pathogenesis of these various retinal conditions due to its role in angiogenesis and vaso-permeability which results in the disruption of blood-retinal barriers [2, 7]. It has 5 different isoforms, and most of the currently available anti-VEGF antibodies block all these isoforms [2]. VEGF has also several physiologic functions that include the regulation of normal vasculogenesis and angiogenesis [8]. It also acts as a survival factor for retinal vessels during their development [9], maintains the choriocapillaris and the photoreceptors [10], and

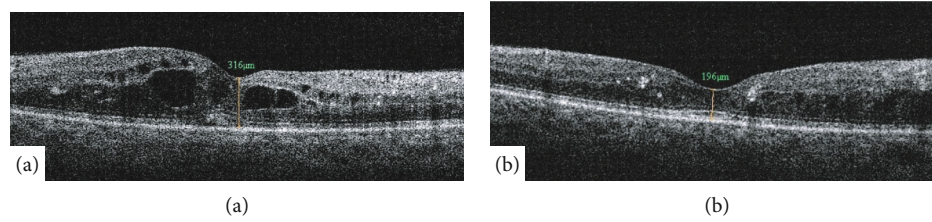


FIGURE 1: Optical coherence tomography (OCT) of the macula of a diabetic patient showing improvement of DME before (a) and after (b) anti-VEGF injections. There is marked improvement in the central foveal thickness as measured by OCT.

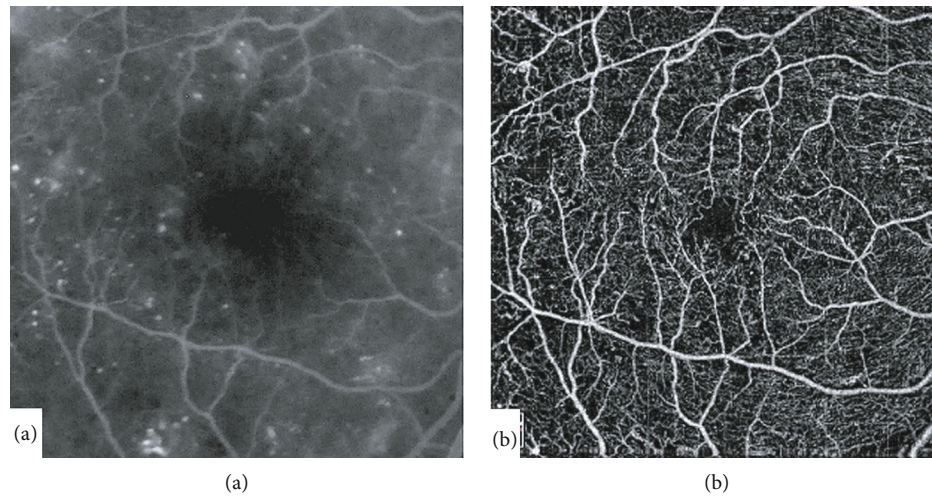


FIGURE 2: Compared to fluorescein angiography (a), optical coherence tomography angiography (Optovue, Inc., Fremont, CA, USA) of the macula (b) allows imaging of the retinal capillaries and foveal avascular zone in high resolution without obscuration by dye leakage or macular xanthophyll pigment shadowing.

possesses a neuroprotective role that reduces neuronal apoptosis [11]. These physiological functions of VEGF may be interrupted during prolonged treatment of retinal conditions with repeated injection of anti-VEGF agents, which raises concerns regarding the safety of the long-term use of these agents [12, 13].

Several animal studies have shown deleterious cellular effects following the inhibition of VEGF [10, 14, 15]. A number of previous studies, however, have evaluated the effect of repeated intravitreal injections of VEGF inhibitors for DME on the macular and retinal perfusion of diabetic patients using fluorescein angiography (FA) with some studies showing worsening and others showing no worsening of perfusion following treatment. These studies, however, assessed mainly the superficial retinal vasculature, were possibly influenced by dye leakage, and depended on trained human graders [16–22]. Optical coherence tomography angiography (OCTA) allows noninvasive and dye-free imaging of the superficial and deep retinal vasculature providing high resolution 3D images of the different retinal vascular layers separately [23, 24]. OCTA has been previously shown to precisely and reliably delineate areas of capillary drop-out and to image the foveal avascular zone (FAZ) without obscuration by dye leakage or macular xanthophyll pigment shadowing compared to FA (Figure 2) [24–26]. It also allows quantitative and automated measurements of the retinal vascular density (VD) and the fractal dimension (FD) reliably and in

a reproducible manner in the macular area without the need for human graders compared to FA [27–31].

Recently, several studies have been performed by various investigators using OCTA to objectively evaluate the effect of repeated intravitreal anti-VEGF injections on the macular perfusion of diabetic patients with DME. In this systematic review, we aim to summarize and compare the methods and findings of these studies.

2. Methods

2.1. Registration, Search Strategy, and Database Search. This systematic review was prospectively registered at PROSPERO on November 25, 2020 (Registration number: CRD42020216343). The study followed the tenets of the Declaration of Helsinki and was approved by the Cairo University research ethics committee. The Preferred Reporting Items for Systematic Reviews and Meta-analyses (PRISMA) guidelines were followed. A systematic literature search using PubMed, Ovid MEDLINE, EMBASE, Science Direct, and Google Scholar for articles published between January 2016 and November 2020 was performed. Keywords searched included different combinations of the following terms: diabetic macular edema, diabetic macular ischemia, diabetic retinopathy, anti-VEGF, VEGF inhibition, ranibizumab, aflibercept, bevacizumab, macular perfusion, macular ischemia, macular microvasculature, retinal ischemia, retinal

perfusion, perifoveal capillaries, foveal avascular zone, capillary reperfusion, capillary non-perfusion, vascular density, and optical coherence tomography angiography. For example, the search strategy in PubMed was as follows: “diabetic macular edema” AND “anti-VEGF OR bevacizumab OR ranibizumab OR aflibercept” AND “macular perfusion OR macular microvasculature OR foveal avascular zone OR diabetic macular ischemia OR vascular density” AND “optical coherence tomography angiography”.

2.2. Selection of Studies. Following the exclusion of duplicates, the identified titles and abstracts were independently reviewed by both investigators, and all relevant studies were included in the review. Any disagreement between both investigators was resolved by an open discussion. The reference lists of identified papers were also examined to find additional relevant articles.

2.3. Inclusion and Exclusion Criteria. Studies in which OCTA was performed before and after anti-VEGF injections for the treatment of DME were included. Studies which did not perform OCTA before injections and studies which only used FA were excluded. Studies which used steroid injections for treatment of DME were also excluded. Only articles that were peer-reviewed and published in the English language were included, and no restrictions were applied to the study type.

2.4. Data Extraction and Assessment of Methodological Quality and Risk of Bias. All included studies were read in full independently by both investigators, and the following data was extracted: name of authors, title, year of publication, the design of the studies, the number of included patients, the scanning protocol and type of machine used, the inclusion and exclusion criteria of patients, the number of injections given and the treatment protocol used, the type of anti-VEGF agents used (Bevacizumab (Avastin, Genentech/Roche, South San Francisco, CA, USA), aflibercept (Eylea, Regeneron, Tarrytown, NY, USA), ranibizumab (Lucentis, Genentech/Roche, South San Francisco, CA, USA), and conbercept (Lumitin, Chengdu Kanghong Biotech, Sichuan, People’s Republic of China)), the outcome measures assessed, and the effect of the injections on different macular perfusion parameters. Data extracted by both investigators was compared, and any discrepancies were discussed, and a consensus was reached. The assessment of the methodological quality and risk of bias in and across the included studies was performed using a customized scoring scale as follows: eight items were scored for each study according to whether they were present or absent. The presence of an item amounted to a score of one while its absence amounted to a score of zero. The maximum score possible was 8, and a higher score meant a higher study quality.

3. Results

A total of 16 studies that evaluated the effect of intravitreal anti-VEGF injections for DME on the macular perfusion using OCTA in the period between January 2016 and November 2020 were included [12, 32–46]. Figure 3 shows the PRISMA flowchart summarizing the results of the search

strategy and reasons for exclusion. All identified studies were noncomparative case series, and so, the Jadad Scale, the Newcastle-Ottawa Scale, and the Cochrane Collaboration’s tool could not be used to assess or compare their methodological quality or risk of bias.

Most of the included studies (14/16, 87.5%) used the RTVue XR Avanti Spectral domain-OCTA machine (Optovue, Inc., Fremont, CA, USA), while two studies (2/16, 12.5%) used the Triton OCTA machine (Topcon Inc, Japan). Only one study compared ischemic to nonischemic eyes [37], while one study compared OCTA to FA findings [41]. The duration of treatment and type of anti-VEGF agent used were variable, and some studies utilized multiple anti-VEGF agents. The design, methods, and results of the included studies are summarized in Tables 1, 2, and 3 according to whether positive, negative, or conflicting effects were found on the macular perfusion, respectively, following treatment. Table 4 summarizes the strengths and limitations of all included studies, while Table 5 presents the customized scale for assessing and comparing the methodological quality of the included studies.

3.1. Studies That Found Stable or Improved Macular Perfusion following Injections (Table 1). A total of 7 studies found stable or improved macular perfusion using OCTA following anti-VEGF injections for DME. In the study by Ghasemi Falavarjani et al. [32], OCTA was prospectively used to evaluate the macular perfusion changes following a single injection of VEGF inhibitors in patients with macular edema due to either DR or central retinal vein occlusion (CRVO). The authors found that neither the FAZ area nor the foveal and parafoveal vascular density of both the superficial (SCP) and deep capillary plexuses (DCP) changed significantly after the single injection. Further evaluation of data from the study showed that the FAZ area increased, and the VD of the foveal area decreased following the single injection, which was not, however, statistically significant. The study, however, included a relatively small number of eyes, used various types of anti-VEGF (bevacizumab in 14 eyes, aflibercept in 3 eyes, and ranibizumab in 1 eye), included 2 different etiologies for the macular edema (13 eyes with DME and 5 eyes with CRVO), involved a single intravitreal injection, had a limited follow-up of one month, and used VD measurements from the built-in machine software. Patients with a history of previous anti-VEGF treatment were also not excluded.

Sorour et al. [33] retrospectively evaluated the effect of repeated injections of VEGF inhibitors for DME or proliferative diabetic retinopathy (PDR) on the macular perfusion using OCTA and found no statistically significant difference in VD measurements after 1, 2, and 3 injections using two scanning protocols. The study included 55 eyes: 46 underwent OCTA imaging after the 1st injection, 28 after the 2nd injection, and 26 after the 3rd injection. Multiple anti-VEGF agents were also used (45.7% bevacizumab, 42.4% aflibercept, and 11.9% ranibizumab) with a mean interval of 47 days between the injections. 23 eyes (50%) that performed OCTA scanning after the 1st injection were not treatment naïve: 13 eyes were included after a washout period of 3

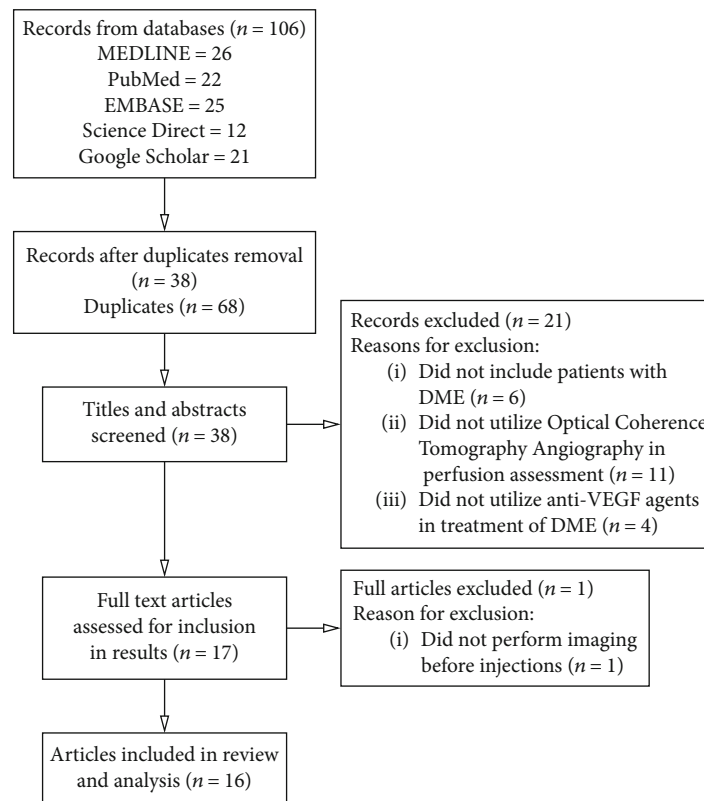


FIGURE 3: Flow diagram showing search results and reasons for exclusion of studies.

months from the last anti-VEGF injection, while 10 eyes were on regular VEGF inhibitors treatment without a washout period.

In the retrospective study by Hsieh et al. [34], a custom-developed Matlab (Mathworks, Natick, MA, USA) software was used for OCTA image processing and analysis. Five OCTA biomarkers including FAZ area, FAZ circulatory index, average vessel caliber, vessel tortuosity, and VD were assessed before and after 3 monthly ranibizumab injections for DME. The authors reported a statistically significant improvement in the FAZ (-31%), the average vessel caliber (-4.3%), and the inner (+6%) and outer (+9%) parafovea VD of the SCP and a statistically significant improvement in the FAZ (-31%), the FAZ circulatory index (-4.2%), and the inner (+9%) and outer (+9.4%) parafovea VD of the DCP following the injections. These biomarkers, however, did not improve to their normal values as compared to a healthy control group. The study did not find significant correlations between OCTA metrics and anatomical improvement but the inner parafoveal VD of the SCP turned out to be the biomarker that most correlated with visual improvement after treatment.

In the retrospective study by Conti et al., patients with DR that underwent aflibercept injections for DME were included, and the FAZ area and retinal VD were measured at baseline and after 6 and 12 months of treatment [35]. No patient was treatment naïve (average of 5.1 injections before the study with an average washout period of 44.4 days), and by 12 months, 26% received monthly aflibercept injections

while 74% received bimonthly injections with an average of 5.2 injections before switching to bimonthly. Although an enlargement of the FAZ area from 0.307 mm^2 to 0.313 mm^2 and decrease in whole image VD from 46.9% to 45.7% was reported at 12 months, these changes were not statistically significant ($p > 0.05$). Changes in choriocapillaris density which was also evaluated by OCTA were also not statistically significant.

Michalska-Malecka and Heinke Knudsen retrospectively reviewed patients imaged before and after treatment with 3 to 5 injections of aflibercept for DME using OCTA [36]. The authors reported little change in the VD measurements of the patients, but found an improvement of vision and central macular thickness.

In a prospective study by Zhu et al. [37], the effect of conbercept injections on the macular perfusion of patients with DME was assessed using OCTA scanning. Patients were divided into two subgroups: ischemic (31 patients) and non-ischemic (19 patients) according to macular perfusion findings on FA and received 3 monthly conbercept injections followed by pro re nata regimen for another 3 months. The FAZ area showed a significant decrease in the ischemic group, while the VD of the SCP increased. Measurements in the nonischemic group did not significantly change.

Mirshani et al. [38] prospectively evaluated changes in macular perfusion following a single bevacizumab injection for DME using OCTA. They measured the retinal VD, FAZ area, vessel diameter index, vascular length density, capillary nonperfusion area, and subfoveal choriocapillaris VD before

TABLE 1: Study design, methods, and results of studies that found stable or improved macular perfusion following injections.

Study	No. of eyes	Design of study	Imaging modality	Agent used and treatment duration	Outcome measure	Study results	Ref.
Ghasemi Falavarjani et al.	13 eyes of 10 patients with DME	Prospective noncomparative case series	OCTA (Optovue) using VD from machine software	Bevacizumab, Ranibizumab, Aflibercept (1 injection by any)	Change in FAZ area (manual) and VD	FAZ-A increased, and VD of foveal area decreased but nonsignificantly ($p > 0.05$)	[32]
Sorour et al.	55 eyes of 35 patients with DME or PDR	Retrospective case series	OCTA (Optovue) 3×3 and 6×6 scans with VD of machine	45.7% Bevacizumab, 42.4% Aflibercept, and 11.9% Ranibizumab	Change in VD after 3 injections	No significant change in VD measurements at 1, 2, and 3 months	[33]
Hsieh et al.	50 eyes of 50 patients with DME	Retrospective case series	OCTA (Optovue) 3×3 with custom developed Matlab software for image processing and analysis	Ranibizumab (3 injections)	Change in FAZ-A, FAZ-CI, AVC, vascular tortuosity, and VD	Improvement of FAZ-A (-31%), AVC (-4.3%), and inner (+5.9%) and outer (+8.8%) PF-VD in the SCP, and FAZ-A (-31%), FAZ-CI (-4.2%), and inner (+9.1%) and outer (+9.4%) PF-VD in DCP ($p \leq 0.05$)	[34]
Conti et al.	19 eyes of 19 patients with DR	Retrospective case series	OCTA (Optovue) 6×6 scan using built-in machine VD	Aflibercept (by 12 months, 26% received monthly while 74% received bimonthly treatment)	Change in FAZ and VD after 6 and 12 months of treatment	FAZ area enlarged from 0.307 to 0.313 mm ² , VD dropped from 46.9% to 45.7% ($p > 0.05$)	[35]
Michalska and Heinke	3 eyes of 3 patients with DME	Retrospective case series	OCTA (Optovue) 3×3 scans	Aflibercept (3-5 injections)	Change in built-in machine VD	Insignificant change in VD ($p > 0.05$)	[36]
Zhu et al.	50 eyes of 50 patients with DME (ischemic and nonischemic)	Prospective case series with predefined outcome measures	OCTA (Optovue) 6×6 scan using machine software	Conbercept (3 monthly injections then pro re nata for 3 months)	Change in built-in machine VD and FAZ area	FAZ area significantly decreased and superficial capillary plexus VD increased in ischemic group (both $p < 0.05$)	[37]
Mirshani et al.	23 eyes of 19 patients with DME	Prospective case series with predefined outcome measures	OCTA (Optovue) 3×3 scan using machine software and custom image processing	Bevacizumab (single injection)	Change in built-in machine VD, manual FAZ area, VDI, and VLD index	No significant change in FAZ area, retinal VD, VDI, or VLD (all $p > 0.05$). Improved subfoveal choriocapillaris VD ($p > 0.05$)	[38]

AVC: average vessel caliber; DCP: deep capillary plexus; DME: diabetic macular edema; DR: diabetic retinopathy; FA: fluorescein angiography; FAZ: foveal avascular zone; FAZ-A: foveal avascular zone area; FAZ-CI: foveal avascular zone circulatory index; OCTA: optical coherence tomography angiography; PDR: proliferative diabetic retinopathy; PF: parafoveal; SCP: superficial capillary plexus; VD: vascular density; VDI: vessel diameter index; VLD: vascular length density.

and after the injection. No significant changes were found after the injection except for a mild improvement in choriocapillaris VD. Only patients with a recent history of VEGF inhibitor treatment were excluded.

3.2. Studies That Found Worsening of Macular Perfusion following Injections (Table 2). A total of 7 studies found worsening of macular perfusion following anti-VEGF injections for DME using OCTA. In the observational study by Couturier et al. [39], patients with DME and severe nonproliferative or proliferative DR injected with ranibizumab or aflibercept for 3 months were included in the study and assessed using

OCTA. Following the injections, there was a decrease in the VD of the SCP from $39.5 \pm 6.9\%$ to $36.6 \pm 4.3\%$ and of the DCP from $44.7 \pm 6.2\%$ to $42.5 \pm 3.8\%$. The result, however, was not statistically significant.

Our group performed a prospective study aimed at evaluating by OCTA the effects of 3 monthly intravitreal injections of bevacizumab on the macular perfusion of treatment naïve diabetic patients with DME (the IMPACT Study) [40]. The FAZ area enlarged by 8.1%, the full retinal thickness (Full) and the SCP FD was reduced by 1.3%, the FD of DCP was reduced by 1.9%, the VD of Full was reduced by 8%, the VD of the SCP was reduced by 9.1%, the VD of

TABLE 2: Study design, methods, and results of studies that found worsening of macular perfusion following injections.

Study	No. of eyes	Design of study	Imaging modality	Agent used and treatment duration	Outcome measure	Study results	Ref.
Couturier et al.	10 eyes of 9 patients with DME	Prospective observational case series	OCTA (Optovue) 3 × 3 scan using machine software for VD	Ranibizumab or Aflibercept (3 injections)	Change in VD after 3 injections using built-in machine software	SCP VD drop from 39.5 ± 6.9% to 36.6 ± 4.3% and DCP VD from 44.7 ± 6.2% to 42.5 ± 3.8% ($p > 0.05$)	[39]
Elnahry et al. (the IMPACT study)	40 eyes of 26 patients with DME	Prospective case series with predefined outcome measures	OCTA (Optovue) 3 × 3 and 6 × 6 scans with custom image processing	Bevacizumab (3 monthly injections)	Change in FD, VD, skeleton VD, and manual FAZ area	Increase in FAZ area and decrease in FD, VD, and skeleton VD of full, SCP, and DCP (all $p < 0.05$)	[40]
Pereira et al.	5 eyes of 5 patients with DME and DMI	Prospective case series	FA, OCTA (Topcon) 3 × 3 or 4.5 × 4.5, and MP	Bevacizumab (6 injections)	Change in FAZ area on FA and OCTA (manually measured in both)	FA FAZ from 1.35 ± 1.44 mm ² to 1.02 ± 1.02 mm ² ($p = 0.19$) and OCTA FAZ from 0.82 ± 0.55 mm ² to 0.92 ± 0.57 mm ² ($p = 0.02$)	[41]
Elnahry et al.	2 eyes of 1 patient with DME	Prospective longitudinal case report	OCTA (Optovue) 6 × 6 scan with machine software	Bevacizumab (repeated 3 monthly injections)	Change in built-in machine VD	Reversible worsening of VD with injections	[12]
Barash et al.	9 eyes with PDR and 5 with DME	Retrospective case series	OCTA (Optovue) macular and peri-papillary scans	Bevacizumab or Aflibercept (immediately after injections)	Macular and peri-papillary VD changes	SCP VD dropped by 7.8% while the DCP VD dropped by 3.5% immediately after injection	[42]
Statler et al.	16 eyes of 16 patients with persistent DME	Prospective case series with predefined outcome measures	OCTA (Optovue) 3 × 3 scan using machine software	Aflibercept (fixed interval injections for 24 months)	Change in built-in machine VD and FAZ area	Whole SCP VD decreased by 5.3% and whole DCP VD decreased by 4.4%. FAZ area increased (all $p < 0.05$)	[43]
Golshani et al. (SWAP-TWO study)	20 eyes of 20 patients with DME	Prospective case series with predefined outcome measures	OCTA (Optovue) 3 × 3 scan using machine software	Aflibercept (monthly dosing till dry then every 2 months thereafter through 12 months)	Change in built-in machine VD and FAZ area	No change in FAZ area, but SCP and DCP VD significantly decreased by 5.2% and 6.3%, respectively ($p \leq 0.05$)	[44]

DCP: deep capillary plexus; DME: diabetic macular edema; DMI: diabetic macular ischemia; FA: fluorescein angiography; FAZ: foveal avascular zone; FD: fractal dimension; Full: full retinal thickness; MP: microperimetry; OCTA: optical coherence tomography angiography; PDR: proliferative diabetic retinopathy; SCP: superficial capillary plexus; VD: vascular density.

DCP was reduced by 10.6%, the skeleton VD of Full was reduced by 13.3%, the skeleton VD of the SCP was reduced by 12.5%, and the skeleton VD of the DCP was reduced by 16.3% in the 6 × 6 mm macular area imaged by OCTA following the injections which were all statistically significant ($p < 0.05$) [40]. Similar findings were also found in the 3 × 3 mm scanning protocol. Automated image alignment before and after treatment was performed using a retinal alignment software (i2k Align Retina, DualAlign, LLC, Clifton Park, NY, USA), and segmentation errors were corrected manually.

In a small prospective study by Pereira et al. that included patients with DME associated with moderate to severe

macular ischemia, the functional and anatomical effects of bevacizumab were assessed using fluorescein angiography, OCTA, and microperimetry [41]. Following 6 intravitreal injections, the mean area of the FAZ on fluorescein angiography was reduced from 1.35 ± 1.44 mm² to 1.02 ± 1.02 mm² ($p = 0.19$) although 3 eyes exhibited an enlargement of the FAZ area. The mean FAZ area on OCTA (3 eyes analyzed) enlarged from 0.82 ± 0.55 mm² to 0.92 ± 0.57 mm² ($p = 0.02$). Microperimetry showed improvement of macular sensitivity from 11.66 ± 0.77 dB to 16.26 ± 3.29 dB ($p = 0.007$) which better correlated with improvement in retinal thickness than with ischemic areas on either fluorescein angiography or OCTA. Three of the 5 included eyes in that study were

TABLE 3: Study design, methods, and results of studies that found conflicting effects following treatment.

Study	No. of eyes	Design of study	Imaging modality	Agent used and treatment duration	Outcome measure	Study results	Ref.
Busch et al.	23 eyes of 23 patients with DME	Retrospective case series	OCTA (Optovue) 3 × 3 scan using machine software for VD	Aflibercept (1-8 monthly injections)	Change in built-in machine VD and FAZ	SCP FAZ increased by 0.07 mm ² and DCP FAZ decreased by 0.04 mm ² ($p > 0.05$)	[45]
Dastiridou et al.	20 eyes of 20 patients with DME	Prospective case series	Swept source OCTA (Topcon) 6 × 6 and 7 × 7 scans	Aflibercept (3 injections)	Change in FAZ area and VD	FAZ of DCP and VD of central area decreased ($p \leq 0.05$)	[46]

DCP: deep capillary plexus; DME: diabetic macular edema; FAZ: foveal avascular zone; OCTA: optical coherence tomography angiography; SCP: superficial capillary plexus; VD: vascular density.

previously treated with anti-VEGF agents while 2 eyes were treatment-naïve.

In a prospective long-term study conducted by our group, 2 eyes of a diabetic patient sequentially treated with repeated monthly bevacizumab injections for DME showed decreased VD measurements of the SCP and DCP following the injections using OCTA. These measurements subsequently returned to their baseline value when the injections were withheld [12]. Treatment of the left eye with injections led to reversible decrease in the VD while the VD of the untreated right eye was stable for 7 months without injections. Following treatment of the right eye there was a similar decrease in the VD.

In the retrospective study by Barash et al., macular and peripapillary VD changes were evaluated immediately following an intravitreal injection of a VEGF inhibitor (bevacizumab or aflibercept) for different pathologies including DR which showed a statistically significant reduction in the VD of most areas of the SCP and DCP in association with elevation of the intraocular pressure, with particularly more affection in the temporal SCP, the optic nerve head, and the radial peripapillary capillary network [42]. The superficial VD was reduced by 8%, while the deep VD was reduced by 3.5% immediately (within 3 minutes) after the injection.

In a prospective, interventional, single-arm study of patients with persistent DME, Statler et al. found a significant decrease in the superficial and deep capillary perfusion density, including the whole, foveal, and parafoveal density, following fixed interval intravitreal injections of aflibercept for 24 months [43]. Better vision correlated with less loss of capillary perfusion density following the injections in the superficial whole and parafoveal areas. Only 16 patients completed the study. All participants had a history of VEGF inhibitor treatment before inclusion in the study.

Golshani et al. [44] prospectively evaluated patients with DME that switched from bevacizumab (95%) or ranibizumab (5%) to aflibercept using OCT and OCTA (SWAP-TWO Study). Patients received monthly aflibercept injections until OCT demonstrated no fluid, followed by fixed dosing once every two months through 12 months. Following treatment, there was no significant change in the FAZ area, but the VD of the SCP significantly decreased by 5.2% ($p = 0.04$),

and the VD of the DCP significantly decreased by 6.3% ($p = 0.05$) by 12 months.

3.3. Studies That Found Conflicting Effects following Treatment (Table 3). In the retrospective study by Busch et al. [45] which analyzed the FAZ area and the VD following repeated aflibercept injections (mean: 2.6 ± 1.3 injections) for DME using OCTA. The authors reported an enlargement of the FAZ area in the SCP from 0.41 ± 0.2 mm² to 0.48 ± 0.24 mm² but a reduction of the FAZ area in the DCP from 0.75 ± 0.34 mm² to 0.71 ± 0.33 mm². These changes, however, were not statistically significant. The VD measurements were also unchanged following the injections.

Dastiridou et al. [46] used swept source OCTA to evaluate the FAZ and VD measurements of eyes of treatment naïve patients with DME following 3 aflibercept injections. There was a statistically significant reduction in the size of the FAZ of the DCP but not of the SCP following the injections with a high intragrader and intergrader agreement for the manual FAZ measurements. The VD of SCP of the central macular area showed a statistically significant 8% reduction following the injections, whereas the decrease in parafoveal VD did not reach statistical significance. The authors hypothesized that the displacement of the capillaries by the macular edema and the associated segmentation errors which occurred and were restored following treatment may have played a role in the findings of their study.

4. Discussion

The effects of repeated intravitreal injections of different VEGF inhibitors for DME on the macular perfusion of diabetic patients has been recently evaluated in several studies that used the relatively new OCTA technology. Originally, this evaluation has depended on the use of FA and expert human graders [16–22], with several studies that later followed that employed ultra widefield FA imaging in order to evaluate the effect of these VEGF inhibitors on the peripheral retinal perfusion of diabetics as well [39, 47–49]. These studies, however, did not provide conclusive results regarding the effect of VEGF inhibition on the status of the macular perfusion of diabetic patients [50].

TABLE 4: Relative strengths and limitations of identified studies.

Study	Strengths	Limitations	Ref.
Ghasemi Falavarjani et al.	Prospective.	Small number of eyes, used various types of VEGF inhibitors, included 2 different etiologies for macular edema, short duration of treatment, used built-in machine VD measurements, and did not exclude patients previously treated with anti-VEGF.	[32]
Sorour et al.	Relatively large number of eyes and used both 3 × 3 and 6 × 6 scans.	Retrospective, short follow-up period, variable anti-VEGF agent used, variable injection interval, used built-in machine VD measurements, did not exclude patients previously treated with anti-VEGF.	[33]
Hsieh et al.	Relatively large number of eyes, used a custom developed software, used one anti-VEGF agent, included one eye of each patient, assessed multiple outcome measures.	Retrospective, used only 3 × 3 scans and did not use automated image alignment.	[34]
Conti et al.	Used one anti-VEGF agent, had a long duration of follow-up, assessed two treatment protocols.	Retrospective, small number of eyes, used only 6 × 6 scans, used built-in machine VD measurements, did not exclude patients previously treated with anti-VEGF.	[35]
Michalska and Heinke	Used one anti-VEGF agent, included one eye of each patient.	Retrospective, small number of eyes, used only 3 × 3 scans, used variable number of injections, used built-in machine VD measurements.	[36]
Zhu et al.	Prospective, divided patients into ischemic and nonischemic groups, included one eye of each patient, used one anti-VEGF agent.	Used only 6 × 6 scans, did not use automated image alignment, used built-in machine VD measurements.	[37]
Mirshani et al.	Prospective, used one anti-VEGF agent, assessed multiple outcome measures.	Small number of eyes, short follow-up period, used only 3 × 3 scans, included both eyes of some patients, did not exclude patients previously treated with anti-VEGF.	[38]
Couturier et al.	Prospective.	Small number of eyes, included both eyes of some patients, used only 3 × 3 scans, used 2 anti-VEGF agents, used built-in machine VD measurements.	[39]
Elnahry et al. (the IMPACT study)	Prospective, registered, relatively large number of eyes, automated image alignment, used a custom developed software, used both 3 × 3 and 6 × 6 scans, used one anti-VEGF agent, patients were treatment-naïve, assessed multiple outcome measures.	Included both eyes of some patients and short follow-up period.	[40]
Pereira et al.	Prospective, relatively long follow-up period, used a single anti-VEGF agent, used microperimetry and fluorescein angiography.	Small number of eyes, assessed FAZ only, not all eyes were treatment naïve.	[41]
Elnahry et al.	Prospective, fellow eye used as control, long duration of follow-up, treatment naïve patient.	Small number of eyes, used built-in machine VD measurements.	[12]
Barash et al.	Only study to assess effect on VD immediately after the injection.	Retrospective, small number of eyes, short duration of follow-up, variable etiologies included, used built-in machine VD measurements, used 2 anti-VEGF agents.	[42]
Statler et al.	Prospective, long follow-up period, used a single anti-VEGF agent.	Small number of eyes, used only 3 × 3 scans, used built-in machine VD measurements, did not exclude patients previously treated with anti-VEGF.	[43]
Golshani et al. (SWAP-TWO study)	Prospective, long follow-up period, used a single anti-VEGF agent.	Small number of eyes, used only 3 × 3 scans, used built-in machine VD measurements, did not exclude patients previously treated with anti-VEGF.	[44]
Busch et al.	Used a single anti-VEGF agent, included one eye of each patient, patients were treatment naïve.	Retrospective, small number of eyes, used only 3 × 3 scans, variable follow-up period, used built-in machine VD measurements.	[45]
Dastiridou et al.	Prospective, used a single anti-VEGF agent, included one eye of each patient.	Small number of eyes, relatively short follow-up period, used built-in machine VD measurements and assessed SCP VD only.	[46]

FAZ: foveal avascular zone; SCP: superficial capillary plexus; VD: vascular density; VEGF: vascular endothelial growth factor.

TABLE 5: A customized scale for assessing and comparing the quality of included studies.

Study	Prospective	More than 30 eyes included	Single anti-VEGF agent	Single eye of included patient	Both 3 × 3 and 6 × 6 scans used	Treatment naive	Follow-up more than 3 months	Customized VD assessment	Total score	Ref.
Ghasemi Falavarjani et al.	1	0	0	0	0	0	0	0	1	[32]
Sorour et al.	0	1	0	0	1	0	0	0	2	[33]
Hsieh et al.	0	1	1	1	0	0	0	1	4	[34]
Conti et al.	0	0	1	1	0	0	1	0	3	[35]
Michalska and Heinke	0	0	1	1	0	0	0	0	2	[36]
Zhu et al.	1	1	1	1	0	0	1	0	5	[37]
Mirshani et al.	1	0	1	0	0	0	0	1	3	[38]
Couturier et al.	1	0	0	0	0	1	0	0	2	[39]
Elnahry et al. (the IMPACT Study)	1	1	1	0	1	1	0	1	6	[40]
Pereira et al.	1	0	1	1	0	0	1	0	4	[41]
Elnahry et al.	1	0	1	0	0	1	1	0	4	[12]
Barash et al.	0	0	0	1	0	0	0	0	1	[42]
Statler et al.	1	0	1	1	0	0	1	0	4	[43]
Golshani et al. (SWAP-TWO study)	1	0	1	1	0	0	1	0	4	[44]
Busch et al.	0	0	1	1	0	1	1	0	4	[45]
Dastiridou et al.	1	0	1	1	0	0	0	0	3	[46]

The presence of an item amounted to a score of one while its absence amounted to a score of zero. Eight items were scored for each study; thus, the maximum score possible for a study was 8. A higher score meant a higher quality.

OCTA is a dye-free imaging modality that depends on comparison of the decorrelation signals between repeated consecutive OCT B-scans acquired in rapid succession at the same retinal location. This allows motion contrast generated by the flow of red blood cells in the retinal vessels to be detected which leads to imaging of perfused retinal vessels and detection of flow-void areas [23–26, 51]. OCTA, therefore, makes it possible to obtain reliable and reproducible measurements of VD and FD, thus allowing an objective and grader-independent assessment of the macular perfusion status [27–31]. Based on these features, OCTA harbors great potential in DR evaluation and is probably more suitable than traditional angiography in analyzing VD changes following VEGF inhibition in diabetics. Nevertheless, OCTA is a still emerging technology with several limitations. First of all, OCTA images may be significantly impacted by low signal strength, resulting in an altered visualization of the small vessels. Moreover, localized loss of signals due to localized media opacities can be misinterpreted as flow-void areas. Finally, it should be considered that vascular OCTA imaging is currently more affected by artifacts and interpretation errors compared to FA. These artifacts include motion and blink artifacts (due to the prolonged scanning time), shadow artifacts, and projection artifacts from superficial

layers [52, 53]. The interpretation of OCTA images should, therefore, be done cautiously with these limitations in mind to avoid reaching misleading or inaccurate conclusions. This could possibly explain why results of studies performed by different investigating groups using OCTA may be different or conflicting. However, as the OCTA technology gets better and faster, many of these limitations and artifacts could be eliminated leading to more reliable and comparable results from studies with more solid conclusions.

A relatively large number of studies that utilized OCTA in the evaluation of macular perfusion changes in diabetics following VEGF inhibition have been recently conducted by several research groups globally. This may reflect the current uncertainty that surrounds the effect of VEGF inhibitors on the macular perfusion status of diabetic patients, which led many researchers to attempt to investigate this effect using the emerging OCTA technology considering its advantages in imaging the retinal vasculature over FA imaging that include its ability to image fine capillary details, especially the perifoveal capillary network and deep capillary plexus, in a higher resolution without obscuration by leakage of dye or macular xanthophyll pigment which allows better detection and quantification of retinal ischemia [54–57]. The studies analyzed in this review, however, yielded

conflicting results with 7 studies showing stable or improved macular perfusion following treatment [32–38], 7 studies showing worsening of macular perfusion following treatment [12, 39–44], and 2 studies showing conflicting results [45, 46]. This could have been due to study design differences, differences in patients' characteristics and inclusion criteria, or methods of image analysis and vascular density quantification. The relative weight of each study and its overall significance in our opinion depended on several factors including the study design, the number of included patients, the duration of treatment and number of injections given, the treatment protocol used, and the method of image analysis, which could not be assessed with any available scale since all the identified studies were noncomparative case series. We therefore developed a customized scoring scale consisting of these items to help compare the methodological quality and risk of bias across the identified studies based on a validated item bank on the risk of bias and precision of case series [58].

Some factors associated with anti-VEGF treatment for DME may result in macular perfusion improvement while others may lead to its worsening, which could explain why some diabetic patients experience macular perfusion improvement following the injections while others experience perfusion worsening, probably depending on which of these factors predominate in each patient. Even in the single patient, it is apparent that some macular areas become better perfused while other areas become worse on OCTA following treatment which suggests that several factors associated with VEGF inhibition that influence macular perfusion are in play [59]. Factors that could result in retinal perfusion improvement after treatment with anti-VEGF antibodies include the reversal of leukostasis, that is induced by excessive VEGF secretion in diabetics and results in increased capillary occlusion [60], restoration of the normal retinal architecture due to decreased intraretinal edema [46], and inhibition of the hypertrophy of endothelial cells that is induced by excessive local VEGF-A production and leads to narrowing and occlusion of capillary lumen [61]. Factors that could justify retinal perfusion worsening following VEGF inhibition include inducing vasoconstriction of the retinal vasculature which was found following bevacizumab and ranibizumab injections for DME possibly due to nitric oxide inhibition which occurs with VEGF inhibition and also leads to systemic hypertension in case of systemic VEGF inhibition [62, 63]. Inhibition of VEGF by bevacizumab also resulted in a decrease of the mean blood flow velocity of the central retinal, the temporal posterior ciliary, and the ophthalmic artery by about 10%, 20%, and 20%, respectively, 4 weeks after one bevacizumab injection in patients with exudative age-related macular degeneration [64]. Loss of pericytes that normally surround mature retinal capillaries and make them nondependent on VEGF for survival could be another cause of decreased capillary density following VEGF inhibition in diabetics [65, 66]. Loss of pericytes is known to occur in early DR and may render capillary endothelial cells susceptible to VEGF inhibition leading to endothelial cell demise and subsequent capillary loss [14, 67]. Another possibility that could also explain the worsening of macular perfusion associated

with VEGF inhibition for DME treatment is the progressive natural history of DR which in this case is incompletely arrested by VEGF inhibition as has been previously reported [21].

The presence of cystoid spaces in chronic diabetic macular edema may resemble areas of capillary nonperfusion on enface OCTA since both may appear as black or grey areas [68, 69]. The appearance of these areas, however, can be variable depending on which OCTA machine is used [69, 70]. Cystoid spaces seen on OCT were also found to colocalize with areas of nonperfusion on OCTA [68, 70]. It is possible that these cystoid spaces may result in lateral displacement of capillaries or preferentially occur in areas of capillary nonperfusion due to the development of nearby leaky microaneurysms [56, 68]. The disappearance of these cystoid spaces following treatment with resultant capillary reperfusion may be another mechanism for an increase in vascular density following treatment [70]. In one study analyzing the effect of treatment on these spaces, however, no reperfusion occurred in nonperfusion areas following resolution of the cystoid spaces [68]. This, however, may have been due to the chronic nature of edema in these cases which requires further validation in cases with the earlier stages of the disease.

The short- and long-term consequences of macular perfusion changes following VEGF inhibition are also still unclear since most of the analyzed studies reported significant visual and anatomical improvements following the injections regardless of the macular perfusion changes. In the study by Hsieh et al. which showed improvement of the macular perfusion following 3 monthly ranibizumab injections, there were no significant correlations between OCTA biomarkers and anatomical improvement; however, the inner parafoveal vascular density of the superficial capillary plexus was the most significantly correlating biomarker with visual improvement following treatment [34], while in the prospective study performed by our group which showed worsening of macular perfusion following 3 monthly bevacizumab injections, changes in the superficial capillary plexus showed a significant negative correlation with changes in the central macular thickness [40]. Other studies, however, did not report significant correlations between OCTA biomarkers and visual or anatomical improvement, with Pereira et al. showing that macular sensitivity measured using microperimetry better correlated with changes in retinal thickness than with ischemic areas on either FA or OCTA [41]. These correlations are important in order to determine the clinical significance of these macular perfusion changes on the short- and long-term functional and anatomical treatment outcomes.

In an interesting study by Alagorie et al. [71] that evaluated the association of intravitreal aflibercept injections with macular VD changes using OCTA in patients with proliferative diabetic retinopathy but without DME, the authors reported no significant macular VD changes following 12 months of intravitreal aflibercept therapy using both monthly and quarterly dosing. The study used the 3 × 3 mm OCTA, however, which may have missed ischemic changes in the perifovea, and only diabetic patients without

DME were included since the authors thought that DME may result in artifacts and segmentation errors in OCTA images which they indicated may have affected the results of previous studies; however, the structure and integrity of the macular microvasculature may differ between patients with and without DME, and so, the direct extrapolation of their results to patients with DME may not be valid. For example, patients with DME may have more structural damage to their macular microvasculature in the form of more pericyte loss which may render their vessels more susceptible to VEGF inhibition compared to patients without DME [40, 65]. Also, because the authors did not compare the baseline macular VD values of included patients with a healthy control group, it is difficult to estimate the initial severity of macular ischemia in the included patients. This is important since patients with more macular ischemia at baseline could be at more risk of worsening of ischemia following VEGF inhibition [72]. Finally, although patients in that study did not have initial macular thickening, there was a decrease in the central macular thickness following treatment below what would be considered a normal macular thickness, raising concerns for progressive macular atrophy associated with long-term VEGF inhibition even in the absence of detectable macular perfusion worsening.

5. Conclusion

In conclusion, several studies have been performed to evaluate the effect of intravitreal injections of various VEGF blocking agents for DME on the macular perfusion status of diabetics using OCTA yielding conflicting results that could have been influenced by study design, patients' inclusion criteria, and method of image analysis used. Analysis of vascular density changes following anti-VEGF treatment for DME using OCTA could benefit from a unified scanning protocol and analysis approach that uses similar study designs and patients' inclusion criteria to eliminate potential sources of bias. This could ultimately provide more definitive conclusions regarding the effect of these injections on the macular perfusion status of diabetics. With future advances in the OCTA technology, including increased speed of scanning, development of better imaging artifacts correction software, and wider scanning protocols, this evaluation will be more reliable and reproducible.

Abbreviations

AVC:	Average vessel caliber
CRVO:	Central retinal vein occlusion
DGP:	Deep capillary plexus
DM:	Diabetes mellitus
DME:	Diabetic macular edema
DR:	Diabetic retinopathy
DRSS:	Diabetic retinopathy severity score
ETDRS:	Early Treatment Diabetic Retinopathy Study
FA:	Fluorescein angiography
FAZ:	Foveal avascular zone
FAZ-A:	Foveal avascular zone area
FAZ-CI:	Foveal avascular zone circulatory index

FD:	Fractal dimension
Full:	Full retinal thickness
IOP:	Intraocular pressure
MP:	Microperimetry
OCT:	Optical coherence tomography
OCTA:	Optical coherence tomography angiography
PDR:	Proliferative diabetic retinopathy
PF:	Parafoveal
SCP:	Superficial capillary plexus
VD:	Vascular density
VDI:	Vessel diameter index
VLD:	Vascular length density
VEGF:	Vascular endothelial growth factor.

Data Availability

All the data used in this study are available within the article.

Additional Points

The authors have read the PRISMA 2009 Checklist, and the manuscript has been prepared and revised according to its guidelines.

Ethical Approval

This report was approved by Cairo University research ethics committee and followed the tenets of the Declaration of Helsinki.

Conflicts of Interest

Ayman G. Elnahry declares that he has no conflict of interest. Gehad A. Elnahry declares that he has no conflict of interest.

Authors' Contributions

AGE has made substantial contribution in the conception and design of the work, and in acquisition, analysis, and interpretation of the data, and in drafting the manuscript. GAE has made substantial contribution in the conception and design of the work and in the revision of the manuscript. Both authors read and approved the final manuscript.

Supplementary Materials

PRISMA 2009 guideline checklist. (*Supplementary Materials*)

References

- [1] J. W. Yau, S. L. Rogers, R. Kawasaki et al., "Global prevalence and major risk factors of diabetic retinopathy," *Diabetes Care*, vol. 35, no. 3, pp. 556–564, 2012.
- [2] B. Bahrani, M. Zhu, T. Hong, and A. Chang, "Diabetic macular oedema: pathophysiology, management challenges and treatment resistance," *Diabetologia*, vol. 59, no. 8, pp. 1594–1608, 2016.
- [3] A. G. Elnahry, F. K. Hassan, and A. A. Abdel-Kader, "Bevacizumab for the treatment of intraretinal cystic spaces in a patient with gyrate atrophy of the choroid and retina," *Ophthalmic Genetics*, vol. 39, no. 6, pp. 759–762, 2018.

- [4] P. U. Dugel, G. J. Jaffe, P. Sallstig et al., “Brolucizumab versus aflibercept in participants with neovascular age-related macular degeneration: a randomized trial,” *Ophthalmology*, vol. 124, no. 9, pp. 1296–1304, 2017.
- [5] A. G. Elnahry, E. M. Sallam, K. J. Guirguis, J. H. Talbet, and A. A. Abdel-Kader, “Vitrectomy for a secondary epiretinal membrane following treatment of adult-onset Coats’ disease,” *American Journal of Ophthalmology Case Reports*, vol. 15, p. 100508, 2019.
- [6] A. G. Elnahry, M. R. Aboufotouh, and G. A. Nassar, “Treatment of intraretinal cystic spaces associated with gyrate atrophy of the choroid and retina with intravitreal bevacizumab,” *Journal of Pediatric Ophthalmology & Strabismus*, vol. 57, no. 6, pp. 400–406, 2020.
- [7] X. Xu, Q. Zhu, X. Xia, S. Zhang, Q. Gu, and D. Luo, “Blood-retinal barrier breakdown induced by activation of protein kinase C via vascular endothelial growth factor in streptozotocin-induced diabetic rats,” *Current Eye Research*, vol. 28, no. 4, pp. 251–256, 2004.
- [8] N. Ferrara and R. S. Kerbel, “Angiogenesis as a therapeutic target,” *Nature*, vol. 438, no. 7070, pp. 967–974, 2005.
- [9] T. Alon, I. Hemo, A. Itin, J. Pe’er, J. Stone, and E. Keshet, “Vascular endothelial growth factor acts as a survival factor for newly formed retinal vessels and has implications for retinopathy of prematurity,” *Nature Medicine*, vol. 1, no. 10, pp. 1024–1028, 1995.
- [10] T. Kurihara, P. D. Westenskow, S. Bravo, E. Aguilar, and M. Friedlander, “Targeted deletion of Vegfa in adult mice induces vision loss,” *Journal of Clinical Investigation*, vol. 122, no. 11, pp. 4213–4217, 2012.
- [11] F. Y. Sun and X. Guo, “Molecular and cellular mechanisms of neuroprotection by vascular endothelial growth factor,” *Journal of Neuroscience Research*, vol. 79, no. 1-2, pp. 180–184, 2005.
- [12] A. G. Elnahry, A. A. Abdel-Kader, K. A. Raafat, and K. Elrakhawy, “Evaluation of the effect of repeated intravitreal bevacizumab injections on the macular microvasculature of a diabetic patient using optical coherence tomography angiography,” *Case Reports in Ophthalmological Medicine*, vol. 2019, Article ID 3936168, 2019.
- [13] K. Manousaridis and J. Talks, “Macular ischaemia: a contraindication for anti-VEGF treatment in retinal vascular disease?,” *British Journal of Ophthalmology*, vol. 96, no. 2, pp. 179–184, 2012.
- [14] M. I. Dorrell, E. Aguilar, L. Schepke, F. H. Barnett, and M. Friedlander, “Combination angiostatic therapy completely inhibits ocular and tumor angiogenesis,” *Proceedings of the National Academy of Sciences*, vol. 104, no. 3, pp. 967–972, 2007.
- [15] F. Baffert, T. Le, B. Sennino et al., “Cellular changes in normal blood capillaries undergoing regression after inhibition of VEGF signaling,” *American Journal of Physiology-Heart and Circulatory Physiology*, vol. 290, no. 2, pp. H547–H559, 2006.
- [16] R. Rajendram, S. Fraser-Bell, A. Kaines et al., “A 2-year prospective randomized controlled trial of intravitreal bevacizumab or laser therapy (BOLT) in the management of diabetic macular edema: 24-month data: report 3,” *Archives of Ophthalmology*, vol. 130, no. 8, pp. 972–979, 2012.
- [17] M. Michaelides, A. Kaines, R. D. Hamilton et al., “A prospective randomized trial of intravitreal bevacizumab or laser therapy in the management of diabetic macular edema (BOLT study) 12-month data: report 2,” *Ophthalmology*, vol. 117, no. 6, pp. 1078–1086.e2, 2010.
- [18] M. Michaelides, S. Fraser-Bell, R. Hamilton et al., “Macular perfusion determined by fundus fluorescein angiography at the 4-month time point in a prospective randomized trial of intravitreal bevacizumab or laser therapy in the management of diabetic macular edema (BOLT Study): Report 1,” *Retina*, vol. 30, no. 5, pp. 781–786, 2010.
- [19] N. Feucht, E. M. Schönbach, I. Lanzl, K. Kotliar, C. P. Lohmann, and M. Maier, “Changes in the foveal microstructure after intravitreal bevacizumab application in patients with retinal vascular disease,” *Clinical Ophthalmology*, vol. 7, pp. 173–178, 2013.
- [20] N. Erol, H. Gursoy, S. Kimyon, S. Topbas, and E. Colak, “Vision, retinal thickness, and foveal avascular zone size after intravitreal bevacizumab for diabetic macular edema,” *Advances in Therapy*, vol. 29, no. 4, pp. 359–369, 2012.
- [21] P. A. Campochiaro, C. C. Wykoff, H. Shapiro, R. G. Rubio, and J. S. Ehrlich, “Neutralization of vascular endothelial growth factor slows progression of retinal nonperfusion in patients with diabetic macular edema,” *Ophthalmology*, vol. 121, no. 9, pp. 1783–1789, 2014.
- [22] C. C. Wykoff, C. Shah, D. Dhoot et al., “Longitudinal retinal perfusion status in eyes with diabetic macular edema receiving intravitreal aflibercept or laser in VISTA study,” *Ophthalmology*, vol. 126, no. 8, pp. 1171–1180, 2019.
- [23] T. S. Hwang, S. S. Gao, L. Liu et al., “Automated quantification of capillary nonperfusion using optical coherence tomography angiography in diabetic retinopathy,” *JAMA Ophthalmology*, vol. 134, no. 4, pp. 367–373, 2016.
- [24] A. Ishibazawa, T. Nagaoka, A. Takahashi et al., “Optical coherence tomography angiography in diabetic retinopathy: a prospective pilot study,” *American Journal of Ophthalmology*, vol. 160, no. 1, 2015.
- [25] J. M. Garcia, T. T. Lima, R. N. Louzada, A. T. Rassi, D. L. Isaac, and M. Avila, “Diabetic macular ischemia diagnosis: comparison between optical coherence tomography angiography and fluorescein angiography,” *Journal of Ophthalmology*, vol. 2016, 2016.
- [26] A. G. Elnahry and D. J. Ramsey, “Automated image alignment for comparing microvascular changes detected by fluorescein angiography and optical coherence tomography angiography in diabetic retinopathy,” *Seminars in Ophthalmology*, 2021.
- [27] A. Rabiolo, F. Gelormini, R. Sacconi et al., “Comparison of methods to quantify macular and peripapillary vessel density in optical coherence tomography angiography,” *PLoS One*, vol. 13, no. 10, 2018.
- [28] J. Lei, M. K. Durbin, Y. Shi et al., “Repeatability and reproducibility of superficial macular retinal vessel density measurements using optical coherence tomography angiography en face images,” *JAMA Ophthalmology*, vol. 135, no. 10, pp. 1092–1098, 2017.
- [29] M. Al-Sheikh, T. C. Tepelus, T. Nazikyan, and S. R. Sadda, “Repeatability of automated vessel density measurements using optical coherence tomography angiography,” *British Journal of Ophthalmology*, vol. 101, no. 4, pp. 449–452, 2017.
- [30] N. Eladawi, M. Elmogy, O. Helmy et al., “Automatic blood vessels segmentation based on different retinal maps from OCTA scans,” *Computers in Biology and Medicine*, vol. 89, pp. 150–161, 2017.

- [31] A. Y. Kim, Z. Chu, A. Shahidzadeh, R. K. Wang, C. A. Puliafito, and A. H. Kashani, "Quantifying microvascular density and morphology in diabetic retinopathy using spectral-domain optical coherence tomography angiography," *Investigative Ophthalmology & Visual Science*, vol. 57, no. 9, 2016.
- [32] K. Ghasemi Falavarjani, N. A. Iafe, J. P. Hubschman, I. Tsui, S. R. Sadda, and D. Sarraf, "Optical coherence tomography angiography analysis of the foveal avascular zone and macular vessel density after anti-VEGF therapy in eyes with diabetic macular edema and retinal vein occlusion," *Investigative Ophthalmology & Visual Science*, vol. 58, no. 1, pp. 30–34, 2017.
- [33] O. A. Sorour, A. S. Sabrosa, A. Yasin Alibhai et al., "Optical coherence tomography angiography analysis of macular vessel density before and after anti-VEGF therapy in eyes with diabetic retinopathy," *International Ophthalmology*, vol. 39, no. 10, pp. 2361–2371, 2019.
- [34] Y. T. Hsieh, M. N. Alam, D. Le et al., "OCT angiography biomarkers for predicting visual outcomes after ranibizumab treatment for diabetic macular edema," *Ophthalmology Retina*, vol. 3, no. 10, pp. 826–834, 2019.
- [35] F. F. Conti, W. Song, E. B. Rodrigues, and R. P. Singh, "Changes in retinal and choriocapillaris density in diabetic patients receiving anti-vascular endothelial growth factor treatment using optical coherence tomography angiography," *International Journal of Retina and Vitreous*, vol. 5, no. 1, 2019.
- [36] K. Michalska-Malecka and K. A. Heinke, "Optical coherence tomography angiography in patients with diabetic retinopathy treated with anti-VEGF intravitreal injections: case report," *Medicine (Baltimore)*, vol. 96, no. 45, 2017.
- [37] Z. Zhu, Y. Liang, B. Yan et al., "Clinical effect of conbercept on improving diabetic macular ischemia by OCT angiography," *BMC Ophthalmology*, vol. 20, no. 1, 2020.
- [38] R. Mirshahi, K. G. Falavarjani, S. Molaei et al., "Macular microvascular changes after intravitreal bevacizumab injection in diabetic macular edema," *Canadian Journal of Ophthalmology*, vol. 56, no. 1, pp. 57–65, 2020.
- [39] A. Couturier, P. A. Rey, A. Erginay et al., "Widefield OCT-angiography and fluorescein angiography assessments of non-perfusion in diabetic retinopathy and edema treated with anti-vascular endothelial growth factor," *Ophthalmology*, vol. 126, no. 12, pp. 1685–1694, 2019.
- [40] A. G. Elnahry, A. A. Abdel-Kader, K. A. Raafat, and K. Elrakhawy, "Evaluation of changes in macular perfusion detected by optical coherence tomography angiography following 3 intravitreal monthly bevacizumab injections for diabetic macular edema in the IMPACT study," *Journal of Ophthalmology*, vol. 2020, Article ID 5814165, 2020.
- [41] F. Pereira, B. R. Godoy, M. Maia, and C. V. Regatieri, "Microperimetry and OCT angiography evaluation of patients with ischemic diabetic macular edema treated with monthly intravitreal bevacizumab: a pilot study," *International Journal of Retina and Vitreous*, vol. 5, no. 1, 2019.
- [42] A. Barash, T. Y. P. Chui, P. Garcia, and R. B. Rosen, "Acute macular and peripapillary angiographic changes with intravitreal injections," *Retina*, vol. 40, no. 4, pp. 648–656, 2020.
- [43] B. Statler, T. F. Conti, F. F. Conti et al., "Twenty-four-month OCTA assessment in diabetic patients undergoing fixed-interval intravitreal aflibercept therapy," *Ophthalmic Surgery, Lasers and Imaging Retina*, vol. 51, no. 8, pp. 448–455, 2020.
- [44] C. Golshani, T. F. Conti, F. F. Conti et al., "Diabetic macular edema treated with intravitreal aflibercept injection after treatment with other anti-VEGF agents (SWAP-TWO study)—12-month analysis," *Journal of VitreoRetinal Diseases*, vol. 4, no. 5, pp. 364–371, 2020.
- [45] C. Busch, T. Wakabayashi, T. Sato et al., "Retinal microvasculature and visual acuity after intravitreal aflibercept in diabetic macular edema: an optical coherence tomography angiography study," *Scientific Reports*, vol. 9, no. 1, 2019.
- [46] A. Dastiridou, K. Karathanou, P. Riga et al., "OCT angiography study of the macula in patients with diabetic macular edema treated with intravitreal aflibercept," *Ocular Immunology and Inflammation*, pp. 1–6, 2020.
- [47] C. C. Wykoff, M. G. Nittala, B. Zhou et al., "Intravitreal Aflibercept for Retinal Nonperfusion in Proliferative Diabetic Retinopathy Study Group. Intravitreal aflibercept for retinal nonperfusion in proliferative diabetic retinopathy: outcomes from the randomized recovery trial," *Ophthalmology Retina*, vol. 3, no. 12, pp. 1076–1086, 2019.
- [48] S. Bonnin, B. Dupas, C. Lavia et al., "Anti-vascular endothelial growth factor therapy can improve diabetic retinopathy score without change in retinal perfusion," *Retina*, vol. 39, no. 3, pp. 426–434, 2019.
- [49] N. Figueiredo, S. K. Srivastava, R. P. Singh et al., "Longitudinal panretinal leakage and ischemic indices in retinal vascular disease after aflibercept therapy: the PERMEATE study," *Ophthalmology Retina*, vol. 4, no. 2, pp. 154–163, 2020.
- [50] A. G. Elnahry, A. A. Abdel-Kader, A. E. Habib, G. A. Elnahry, K. A. Raafat, and K. Elrakhawy, "Review on recent trials evaluating the effect of intravitreal injections of anti-VEGF agents on the macular perfusion of diabetic patients with diabetic macular edema," *Reviews on Recent Clinical Trials*, vol. 15, no. 3, pp. 188–198, 2020.
- [51] A. Gill, E. D. Cole, E. A. Novais et al., "Visualization of changes in the foveal avascular zone in both observed and treated diabetic macular edema using optical coherence tomography angiography," *International Journal of Retina and Vitreous*, vol. 3, 2017.
- [52] R. F. Spaide, J. G. Fujimoto, N. K. Waheed, S. R. Sadda, and G. Staurenghi, "Optical coherence tomography angiography," *Progress in Retinal and Eye Research*, vol. 64, pp. 1–55, 2018.
- [53] R. F. Spaide, J. G. Fujimoto, and N. K. Waheed, "Image artifacts in optical coherence tomography angiography," *Retina*, vol. 35, no. 11, pp. 2163–2180, 2015.
- [54] R. F. Spaide, J. M. Klancnik Jr., and M. J. Cooney, "Retinal vascular layers imaged by fluorescein angiography and optical coherence tomography angiography," *JAMA Ophthalmology*, vol. 133, no. 1, pp. 45–50, 2015.
- [55] A. G. Elnahry and D. J. Ramsey, "Optical coherence tomography angiography imaging of the retinal microvasculature is unimpeded by macular xanthophyll pigment," *Clinical & Experimental Ophthalmology*, vol. 48, no. 7, pp. 1012–1014, 2020.
- [56] A. M. Mansour, A. G. Elnahry, K. Tripathy et al., "Analysis of optical coherence angiography in cystoid macular oedema associated with gyrate atrophy," *Eye*, 2020.
- [57] A. Couturier, V. Mané, S. Bonnin et al., "Capillary plexus anomalies in diabetic retinopathy on optical coherence tomography angiography," *Retina*, vol. 35, no. 11, pp. 2384–2391, 2015.
- [58] M. Viswanathan and N. D. Berkman, *Development of the RTI Item Bank on Risk of Bias and Precision of Observational*

- Studies Methods research report*, Prepared by the RTI International–University of North Carolina Evidence-based Practice Center under Contract No. 290-2007-0056-I AHRQ Publication No. 11-EHC028-EF, Rockville, MD: Agency for Healthcare Research and Quality, 2011, <http://www.effectivehealthcare.ahrq.gov/reports/final.cfm>.
- [59] R. Rosen, J. S. Romo, M. V. Toral et al., “Reference-based OCT angiography perfusion density mapping for identifying acute and chronic changes in eyes with retinopathy over time,” *Invest Ophthalmol Vis Sci*, vol. 60, no. 11, 2019.
- [60] M. J. Tolentino, J. W. Miller, E. S. Gragoudas et al., “Intravitreal injections of vascular endothelial growth factor produce retinal ischemia and microangiopathy in an adult primate,” *Ophthalmology*, vol. 103, no. 11, pp. 1820–1828, 1996.
- [61] P. Hofman, B. C. van Blijswijk, P. J. Gaillard, G. F. Vrensen, and R. O. Schlingemann, “Endothelial cell hypertrophy induced by vascular endothelial growth factor in the retina: new insights into the pathogenesis of capillary nonperfusion,” *Archives of Ophthalmology*, vol. 119, no. 6, pp. 861–866, 2001.
- [62] M. M. Kurt, O. Çekiç, Ç. Akpolat, and M. Elçioglu, “Effects of intravitreal ranibizumab and bevacizumab on the retinal vessel size in diabetic macular edema,” *Retina*, vol. 38, no. 6, pp. 1120–1126, 2018.
- [63] X. Zhu, S. Wu, W. L. Dahut, and C. R. Parikh, “Risks of proteinuria and hypertension with bevacizumab, an antibody against vascular endothelial growth factor: systematic review and meta-analysis,” *American Journal of Kidney Diseases*, vol. 49, no. 2, pp. 186–193, 2007.
- [64] P. Bonnin, J. A. Pournaras, Z. Lazrak et al., “Ultrasound assessment of short-term ocular vascular effects of intravitreal injection of bevacizumab (Avastin®) in neovascular age-related macular degeneration,” *Acta Ophthalmologica*, vol. 88, no. 6, pp. 641–645, 2010.
- [65] L. E. Benjamin, I. Hemo, and E. Keshet, “A plasticity window for blood vessel remodelling is defined by pericyte coverage of the preformed endothelial network and is regulated by PDGF-B and VEGF,” *Development*, vol. 125, no. 9, pp. 1591–1598, 1998.
- [66] P. Lindahl, B. R. Johansson, P. Levéen, and C. Betsholtz, “Pericyte loss and microaneurysm formation in PDGF-B-deficient mice,” *Science*, vol. 277, no. 5323, pp. 242–245, 1997.
- [67] A. W. Stitt, T. A. Gardiner, and D. B. Archer, “Histological and ultrastructural investigation of retinal microaneurysm development in diabetic patients,” *British Journal of Ophthalmology*, vol. 79, no. 4, pp. 362–367, 1995.
- [68] V. Mané, B. Dupas, A. Gaudric et al., “Correlation between cystoid spaces in chronic diabetic macular edema and capillary nonperfusion detected by optical coherence tomography angiography,” *Retina*, vol. 36, Supplement 1, pp. S102–S110, 2016.
- [69] M. Parravano, E. Costanzo, E. Borrelli et al., “Appearance of cysts and capillary non perfusion areas in diabetic macular edema using two different OCTA devices,” *Scientific Reports*, vol. 10, no. 1, p. 800, 2020.
- [70] T. E. de Carlo, A. T. Chin, T. Joseph et al., “Distinguishing diabetic macular edema from capillary nonperfusion using optical coherence tomography angiography,” *Ophthalmic Surgery, Lasers and Imaging Retina*, vol. 47, no. 2, pp. 108–114, 2016.
- [71] A. R. Alagorie, M. G. Nittala, S. Velaga et al., “Association of intravitreal aflibercept with optical coherence tomography angiography vessel density in patients with proliferative diabetic retinopathy: a secondary analysis of a randomized clinical trial,” *JAMA Ophthalmology*, vol. 138, no. 8, pp. 851–857, 2020.
- [72] E. J. Chung, M. I. Roh, O. W. Kwon, and H. J. Koh, “Effects of macular ischemia on the outcome of intravitreal bevacizumab therapy for diabetic macular edema,” *Retina*, vol. 28, no. 7, pp. 957–963, 2008.

Research Article

Behavior of SD-OCT Detectable Hyperreflective Foci in Diabetic Macular Edema Patients after Therapy with Anti-VEGF Agents and Dexamethasone Implants

Anne Rübsam ^{1,2}, Laura Wernecke,¹ Saskia Rau,¹ Dominika Pohlmann,^{1,2} Bert Müller,¹ Oliver Zeitz,^{1,2} and Antonia M. Jousen^{1,2}

¹Department of Ophthalmology, Charité Universitätsmedizin Berlin, Corporate Member of Freie Universität Berlin, Humboldt-Universität zu Berlin and Berlin Institute of Health, Germany

²Berlin Institute of Health (BIH), Berlin, Germany

Correspondence should be addressed to Anne Rübsam; anne.ruebsam@charite.de

Received 29 September 2020; Revised 16 March 2021; Accepted 27 March 2021; Published 14 April 2021

Academic Editor: Hiroshi Okamoto

Copyright © 2021 Anne Rübsam et al. This is an open access article distributed under the Creative Commons Attribution License, which permits unrestricted use, distribution, and reproduction in any medium, provided the original work is properly cited.

Purpose. Diabetic macular edema (DME) is the most common cause of blindness in the working-age population. Spectral-domain optical coherence tomography (SD-OCT) allows detection and monitoring of the edema and a detailed analysis of the retinal structure. Hyperreflective foci (HF) are small, circumscribed lesions on OCT, and their origin is yet to be determined. Our study was aimed to shed light on HF pathophysiology, by analyzing their number and location in DME patients at baseline and after therapy. **Methods.** A prospective, observational study on 59 eyes of 51 DME patients who were treated with anti-vascular endothelial growth factor (VEGF) therapy (VEGF group, $n = 40$ eyes) or dexamethasone implant (DEX group, $n = 19$). HF and hard exudates (HE) were discriminated by their appearance on fundus photographs and their size on OCT. Quantity and location of HF and HE were analyzed at baseline and after therapy. **Results.** DME decreased in 75% of patients in the VEGF (455.5 μm vs. 380.8 μm , $p = 0.02$) and in 95% of patients in the DEX group (471.6 μm vs. 381.9 μm , $p = 0.007$). The number of foci decreased in 62.5% of patients after anti-VEGF (130.6 vs. 111.1, $p = 0.07$) and in 68% of patients after dexamethasone injection ((123.4 vs. 94.9, $p = 0.02$) 5.1). A subgroup of 15% of eyes, all treated with anti-VEGF, showed accumulation of larger HF in outer retinal layers to visible HE during DME resolution, whereas smaller HF, found in all retinal layers, remained unchanged. There was a trend towards a dynamic shift of the foci from inner to outer retinal layers. **Conclusion.** The dynamic rearrangement of the small HF and their slightly greater reduction after anti-inflammatory therapy suggest inflammatory cells as their origin, whereas larger HF in the outer retinal layers correspond to microexudates. Furthermore, we found a more favourable outcome in patients with HF after treatment with dexamethasone implants compared to anti-VEGF agents.

1. Introduction

Diabetic macular edema (DME), a common complication of diabetes, is the primary cause of visual impairment in the working-age population of the Western world [1]. Clinical evidence indicates that there is a combination of capillary occlusion and an increased capillary permeability in DME. The ability of vascular endothelial growth factor (VEGF), to promote both vascular permeability and angiogenesis, made it a likely contributor to the vascular dysfunctions observed in DME [2, 3]. Although significant success could be demon-

strated with anti-VEGF therapy, a number of limitations exist: ranging from the need for repeated intraocular injections; the socioeconomic burden of the repeated therapy; and most importantly, the fact that only approximately half of the patients show a reduction of DME after anti-VEGF therapy [4].

In the past decade, varieties of physiologic and molecular changes consistent with a role of inflammation have been found in the retinas or vitreous humor of diabetic animals and patients [5–11]. While the detailed mechanisms and their contribution to pathologies observed in diabetic retinopathy

(DR) remain to be specified, these inflammatory changes seem to play a key important role in the development of DR and DME, as their inhibition has been shown to impact the development of retinal alterations in animal models of diabetes [12]. Studies using anti-inflammatory agents such as salicylates or minocycline in patients with DR gave further evidence that regulating the inflammatory response has a potentially beneficial effect, by preventing irreversible vascular and neuronal perturbations over time [13]. Dexamethasone (DEX) intravitreal implant (Ozurdex[®]) has been shown to be effective in the treatment of DME, with an improvement in visual acuity (VA) and a decrease in retinal thickness [14–16], even in eyes with DME refractory to anti-VEGF [15, 16]. Furthermore, as for anti-VEGF therapies [17], delay of progression and even improvement of diabetic retinopathy severity have been shown after therapy with DEX implants [18].

Recently, several authors identified baseline spectral-domain optical coherence tomography (SD-OCT) measures which can serve as biomarkers for predicting VA outcome after treatment for DME, either with DEX implants [19, 20] or anti-VEGF therapies [21–23]. The presence of subretinal fluid (SRF), continuity of the inner segment/outer segment (IS/OS) line, and the absence of HF predict better visual outcomes after treatment in eyes with DME [19, 20, 24]. Furthermore, the absence of HFs led to significantly greater VA improvement and a greater reduction in central retinal thickness (CRT) after anti-VEGF therapy [22]. HF are discrete, well-circumscribed, intraretinal lesions with greater reflectivity than the retinal pigment epithelium (RPE) band on SD-OCT [25]. The role of HF has also been investigated in several other neurovascular disorders like retinitis pigmentosa [26], retinal vein occlusion [27], morbus coats [28], and age-related macular degeneration (AMD) [29]. The exact origin of these foci is yet to be determined. They may represent subclinical features of lipoprotein extravasation after the breakdown of the inner blood-retinal barrier (BRB), which form visible hard exudates at later stages of the disease [30] and/or represent activated inflammatory cells such as microglia [31–33] or migrating RPE cells (in AMD only) [25].

The purpose of this study was to gain more insight into the pathophysiology of HF. This was done through analyzing the quantity and location of retinal HF at baseline and after therapy with one intravitreal injection of an anti-VEGF drug or a dexamethasone implant in DME patients. We hypothesized that primarily anti-inflammatory therapy by dexamethasone should influence HF differently than primarily antiangiogenic therapy by VEGF inhibition.

2. Material and Methods

In this noninterventive, observational, and prospective study, we recruited 59 eyes of 51 consecutive patients affected by type 2 diabetes. They were all treated at the Retina Service of the Department of Ophthalmology, Charité Universitätsmedizin Berlin, between September 2018 and June 2019. All the research and measurements adhered to the tenets of the Declaration of Helsinki; the local ethics committee approved the study. Informed consent was given by the patients via prior study enrollment.

The inclusion criteria was those aged 18 years or older with the presence of a fovea involving clinically significant DME, which necessitates DME therapy with one of the three currently available anti-VEGF agents (VEGF group): bevacizumab (Avastin[®]), ranibizumab (Lucentis[®]), aflibercept (Eylea[®]), or the intravitreal injection of a Dexamethasone Implant (Ozurdex[®], DEX group). Patients were not randomized, but prospectively included based on their treatment (either VEGF or DEX group). Treatment modality was chosen at the discretion of the treating retina specialist.

The exclusion criteria were the presence of significant media opacities and severe visual impairment leading to low-quality SD-OCT images, planned retinal laser treatment or intraocular surgery within the follow-up period or within the past 3 months, a refractive error greater than minus 5 diopters, and a sign of any other active retinal disease in the study eye (including the presence of an epiretinal membrane or vitreomacular traction syndrome).

2.1. Patient Data. Baseline diagnostic procedures included a best-corrected visual acuity (BCVA) assessment in Logarithm of the Minimum Angle of Resolution (logMAR), anterior and posterior segment examination, SD-OCT (Heidelberg Spectralis, Heidelberg Engineering, Heidelberg, Germany), fluorescein angiography (FA, Heidelberg Spectralis, Heidelberg Engineering, Heidelberg, Germany), color fundus photography (CFP, Zeiss Mediatec, Jena, Germany), and OCT-angiography (OCTA, Heidelberg Engineering, Heidelberg, Germany). We performed follow-up examinations including SD-OCT and CFP 15 days after the anti-VEGF injection. Another follow-up visit with SD-OCT and CFP assessment and visual acuity testing was conducted 30 days after the intravitreal anti-VEGF injection and 30 days after the injection of the intravitreal dexamethasone implant (Ozurdex[®]). We chose a follow-up interval of 30 days for Ozurdex[®], because the maximum reduction of the CRT after the injection is detectable 30 days after treatment [34].

2.2. OCT Data. Standard settings for OCT recordings were 20° × 20° volume scan, 49 sections at a distance of 122 μm. Central retinal thickness (CRT) in μm was automatically calculated by the device software (software version 5.1.2.0), as the distance from the RPE to the inner limiting membrane (ILM) at the highest point within a circle of 1 mm radius, centered on the fovea. We also assessed the disruption of the junction between the photoreceptor inner and outer segments (IS/OS line). An intact IS/OS line was defined as a continuous hyperreflective line on each OCT scan and a disrupted IS/OS line as the loss or discontinuity of the hyperreflective line, if present, in any of the 49 scans.

Two masked, independent investigators (LW and SR) manually counted the HF within each scan. HF were defined as discrete and well-circumscribed dots of identical reflectivity as the RPE band. The largest diameter of small HF (also referred to as hyperreflective dots) was limited to 30 μm. Additional larger foci with a diameter of >30 μm could be identified in a subset of patients. By utilizing these size criteria, we excluded small noise signals and large hyperreflective clumps, which are detectable as hard exudates on

fundus photography. The total number of HF in each scan was counted, as well as the number of foci within the inner (from the ILM to inner nuclear layer, INL) and outer (outer plexiform layer, OPL to the RPE) retinal layers.

The eyes of the DME patients were further classified into two groups according to their pattern of edema. Focal edema was defined as a localized retinal fluid collection, mostly in the outer retinal layers (also referred to as outer retinal edema), contrary to a diffuse cystoid or noncystoid retinal thickening, derived from breakdown of the inner blood-retinal barrier. FA was performed for evaluation of retinal ischemia and vascular leakage.

2.3. Color Fundus Photography. Each OCT image with a hyperreflective focus was overlaid with a corresponding CFP and with the corresponding red-free image that is available for tracking on the Heidelberg Spectralis device, using the device software. For each HF on SD-OCT, we thereby ruled out other causes of hyperreflectivity such as microaneurysms, haemorrhages, cotton wool spots, retinal vessels, and hard exudates. All of which are visible on CFPs and/or near-infrared images. If any of these were found to account for the HF, these foci were excluded from the analysis.

2.4. Optical Coherence Tomography Angiography. For the OCTA examinations, 70,000 A-Scans were made and a $15 \times 15^\circ$ scan angle protocol was used to gain a total of 261 B-scans, resulting in images with an axial resolution of approximately $4 \mu\text{m}$. This was within the B-scan resolution of approximately $11 \mu\text{m}$ and between the B-scan resolution of approximately also $11 \mu\text{m}$. The standard OCTA viewing module 6.9.5.0 and a manual segmentation of the retinal layers was used for the evaluation of the qualitative relationship between HF on B-scan OCT images and the retinal vasculature on en face OCTA images. Instead of using the program's predefined automated segmentation, we manually selected the thickness of the vascular slab to be displayed exactly at the border of the foci to display only blood vessels adjacent to the HF. To do so, we manually moved the two depicted dashed red lines in the Angio mode B-scan, which indicate the vascular slab to be displayed at the corresponding two-dimensional en face OCTA image (with transversal slab orientation), to the border of the HF (Figure 1). The corresponding area in the en face OCTA image was then compared to the OCT scan and analyzed for the overlay of the HF with vasculature.

2.5. Statistical Analysis. The means \pm SEM and statistically significant differences are reported. The correlation between the baseline characteristics and between the baseline and the follow-up visit were calculated with Pearson's correlation coefficient r based on the assumption of a Gaussian distribution. The differences in the parameters between the baseline and final visit were evaluated using a two-tailed t -test. A p value inferior to 0,05 was considered significant. The statistical analysis, except for the kappa coefficient, was performed using GraphPad Prism (GraphPad Software, San Diego, CA, USA). Calculation of the intraclass correlation coefficient (Cohen's kappa), for evaluation of interobserver con-

cordance of HF counting was performed using SPSS (IBM Software, Armonk, New York, USA), based on a mean rating ($k = 2$), absolute agreement, and 2-way mixed effects model.

3. Results

3.1. Baseline. The baseline characteristics of the subjects are listed in Table 1. The patients' mean age was 58.9 ± 8 years. Although DME occurred during all DR stages, more than half of the study patients had a proliferative stage. Of note, almost all DME patients with HF presented with a diffuse retinal thickening. Disruption of the IS/OS line was present in 7/59 eyes (12%) at the baseline visit. The numbers of HF ranged from 17 to 375 foci per eye at baseline (mean 131.1 ± 103). There was an excellent interrater agreement (0.938) regarding the number of counted HF.

The baseline HF number was positively correlated with the baseline CRT ($r = 0.535$, $p < 0.001$), but no significant correlation was found between the baseline presence of foci and the disruption of the IS/OS line, the DME type or DR stage at baseline, and in regard to the final number of HF and final CRT. The number of baseline HF further significantly correlated with baseline VA ($r = 0.502$, $p < 0.001$) and final VA ($r = 0.398$, $p = 0.003$). There was no difference regarding the distribution of foci and their impact on visual acuity as both, inner retinal layer and outer retinal layer HF, correlated significantly with baseline and final VA (IRL foci: $r = 0.391$, $p = 0.003$ for baseline VA and $r = 0.351$, $p = 0.008$ for final VA; ORL foci: $r = 0.493$, $p = 0.001$ for baseline VA and $r = 0.356$, $p = 0.007$ for final VA).

OCT imaging demonstrated that 64% hyperreflective foci (large and small) were deposited in the outer retinal layers (OPL to RPE, Figure 1), mostly adjacent to cystoid spaces. The other 36% foci, all fine hyperreflective dots, were found to be randomly deposited in the inner retinal layers (ILM to INL, Figure 2(b)). Hard exudates were found only in the outer retinal layers (Figure 2(e)). A comparative analysis of HF on SD-OCT and corresponding OCTA scans revealed that HF were associated with blood vessels depending on their location within the retina. Whereas inner retinal layer foci were elusively attached to vessels of the superficial capillary plexus, we found outer retinal layer foci that are attached to the wall of cystoid spaces, in areas without any sign of vascularization on OCTA (Figure 2(c)). Hard exudates that are located between the IPL and the OPL were attached to vessels of the deep capillary plexus on OCTA (Figure 2(f)).

DME: diabetic macular edema; IS/OS: inner segment/outer segment; NPDR: nonproliferative diabetic retinopathy; PDR: proliferative diabetic retinopathy.

3.2. Follow-Up. After therapy, the overall mean CRT decreased significantly from $414.2 \pm 79 \mu\text{m}$ to $378.4 \pm 76 \mu\text{m}$ ($p < 0.001$). The overall mean number of foci decreased from 131.7 ± 103 to 115.6 ± 100 ($p = 0.004$). The mean number of HE remained unchanged after treatment (13.9 ± 18 to 13.1 ± 16 , $p = 0.223$). The mean BCVA also remained unchanged (0.41 ± 0.31 to 0.41 ± 0.31 , $p = 0.929$).

3.3. Central Retinal Thickness. In the VEGF group, mean CRT decreased significantly from baseline to day 15 ($p = 0.001$) and

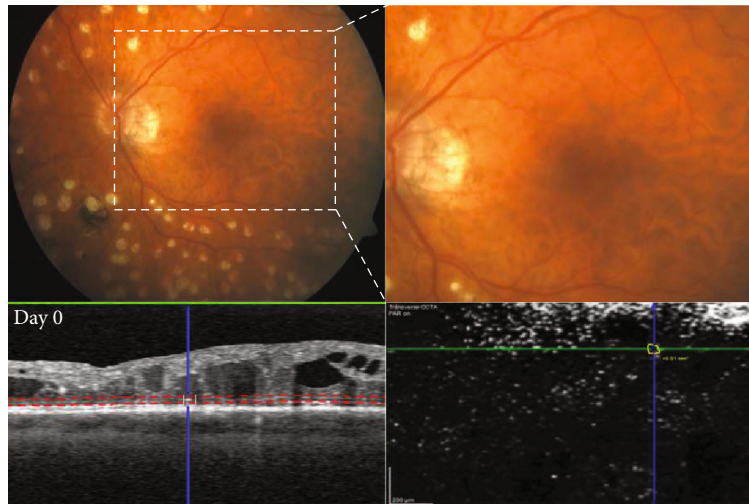


FIGURE 1: Multimodal imaging of a nonvascularized outer retinal layer (ORL) hyperreflective foci (HF). Figure shows the distribution of a HF in a 42-year-old patient with proliferative diabetic retinopathy (PDR) at baseline. Upper panel: HF in the absence of any visible HE on corresponding color fundus photographs (CFP) could be detected. Higher magnification image of the macular area marked with a dashed square. Lower panel: visualization of an outer nuclear layer HF adjacent to a cystoid space on optical coherence tomography (OCT) B-scan with manual segmentation of the vascular slabs of this region visualized as dashed red lines (left). Corresponding en face OCT-angiography (OCTA, right) image of the manually outlined vascular slab confirms, which the HF is not attached to blood vessels. HF border is outlined in yellow and area in mm^2 is calculated by the device software.

TABLE 1: Baseline characteristics of 40 diabetic study patients.

No. of eyes (patients)	59 (51)
Male/female	39/12
Age, years	58,9 (± 8)
Diabetic retinopathy stage	
Mild NPDR	7
Moderate NPDR	11
Severe NPDR	16
PDR	25
Intravitreal medication	
Bevacizumab	19
Ranibizumab	10
Aflibercept	11
Dexamethasone	19
DME type	
Focal	8
Diffuse:	51
Central retinal thickness, μm	414.2 (± 79.8)
No. hyperreflective foci	131.1 (± 103)
No. hard exudates	13.9 (± 18)
IS/OS disruption	
Yes	7
No	52

decreased further significantly to day 30 ($p = 0.021$). In the DEX group, mean CRT also decreased significantly from baseline to day 30 ($p = 0.007$). The details are listed in Table 2 and illustrated in Figure 3. An additional excel file with all patient data, relevant for the analysis, is available as a supplemental file (see Online Resource 1).

There was no difference between patients treated with anti-VEGF and dexamethasone, regarding the reduction of retinal thickness (VEGF group: 12% reduction after 15 days, 17% after 1 month, DEX group: 22% after 1 month). Of note, the percentage of eyes, without any persistent macular fluid or a decreased edema at day 30, was higher when Ozurdex[®] had been injected (Table 3).

3.4. Hyperreflective Foci. In the VEGF group, the mean number of foci decreased only slightly after 15 days ($p = 0.105$). Then, 30 days after the injection, the mean number of foci decreased further, but without statistical significance (130.6 vs. 111.1, $p = 0.062$). In the DEX group, the mean number of foci decreased significantly after 30 days (123.4 vs. 94.9, $p = 0.020$). The details are listed in Table 2 and illustrated in Figure 3.

The percentage of eyes with a reduction of the number of foci at the end at one month was, as for the reduction of the DME, slightly higher in the DEX group (62.5% anti-VEGF vs. 68% for Ozurdex[®], Table 2). In the VEGF group, 75% of the patients with a decreased number of foci had a decreased edema, 10% of patients presented unchanged, and 15% increased macular fluid. Of the 13/19, 68% of eyes in the DEX group had a reduced number of foci; all eyes showed a reduction in CRT, with seven patients having a dry macula 1 month after the treatment. A representative patient of the DEX group is illustrated in Figure 4.

The fine HF were scattered throughout all retinal layers at the follow-up examination, with a trend towards a downward shift of the foci from the inner to the outer retinal layers. Before therapy, the percentage of HF in the inner retinal layers was 34%, and 66% were distributed in the outer retinal layers. After treatment, 6% of the inner retinal layer foci shifted into outer retinal layers (Figure 5).

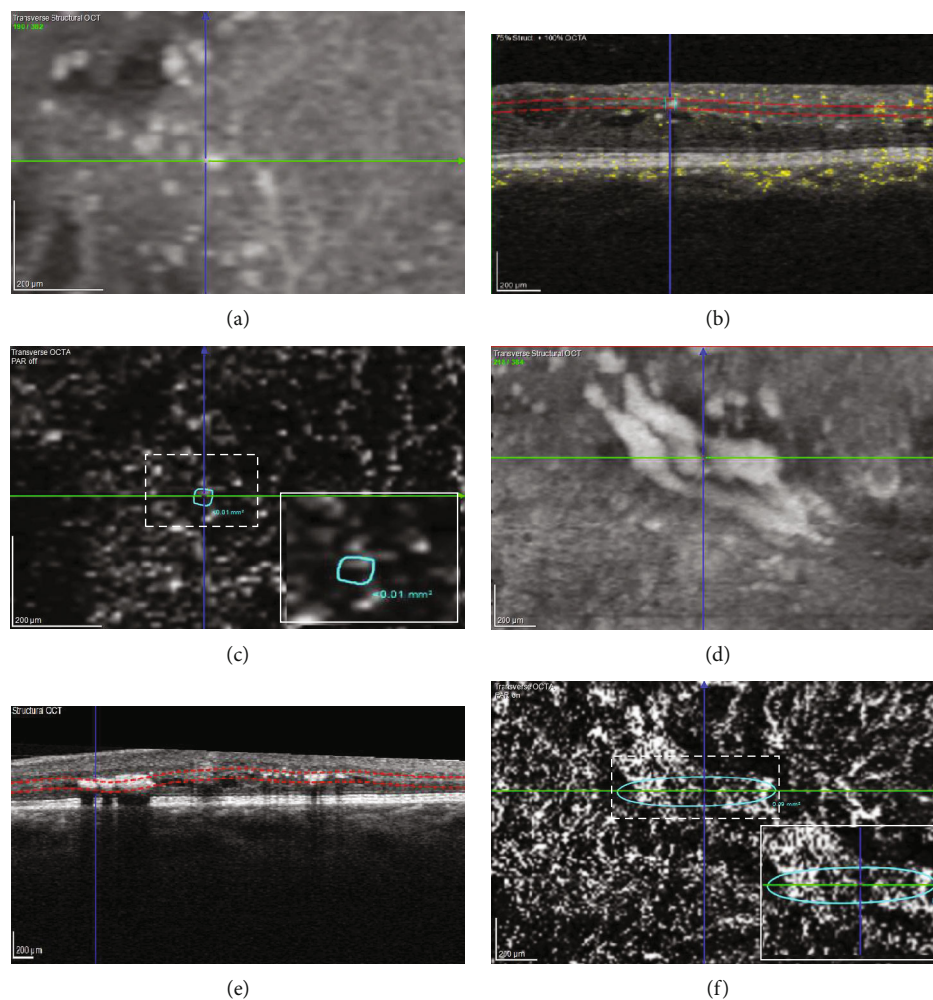


FIGURE 2: Multimodal imaging of vascularized inner retinal layer (IRL) hyperreflective foci (HF) and hard exudates (HE). (a, d) The structural optical coherence tomography (OCT) delineates dot-like HF (a–c) and spot-like HE (d–f) in a 39-year-old patient with mild nonproliferative diabetic retinopathy (NPDR) at baseline. (b, e) B-scan with manual segmentation of the vascular slabs of the region visualized as dashed red line, depicting HF in the inner nuclear layer (INL) and HE in the outer plexiform layer (OPL). (c, f) Corresponding en-face OCT-angiography (OCTA) images of the manually outlined vascular slabs demonstrate HF and HE deposited adjacent to blood vessels. Higher magnification images of the HF and HE are marked by a dash square. Both HF and HE borders are outlined in turquoise, and area in mm^2 is calculated by the device software.

3.5. Hard Exudates. In the VEGF group, the mean number of HE remained unchanged after treatment (17.9 ± 20 to 16.1 ± 19 , $p = 0.223$ after 15 and 13.3 ± 16 , $p = 0.411$ after 30 days). In the DEX group, the mean number of HE also remained unchanged after treatment (4.75 ± 5 to 5.1 ± 8 , $p = 0.562$, Figure 3). A subgroup of 7/46 (15%) of eyes showed an accumulation of visible HE in the OPL during the study period. This was in an area where we detected only larger HF ($>30 \mu\text{m}$) at baseline. All of these patients were treated with anti-VEGF and DME decreased in 71.4% of these patients and remained unchanged or increased in each 14.3% (Figure 6).

4. Discussion

We saw a significant reduction of DME, independent of whether anti-VEGF or dexamethasone had been injected. The number of HF, as well as the number of HE, did not

diminish clearly after either treatment. However, the percentage of eyes with a reduction in the number of foci at the end of the study period was as for the reduction of the CRT, slightly higher in the DEX group. There was also a trend towards a dynamic shift of the foci from the inner to the outer retinal layers. Fifteen percent of eyes showed an accumulation of larger diameter HF to visible HE over time, all treated with anti-VEGF agents, and the conversion of HF to HEs in these patients was independent of the change in macular fluid.

In the literature, various different hypotheses about the origin of HF have emerged that might in fact coexist. HF could be precursors of hard exudates, migrating RPE cells (in AMD), degenerated photoreceptor cells, or aggregations of activated immune cells, such as microglia. Bolz et al. first described such HF in 12 patients with DME using different OCT techniques [30]. These foci were interpreted as the morphologic sign of lipid extravasation obviously forming HEs,

TABLE 2: Mean change in central retinal thickness and number of hyperreflective foci of 51 diabetic study patients at the baseline visit and during follow-up.

Group	Number of eyes (patients) visit 1	Number of eyes (patients) visit 2	Mean CRT + SD at baseline (μm)	Mean CRT + SD at visit 1 (μm) (* <i>p</i> value)	Mean CRT + SD at visit 2 (μm) (* <i>p</i> value)	Mean number of foci + SD at baseline (μm)	Mean number of foci + SD at visit 1 (μm) (* <i>p</i> value)	Mean number of foci + SD at visit 2 (μm) (* <i>p</i> value)
VEGF group	40 (35)	32 (27)	455.5 ± 139	402.5 ± 13 (<i>p</i> = 0.001)	380.8 ± 123 (<i>p</i> = 0.021)	130.6 ± 100	120.2 ± 94 (<i>p</i> = 0.105)	111.1 ± 88 (<i>p</i> = 0.062)
DEX group		19 (16)	471.6 ± 112		381.9 ± 99 (<i>p</i> = 0.007)	123.4 ± 94		94.9 ± 89 (<i>p</i> = 0.020)

CRT: central retinal thickness; SD: standard deviation; visit 1: 15 days; visit 2: 30 days; * two-tailed *t*-test.

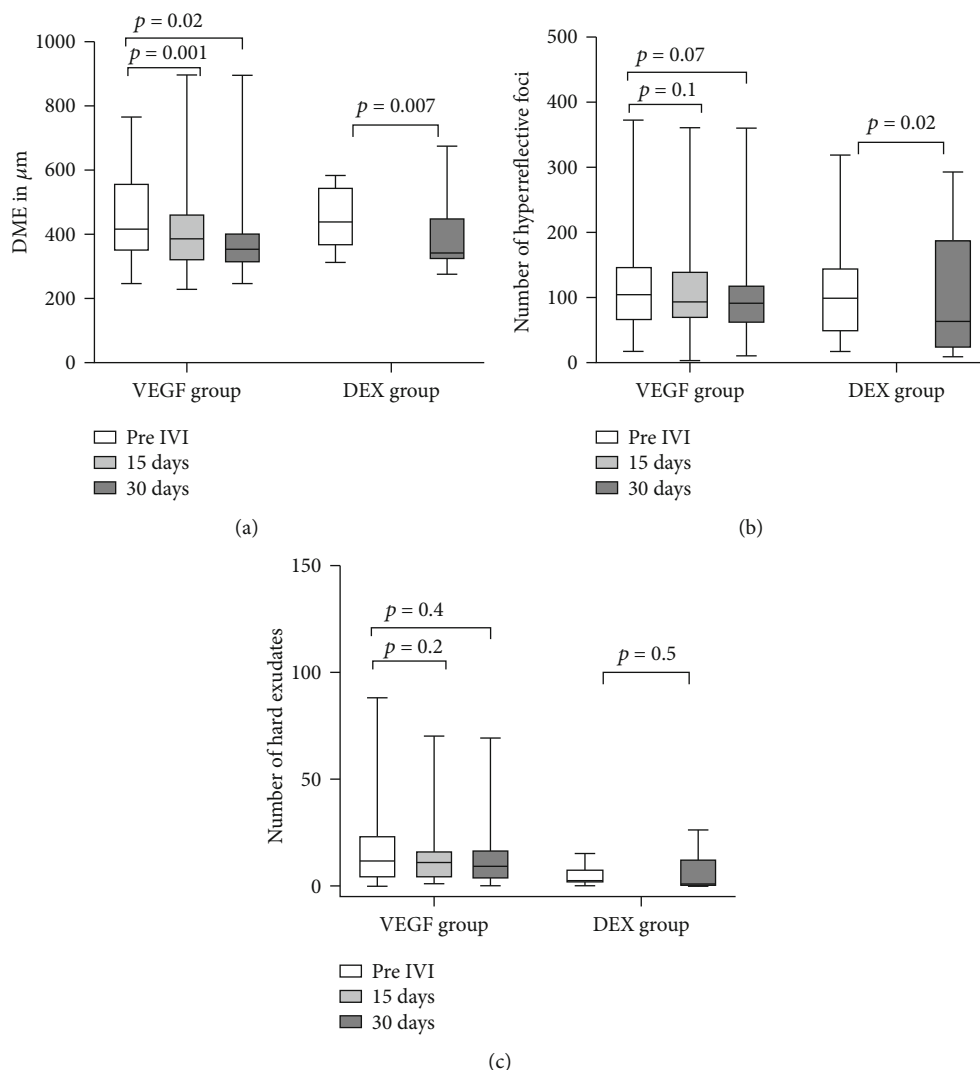


FIGURE 3: Boxplot graph representing changes in central retinal thickness (CRT), number of hyperreflective foci (HF), and number of hard exudates (HE) after anti-VEGF therapy (VEGF group) or dexamethasone implantation (DEX group) in patients with diabetic macular edema (DME). Figure shows the difference in change in (a) CRT in μm (b) number of HF, and (c) number of HE for the VEGF and DEX group at baseline versus 15 or 30 days after the injection.

TABLE 3: Assessment percentage of eyes with a change in macular edema and change in the number of hyperreflective foci at the end of the treatment period.

Group	Macular edema				Number of foci	
	Dry	Decreased	Unchanged	Increased	Decreased	Increased
VEGF group	2/32 (6.25%)	22/32 (68.75%)	4/32 (12.5%)	4/32 (12.5%)	20/32 (62.5%)	12/32 (37.5%)
DEX group	8/19 (42%)	10/19 (53%)	1/19 (5%)	—	13/19 (68%)	6/19 (32%)

and they were not observable in classic examinations such as those using ophthalmoscopy or fundus photographs [30]. Retinal HEs are composed of lipid and proteinaceous material, such as fibrinogen and albumin that leak from the impaired BRB. They are deposited primarily in the OPL of the retina. Pemp et al. also demonstrated subretinal HF on OCT in patients with DME which may be associated with the future subfoveal deposition of HEs [23]. During the three-month treatment period, the HF in 24 eyes with

DME, which were initially distributed through all retinal layers, shifted downwards and formed larger aggregates, although a rapid reduction in DME was seen in all patients [35]. When the aggregates reached a diameter of about 100 μm in SD-OCT, HE appeared at corresponding locations of fundus photographs. A possible source of these deposits was thought to be microaneurysms, and the larger a vessel was in diameter, the more deposits could be observed at the vessel wall [23]. Similarly, in our study of a subgroup of

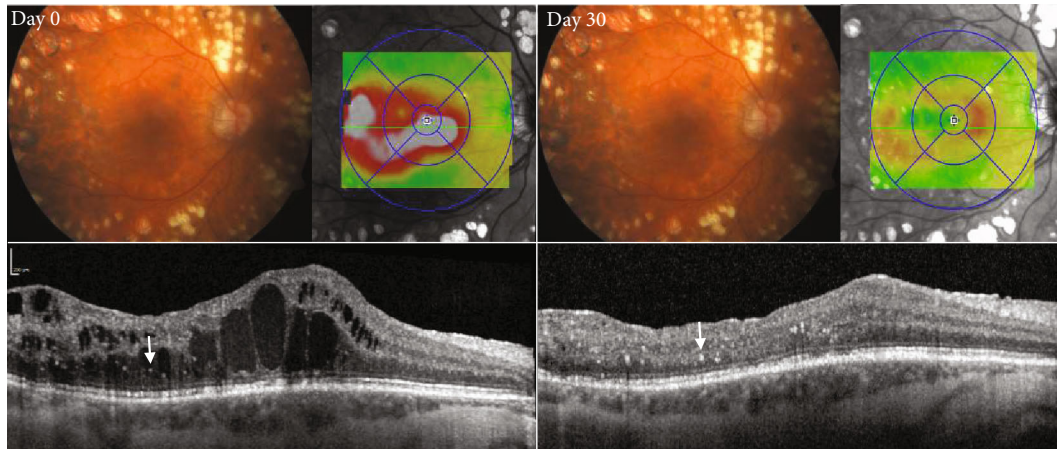


FIGURE 4: Treatment response of hyperreflective foci (HF) after dexamethasone implantation in a patient with diabetic macular edema (DME). Color fundus photograph (CFP), spectral-domain optical coherence tomography (SD-OCT) B-scan, and infrared image with Early Treatment Diabetic Retinopathy Study (EDTRS) grid depicting extent of DME (red and grey color) at baseline (left panel, day 0) and one month after dexamethasone injection (right panel, day 30) in the same patient as in Figure 1. HF are found adjacent to cystoid spaces in the outer retinal layers. After therapy, the DME resolved and the number of HF clearly decreased.

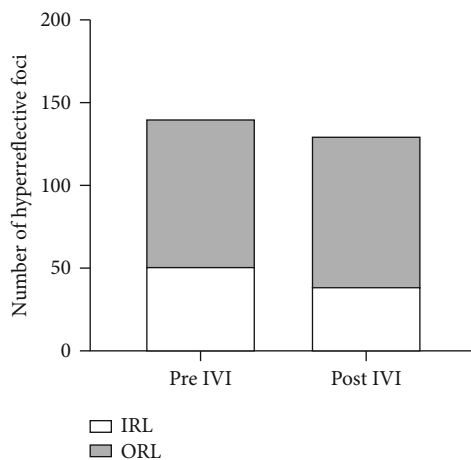


FIGURE 5: Bar graph representing changes in the distribution of hyperreflective foci (HF) in patients with diabetic macular edema (DME) treated with anti-VEGF or dexamethasone implant. Figure shows the difference in the distribution of HF between the inner retinal layers (IRL, from the ILM to inner nuclear layer, INL) and the outer retinal layers (ORL, from the outer plexiform layer, OPL to the retinal pigment epithelium, RPE) at baseline compared to 30 days after the injection.

patients, HF in outer retinal layers accumulated to visible HE during the follow-up period of one to two months after the treatment (Figure 6). During therapy, HE increased significantly in number and size in these patients, while DME resolved. Of note, the HF that accumulated were larger in size than the fine hyperreflective dots, which were still detectable before and after therapy (Figure 6). We think these larger HF correspond to microexudates similar to what has been postulated by Bolz et al. and Pemp et al. [23, 30], and that the small HF or hyperreflective dots could resemble cells of macrophage origin, that might aim to phagocytose the accumulated lipids and proteins. As such, their occurrence is independent of the state of fluid accumulation.

We did not find the large HF as precursors of exudates in a majority of our patients contrary to the study by Pemp et al. [23]. All patients in their study had severe DME, which did not respond to previous therapy with focal or grid laser therapy. Thus, a specific subgroup of recalcitrant DME patients was selected from our study cohort in the matter that the exudative pathophysiology might have been predominant in their patients. Furthermore, in our study, we found HEs only in 54% of patients at baseline on SD-OCT images and CFPs. Similarly, Ota et al. also found HEs in 50% of their patients, but they used only CFPs for analysis [36]. Thus, HF do not form HE in all patients and therefore might represent a different entity than microexudates.

We found that the HF that evolved to HE are larger HF which are primarily found in the outer retina. As well as this, we detected HF scattered through all retina layers. Before therapy, this occurred even more frequently in the inner retinal layers in part in proximity to blood vessels (Figure 1). This is in line with some authors also suggesting that HF are a different entity than exudates, because the foci are distributed throughout all retinal layers, and thus, they are unrelated to microaneurysms as their source. In our study, ORL foci were especially found in foveal cystoid spaces (Figure 1), although HEs are rarely deposited in cystoid spaces. Moreover, the ELM, which corresponds to the adherent junction between Müller glial cells and photoreceptors, would restrict the migration of extravasated material and macromolecules into the outer retinal layers. Thus, HF might also represent a different entity such as inflammatory monocytic cells like activated microglia or macrophages. Microglia are the resident immune cells in the retina. Ramified (“resting”) microglia reside in the inner and outer plexiform layers where they continuously monitor their environment. When activated, they shift towards an amoeboid morphology [35], where they exhibit a larger cell body with shorter processes, they are therefore more likely to be detected as bright dots on SD-OCT. Both microglia and HF are also primarily found

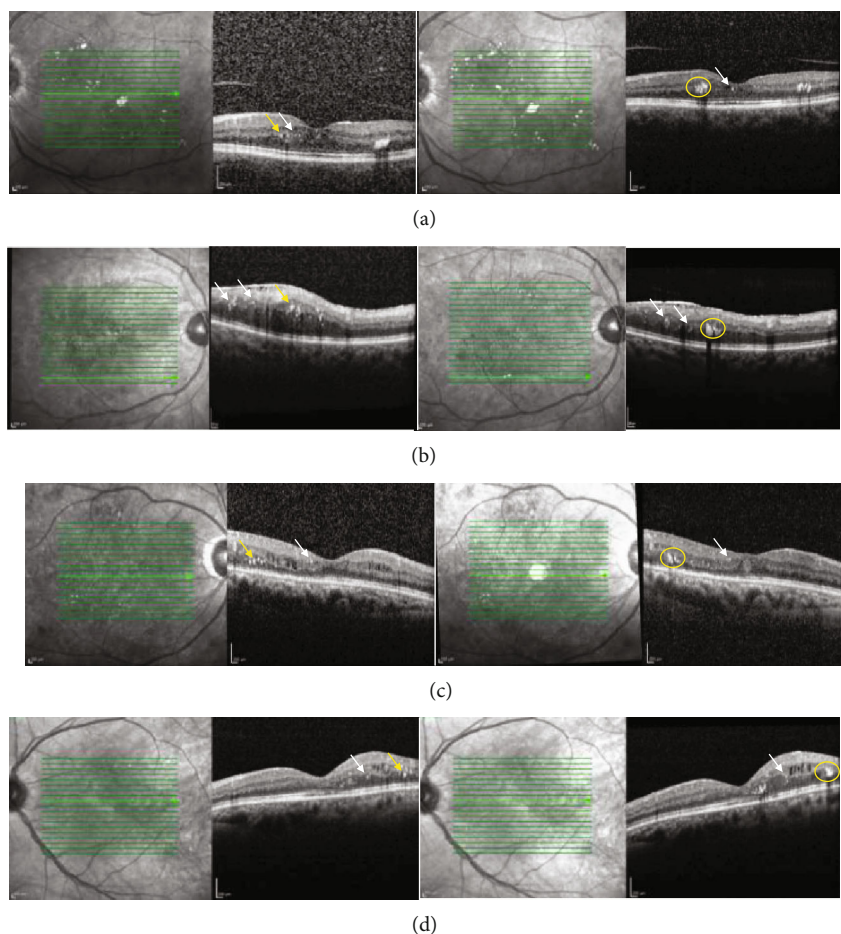


FIGURE 6: Accumulation of large hyperreflective foci (HF) to form hard exudates (HE) in patients with diabetic macular edema (DME) after anti-VEGF therapy. Figure shows infrared images and corresponding spectral-domain optical coherence tomography (SD-OCT) scans at (left panel, a–d) baseline and (right panel, a, b) two months or (right panel, c, d) one month after anti-VEGF injection. In the region of interest on SD-OCT, large HF (yellow arrows) in the outer retinal layers (outer plexiform layer (OPL) and outer nuclear layer (ONL)) increase in density and area to form HEs (yellow circles), which are visible on corresponding infrared images (right panel, a, b). Small HF (white arrows), which might resemble phagocytosing macrophages, are scattered through all retinal layers and do not change in number or size after treatment.

in the inner retina in DR and shift towards the outer retinal layers during DR progression, similar to what we found in our study (Figure 5). Case studies using histological techniques on retinal cross-sections revealed increasing numbers of moderately hypertrophic microglial cells in the plexiform layers of NPDR patients [37]. As DME arises, microglia have been observed in the outer retina and subretinal space [38]. In tissues from PDR patients, clusters of microglial cells could be found surrounding ischemic areas and new vessels together with a significant rise in their total number [38]. Furthermore, some authors insisted that HF are distinct in nature from lipoprotein exudates, because they detected HF in diabetic patients at the initial stages of DR and also in those without DR who had no detectable sign of a disrupted BRB on FA or without any sign of DME on OCT [33]. In addition, Lee et al. also observed a positive correlation between the level of soluble cluster of differentiation (CD) 14; a cytokine associated with the innate immune response expressed in microglia, monocytes, and macrophages; and the number of HF in the inner retina in DME patients [31].

Another fact that points towards monocytes is the fact that HE could regress after treatment, but very slowly, usually in a few months or at least many weeks after fluid reabsorption. This is different from the greater resolution of HF only one month after anti-inflammatory treatment compared to anti-VEGF therapy in our study. Therefore, we speculate that such a rapid response supports the fact that the fine HF that are distributed through all retinal layers in patients without visible HEs represent activated and swelled microglia as part of an inflammatory response.

As aforementioned, anti-VEGF agents, such as ranibizumab, have been successfully used to treat DME [39, 40]. Steroids are presumed to have more potent anti-inflammatory properties compared with anti-VEGF agents and have also been shown to effectively cause resolution of DME [14, 16]. Although complete resolution of DME may be achieved with both these treatment options, there may be several factors that predict the treatment response dependent on the agent used to treat the DME. In a study by Chatziralli, the reduction of the numbers of HF was not

influenced by the choice of treatment option used to reduce the DME (ranibizumab or dexamethasone implant) [34]. In our study, there was a trend towards a greater reduction of HF in the DEX group, suggesting that inflammation and hyperpermeability with subsequent lipoprotein extravasation are potentially both implicated in the pathogenesis of HF and DME. Furthermore, VEGF has been demonstrated to induce microglial activation and anti-VEGF agents and, thus, also counteract this activation [41]. This might explain why there is not the obvious advantage of steroids over anti-VEGF in the reduction of the number of foci. In line with most studies that demonstrated a significant reduction of HF in DME and wet AMD patients after treatment [22, 34, 42–47], we did not find a significant reduction in the number of HF, along with a significant reduction in CRT. Most studies used a standardized three-time loading phase, and since postoperative observation in the present study took place two to four weeks after only one injection, no exact comparison is possible. It can be speculated that the reduction in HF numbers might have been greater if examination had been performed after three injections. Another explanation for the only slight decrease in the number of foci might be due to improve detection of hyperreflective foci/dots after resorption of edema. As the retinal architecture is restored, the foci are just easier to detect.

An important consideration is the fact that HF, among other OCT detectable morphological features, might serve as a better predictor of visual outcome in DME patients than the quantitative reduction of macular fluid as studies demonstrated only a moderate correlation of CRT with VA in DME patients [48, 49]. The integrity of the ellipsoid zone and the ELM has been shown to be the best predictor of visual outcome so far [20, 21]. We found HF as strong predictors of visual outcome in DME patients, demonstrated by a highly significant correlation of baseline HF (IRL and ORL foci) with baseline VA and final VA. This is in line with the literature on HF in DME patients [19, 22, 23]. Similar observations have also been reported in patients with age-related macular degeneration [44] and branch retinal vein occlusion [50]. Especially, HF in the outer layers correlated with poor visual function and with the disruption of the ELM and IS/OS line in patients with DME [51]. Hyperreflective foci, IS/OS, and ELM line disruption seems to represent outer blood-retinal barrier breakdown and photoreceptor dysfunction [51]. Fewer HF might represent better retinal tissue integrity, whereas the presence of many HF reflects tissue disintegration, a higher grade of inflammation, and more severe DME conditions. Since damaged ELM and/or IS/OS are not necessarily accompanied by macular edema in DME, this might be a good explanation for why visual acuity does not always improve after therapy in DME patients.

Further, we wanted to gain more insight into HF pathophysiology by performing OCTA in our patients. OCTA is a noninvasive imaging modality that enables a visualization of the retinal microvasculature. A comparative analysis of HF on SD-OCT and corresponding OCTA scans revealed that HF in the outer retinal layers were not attached to blood vessels in our patients. We identified them in spaces without any sign of vascularization, thus suggesting resident micro-

glia as their origin, rather than exudation from leaking blood vessels. So far, only one other study evaluated HF on OCTA, but the authors looked only at HF in the INL and the Henle fiber layer (HFL), which is located at the border between ONL and OPL [52]. Murakami et al. found HF in the INL to be frequently attached to capillaries on OCTA images, which therefore might represent lipid-laden macrophages or precursors of HEs. In the HFL, HF were found to be in part enwrapped by a “reflectance decorrelation signal” [52]. They hypothesized that these HF contribute to photoreceptor damage and neuroglial dysfunction and might be of microglial/macrophage origin, because of the correlation between the “reflectance decorrelation signal” and visual impairment and disruption of the ellipsoid zone of the photoreceptors on OCT [52].

One important consideration is the image modality chosen to detect the HF, which has a potential effect on the detection rate. One study by Bolz et al. compared the detection rate of HF on three different OCT devices (two time-domain OCT devices, one SD-OCT) [30]. The study concluded that all three devices were able to detect the same HF in the same intraretinal locations; however, their features, density, and distribution throughout the retinal layers could be determined more precisely on SD-OCT, due to the higher resolution [30]. Furthermore, the eye-tracking system of the device offers the possibility of comparing the same retinal location in repeated examination. More recent OCT technologies include enhanced deep imaging OCT (EDI-OCT), which allows better visualization of the choroid and the swept-source (SS) OCT. This also allows a faster and more in detail visualization of the retinal and choroidal architecture and is less prone for artefacts due to media opacities or due to eye movement. A recent study found more HF on the Spectralis SD-OCT, the same device that we used for this study, compared to a SS-OCT device [53]. This was most likely due to the higher contrast delivered by the Spectralis SD-OCT [53]. Thus, currently, there is no obvious advantage of using the most recent SS-OCT technology when assessing OCT biomarkers like HF, apart from the shorter acquisition time and easier acquisition protocol. Most importantly, specialists should use the same device at every follow-up examination, when assessing HF or other biomarkers of treatment response.

The strengths of our study are its prospective design and the direct comparison of the two different treatment options for DME on the quality and quantity of HF. Limitations are the following: a relatively small sample size, short follow-up, and the fact that no histological samples were collected. Without histological correlation of the lesions on SD-OCT with immunohistochemistry markers for reactive RPE or microglial cells, we cannot definitively conclude on the origin of HF.

5. Conclusion

In conclusion, this is the first prospective study to comparatively study the quality and quantity of HF on OCT and OCTA in patients with DR, before and after treatment, with either primarily antiangiogenic or anti-inflammatory therapy. We assume HF to be related to microexudates in a subset of

patients. These foci are larger in diameter on SD-OCT and found in outer retinal layers, whereas the fine hyperreflective dots, which are scattered through all retinal layers, correspond to monocytes such as microglia or macrophages.

We suggest that HF might predict treatment responses in patients with DME, as we could demonstrate a greater decrease in the number of HF in patients treated with dexamethasone implants compared to anti-VEGF agents. Further investigation is warranted to determine whether HF could serve as a biomarker to develop new endpoints for clinical imaging trials and more accurate disease monitoring in clinical practice. Further studies on HF should implement a longer follow-up period and automated, objective assessment of HF using specific software. This knowledge may contribute to the development of proper risk assessment, and therefore enable personalized decision making.

Data Availability

All clinical data is available for the reader in the supplemental file.

Disclosure

This research received no specific grant from any funding agency in the public, commercial, or not-for-profit sectors. The clinical data was collected as part of the employment for Charité University Medicine Berlin and the Berlin Institute of Health.

Conflicts of Interest

The authors declare that they have no conflict of interest.

Acknowledgments

We would like to acknowledge D. Scharf and R. Strothmann for the image acquisition and Jessamy Hardie for proofreading.

Supplementary Materials

Supplemental word file with an overview over the included study patients. Date of birth, gender, type of diabetic macular edema, disruption of inner segment/outer segment line, central retinal thickness, number and location of hyperreflective foci and hard exudates at baseline, and 15 and/or 30 days after therapy are shown. (*Supplementary Materials*)

References

- [1] B. E. Klein, "Overview of epidemiologic studies of diabetic retinopathy," *Ophthalmic Epidemiology*, vol. 14, no. 4, pp. 179–183, 2007.
- [2] J. W. Miller, A. P. Adamis, D. T. Shima et al., "Vascular endothelial growth factor/vascular permeability factor is temporally and spatially correlated with ocular angiogenesis in a primate model," *The American Journal of Pathology*, vol. 145, no. 3, pp. 574–584, 1994.
- [3] N. Ferrara and T. Davis-Smyth, "The biology of vascular endothelial growth factor," *Endocrine Reviews*, vol. 18, no. 1, pp. 4–25, 1997.
- [4] M. A. Singer, D. S. Kermany, J. Waters, M. E. Jansen, and L. Tyler, "Diabetic Macular Edema: It Is More Than Just Vegf," *F1000Res*, vol. 5, 2016.
- [5] H. Funatsu, H. Noma, T. Mimura, S. Eguchi, and S. Hori, "Association of vitreous inflammatory factors with diabetic macular edema," *Ophthalmology*, vol. 116, no. 1, pp. 73–79, 2009.
- [6] S. G. Elner, V. M. Elner, G. J. Jaffe, A. Stuart, S. L. Kunkel, and R. M. Strieter, "Cytokines in proliferative diabetic retinopathy and proliferative vitreoretinopathy," *Current Eye Research*, vol. 14, no. 11, pp. 1045–1053, 1995.
- [7] A. M. Abu El-Asrar, S. Struyf, D. Kangave, K. Geboes, and J. Van Damme, "Chemokines in proliferative diabetic retinopathy and proliferative vitreoretinopathy," *European Cytokine Network*, vol. 17, no. 3, pp. 155–165, 2006.
- [8] Y. Mitamura, S. Takeuchi, A. Matsuda, Y. Tagawa, Y. Mizue, and J. Nishihira, "Monocyte chemotactic protein-1 in the vitreous of patients with proliferative diabetic retinopathy," *Ophthalmologica*, vol. 215, no. 6, pp. 415–418, 2001.
- [9] D. Muramatsu, Y. Wakabayashi, Y. Usui, Y. Okunuki, T. Kezuka, and H. Goto, "Correlation of complement fragment C5a with inflammatory cytokines in the vitreous of patients with proliferative diabetic retinopathy," *Graefé's Archive for Clinical and Experimental Ophthalmology*, vol. 251, no. 1, pp. 15–17, 2013.
- [10] Y. Wakabayashi, Y. Usui, Y. Okunuki et al., "Correlation of vascular endothelial growth factor with chemokines in the vitreous in diabetic retinopathy," *Retina*, vol. 30, no. 2, pp. 339–344, 2010.
- [11] D. Zur, M. Igllicki, and A. Loewenstein, "The role of steroids in the management of diabetic macular edema," *Ophthalmic Research*, vol. 62, no. 4, pp. 231–236, 2019.
- [12] A. M. Joussen, T. Murata, A. Tsujikawa, B. Kirchhof, S. E. Bursell, and A. P. Adamis, "Leukocyte-mediated endothelial cell injury and death in the diabetic retina," *The American Journal of Pathology*, vol. 158, no. 1, pp. 147–152, 2001.
- [13] J. K. Krady, A. Basu, C. M. Allen et al., "Minocycline reduces proinflammatory cytokine expression, microglial activation, and caspase-3 activation in a rodent model of diabetic retinopathy," *Diabetes*, vol. 54, no. 5, pp. 1559–1565, 2005.
- [14] D. S. Boyer, Y. H. Yoon, R. Belfort Jr. et al., "Three-year, randomized, sham-controlled trial of dexamethasone intravitreal implant in patients with diabetic macular edema," *Ophthalmology*, vol. 121, no. 10, pp. 1904–1914, 2014.
- [15] P. Mello Filho, G. Andrade, A. Maia et al., "Effectiveness and safety of intravitreal dexamethasone implant (Ozurdex) in patients with diabetic macular edema: a real-world experience," *Ophthalmologica*, vol. 241, no. 1, pp. 9–16, 2018.
- [16] M. Igllicki, C. Busch, D. Zur et al., "Dexamethasone implant for diabetic macular edema in naive compared with refractory eyes: the international retina group real-life 24-month multicenter study. The Irgrel-Dex study," *Retina*, vol. 39, no. 1, pp. 44–51, 2019.
- [17] J. G. Gross, A. R. Glassman, D. Liu et al., "Five-year outcomes of panretinal photocoagulation vs intravitreal ranibizumab for proliferative diabetic retinopathy: a randomized clinical trial," *JAMA Ophthalmology*, vol. 136, no. 10, pp. 1138–1148, 2018.

- [18] M. Iglicki, D. Zur, C. Busch, M. Okada, and A. Loewenstein, "Progression of diabetic retinopathy severity after treatment with dexamethasone implant: a 24-month cohort study the 'Dr-Pro-Dex Study'," *Acta Diabetologica*, vol. 55, no. 6, pp. 541–547, 2018.
- [19] D. Zur, M. Iglicki, C. Busch et al., "Oct biomarkers as functional outcome predictors in diabetic macular edema treated with dexamethasone implant," *Ophthalmology*, vol. 125, no. 2, pp. 267–275, 2018.
- [20] D. Zur, M. Iglicki, A. Sala-Puigdollers et al., "Disorganization of retinal inner layers as a biomarker in patients with diabetic macular oedema treated with dexamethasone implant," *Acta Ophthalmologica*, vol. 98, no. 2, pp. e217–e223, 2020.
- [21] J. K. Sun, S. H. Radwan, A. Z. Soliman et al., "Neural retinal disorganization as a robust marker of visual acuity in current and resolved diabetic macular edema," *Diabetes*, vol. 64, no. 7, pp. 2560–2570, 2015.
- [22] T. Murakami, K. Suzuma, A. Uji et al., "Association between characteristics of foveal cystoid spaces and short-term responsiveness to ranibizumab for diabetic macular edema," *Japanese Journal of Ophthalmology*, vol. 62, no. 3, pp. 292–301, 2018.
- [23] B. Pemp, G. Deak, S. Prager et al., "Distribution of intraretinal exudates in diabetic macular edema during anti-vascular endothelial growth factor therapy observed by spectral domain optical coherence tomography and fundus photography," *Retina*, vol. 34, no. 12, pp. 2407–2415, 2014.
- [24] M. Iglicki, A. Lavaque, M. Ozimek et al., "Biomarkers and predictors for functional and anatomic outcomes for small gauge pars plana vitrectomy and peeling of the internal limiting membrane in naïve diabetic macular edema: the vital study," *PLoS One*, vol. 13, no. 7, article e0200365, 2018.
- [25] J. Ho, A. J. Witkin, J. Liu et al., "Documentation of intraretinal retinal pigment epithelium migration via high-speed ultrahigh-resolution optical coherence tomography," *Ophthalmology*, vol. 118, no. 4, pp. 687–693, 2011.
- [26] M. Kuroda, Y. Hirami, M. Hata, M. Mandai, M. Takahashi, and Y. Kurimoto, "Intraretinal hyperreflective foci on spectral-domain optical coherence tomographic images of patients with retinitis pigmentosa," *Clinical Ophthalmology*, vol. 8, pp. 435–440, 2014.
- [27] K. Ogino, T. Murakami, A. Tsujikawa et al., "Characteristics of optical coherence tomographic hyperreflective foci in retinal vein occlusion," *Retina*, vol. 32, no. 1, pp. 77–85, 2012.
- [28] Q. Yang, W. Wei, X. Shi, and L. Yang, "Successful use of intravitreal ranibizumab injection and combined treatment in the management of Coats' disease," *Acta Ophthalmologica*, vol. 94, no. 4, pp. 401–406, 2016.
- [29] O. Segal, E. Barayev, A. Y. Nemet, N. Geffen, I. Vainer, and M. Mimouni, "Prognostic value of hyperreflective foci in neovascular age-related macular degeneration treated with bevacizumab," *Retina*, vol. 36, no. 11, pp. 2175–2182, 2016.
- [30] M. Bolz, U. Schmidt-Erfurth, G. Deak et al., "Optical coherence tomographic hyperreflective foci: a morphologic sign of lipid extravasation in diabetic macular edema," *Ophthalmology*, vol. 116, no. 5, pp. 914–920, 2009.
- [31] H. Lee, H. Jang, Y. A. Choi, H. C. Kim, and H. Chung, "Association between soluble Cd14 in the aqueous humor and hyperreflective foci on optical coherence tomography in patients with diabetic macular edema," *Investigative Ophthalmology & Visual Science*, vol. 59, no. 2, pp. 715–721, 2018.
- [32] U. De Benedetto, R. Sacconi, L. Pierro, R. Lattanzio, and F. Bandello, "Optical coherence tomographic hyperreflective foci in early stages of diabetic retinopathy," *Retina*, vol. 35, no. 3, pp. 449–453, 2015.
- [33] S. Vujosevic, S. Bini, G. Midena, M. Berton, E. Pilotto, and E. Midena, "Hyperreflective intraretinal spots in diabetics without and with nonproliferative diabetic retinopathy: an in vivo study using spectral domain Oct," *Journal Diabetes Research*, vol. 2013, article 491835, pp. 1–5, 2013.
- [34] I. P. Chatziralli, T. N. Sergentanis, and S. Sivaprasad, "Hyperreflective foci as an independent visual outcome predictor in macular edema due to retinal vascular diseases treated with intravitreal dexamethasone or ranibizumab," *Retina*, vol. 36, no. 12, pp. 2319–2328, 2016.
- [35] E. J. Davis, T. D. Foster, and W. E. Thomas, "Cellular forms and functions of brain microglia," *Brain Research Bulletin*, vol. 34, no. 1, pp. 73–78, 1994.
- [36] M. Ota, K. Nishijima, A. Sakamoto et al., "Optical coherence tomographic evaluation of foveal hard exudates in patients with diabetic maculopathy accompanying macular detachment," *Ophthalmology*, vol. 117, no. 10, pp. 1996–2002, 2010.
- [37] M. Karlstetter, R. Scholz, M. Rutar, W. T. Wong, J. M. Provis, and T. Langmann, "Retinal microglia: just bystander or target for therapy?," *Progress in Retinal and Eye Research*, vol. 45, pp. 30–57, 2015.
- [38] H. Y. Zeng, W. R. Green, and M. O. Tso, "Microglial activation in human diabetic retinopathy," *Archives of Ophthalmology*, vol. 126, no. 2, pp. 227–232, 2008.
- [39] D. M. Brown, U. Schmidt-Erfurth, D. V. Do et al., "Intravitreal aflibercept for diabetic macular edema: 100-week results from the vista and vivid studies," *Ophthalmology*, vol. 122, no. 10, pp. 2044–2052, 2015.
- [40] Q. D. Nguyen, D. M. Brown, D. M. Marcus et al., "Ranibizumab for diabetic macular edema: results from 2 phase III randomized trials: RISE and RIDE," *Ophthalmology*, vol. 119, no. 4, pp. 789–801, 2012.
- [41] A. Couturier, E. Bousquet, M. Zhao et al., "Anti-vascular endothelial growth factor acts on retinal microglia/macrophage activation in a rat model of ocular inflammation," *Molecular Vision*, vol. 20, pp. 908–920, 2014.
- [42] K. Abri Aghdam, A. Pielen, C. Framme, and B. Junker, "Correlation between hyperreflective foci and clinical outcomes in neovascular age-related macular degeneration after switching to aflibercept," *Investigative Ophthalmology & Visual Science*, vol. 56, no. 11, pp. 6448–6455, 2015.
- [43] J. W. Kang, H. Chung, and H. Chan Kim, "Correlation of optical coherence tomographic hyperreflective foci with visual outcomes in different patterns of diabetic macular edema," *Retina*, vol. 36, no. 9, pp. 1630–1639, 2016.
- [44] G. Coscas, U. De Benedetto, F. Coscas et al., "Hyperreflective dots: a new spectral-domain optical coherence tomography entity for follow-up and prognosis in exudative age-related macular degeneration," *Ophthalmologica*, vol. 229, no. 1, pp. 32–37, 2013.
- [45] C. Framme, P. Schweizer, M. Imesch, S. Wolf, and U. Wolf-Schnurrbusch, "Behavior of Sd-Oct-detected hyperreflective foci in the retina of anti-VEGF-treated patients with diabetic macular edema," *Investigative Ophthalmology & Visual Science*, vol. 53, no. 9, pp. 5814–5818, 2012.
- [46] H. Lee, B. Ji, H. Chung, and H. C. Kim, "Correlation between optical coherence tomographic hyperreflective foci and visual

- outcomes after anti-VEGF treatment in neovascular age-related macular degeneration and polypoidal choroidal vasculopathy,” *Retina*, vol. 36, no. 3, pp. 465–475, 2016.
- [47] V. Schreur, L. Altay, F. van Asten et al., “Hyperreflective foci on optical coherence tomography associate with treatment outcome for anti-VEGF in patients with diabetic macular edema,” *PLoS One*, vol. 13, no. 10, article e0206482, 2018.
- [48] A. S. Maheshwary, S. F. Oster, R. M. Yuson, L. Cheng, F. Mojana, and W. R. Freeman, “The association between percent disruption of the photoreceptor inner segment-outer segment junction and visual acuity in diabetic macular edema,” *American Journal of Ophthalmology*, vol. 150, no. 1, pp. 63–67.e1, 2010.
- [49] Diabetic Retinopathy Clinical Research, Network, D. J. Browning, A. R. Glassman et al., “Relationship between optical coherence tomography-measured central retinal thickness and visual acuity in diabetic macular edema,” *Ophthalmology*, vol. 114, no. 3, pp. 525–536, 2007.
- [50] B. Mo, H. Y. Zhou, X. Jiao, and F. Zhang, “Evaluation of hyperreflective foci as a prognostic factor of visual outcome in retinal vein occlusion,” *International Journal of Ophthalmology*, vol. 10, no. 4, pp. 605–612, 2017.
- [51] A. Uji, T. Murakami, K. Nishijima et al., “Association between hyperreflective foci in the outer retina, status of photoreceptor layer, and visual acuity in diabetic macular edema,” *American Journal of Ophthalmology*, vol. 153, no. 4, pp. 710–717.e1, 2012.
- [52] T. Murakami, K. Suzuma, Y. Dodo et al., “Decorrelation signal of diabetic hyperreflective foci on optical coherence tomography angiography,” *Scientific Reports*, vol. 8, no. 1, article 8798, 2018.
- [53] C. Mitsch, J. Lammer, S. Karst, C. Scholda, E. Pablik, and U. M. Schmidt-Erfurth, “Systematic ultrastructural comparison of swept-source and full-depth spectral domain optical coherence tomography imaging of diabetic macular oedema,” *The British Journal of Ophthalmology*, vol. 104, no. 6, pp. 868–873, 2020.

Research Article

Atg16L1 as a Novel Biomarker and Autophagy Gene for Diabetic Retinopathy

Xinxiao Gao ^{1,2}, Yunhui Du,³ Wayne Bond Lau,⁴ Yu Li,³ Siquan Zhu,²
and Xin-Liang Ma ^{1,4}

¹Department of Physiology and Pathophysiology, School of Basic Medical Sciences, Capital Medical University, Beijing 100069, China

²Department of Ophthalmology, Beijing Anzhen Hospital, Capital Medical University, Beijing 100029, China

³Beijing Anzhen Hospital, Capital Medical University, Beijing Institute of Heart, Lung and Blood Vessel Diseases, Beijing 100029, China

⁴Department of Emergency Medicine, Thomas Jefferson University, 1025 Walnut Street, College Building, Suite 808, Philadelphia, PA 19107, USA

Correspondence should be addressed to Xin-Liang Ma; drxin.ma@hotmail.com

Received 25 June 2020; Revised 14 February 2021; Accepted 12 March 2021; Published 19 March 2021

Academic Editor: Maria Vittoria Cicinelli

Copyright © 2021 Xinxiao Gao et al. This is an open access article distributed under the Creative Commons Attribution License, which permits unrestricted use, distribution, and reproduction in any medium, provided the original work is properly cited.

Objective. Accumulating evidence suggests the critical role of autophagy in the pathogenesis of diabetic retinopathy (DR). In the current study, we aim to identify autophagy genes involved in DR via microarray analyses. **Methods.** Gene microarrays were performed to identify differentially expressed lncRNAs/mRNAs between normal and DR retinas. Gene Ontology and Kyoto Encyclopedia of Genes and Genomes analyses of lncRNA-coexpressed mRNAs were used to determine the related pathological pathways and biological modules. Real-time polymerase chain reactions (PCR) were conducted to validate the microarray analyses. **Results.** A total of 2474 significantly dysregulated lncRNAs and 959 differentially expressed mRNAs were identified in the retina of DR. Based upon Signalnet analysis, Bcl2, Gabarapl2, Atg4c, and Atg16L1 participated the process of cell death in DR. Moreover, real-time PCR revealed significant upregulation of Atg16L1. **Conclusion.** This study indicated the importance and potential role of Atg16L1, one of the autophagy genes, as a biomarker in DR development and progression.

1. Introduction

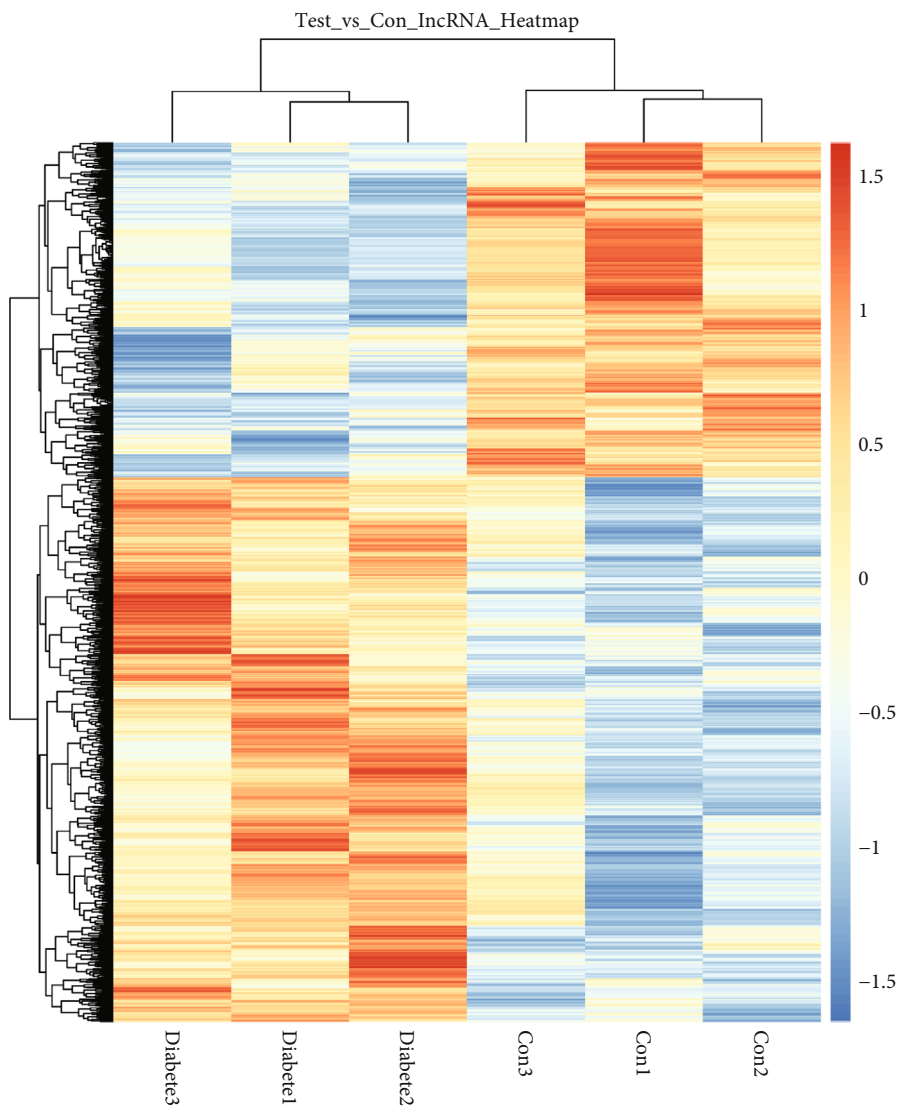
Diabetic retinopathy (DR) is a major contributor to vision loss in patients with diabetes mellitus [1]. DR incidence has been increasing rapidly in recent years, from 127 million in 2010 to a projected 191 million by 2030 [2]. The underlying key biochemical pathways may include genetic and epigenetic factors, polyol pathway activation, production of advanced glycation endproducts (AGEs), protein kinase C (PKC) activation, hexosamine pathway activation, and poly (ADP-ribose) polymerase upregulation. However, DR pathogenesis is complex and remains incompletely understood [3].

Autophagy is the primary intracellular catabolic mechanism mediating degradation and recycling of proteins and organelles. Due to its essential role in development, aging, starvation, cellular differentiation, and cell death, autophagy has

attracted marked attention in recent years. Dysregulation of autophagy and lysosomal pathways is the hallmark of many diseases, from diabetes to neurodegenerative disorders and lysosomal storage diseases [4–6]. Moreover, growing data have suggested the crucial role of autophagy in DR pathophysiology [7, 8]. Heretofore, there remains limited understanding regarding the exact autophagy genes involved in DR development and progression. The advent of microarray technology has facilitated detection of the comprehensive pattern of simultaneous transcript expression [9]. In this study, we aim to identify the autophagy genes involved in DR by microarray analyses.

2. Methods

2.1. Diabetic Mouse Model. All animal procedures were approved in accordance with the Association of Research in



(a)

FIGURE 1: Continued.

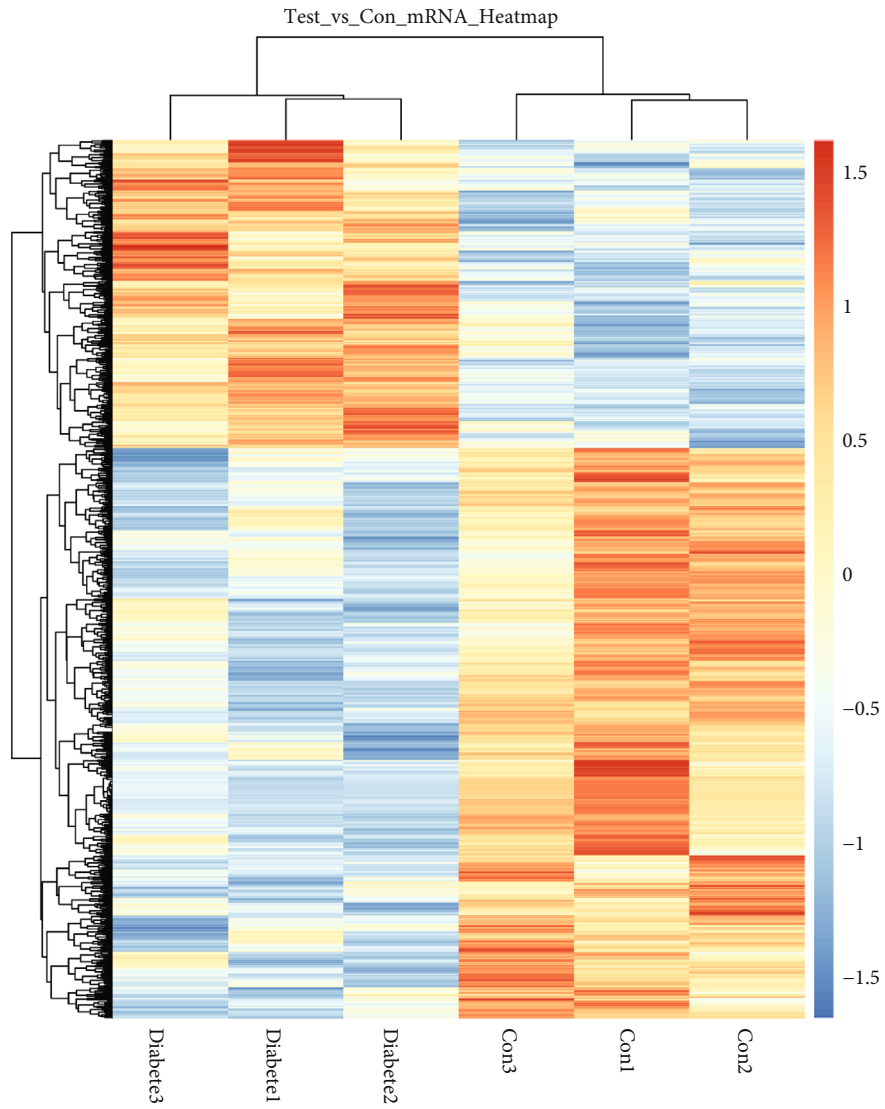
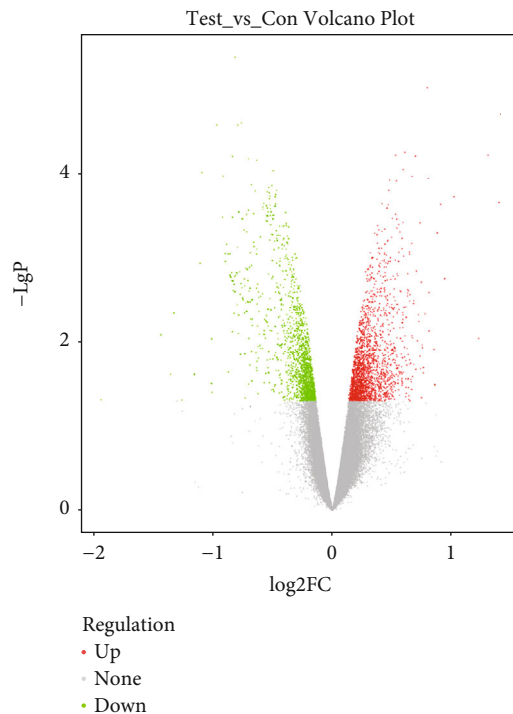


FIGURE 1: Continued.



(c)

FIGURE 1: Identification of DR-related lncRNAs/mRNAs by microarray analysis. (a) Heatmap from the hierarchical clustering analysis demonstrating the differentially expressed lncRNAs between nondiabetic and diabetic retinas. (b) Heatmap demonstrating the dysregulated mRNAs between nondiabetic and diabetic retinas. (c) Volcano plot illustrating the differentially expressed lncRNAs in nondiabetic and diabetic retinas.

Vision and Ophthalmology Treatment of Animals in Research and the Capital Medical University's Animal Care and Use Committee Guidelines. All in vivo experiments were performed upon adult male C57BL/6 mice (8 weeks old). Experimental mice were randomized to receive HFD (60 kcal%) (Research Diets Inc. D12492i) or normal diet control (ND, D12450Bi). Eight months after ND or HFD, mice were anesthetized with 2% isoflurane. Blood glucose concentrations were measured 48 hours after STZ injection and weekly thereafter. Only animals with blood glucose levels exceeding 250 mg/dL were considered diabetic. After 10–12 weeks, the animals were sacrificed by pentobarbital overdose. The retinas were quickly removed, placed in liquid nitrogen, and stored at -80°C for biochemical measurement.

2.2. Microarray Analysis. Total RNAs were isolated from the retinas of diabetic mice and age-matched controls using TRIzol reagent (Life Technologies, Carlsbad, CA, USA) and purified with an RNeasy mini kit (Qiagen, Valencia, CA, USA) per manufacturer's protocol. Microarray profiling was performed by mouse Clariom™ D Assay (Affymetrix GeneChip®, USA, an assay containing 65956 gene-level probe sets). Raw data were normalized at the transcript level by the TAC software (Transcriptome Analysis Console; version: 4.0.1) using Affymetrix default analysis settings (Robust Multichip Analysis workflow). The median summarization of transcript expressions was calculated.

Based upon differentially expressed lncRNAs, hierarchical clustering was performed by R package heatmap (version:

TABLE 1: Top ten differentially expressed lncRNAs in diabetic retinas compared to undiabetic retinas.

lncRNAs	Strand	P value	Fold change
<i>Upregulated</i>			
Chr18: 65390334-65393029	Forward	0.0002	2.63
Chr10: 122606616-122609483	Reverse	0.0005	1.84
Chr15: 73979542-73994040	Forward	0.0007	1.58
Chr7: 35838522-35839628	Forward	0.0008	1.56
Chr4: 129830892-129833771	Forward	0.0015	1.55
Chr5: 43784046-43786117	Reverse	0.0017	1.44
Chr12: 81308672-81311207	Reverse	0.0018	1.37
Chr6: 84883190-84884193	Reverse	0.0025	1.35
Chr1: 132943512-132945320	Reverse	0.0028	1.33
Chr2: 129082743-129084444	Forward	0.0034	1.25
<i>Downregulated</i>			
Chr4: 10136920-10138026	Reverse	0.0001	1.60
Chr11: 3193516-3194263	Reverse	0.0008	1.55
Chr13: 51168717-51170674	Reverse	0.0020	1.38
Chr4: 3089552-3091186	Forward	0.0022	1.38
Chr1: 84984529-84984611	Forward	0.0026	1.36
Chr14: 42037609-42040012	Reverse	0.0028	1.29
Chr5: 131041336-131044079	Reverse	0.0028	1.27
Chr8: 73353725-73362159	Forward	0.0041	1.25
Chr10: 61858666-61859663	Reverse	0.0043	1.23
Chr7: 21523277-21524200	Reverse	0.0045	1.20

TABLE 2: Top ten differentially expressed mRNAs in diabetic retinas compared to undiabetic retinas.

Gene symbol	Description	<i>P</i> value	Fold change
<i>Upregulated</i>			
Hdc	Histidine decarboxylase	0.0004	1.66
Dnah7b	Dynein, axonemal, heavy chain 7B	0.0009	1.47
Erap1	Endoplasmic reticulum aminopeptidase 1	0.0010	1.47
Alpk2	Alpha-kinase 2	0.0011	1.36
Gsc2	Goosecoid homeobox 2	0.0016	1.36
N4bp2l1	NEDD4 binding protein 2-like 1	0.0027	1.27
Skap2	src family-associated phosphoprotein 2	0.0028	1.25
Zscan29	Zinc finger SCAN domains 29	0.0033	1.25
Tmprss7	Transmembrane serine protease 7	0.0039	1.24
Atg16l1	Autophagy-related 16-like 1	0.0043	1.18
<i>Downregulated</i>			
Camk1g	Calcium/calmodulin-dependent protein kinase I gamma	0.0002	1.44
Vmn1r121	Vomerolateral 1 receptor 121	0.0003	1.43
Sly	Sycp3 like Y-linked	0.0003	1.40
Serinc5	Serine incorporator 5	0.0004	1.33
Clybl	Citrate lyase beta like	0.0018	1.32
Hist1h1c	Histone cluster 1, H1c	0.0018	1.31
Ubt2	Ubiquitin domain containing 2	0.0022	1.27
Ttc12	Tetratricopeptide repeat domain 12	0.0030	1.26
Rhobtb1	Rho-related BTB domain containing 1	0.0036	1.26
Duxbl2	Double homeobox B-like 2	0.0037	1.25

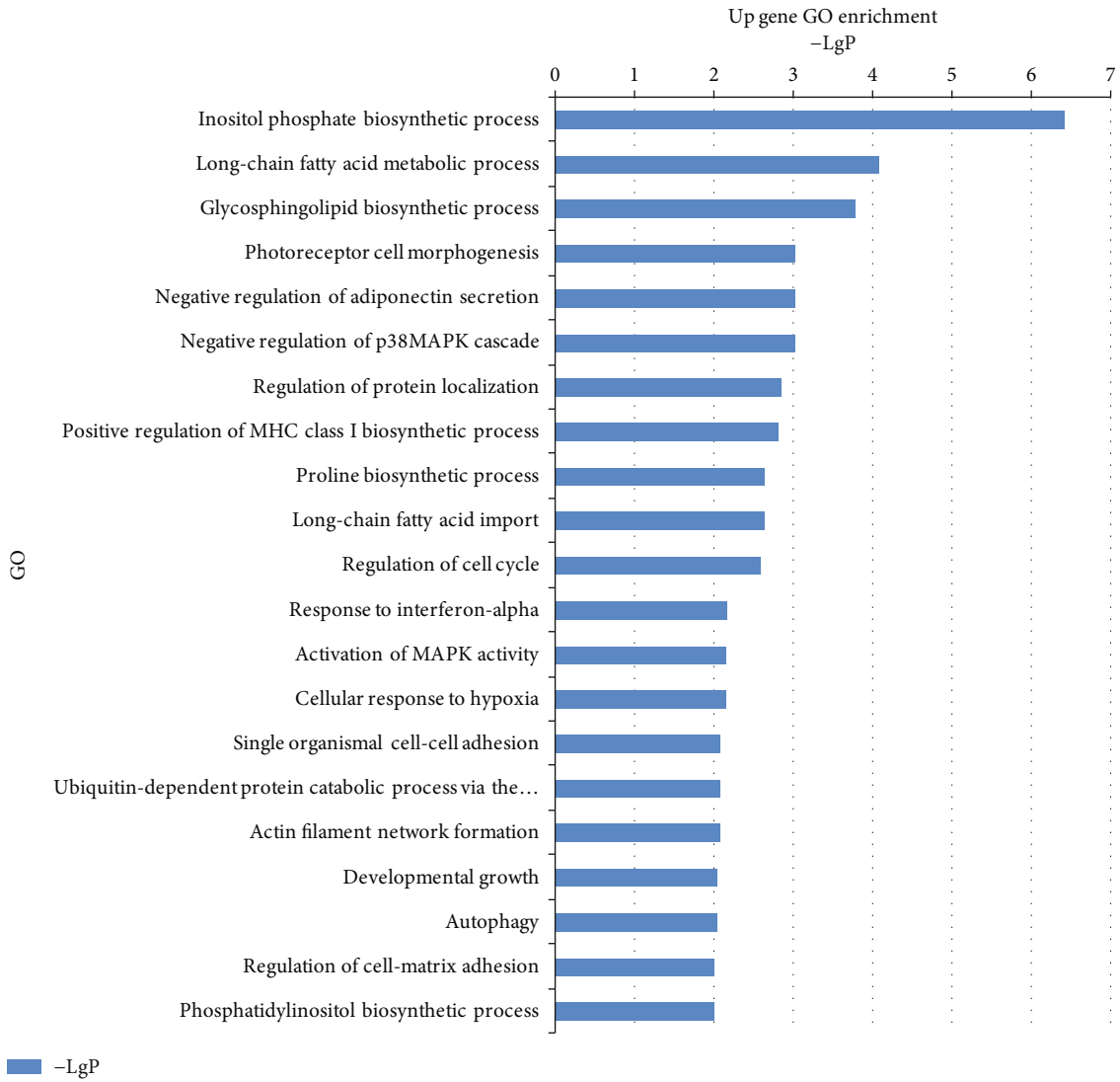
1.0.12). Gene Ontology (GO) analysis determined the main function of the differentially expressed genes, yielding the likely gene regulatory network on the basis of biological processes and molecular function. Specifically, a two-sided Fisher's exact test and chi-square test were used to classify the GO category. The false discovery rate (FDR) was calculated to correct the *P* value (the smaller the FDR, the smaller the error in judging the *P* value). Pathway analysis was conducted upon the differential genes identified, per Kyoto Encyclopedia of Genes and Genomes (KEGG) databases. Fisher's exact test was performed to select the significant pathway. The threshold of significance was considered $P < 0.05$. Based on the interactions of genes in the KEGG database, global signal transduction network (Signalnet) was generated to demonstrate the interaction between the differentially expressed genes in treated groups. The visualization of network was built by software Cytoscape (version: 3.6.0).

2.3. Real-Time Quantitative PCR. Quantitative real-time PCR (qRT-PCR) was applied to validate the selected genes from the microarray analyses. Total RNAs were extracted using TRIzol reagent (Invitrogen, Carlsbad, Canada) and reverse-transcribed per manufacturer's instructions. qRT-PCR reaction was monitored by the ABI Prism 7500 Sequence Detection System (Applied Biosystems, Foster City, CA) and run in duplicate for each sample. The PCR reaction mixture (20 μ l) contained 2 μ l of cDNA template, 0.6 μ l forward and reverse primers, and 10 μ l of 2 \times SYBR-Green PCR Mix (Takara). The level of mRNA expression

was calculated from the fluorescence intensity (b-actin served as internal control). Primers targeting Atg4c (F: 5'-GATGAAAGCAAGATGTTGCCTG-3' and R: 5'-TCTTCCCTGTAGGTCAGCCAT-3') and Atg16L1 (F: 5'-CAGAGCAGCTACTAAGCGACT-3' and R: 5'-AAAAGGGGAGATTCGGACAGA-3') were used for real-time RT-PCR amplification. The relative gene expression was calculated by the $\Delta\Delta$ threshold cycle (Ct) method. Real-time PCR reaction was run in biological triplicates for each sample. Melting curve analysis was used to verify the product purity at the end of the PCR run.

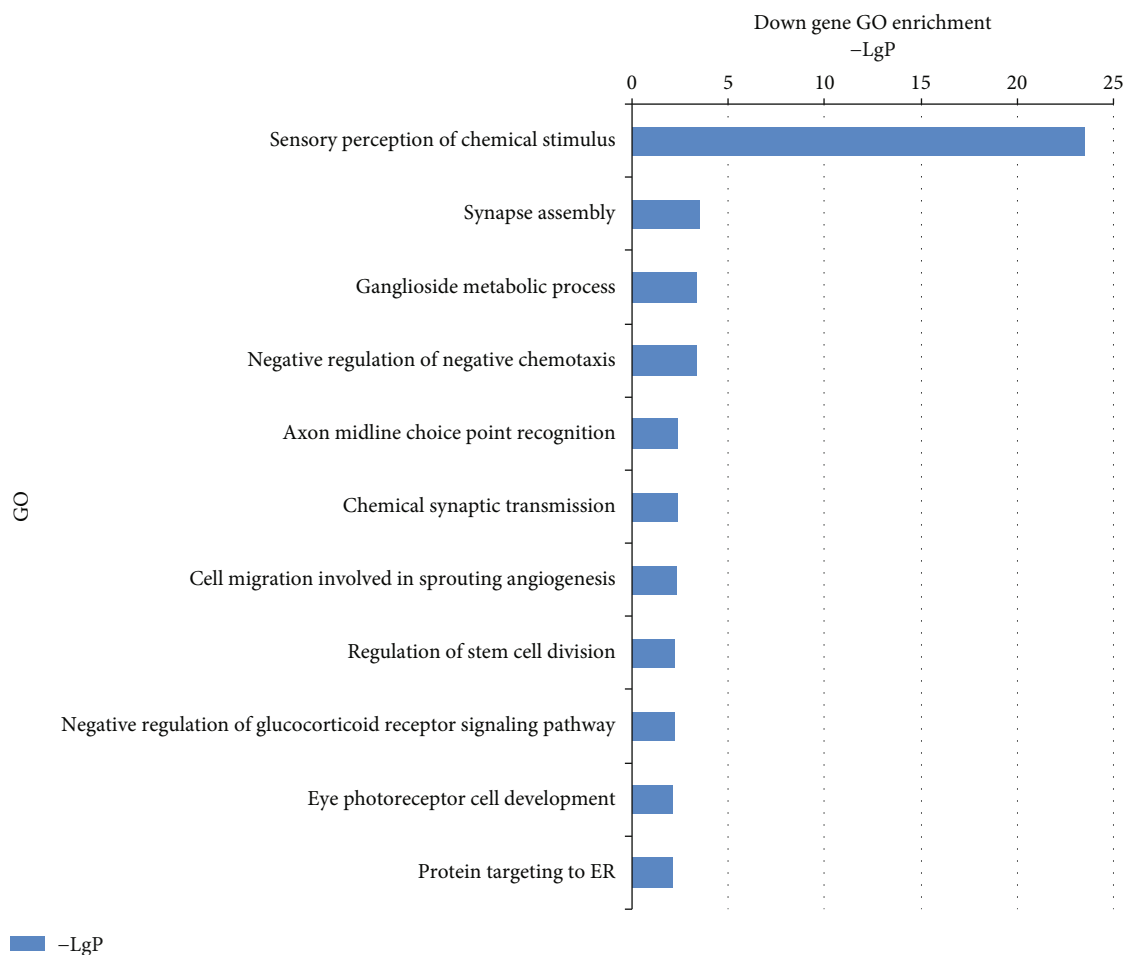
3. Results

3.1. Overview of lncRNA-mRNA Microarray Analysis. To reveal a differential gene expression profile, hierarchical clustering analysis compared lncRNA-mRNA expression between diabetic and nondiabetic retinas (Figures 1(a) and 1(b)). Differentially expressed lncRNAs (with statistical significance) between the two groups were identified via volcano plot filtering (Figure 1(c)). The combined criteria of a *P* value < 0.05 and fold change > 1.1 identified 2474 lncRNAs expressed differentially, including 1487 upregulated and 987 downregulated lncRNAs. 317 significantly increased and 642 decreased mRNAs were also identified. The top 10 differentially expressed lncRNAs and mRNAs between diabetic and nondiabetic retinas are listed in Tables 1 and 2, respectively.

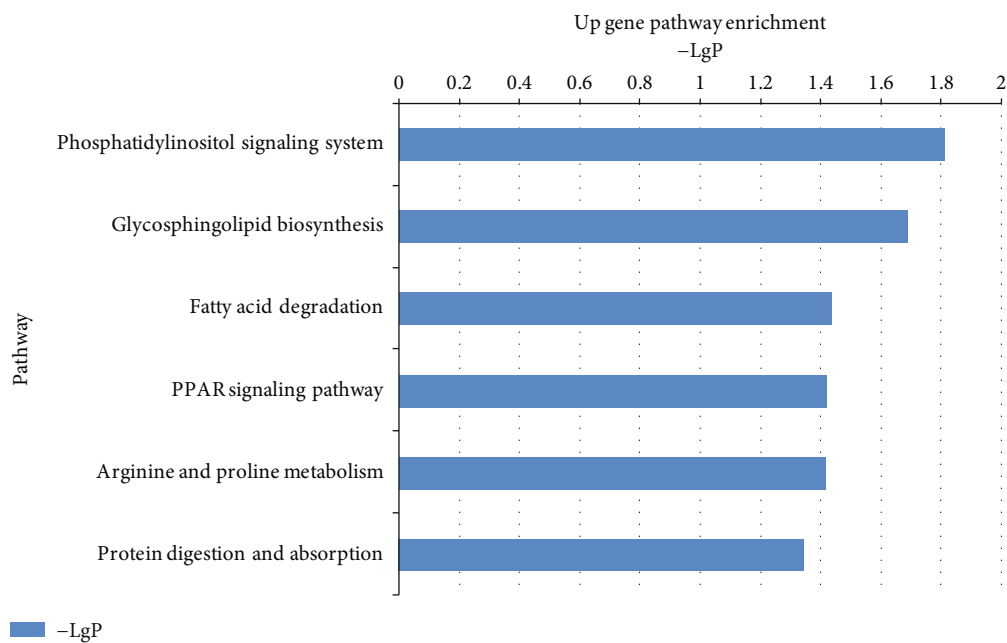


(a)

FIGURE 2: Continued.



(b)



(c)

FIGURE 2: Continued.

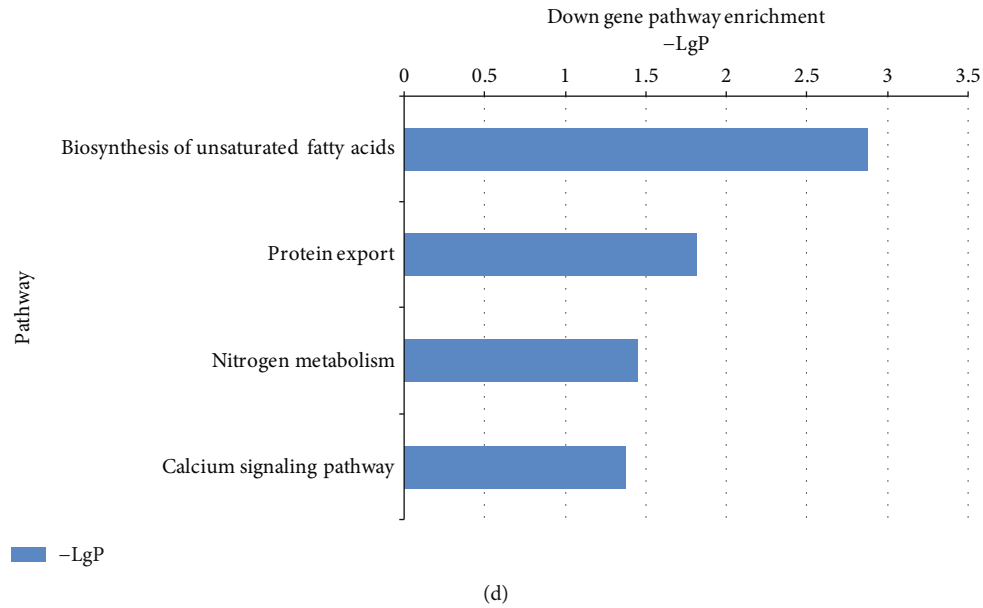


FIGURE 2: Gene Ontology (GO) analyses and KEGG analysis of the dysregulated lncRNAs with top enrichment scores of biological processes. (a) Significantly upregulated differentially expressed genes, by GO analysis. (b) Significantly downregulated differentially expressed genes, by GO analysis. (c) Significant pathways of differentially expressed upregulated genes. (d) Significant pathways of differentially expressed downregulated genes.

TABLE 3: The involved genes in signaling pathways relevant to retinal function.

Pathway name	P value	Gene symbol
Photoreceptor cell morphogenesis	0.000933385	Cabp4, Grk1
Activation of MAPK activity	0.006855100	Map3k13, Fgf2, Adam9
Autophagy	0.009045081	Atg4c, Atg16L1

3.2. Gene Enrichment and Pathway Analysis of lncRNA-Coexpressed mRNAs. GO analysis determined the main gene functions and gene product enrichment affected by diabetes. The GO database revealed (of 21 upregulated GOs) photoreceptor cell morphogenesis, activation of MAPK activity, and autophagy were related to retinal function (Figure 2(a)). Of 11 downregulated GOs, only eye photoreceptor cell development was directly related to retinal function (Figure 2(b)). The summaries of those genes involved in the significant signaling pathways relevant to retinal function are listed in Table 3. KEGG analysis revealed highly enriched upregulated signaling pathways included phosphatidylinositol signaling system, glycosphingolipid biosynthesis, fatty acid degradation, PPAR signaling pathway, arginine and proline metabolism, and protein digestion and absorption (Figure 2(c)). Significantly downregulated pathways included biosynthesis of unsaturated fatty acids, protein export, nitrogen metabolism, and calcium signaling pathway (Figure 2(d)).

3.3. Construction of the lncRNA-mRNA Coexpression Network and Identification of Genes in the Process of Cell Death. Based upon significant pathway and GO analysis, the Signalnet analysis screened the key genes associated with

DR pathogenesis. A total of 369 key genes were identified in the transduction network. Specifically, Bcl2, Gabarapl2, Atg4c, and Atg16L1 were involved in the process of cell death. Figure 3 showed the Signalnet of cell death-related lncRNA-mRNA coexpression network. To evaluate the expression of these 4 specific genes in diabetic and nondiabetic retinas, hierarchical clustering analysis was further performed. The heatmap (Figure 4(a)) suggested the good classification of mRNA expression profile between those two groups.

3.4. Confirmation of Gene Expression in Autophagy by RT-PCR. To further validate the microarray analysis results, we conducted qPCR assays for the genes involved in autophagy. qRT-PCR analysis revealed significantly upregulated expression of Atg16L1 compared to control, while Atg4c expression was unremarkable (Figure 4(b)). The potential role of Atg16L1 in DR pathogenesis was further supported.

4. Discussion

The pathogenesis of DR is hugely complex and likely implicates the dysregulation of many biochemical and molecular

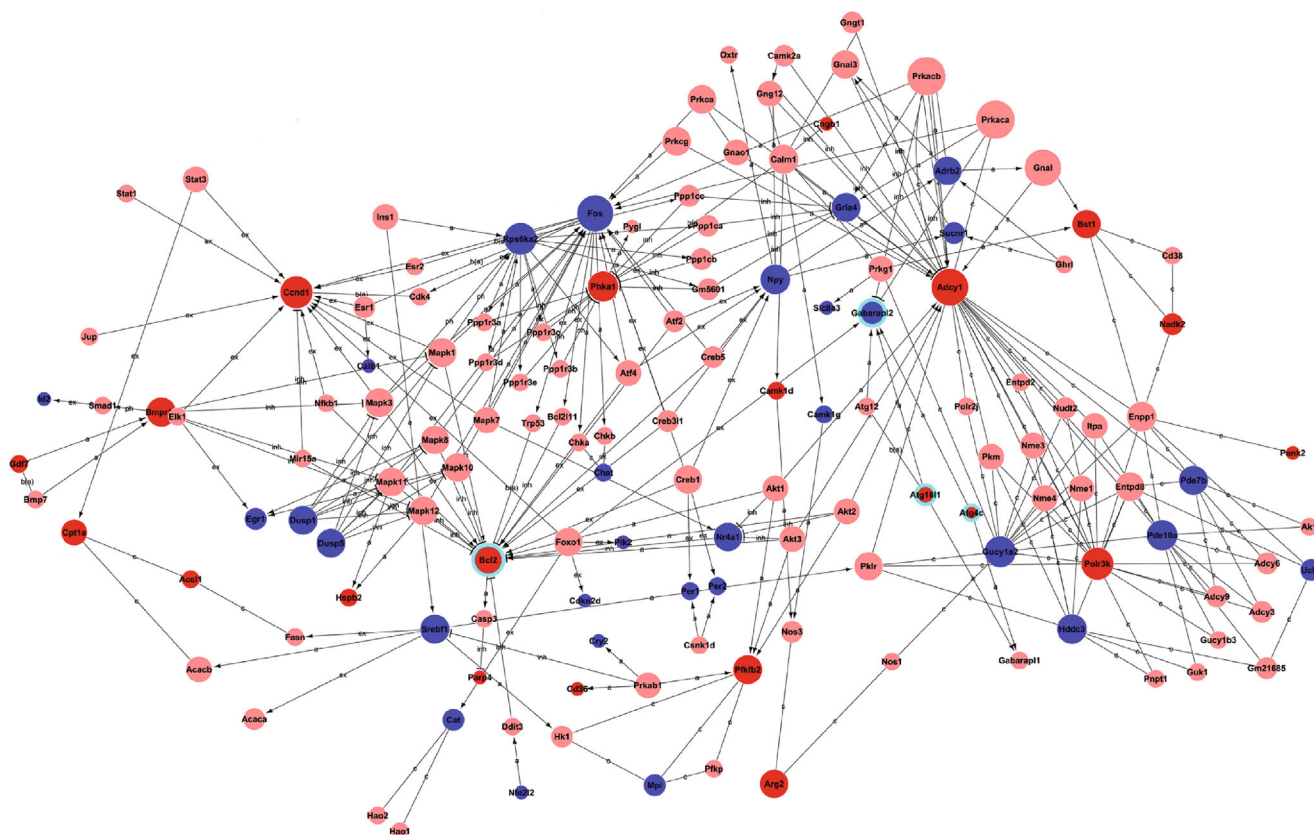


FIGURE 3: Signalnet of cell death-related lncRNA-mRNA coexpression network (the circles highlighted with green ring). The red circles represent upregulated genes, and blue circles represent downregulated genes. Interaction between the genes is shown as follows: a: activation; b: binding/association; c: compound; ex: expression; inh: inhibition; ph: phosphorylation; ubi: ubiquination.

signaling pathways. Despite great strides, the detailed molecular mechanisms responsible for DR are incompletely known. Recent studies have demonstrated that autophagy participates in DR pathology [10, 11], but the underlying responsible genes are unclear. To better understand the significance of autophagy in DR, we evaluated the associated genes by microarray analyses. Signalnet analysis suggests the involvement of Bcl2, Gabarapl2, Atg4c, and Atg16L1 in the process of cell death in DR. As expression of Atg16L1 was significantly increased, this particular molecule may be an important participant in DR development and progression.

lncRNAs/mRNAs have garnered attention in recent years for their potential regulatory role in DR [12, 13]. Additionally, the important roles of lncRNAs were investigated in PDR by harvesting fibrovascular membranes [14]. In the current study, we identified 2474 significantly dysregulated lncRNAs and 959 differentially expressed mRNAs, further confirmed by PCR analysis. In another prior study, lncRNAs were investigated with respect to DR pathogenesis in a mouse streptozotocin-induced diabetic model, utilizing microarray analyses. Only 303 aberrantly expressed lncRNAs were identified in the retinas of early DR [13]. Different animal models and protocol may lead to this discrepancy. Future bioinformatic analysis of the lncRNAs/mRNAs will be helpful to confirm these results.

Accumulating evidence suggests that autophagy plays an essential role and may act as a double-edged sword in DR [15, 16]. Activation of autophagy results in cell survival under mild stress in DR, while dysregulated autophagy can lead to massive cell death during severe stress conditions. In high glucose concentrations, autophagy activation in cultured ARPE-19 cells decreases proinflammatory cytokine production [17]. High glucose upregulates autophagy in retinal Müller cells during early DR pathogenesis phases [10]. In agreement with these previous studies, we demonstrate (based on GO analysis) that autophagy is upregulated during DR. While the contribution of autophagy to DR development requires further study, our findings may open interesting perspectives for novel therapies.

Interestingly, two conserved mRNAs, including Atg16L1, were identified to be involved with autophagy in the current study. As a key player in early autophagy initiation, Atg16L1 also regulates subsequent steps of this pathway [18]. Moreover, recent progress has demonstrated that Atg16L1 may be involved in diabetic pathophysiology by regulating autophagy [19, 20]. In consistent fashion, we report significantly increased expression of Atg16L1 in diabetic mouse retinas. Based upon these findings, we hypothesize that Atg16L1 may be an important component of the DR pathological process. Further studies are warranted to better understand the functional role of this novel mRNA in DR.

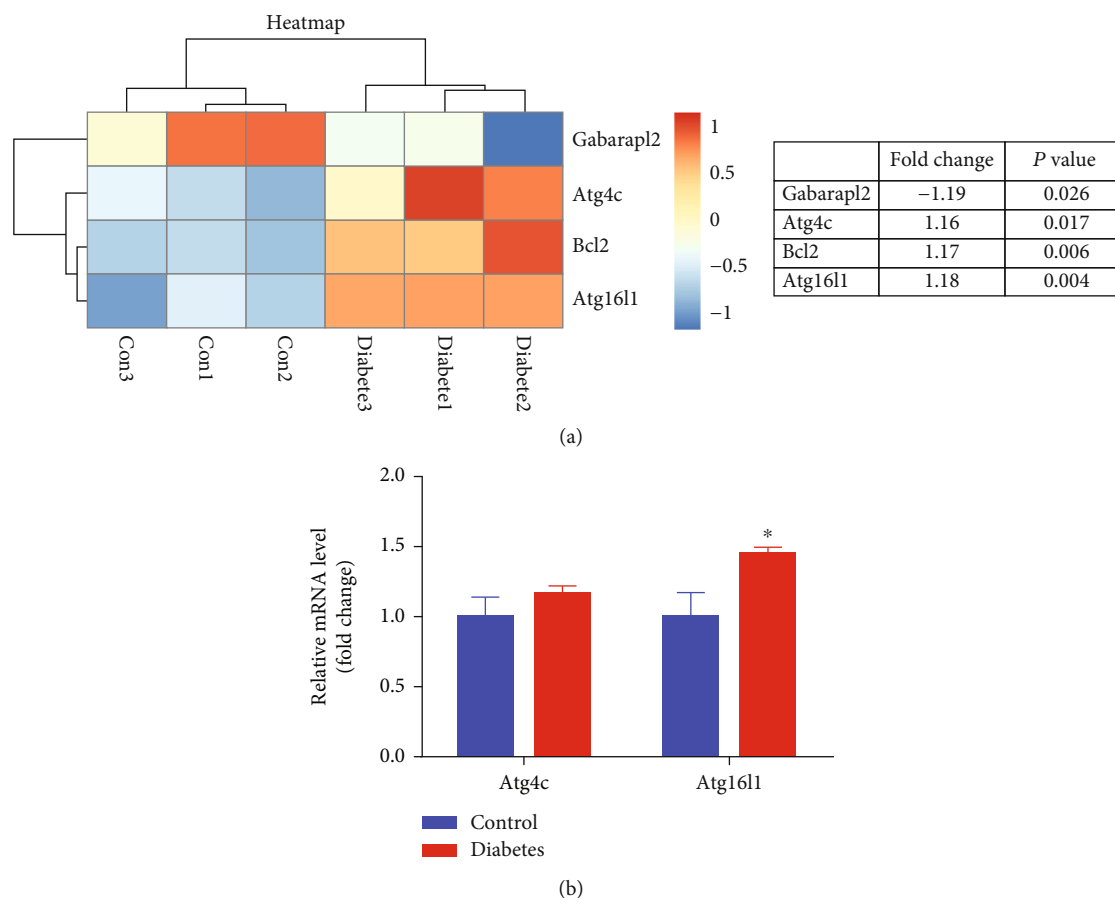


FIGURE 4: Differential expression of cell death-related genes between nondiabetic and diabetic retinas. (a) Heatmap from microarray analysis of gene expression related to the process of cell death. (b) qRT-PCR analysis was performed on the two genes involved in the process of autophagy. The results showed that, compared to control, Atg16L1 was significantly upregulated while Atg4c expression was unchanged in diabetic retinas.

In conclusion, we identified dysregulated autophagy genes involved in DR by microarray analyses. Atg16L1 may be a potential biomarker for the diagnosis and prognosis of DR. It may serve as a potential therapeutic target blocking and slowing DR progression. Future work is required to confirm these findings and elucidate the specific underlying molecular signaling mechanisms.

Data Availability

The data used to support the findings of this study are available from the corresponding authors upon request.

Disclosure

Our results have been accepted to be presented at the Association for Research in Vision and Ophthalmology (ARVO) Annual Meeting in 2020.

Conflicts of Interest

All authors declare that there are no conflicts of interest regarding the publication of this paper.

Authors' Contributions

All authors have significantly contributed in the present review. All authors are in agreement with the content of the manuscript.

Acknowledgments

This study was funded by Beijing Natural Science Foundation (Grant No. 7192049) and China Postdoctoral Science Foundation (Grant No. 2016M600107).

References

- [1] D. A. Antonetti, R. Klein, and T. W. Gardner, "Diabetic retinopathy," *The New England Journal of Medicine*, vol. 366, no. 13, pp. 1227–1239, 2012.
- [2] A. W. Stitt, T. M. Curtis, M. Chen et al., "The progress in understanding and treatment of diabetic retinopathy," *Progress in Retinal and Eye Research*, vol. 51, pp. 156–186, 2016.
- [3] M. Whitehead, S. Wickremasinghe, A. Osborne, P. Van Wijngaarden, and K. R. Martin, "Diabetic retinopathy: a complex pathophysiology requiring novel therapeutic strategies," *Expert Opinion on Biological Therapy*, vol. 18, no. 12, pp. 1257–1270, 2018.

- [4] J. F. Rivera, S. Costes, T. Gurlo, C. G. Glabe, and P. C. Butler, "Autophagy defends pancreatic beta cells from human islet amyloid polypeptide-induced toxicity," *The Journal of Clinical Investigation*, vol. 124, no. 8, pp. 3489–3500, 2014.
- [5] R. A. Nixon, "The role of autophagy in neurodegenerative disease," *Nature Medicine*, vol. 19, no. 8, pp. 983–997, 2013.
- [6] M. P. Ordonez, "Defective mitophagy in human Niemann-Pick type C1 neurons is due to abnormal autophagy activation," *Autophagy*, vol. 8, pp. 1157–1158, 2014.
- [7] P. Boya, L. Esteban-Martínez, A. Serrano-Puebla, R. Gómez-Sintes, and B. Villarejo-Zori, "Autophagy in the eye: development, degeneration, and aging," *Progress in Retinal and Eye Research*, vol. 55, pp. 206–245, 2016.
- [8] J. M. Lopes de Faria, D. A. Duarte, C. Montemurro, A. Papadimitriou, S. R. Consonni, and J. B. Lopes de Faria, "Defective autophagy in diabetic retinopathy," *Investigative Ophthalmology & Visual Science*, vol. 57, no. 10, pp. 4356–4366, 2016.
- [9] J. D. Hoheisel, "Microarray technology: beyond transcript profiling and genotype analysis," *Nature Reviews. Genetics*, vol. 7, no. 3, pp. 200–210, 2006.
- [10] I. Piano, E. Novelli, L. Della Santina, E. Strettoi, L. Cervetto, and C. Gargini, "Involvement of autophagic pathway in the progression of retinal degeneration in a mouse model of diabetes," *Frontiers in Cellular Neuroscience*, vol. 10, p. 42, 2016.
- [11] W. Wang, Q. Wang, D. Wan et al., "Histone HIST1H1C/H1.2 regulates autophagy in the development of diabetic retinopathy," *Autophagy*, vol. 13, no. 5, pp. 941–954, 2017.
- [12] M. A. Reddy, Z. Chen, J. T. Park et al., "Regulation of inflammatory phenotype in macrophages by a diabetes-induced long noncoding RNA," *Diabetes*, vol. 63, no. 12, pp. 4249–4261, 2014.
- [13] B. Yan, Z. F. Tao, X. M. Li, H. Zhang, J. Yao, and Q. Jiang, "Aberrant expression of long noncoding RNAs in early diabetic retinopathy," *Investigative Ophthalmology & Visual Science*, vol. 55, no. 2, pp. 941–951, 2014.
- [14] K. Ishikawa, S. Yoshida, Y. Kobayashi et al., "Microarray analysis of gene expression in fibrovascular membranes excised from patients with proliferative diabetic retinopathy," *Investigative Ophthalmology & Visual Science*, vol. 56, no. 2, pp. 932–946, 2015.
- [15] P. Chai, H. Ni, H. Zhang, and X. Fan, "The evolving functions of autophagy in ocular health: a double-edged sword," *International Journal of Biological Sciences*, vol. 12, no. 11, pp. 1332–1340, 2016.
- [16] D. Fu, J. Y. Yu, S. Yang et al., "Survival or death: a dual role for autophagy in stress-induced pericyte loss in diabetic retinopathy," *Diabetologia*, vol. 59, no. 10, pp. 2251–2261, 2016.
- [17] H. Shi, Z. Zhang, X. Wang et al., "Inhibition of autophagy induces IL-1 β release from ARPE-19 cells via ROS mediated NLRP3 inflammasome activation under high glucose stress," *Biochemical and Biophysical Research Communications*, vol. 463, no. 4, pp. 1071–1076, 2015.
- [18] E. Zavodszky, M. Vicinanza, and D. C. Rubinsztein, "Biology and trafficking of ATG9 and ATG16L1, two proteins that regulate autophagosome formation," *FEBS Letters*, vol. 587, no. 13, pp. 1988–1996, 2013.
- [19] B. C. King, K. Kulak, U. Krus et al., "Complement component C3 is highly expressed in human pancreatic islets and prevents β cell death via ATG16L1 interaction and autophagy regulation," *Cell Metabolism*, vol. 29, no. 1, pp. 202–210.e6, 2019.
- [20] B. C. King, E. Renström, and A. M. Blom, "Intracellular cytosolic complement component C3 regulates cytoprotective autophagy in pancreatic beta cells by interaction with ATG16L1," *Autophagy*, vol. 15, no. 5, pp. 919–921, 2019.

Research Article

Diabetic Macular Edema Treatment with Bevacizumab Does Not Depend on the Retinal Nonperfusion Presence

Bogumiła Sędziak-Marcinek ¹, Sławomir Teper ¹, Elżbieta Chełmecka ²,
Adam Wylęgała ³, Mateusz Marcinek ⁴, Mateusz Bas ⁵ and Edward Wylęgała ¹

¹Chair and Department of Ophthalmology, Faculty of Medical Sciences in Zabrze, Medical University of Silesia, 40-760 Katowice, Poland

²Department of Statistics, Department of Instrumental Analysis, Faculty of Pharmaceutical Sciences in Sosnowiec, 41-200 Sosnowiec, Medical University of Silesia, Katowice, Poland

³Health Promotion and Obesity Management Unit, Department of Pathophysiology, Faculty of Medical Sciences in Katowice, Medical University of Silesia, 40-728 Katowice, Poland

⁴Department of Urology, Faculty of Medical Sciences in Katowice, Medical University of Silesia, 40-760 Katowice, Poland

⁵Faculty of Biomedical Engineering, Silesian University of Technology, 41-800 Zabrze, Poland

Correspondence should be addressed to Bogumiła Sędziak-Marcinek; bogsedziak@gmail.com

Received 28 December 2020; Revised 7 February 2021; Accepted 14 February 2021; Published 27 February 2021

Academic Editor: Irini Chatziralli

Copyright © 2021 Bogumiła Sędziak-Marcinek et al. This is an open access article distributed under the Creative Commons Attribution License, which permits unrestricted use, distribution, and reproduction in any medium, provided the original work is properly cited.

This study evaluated the relationship between the retinal nonperfusion area (NPA) presence and the effectiveness of bevacizumab treatment (IVB) in patients with diabetic macular edema (DME). It also tested the prognostic usefulness of ultra-wide-field fluorescein angiography (UWFFA) and OptosAdvance software for diabetic retinopathy monitoring. Eighty-nine patients with DME with a macular central subfield thickness (CST) $\geq 250 \mu\text{m}$, with ($N = 49$ eyes) and without ($N = 49$ eyes) retinal NPA, underwent nine bevacizumab injections over 12 months. NPA distribution, leakage area distribution, microaneurysm (MA) count, macular CST, diabetic retinopathy severity, and best-corrected visual acuity (BCVA) were assessed. The results show that bevacizumab reduced the macular CST from 420 to 280 μm ($p < 0.001$) and improved BCVA ($p < 0.001$) by about 10 ETDRS letters in both groups of patients. Additionally, the therapy reduced total retinal NPA from 29 (14-36) mm^2 to 12 (4-18) mm^2 (Me (Q1-Q3); $p < 0.001$) in patients with diagnosed nonperfusion. The effect of the therapy measured with vascular leakage, MA count, $\text{BCVA}_{\text{relative}}$ and $\text{CST}_{\text{relative}}$ strongly depended on the zone of the retina and the NPA distribution. We conclude that the bevacizumab treatment had a positive effect on DME and BCVA in both study groups and on the size of retinal NPA in patients with retinal nonperfusion.

1. Introduction

Diabetic retinopathy (DR) is considered the most common microvascular complication of diabetes [1]. Some authors suggested that almost all T1DM (type 1 diabetes mellitus) patients would have some degree of retinopathy 20 years from T1DM diagnosis, as would more than 80% of insulin-treated T2DM (type 2 diabetes mellitus) patients and 50% of those not requiring insulin [2, 3]. The diabetic retinopathy lesions may occur in different areas of the retina influencing the severity and progression of this disease [4, 5]. It was

shown that the extent of capillary nonperfusion can increase from the peripapillary retina in ascending order and that the areas of nonperfusion occur in the midperiphery [4]. DR lesions first develop in the peripheral retina, and they are predominantly associated with a significantly larger area of retinal nonperfusion [4, 5]. Moreover, Silva et al. reported that the extent of capillary nonperfusion in the midperiphery increased as DR progressed [4].

The most common cause of vision loss in diabetic patients is diabetic macular edema (DME). DME is defined as a retinal thickening at the center of the macula or the

thickening approaching this center [6]. The pathophysiological process is related to a decrease in the retinal oxygen saturation, which makes retinal capillaries hyperpermeable [7]. The whole process is mediated by the upregulation of vascular endothelial growth factor (VEGF) and subsequent deterioration of retinal capillary autoregulation [7]. DME-related nonperfusion increases the risk of more complex ophthalmic disease development. Impaired macular perfusion is frequently asymptomatic until the later stages, leading to more acute and severe vision loss. Thus, it is essential to recognize and quantify these microvascular transformations to assess disease severity and implement optimal treatment protocol to prevent vision loss [8].

Bevacizumab (IVB) is a monoclonal, humanized, full-length antibody inhibiting vascular endothelial growth factor (VEGF). Currently, bevacizumab is widely used in DME treatment as an off-label drug [9–11].

Ultra-wide-field fluorescein angiography (UWFFA) allows producing high-resolution images with a 200° field view covering >80% of the retinal surface while traditional angiograms cover only 30–50° field view of the retina. The newest UWFFA stereographical images allow for correction of the inherent peripheral retinal distortion. This allows for accurate measurements of both posterior and peripheral areas of the retina [12–14]. UWFFA imaging has become the standard technique of peripheral nonperfusion assessment in retinal vascular diseases and is used to study the relationship between retinal nonperfusion and DME severity [4, 15].

In this study, we evaluated the relation between the retinal nonperfusion area presence and the effectiveness of bevacizumab treatment in patients with diabetic macular edema that were not subjected to the previous treatment. We also evaluated the usefulness of UWFFA imaging for prognostic purposes in patients with diabetic macular edema.

2. Materials and Methods

2.1. Permissions and Ethical Statements. The study was approved by the Ethics Committee of the Medical University of Silesia (decision KNW/0022/KB1/125/I/18/19). The study was conducted following the Declaration of Helsinki. The participants were informed about the study purpose, the study protocol, and the benefits and possible risks related to the study. The written consent had been obtained from all participants enrolled in the study.

2.2. Study Group. The participants were recruited from the ophthalmological outpatient clinic of the Clinical Department of Ophthalmology, Faculty of Medical Science, Medical University of Silesia. The inclusion and exclusion criteria in the study are presented in Table 1.

The patients' recruitment, diagnostics, and intravitreal treatment were carried out in the outpatient clinic throughout 2018–2020.

Based on studies by Ekinici et al. that reported CST changes after bevacizumab treatment [16], the necessary sample size for this study was calculated as 25 samples. Since the purpose of this study was to differentiate between the two

groups of subjects, with and without nonperfusion, a group of 98 patients was selected for the study: 49 with nonperfusion and 49 without nonperfusion. With this sample size, it was possible to meet the assumption of a minimum sample size for a significance level of 0.05 and a test power of 0.8.

2.3. Recruitment and Diagnostics of the Participants. Patients of the ophthalmological outpatient clinic were interviewed and initially examined during the routine appointment.

The interview consisted of a chart survey, and the following data were recorded: sex, age, type and duration of diabetes, serum glycosylated hemoglobin (HbA1c) level, and the following qualitative variables such as hypertension, current medication with blood thinners, and renal failure.

The initial examination was done with a slit lamp and was aimed at assessing the anterior and posterior segments of the eye.

2.3.1. Retinal Nonperfusion and Diabetic Macular Edema Diagnostics. The patients were subjected to further diagnostics to identify those with retinal nonperfusion and diabetic macular edema.

Ultra-wide-field fluorescein angiography (UWFFA) allowed analyzing the distribution of nonperfusion areas (NPA), distribution of leakage area, and microaneurysm (MA) count and assessing the severity of the diabetic retinopathy.

Swept-source optical coherence tomography (SS-OCT) enabled the assessment of diabetic macular edema by measuring central subfield thickness (CST).

The patients with DME and with central subfield thickness (CST) $\geq 250 \mu\text{m}$ were enrolled in the study and divided into two subgroups according to the retinal nonperfusion presence: patients with retinal nonperfusion ($N = 49$ eyes) and patients without retinal nonperfusion ($N = 49$ eyes). UWFFA and SS-OCT imaging allowed assessing the effectiveness of the bevacizumab treatment, monitoring the changes in retinal nonperfusion, and assessing the usefulness of UWFFA for retinal nonperfusion prognosis.

2.4. Bevacizumab Treatment Protocol. Ninety-eight eyes were qualified for bevacizumab treatment. The intravitreal injections were performed in the ophthalmological outpatient clinic of the Clinical Department of Ophthalmology of Faculty of Medical Science of the Medical University of Silesia. The injections were administered by an ophthalmologist. The eyes were locally anesthetized with proxymetacaine hydrochloride, disinfected with 5% iodine povidone, and then injected with 0.5 mg/0.05 ml bevacizumab (Avastin, Roche, Swiss). The first five injections were administered every month, and the next four injections were administered every two months. Each eye received 9 injections over 12 months to reach the loading dose of bevacizumab [11, 17, 18].

Before the first and one month after the last injection (on the 13th month of the study), the patients were subjected to the UWFFA and BCVA test. Also, before each injection, the central subfield thickness (CST) was measured to assess diabetic macular edema.

TABLE 1: The inclusion and exclusion criteria for patients with diabetic macular edema participating in the study evaluating the effectiveness of intravitreal bevacizumab treatment.

Inclusion criteria	Exclusion criteria
≥18 years old	Previous intravitreal anti-VEGF or steroid therapy
Diabetes mellitus type 1 or 2	Retinal photocoagulation
DME with CST ≥ 250 μm	History of pars plana vitrectomy or cataract surgery with posterior capsule rupture
Nonproliferative diabetic retinopathy	Media opacity disabling to assess the fundus of the eye
	Vitreoretinal traction in the macula
	Epiretinal membrane influencing BCVA
	Proliferative diabetic retinopathy
BCVA of 24-78 ETDRS letters	Systemic treatment influencing the retina or DME
	Nonperfusion of the foveal area
	Any concurrent nondiabetic retinal disease

Abbreviation: CST = central subfield thickness.

2.5. Diagnostic Methodology

2.5.1. Ultra-Wide-Field Fluorescein Angiography (UWFFA). Ultra-wide-field fluorescein angiography (UWFFA) images were obtained using the Optos California P200DTx (Optos, Dunfermline, Scotland, UK) scanning laser ophthalmoscope imaging system equipped with the OptosAdvance Software v4.2.31 (Figures 1(a) and 1(b)). The preparation and image analysis were done according to the methodology by Fan et al. and Fang et al. [19, 20].

(1) *Preparation.* The pupils were dilated by topical administration of tropicamide 1% (Polpharma, Starogard Gdański, Poland) and phenylephrine 2.5% to the conjunctival sac. Sodium fluorescein (250 mg; SERB, Paris, France) was administered intravenously *via* the median ulnar vein, and the images were captured at 45 s, 2 min, and 5 min of fluorescein angiography (early, middle, and late phase, respectively).

(2) *Image Analysis.* The images obtained for each eye were reviewed to check the image quality and its eligibility for the quantitative variables and diabetic retinopathy severity assessment.

The initial and after-treatment UWFFA images were analyzed by two trained UWFFA graders/ophthalmologists using OptosAdvance software v4.2.31 that allows for accurate measurements of the total visible retinal area in square millimeters (mm²) and adjusts for peripheral distortion. The graders were allowed to adjust the contrast and brightness to obtain optimal visualization. They analyzed each image and each step until a unanimous decision was reached. On the obtained UWFFA images, the graders manually delineated the peripheral extent of the visible retina—the total visible retina. The total visible retina was defined as the region where the blood vessels of the retina were visible and easily assessed for the capillary nonperfusion presence. The peripheral artifacts (i.e., eyelids and eyelashes) and the areas of poor image quality were excluded from this region. Pairs of

UWFFA images (initial and after treatment) were applied on top of each other so their surfaces were identical and to make sure that no errors in before- and after-treatment image analyses were possible. After the delineation of the total visible retina, the graders manually delineated the border of the nonperfusion area (NPA) and the leakage area.

(3) *Nonperfusion Area (NPA) Distribution.* The nonperfusion area was assessed using early phase UWFFA images (captured at 45 s of fluorescein angiography). First, the prespecified custom grid was applied to the images. The grid consisted of two circles of 10 and 15 mm radii, centered on the fovea. The circles divided the UWFFA image into three zones: a posterior (<10 mm radius), a midperiphery (10-15 mm radii), and a far periphery (>15 mm radius) (Figure 2). Then, the graders manually delineated the nonperfusion areas in the posterior, midperiphery, and far-periphery zones (Figure 3). The foveal area was excluded from the posterior zone analysis due to the possibility of bias. The nonperfusion area (NPA) was identified by the absence of retinal arterioles and/or capillaries with overall hypofluorescence relative to the overall background. Additionally, the image was compared to the respective fundus color image in search of intraretinal hemorrhages that could suppress fluorescence and simulate nonperfusion areas. Finally, the surface of nonperfusion areas in each zone was counted against the grid and expressed in square millimeters (mm²).

(4) *Leakage Area Distribution.* The leakage area distribution was assessed using the same prespecified grid and methodology as for the nonperfusion area distribution, but the leakage area was assessed using late phase UWFFA images (captured at 5 min of fluorescein angiography) and was identified by hyperfluorescence relative to the overall background (Figure 4). Basing on the leakage area distribution, we were able to distinguish between focal and diffuse DME. Focal DME is characterized by localized leakage from microaneurysms (MA), while in diffuse DME, the leakage involves the entire circumference of the fovea and the area has no clear edges [21].

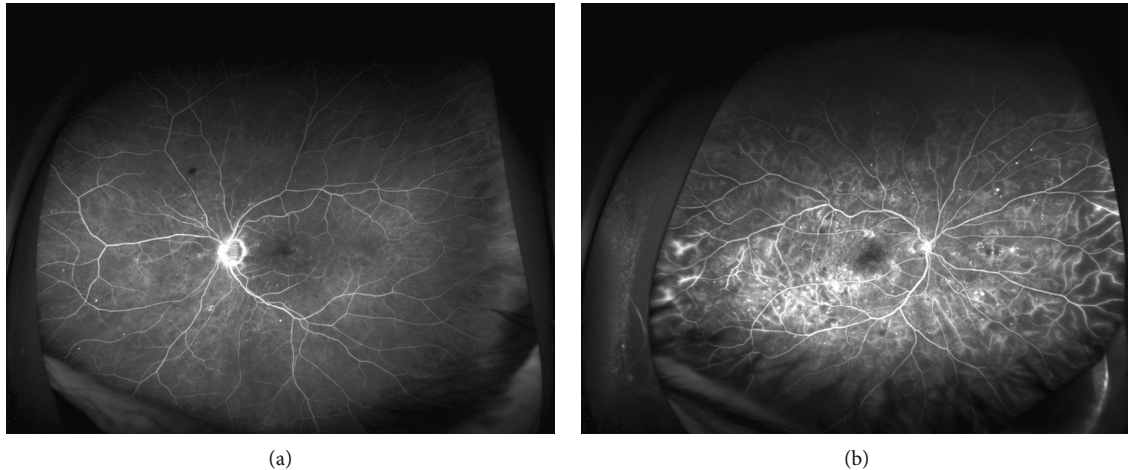


FIGURE 1: The ultra-wide-field fluorescein angiography (UWFFA) images of diabetic macular edema (DME) (a) without retinal nonperfusion and (b) with retinal nonperfusion. The images were obtained using the Optos California P200DTx scanning laser ophthalmoscope and the OptosAdvance Software v4.2.31.

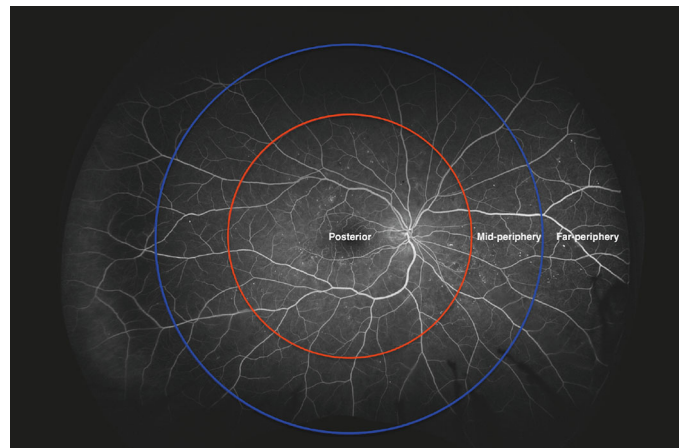


FIGURE 2: Zones of the retina relative to the center of the fovea: posterior zone (radius < 10 mm), midperiphery zone (radius = $10 - 15$ mm), and far-periphery zone (radius > 15 mm). The ultra-wide-field fluorescein angiography (UWFFA) image was obtained using the Optos California P200DTx scanning laser ophthalmoscope and the OptosAdvance Software v4.2.31.

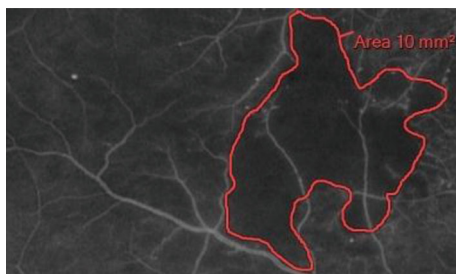


FIGURE 3: Nonperfusion area delineation and measurement on the ultra-wide-field fluorescein angiographic (UWFFA) image. The nonperfusion area is outlined in red. The size of the nonperfusion area (mm^2) was measured automatically using the OptosAdvance software v4.2.31.

(5) *Vascular Leakage Determination.* The vascular leakage was assessed using the late phase UWFFA images (captured at 5 min of fluorescein angiography) and the same prespecified grid as the one used for the NPA and leakage area distri-

bution. Vascular leakage was identified by late venous or arterial hyperfluorescence relative to the overall background (Figure 5).

(6) *Microaneurysm (MA) Count and Microaneurysm Segmentation.* The microaneurysm (MA) count was assessed using early phase UWFFA images (captured at 45 s of fluorescein angiography) (Figure 6). The MA count segmentation was performed with a fully automated algorithm platform developed for the study by Silesian University of Technology.

First, the input UWFFA image pairs were normalized for pixel intensity values, and the histograms were equalized. Then, masks of retinal blood vessels were generated using Hessian matrices and enhanced using mathematical morphology operations (closing and dilation). Structures that were too small to be classified as vessels were removed. Next, masks of microaneurysms were generated using



FIGURE 4: Leakage area delineation and measurement on the ultra-wide-field fluorescein angiographic (UWFFA) image. The leakage areas are outlined in blue. The size of leakage areas (mm^2) was measured automatically using the OptosAdvance software v4.2.31.

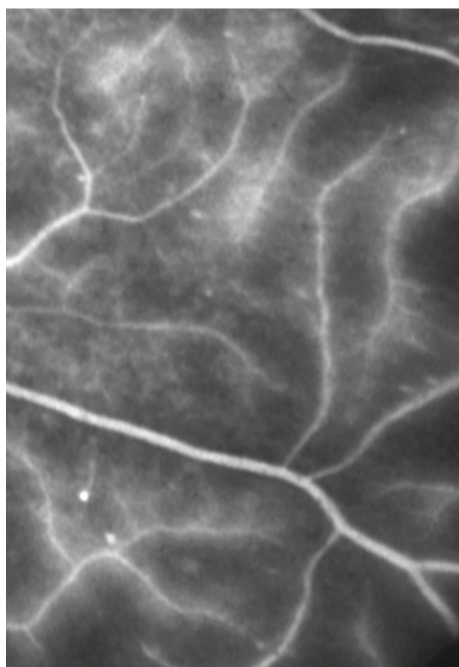


FIGURE 5: Vascular leakage on the ultra-wide-field fluorescein angiographic (UWFFA) image.

Hessian matrices. Masks of the retinal area were generated using previously prepared masks of retinal blood vessels. This way, the mask of the retinal area covered most of the retinal blood vessel range. The masks of microaneurysms with areas too large to be classified as microaneurysms were removed using mathematical morphology operations. Masks of microaneurysms that occurred on the retinal blood vessels or outside the retinal area were removed using previously obtained retinal blood vessel and retinal area masks. Finally, the microaneurysms occur-

ring in the posterior and peripheral parts of the retina were counted using the MATLAB® program (The MathWorks Inc., Natick, Massachusetts, USA).

(7) *Diabetic Retinopathy Severity*. The severity of diabetic retinopathy was assessed according to the diabetic retinopathy severity scale (DRSS) as mild, moderate, or severe nonperfusion diabetic retinopathy (NPDR) based on ultra-wide photograph of the fundus of the eye [22].

2.5.2. *Swept-Source Optical Coherence Tomography (SS-OCT)*. Swept-source optical coherence tomography images were obtained using the DRI OCT Triton tomograph (Topcon, Japan).

The images were taken using a 6×6 mm scanning protocol of a central macular field with an ETDRS grid to obtain thickness data. The central subfield thickness (CST; in μm) was defined as the retinal thickness at the fovea. The diabetic macular edema was diagnosed when CST was $\geq 250 \mu\text{m}$.

2.6. *Analysis of the Effectiveness of Bevacizumab Treatment in Particular Areas of the Retina in Patients with Retinal Nonperfusion*. To assess the effects of the therapy in each zone of the retina, the relative macular central subfield thickness ($\text{CST}_{\text{relative}}$) (equation (1)) and relative best-corrected visual acuity ($\text{BCVA}_{\text{relative}}$) (equation (2)) were calculated for patients with diagnosed retinal nonperfusion. For the remaining variables, an analogous, general formula of equation (3) was used:

$$\text{CST}_{\text{relative}} = \frac{\text{CST}_{\text{after therapy}} - \text{CST}_{\text{before therapy}}}{\text{CST}_{\text{before therapy}}} \cdot 100\%, \quad (1)$$

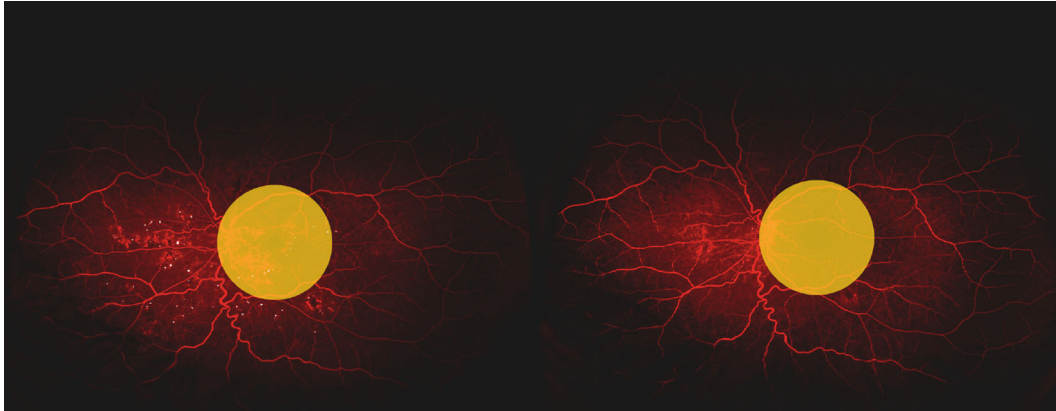


FIGURE 6: Microaneurysms (white dots) before bevacizumab therapy (left side) and after bevacizumab therapy (right side) counted by the automated platform. Yellow circles indicate the posterior retinal area. The ultra-wide-field fluorescein angiography (UWFFA) images were obtained using the Optos California P200DTx scanning laser ophthalmoscope and the OptosAdvance Software v4.2.31.

$$BCVA_{\text{relative}} = \frac{BCVA_{\text{after therapy}} - BCVA_{\text{before therapy}}}{BCVA_{\text{before therapy}}} \cdot 100\%, \quad (2)$$

$$\text{Variable}_{\text{relative}} = \frac{\text{variable}_{\text{after therapy}} - \text{variable}_{\text{before therapy}}}{\text{variable}_{\text{before therapy}}} \cdot 100\%. \quad (3)$$

2.7. Statistical Analysis. Qualitative variables are presented using the percentages. The χ^2 test was used to determine the relationship between nonmeasurable features, and then the odds ratio (OR), with 95% confidence intervals (CI), was calculated in case of a statistically significant relationship.

Quantitative variables are presented as mean and standard deviation (for data with normal distribution) or as median and lower-upper quartiles (for data with nonnormal or skewed distribution). Data distribution normality for quantitative characteristics at the beginning and at the end of the therapy was checked with the Shapiro-Wilk test and quantile plots and then the Student t -test for dependent samples or the nonparametric Wilcoxon pairwise test was used accordingly. In the central subfield thickness (CST) analysis, depending on the injection sequence number, an analysis of variance for repeated measurements with contrast analysis was used. The homogeneity of variances was checked with Levene's test. The variables with nonnormal distribution were analyzed using Friedman's ANOVA test. Whenever necessary, the normality of variables was improved using a logarithmic transformation. To determine the correlation between quantitative variables, Spearman's rank correlation coefficient was calculated. All statistical calculations were done using the Statistica v. 13.1 program (TIBCO, Palo Alto, USA), and statistical significance was set at $p < 0.05$.

3. Results

3.1. Retinal Nonperfusion Occurrence and Cooccurrence with Diabetic Retinopathy Parameters. Our analyses (please see

Table 2 for reference) showed that the occurrence of retinal nonperfusion was independent of gender ($p = 0.838$) and the treated eye ($p = 0.418$). However, it correlated with phakic eye presence ($p < 0.05$).

The occurrence of retinal nonperfusion was related to diffuse ($p < 0.001$) and focal ($p < 0.001$) macular edema presence. Diffuse macular edema was four times more frequent in patients with retinal nonperfusion (OR = 4.7, 95% CI: 2.0-11.0), while focal macular edema showed four times higher occurrence in patients without retinal nonperfusion (OR = 4.7, 95% CI: 2.0-11.0).

Similarly, our analyses showed that retinal nonperfusion was correlated with vascular leakage ($p < 0.001$ for all three examined zones: far-periphery, midperiphery, and posterior zones). We found that retinal nonperfusion increases the chance for a vascular leakage by about twenty-six times (OR = 26.4, 95% CI: 7.2-97.3) in the far-periphery zone of the retina, almost sixty times (OR = 58.8, 95% CI: 12.5-275.4) compared to that in the midperiphery zone and about five times compared to that in the posterior retina (OR = 5.2, 95% CI: 2.2-12.4).

Retinal nonperfusion also correlated with the severity of nonproliferative diabetic retinopathy (NPDR) ($p < 0.001$). Approximately half (51%) of each group of patients, with and without retinal nonperfusion, was diagnosed with moderate NPDR. Mild NPDR was observed more frequently in diabetic patients without observed retinal nonperfusion (49% vs. 4% for patients with retinal nonperfusion), whereas severe NPDR was observed in patients with diagnosed retinal nonperfusion (45% vs. 0% for patients without observed nonperfusion).

The occurrence of retinal nonperfusion was not related to the ongoing insulin ($p = 0.414$) or anticoagulant treatment ($p = 0.073$), the presence of hypertension ($p = 0.134$) or coronary heart disease ($p = 0.789$), and the elevated cholesterol levels ($p = 0.154$). However, it was negatively correlated with renal failure ($p < 0.05$). No patient without observed nonperfusion reported renal failure, and 14% of patients with retinal nonperfusion reported experiencing renal failure at any stage of diabetes.

TABLE 2: Comparison of diabetic retinopathy qualitative variables of patients with diabetic macular edema (DME) without ($N = 49$) or with ($N = 49$) diagnosed retinal nonperfusion qualified for intravitreal bevacizumab treatment. The results are presented as mean \pm standard deviation using the chi-squared (χ^2) test. Statistical significance was set at $p < 0.05$.

Variable	Variant	Patients without nonperfusion ($N = 49$)	Patients with nonperfusion ($N = 49$)	χ^2	p
Sex	Woman	29 (59%)	28 (57%)	0.04	0.838
	Man	20 (41%)	21 (43%)		
Eye	Right	21 (43%)	25 (51%)	0.66	0.418
	Left	28 (57%)	24 (49%)		
Lens status	Phakic	19 (39%)	31 (63%)	5.88	<0.05
	Pseudophakic	30 (61%)	18 (37%)		
Diabetic macular edema	Diffuse	16 (33%)	34 (69%)	13.23	<0.001
	Focal	33 (67%)	15 (31%)		
Vascular leakage (far-periphery zone)	Yes	3 (6%)	31 (63%)	35.31	<0.001
	No	46 (94%)	18 (37%)		
Vascular leakage (midperiphery zone)	Yes	2 (4%)	35 (71%)	47.28	<0.001
	No	47 (96%)	14 (29%)		
Vascular leakage (posterior zone)	Yes	17 (35%)	36 (73%)	14.83	<0.001
	No	32 (65%)	13 (27%)		
Nonproliferative diabetic retinopathy	Mild	24 (49%)	2 (4%)	40.62	<0.001
	Moderate	25 (51%)	25 (51%)		
	Severe	0 (0%)	22 (45%)		
Insulin treatment	Yes	26 (53%)	30 (61%)	0.67	0.414
	No	23 (47%)	19 (39%)		
Hypertension	Yes	36 (73%)	29 (59%)	2.24	0.134
	No	13 (27%)	20 (41%)		
Hypercholesterolemia	Yes	31 (63%)	24 (49%)	2.03	0.154
	No	18 (37%)	25 (51%)		
Coronary heart disease	Yes	8 (16%)	9 (18%)	0.07	0.789
	No	41 (84%)	40 (82%)		
Renal failure	Yes	0 (0%)	7 (14%)	—	<0.05
	No	49 (100%)	42 (86%)		
Anticoagulant treatment	Yes	7 (14%)	2 (4%)	3.22	0.073
	No	42 (86%)	47 (96%)		

Abbreviations: DME = diabetic macular edema.

All patients included in the study were suffering from type 2 diabetes mellitus. Our analyses showed that the patients without retinal nonperfusion differed in age from patients with retinal nonperfusion ($p < 0.05$), and they were on average 2.9 years older (95% CI: 0.1-5.8).

Body mass index (BMI) of the patients without retinal nonperfusion was the same as BMI of patients with retinal nonperfusion ($p = 0.736$), but these two groups of patients differed in the duration of type 2 diabetes mellitus (T2DM) ($p < 0.05$) and in the glycated hemoglobin (HbA1c) level ($p < 0.001$) (Table 3). Simultaneously, HbA1c level in patients with retinal nonperfusion was higher by about 0.5 mg/dl (95% CI: 0.3-0.7) as compared to patients without retinal nonperfusion.

3.2. Effect of Long-Term Bevacizumab Treatment on the Retinal Nonperfusion Areas. Forty-nine of the patients included in the study were diagnosed with retinal nonperfusion.

Our results show that intravitreal treatment with bevacizumab reduced the area of retinal nonperfusion in the patients with diabetic macular edema (DME). The area of the retinal nonperfusion was significantly smaller after 9 bevacizumab injections in the far-periphery ($p < 0.001$), midperiphery ($p < 0.001$), and posterior ($p < 0.001$) zones of the retina and in the total retinal area ($p < 0.001$) (Table 4).

Total area of retinal nonperfusion negatively correlated with BCVA (best-corrected visual acuity) before (high correlation, $\rho = -0.544$) and after (high correlation, $\rho = -0.500$)

TABLE 3: Comparison of diabetic retinopathy quantitative variables of patients with diabetic macular edema (DME) without ($N = 49$) or with ($N = 49$) diagnosed retinal nonperfusion qualified for long-term intravitreal bevacizumab treatment. t -test for two independent samples. The results are presented as mean \pm standard deviation. Statistical significance was set at $p < 0.05$.

Variable	Patients without nonperfusion ($N = 49$)	Patients with nonperfusion ($N = 49$)	t	p
Age (years)	70.0 \pm 5.5	67.1 \pm 8.4	2.02	<0.05
BMI (kg/m ²)	26.4 \pm 1.8	26.3 \pm 1.9	0.34	0.736
HbA1c serum concentration (mg/dl)	6.6 \pm 0.4	7.0 \pm 0.5	4.62	<0.001

Abbreviations: T2DM = type 2 diabetes mellitus; BMI = body mass index; HbA1c = glycated hemoglobin.

TABLE 4: Comparison of retinal nonperfusion area according to retinal zone before and after bevacizumab intravitreal treatment in patients with diabetic macular edema (DME) ($N = 49$) using the Wilcoxon signed-rank test. The results are presented as median (lower-upper quartile). Statistical significance was set at $p < 0.05$.

Nonperfusion area according to retinal zone (mm ²)	Before bevacizumab therapy	After bevacizumab therapy	$\Delta =$ before – after	Z	p
Total retinal area	29 (14-36)	12 (4-18)	12 (5-24)	5.86	<0.001
Far periphery	10 (0-23)	2 (0-10)	2 (0-11)	4.37	<0.001
Midperiphery	6 (3-10)	1 (0-4)	4 (1-8)	5.11	<0.001
Posterior	4 (1-11)	1 (0-5)	2 (0-5)	4.46	<0.001

bevacizumab treatment (Table 5). Reversely, total area of retinal nonperfusion positively correlated with macular central subfield thickness (CST). The correlation was high before ($\rho = 0.672$) and average after ($\rho = 0.493$) bevacizumab treatment. We found that a larger total area of retinal nonperfusion corresponded to a greater total microaneurysm (MA) count (average correlation, $\rho = 0.380$) and a greater MA count in the posterior retinal zone (average correlation, $\rho = 0.491$) before the treatment and after it (average correlation, $\rho = 0.482$ for total MA count; high correlation, $\rho = 0.588$ for MA count in the posterior retinal zone). Also, a greater total area of retinal nonperfusion corresponded to a greater total leakage area (high correlation, $\rho = 0.522$), far-periphery leakage area (average correlation, $\rho = 0.490$), and midperiphery leakage area (average correlation, $\rho = 0.450$) before bevacizumab treatment and after it (average correlation for all three parameters: $\rho = 0.468$, $\rho = 0.365$, and $\rho = 0.393$, respectively). There was no statistically significant correlation between the total area of retinal nonperfusion and the leakage area in the posterior zone of the retina ($p = 0.5255$).

In order to present the relationships between the analyzed variables, we calculated the relative parameters (Table 5) according to equation (3) presented in Section 2.6. We found that the decrease in the total area of retinal nonperfusion was related to the decrease in the macular CST (average correlation, $\rho = 0.340$), the decrease in total MA count (high correlation, $\rho = 0.554$), the decrease in the MA count in the posterior retinal zone (average correlation, $\rho = 0.479$), the decrease in the total leakage area (high correlation, $\rho = 0.607$), and the decrease in the leakage area in the posterior retinal zone (high correlation, $\rho = 0.541$). We also found that the decrease in the far-periphery nonperfusion area was accompanied by the decrease in the total MA count (average correlation, $\rho = 0.360$).

3.3. Effect of Long-Term Bevacizumab Treatment on Best-Corrected Visual Acuity (BCVA). We found that best-corrected visual acuity (BCVA) improved after bevacizumab treatment regardless of the retinal nonperfusion presence ($p < 0.001$) (Table 6). However, the analyses showed no effect of retinal nonperfusion ($p = 0.165$) and no interaction between the study time and retinal nonperfusion ($p = 0.935$) (Table 6). Analyzing each group of patients separately before and after bevacizumab treatment, we found no statistically significant differences in BCVA improvement ($p = 0.239$ and $p = 0.163$, respectively).

The analyses showed that the ETDRS score significantly depended on the therapy in both groups of patients with ($\chi^2 = 41.79$; $p < 0.001$) and without retinal nonperfusion ($\chi^2 = 35.93$; $p < 0.001$). The number of people showing the same change in BCVA test score was similar in both groups of patients ($\chi^2 = 1.21$; $p = 0.751$) (Table 7).

3.4. Effect of Bevacizumab Treatment on Macular Central Subfield Thickness (CST). The analyses of macular central subfield thickness (CST) showed that bevacizumab treatment reduced macular edema ($p < 0.001$), and this effect did not depend on retinal nonperfusion presence ($p = 0.859$) (Table 6). CST in patients with and without retinal nonperfusion was the same before ($p = 0.852$) and after ($p = 0.936$) bevacizumab treatment, when analyzed separately for each group (Table 6).

In the group of patients with diagnosed retinal nonperfusion, the administration of earlier doses of bevacizumab had a more substantial effect on macular CST reduction. We found significant differences in macular CST between patients with and without retinal nonperfusion. These differences were recorded for measurements taken at subsequent, early (from the 2nd to the 4th) appointments when following injections of the bevacizumab were administered. We could

TABLE 5: Spearman's rank correlation (Spearman's ρ) between examined parameters in the total retinal area and far-periphery retinal area before and after bevacizumab intravitreal treatment of patients with diabetic macular edema (DME) and with diagnosed retinal nonperfusion ($N = 49$). Statistical significance was set at $p < 0.05$.

Relative retinal nonperfusion area	Examined relative parameter	ρ	p
(Total retinal NPA) _{relative}	BCVA _{relative}	-0.071	0.631
	CST _{relative}	0.340	<0.05
	(Total MA count) _{relative}	0.554	<0.001
	(MA count in posterior) _{relative}	0.479	<0.001
	(Total leakage area) _{relative}	0.607	<0.001
	(Leakage area in far periphery) _{relative}	0.143	0.384
	(Leakage area in midperiphery) _{relative}	0.219	0.159
	(Leakage area posterior) _{relative}	0.541	<0.001
(Far – periphery NPA) _{relative}	BCVA _{relative}	0.037	0.835
	CST _{relative}	0.162	0.359
	(Total MA count) _{relative}	0.360	<0.05
	(MA count in posterior) _{relative}	0.337	0.051
	(Total leakage area) _{relative}	0.318	0.067
	(Leakage area in far periphery) _{relative}	0.256	0.181
	(Leakage area in midperiphery) _{relative}	0.106	0.583
	(Leakage area posterior) _{relative}	0.200	0.256

ρ : Spearman's rank correlation coefficient; BCVA: best-corrected visual acuity; CST: central subfield thickness; MA: microaneurysm; NPA: nonperfusion area.

observe the positive results of the bevacizumab treatment immediately after the first injection (Table 8).

3.5. Effect of Bevacizumab Treatment on Retinal Microaneurysm (MA) Count. Analysis of total MA count and MA count in the posterior zone of the retina showed statistically significant differences after the treatment (for both variables, $p < 0.001$), and retinal nonperfusion occurrence (for both variables, $p < 0.001$) (Table 6). We also found interactions between the treatment and retinal nonperfusion occurrence ($p < 0.001$ for total MA count and $p < 0.05$ for MA count in the posterior zone of the retina). Also, total MA count and MA count in the posterior zone of the retina recorded for patients with retinal nonperfusion before bevacizumab treatment were higher than in patients without retinal nonperfusion at the same time ($p < 0.001$). After the therapy, values for both variables decreased in both groups. In the case of total MA count, the values differed between both analyzed groups ($p < 0.001$), while for MA count in the posterior zone of the retina, the values were similar in both analyzed groups ($p = 0.077$) (Table 6). We conclude that bevacizumab therapy was equally effective for diabetic patients with and without retinal nonperfusion, when assessed with MA count in the posterior zone of the retina.

3.6. Effect of Bevacizumab Treatment on Leakage Area. Our analyses showed statistically significant differences in total leakage area before and after bevacizumab treatment

($p < 0.001$) (Table 6). Differences resulting from retinal nonperfusion occurrence ($p < 0.001$) were found regardless of the treatment, and no interaction between the treatment and nonperfusion occurrence was recorded ($p = 0.086$). Significantly higher values of total leakage area were noted in the group of patients with retinal nonperfusion before bevacizumab treatment ($p < 0.001$), and this tendency was noted when comparing the two groups after the treatment ($p < 0.001$).

Analyses for the far-periphery zone showed a significant reduction in leakage area in both groups of patients ($p < 0.05$ for patients with nonperfusion; $p < 0.001$ for patients without nonperfusion) (Table 6). Patients with retinal nonperfusion had a larger leakage area in the far-periphery zone before bevacizumab treatment when compared to the group of patients without retinal nonperfusion ($p < 0.001$), while after the treatment, the leakage areas did not differ statistically ($p = 0.83$, Table 6).

The leakage area in the midperiphery and posterior zones of the retina before and after bevacizumab treatment differed significantly between the groups (for both variables and groups, $p < 0.001$). The treatment reduced the leakage area in each of the analyzed zones in both groups of patients. Also, the leakage areas in the midperiphery ($p < 0.001$) and posterior zones of the retina ($p < 0.001$) were always (before and after the treatment) larger in the group of patients diagnosed with retinal nonperfusion (for the midperiphery zone before and after treatment, $p < 0.001$; for the posterior zone before treatment, $p < 0.001$; and after treatment, $p < 0.05$) (Table 6).

TABLE 6: Comparison of examined parameters of patients with diabetic macular edema (DME) without ($N = 49$) or with ($N = 49$) diagnosed retinal nonperfusion before and after intravitreal bevacizumab treatment using two-way analysis of variance. The results are presented as mean \pm standard deviation or median (lower-upper quartile). Statistical significance was set at $p < 0.05$.

Examined parameters	Study group	Before bevacizumab therapy	After bevacizumab therapy	P_{time}	$P_{\text{nonperfusion}}$	$P_{\text{interactions}}$
BCVA (ETDRS letters)	Patients <i>without</i> nonperfusion	68.0 \pm 7.3	76.8 \pm 5.6	<0.001	0.165	0.935
	Patients <i>with</i> nonperfusion	66.1 \pm 8.7	74.7 \pm 8.4			
	$P_{\text{without nonperfusion vs. with nonperfusion}}$	0.239	0.163			
CST (μm)	Patients <i>without</i> nonperfusion	419.3 \pm 86.1	287.3 \pm 49.7	<0.001	0.859	0.888
	Patients <i>with</i> nonperfusion	422.7 \pm 94.8	288.2 \pm 58.3			
	$P_{\text{without nonperfusion vs. with nonperfusion}}$	0.852	0.936			
Total MA count (N)	Patients <i>without</i> nonperfusion	115.4 \pm 35.5	71.1 \pm 32.1	<0.001	<0.001	<0.001
	Patients <i>with</i> nonperfusion	188.2 \pm 60.7	109.9 \pm 50.7			
	$P_{\text{without nonperfusion vs. with nonperfusion}}$	<0.001	<0.001			
MA count (N)—posterior zone	Patients <i>without</i> nonperfusion	84.7 \pm 31.1	48.1 \pm 27.9	<0.001	<0.001	<0.05
	Patients <i>with</i> nonperfusion	117.1 \pm 49.2	59.8 \pm 36.0			
	$P_{\text{without nonperfusion vs. with nonperfusion}}$	<0.001	0.077			
Total leakage area (mm^2)*	Patients <i>without</i> nonperfusion	18.0 (12.0-24.0)	4.0 (2.0-6.0)	<0.001*	<0.001	0.086
	Patients <i>with</i> nonperfusion	60.0 (32.0-107.0)	11.0 (4.0-16.0)			
	$P_{\text{without nonperfusion vs. with nonperfusion}}$	<0.001	<0.001			
Leakage area in far-periphery zone (mm^2)	Patients <i>without</i> nonperfusion	0.0 (0.0-0.0)	0.0 (0.0-0.0)	<0.05	—	—
	Patients <i>with</i> nonperfusion	8.0 (2.0-23.0)	0.0 (0.0-1.0)			
	$P_{\text{without nonperfusion vs. with nonperfusion}}$	<0.001	0.083			
Leakage area in midperiphery zone (mm^2)	Patients <i>without</i> nonperfusion	0.0 (0.0-3.0)	0.0 (0.0-0.0)	<0.001		
	Patients <i>with</i> nonperfusion	11.0 (4.0-25.0)	2.0 (0.0-4.0)			
	$P_{\text{without nonperfusion vs. with nonperfusion}}$	<0.001	<0.001			
Leakage area in posterior zone (mm^2)**	Patients <i>without</i> nonperfusion	16.0 (9.0-21.0)	4.0 (2.0-6.0)	<0.001		
	Patients <i>with</i> nonperfusion	24.0 (16.0-69.0)	6.0 (3.0-12.0)			
	$P_{\text{without nonperfusion vs. with nonperfusion}}$	<0.001	<0.05			

*Two-way ANOVA after log transformation of variables. **The Friedman test. BCVA: best-corrected visual acuity; CST: central subfield thickness; ETDRS: Early Treatment Diabetic Retinopathy Study; MA: microaneurysm.

TABLE 7: Change in best-corrected visual acuity (BCVA) of patients with diabetic macular edema (DME) without ($N = 49$) or with ($N = 49$) diagnosed retinal nonperfusion before and after bevacizumab treatment. The results are presented as the number of patients showing the change.

Change in BCVA	Patients without nonperfusion	Patients with nonperfusion
Deterioration	0	1
No improvement	11	9
Improvement by 10 ETDRS letters (1 aggregated unit)	33	34
Improvement by 20 ETDRS letters (2 aggregated units)	5	5

Abbreviations: BCVA = best-corrected visual acuity; ETDRS = Early Treatment Diabetic Retinopathy Study.

3.7. *Effect of Bevacizumab Treatment in Particular Areas of the Retina in Patients with Retinal Nonperfusion.* We found a high positive correlation between the treatment effect assessed with the BCVA test and the total area of nonperfu-

sion ($p < 0.001$) (Table 9), and average positive correlations with the NPA in the far-periphery and the midperiphery zones of the retina ($p < 0.01$ for both zones). Simultaneously, we noted statistically significant highly negative correlation

TABLE 8: Central subfield thickness (CST) at the fovea of the retina in patients with diabetic macular edema (DME) without ($N = 49$) or with ($N = 49$) retinal nonperfusion during subsequent intravitreal bevacizumab (0.5 mg/0.05 ml) injections. The results are presented as mean \pm standard deviation. Statistical significance was set at $p < 0.05$.

Time of therapy (months)	Bevacizumab injection no	CST (μm) in patients without nonperfusion ($N = 49$)	CST (μm) in patients with nonperfusion ($N = 49$)	$P_{\text{without nonperfusion vs. with nonperfusion}}$
0	I	419.3 \pm 86.1	422.7 \pm 94.8	0.852
1	II	376.8 \pm 79.7	344.8 \pm 78.4	<0.05
2	III	358.4 \pm 71.8	316.3 \pm 74.5	<0.01
3	IV	341.0 \pm 75.5	307.5 \pm 77.7	<0.05
4	V	316.8 \pm 56.9	297.8 \pm 62.7	0.120
6	VI	300.5 \pm 62.0	299.3 \pm 75.3	0.930
8	VII	293.0 \pm 55.4	298.0 \pm 71.4	0.704
10	VIII	293.0 \pm 55.4	292.7 \pm 61.5	0.871
12	IX	287.3 \pm 49.7	288.2 \pm 58.3	0.936

Abbreviation: CST = central subfield thickness.

TABLE 9: Spearman's rank correlation (Spearman's ρ) between relative best-corrected visual acuity ($\text{BCVA}_{\text{relative}}$), relative central subfield thickness ($\text{CST}_{\text{relative}}$), and zone of the retina in patients with diabetic macular edema (DME) with ($N = 49$) diagnosed retinal nonperfusion qualified for intravitreal bevacizumab treatment. Statistical significance was set at $p < 0.05$.

	Zone of retinal nonperfusion before therapy	ρ	p
$\text{BCVA}_{\text{relative}}$ (%)	Total area of the retina	0.589	<0.001
	Far periphery	0.402	<0.01
	Midperiphery	0.441	<0.01
	Posterior	0.045	0.760
$\text{CST}_{\text{relative}}$ (%)	Total area of the retina	-0.614	<0.001
	Far periphery	-0.432	<0.01
	Midperiphery	-0.427	<0.01
	Posterior	-0.048	0.740

ρ : Spearman's rank correlation coefficient.

between the treatment effect assessed with macular central subfield thickness (CST) and the total area of retinal nonperfusion ($p < 0.001$), and average negative correlations with the NPA in the far-periphery and midperiphery retinal zones ($p < 0.01$ for both zones). The treatment effect assessed with relative BCVA and relative CST did not correlate with the retinal nonperfusion area in the posterior zone of the retina ($p = 0.760$ and $p = 0.740$, respectively). The effect of bevacizumab treatment did not depend on the area of nonperfusion in the posterior zone of the retina, and it was positive regardless of the size of the nonperfusion area.

4. Discussion

In this study, we analyzed the relation between the size of retinal nonperfusion areas (NPA) and the effectiveness of 12-month intravitreal bevacizumab (IVB) therapy in patients with treatment-naïve diabetic macular edema (DME). The effectiveness of the treatment was assessed using ultra-

wide-field fluorescein angiography (UWFFA) and swept-source optical coherence tomography (SS-OCT). The results showed that (i) retinal NPA decreased in the far-periphery, midperiphery, and posterior zones of the retina during bevacizumab treatment in patients with DME; (ii) there was no progression of diabetic retinopathy in patients with DME after the bevacizumab treatment; (iii) the size of retinal NPA was associated with diabetic retinopathy severity, but bevacizumab treatment stabilized or reversed it; (iv) patients with DME responded well to bevacizumab treatment regardless of the presence of retinal nonperfusion—retinal nonperfusion did not affect the efficacy of bevacizumab treatment aimed at reducing DME; (v) peripheral retinal nonperfusion did not affect the pattern of visual acuity, the severity of DME, and the efficacy of bevacizumab therapy; (vi) bevacizumab treatment was equally effective in treating microaneurysms in the posterior zone of the retina in patients with and without retinal nonperfusion; (vii) patients with retinal nonperfusion were more frequently diagnosed with diffuse macular edema, while patients without retinal nonperfusion were diagnosed with focal macular edema; (viii) retinal nonperfusion was associated with vascular leakage; and (ix) patients with retinal nonperfusion had faster progression of diabetic retinopathy compared to patients without retinal nonperfusion and higher HbA1c (glycated hemoglobin) levels.

The UWFFA effectively detects the peripheral retinal nonperfusion that correlates with increased risk of DME in patients with diabetic retinopathy (DR) [23, 24]. In this study, we used UWFFA with a 200° field view in a single image. We demonstrated that intravitreal bevacizumab treatment strongly reduced the NPA in the far-periphery, midperiphery, and posterior zones of the retina in the analyzed groups of patients with DME, when comparing the results before and after the treatment. The most effective changes in NPA occurred in the midperiphery zone of the retina. Xue et al. also reported a positive response to 4-month anti-VEGF treatment with ranibizumab in patients with DME with significant peripheral retinal nonperfusion. They observed that the reduction of absolute and relative central

retinal thickness was associated with the number of microaneurysms, peripheral nonperfusion, and neovascularization [25]. Wykoff et al. showed that aflibercept treatment not only slowed the worsening of retinal perfusion but also improved it in some cases by decreasing areas of retinal nonperfusion [26]. Since Yoo et al. observed that macular edema recurred in 65.1% of the eyes after initial bevacizumab (IVB) injection [27], we hope that our approach (9 injections over 12 months) will ensure long-lasting effects in the studied groups of patients. We observed that macular CST significantly decreased after three initial doses of bevacizumab, more in patients with retinal NPA than in patients without NPA. The next doses maintained the reductive effect of bevacizumab, but we would need to investigate further if the effect lasts after this 12-month treatment. The odds are high as Cai et al. proved the therapeutic efficiency of anti-VEGF agents injected 9-10 times during the first year and 5-6 times during the second year of DME treatment [18].

UWFFA showed that peripheral retinal nonperfusion did not affect the best-corrected visual acuity (BCVA), the severity of DME, and the efficacy of bevacizumab treatment. The total NPA was highly positively correlated with macular CST (central subfield thickness) and highly negatively correlated with BCVA in the group of patients with retinal nonperfusion. BCVA after the treatment was better both in patients without retinal nonperfusion and with retinal nonperfusion, but the effects of the therapy did not differ significantly between the analyzed groups. Bevacizumab treatment applied in our study had a positive effect on visual acuity. This does not correspond with other studies reporting that macular NPA may have hindered the visual acuity in patients with DME 3 months after intravitreal bevacizumab injections [28]. The difference may result from a different time at which the visual acuity was evaluated. In our study, we evaluated it one month after the last bevacizumab injection. Nevertheless, other reports confirm that a thoroughly selected approach offers the opportunity to individualize management while minimizing the burden of the treatment [29–31].

Our study showed that bevacizumab treatment reduced macular CST, but the effect was independent of the NPA presence. Intergroup comparison between patients with retinal nonperfusion and those without it showed no difference in macular CST between these groups before and after bevacizumab treatment. Mushtaq et al. also demonstrated a significant improvement in central retinal thickness after bevacizumab treatment. They reported that the greatest improvement was observed in the group of patients with central retinal thickness $> 400 \mu\text{m}$ [32]. Other authors, like Yoo et al. [27], studying patients with branch retinal vein occlusion with nonperfusion larger than a 0.5 mm ETDRS (Early Treatment Diabetic Retinopathy Study) circle zone or with an initial central retinal thickness $> 570 \mu\text{m}$, noticed that these patients should be closely monitored after the treatment. Their results showed that macular edema recurred within six months after a single bevacizumab injection in most patients [27]. This agrees with our observation that a more frequent injection regimen is a key factor for the positive outcome of the treatment. The other studies showed that bevacizumab treatment resulted in a better visual outcome

regardless of initial macular edema and initial central macular thickness but only at 6 weeks [33]. In our study, the average macular CST in both analyzed groups before bevacizumab treatment was $> 400 \mu\text{m}$; after bevacizumab treatment, it was $< 300 \mu\text{m}$. This change was accompanied by an improvement in the BCVA score by about 10 ETDRS letters also in both analyzed groups. More importantly, the effects of bevacizumab treatment on DME reduction did not depend on the retinal nonperfusion presence. First doses of bevacizumab had a more substantial effect on macular CST reduction in patients with retinal nonperfusion: macular CST was lower in patients with retinal nonperfusion than in patients without nonperfusion after injections I-III, and this pattern was not observed after injections IV-IX. The randomized clinical trials examining severe disease reported a significant improvement in BCVA and reduction of central macular thickness after three intravitreal injections with bevacizumab. However, the effect decreased gradually as both measured variables returned to near-baseline values 3 months after the last intravitreal injection [34]. Several reports indicate that bevacizumab injections may have a beneficial effect on macular thickness and visual acuity in diffuse DME [35]. According to authors, bevacizumab monotherapy improves visual function, measured by fluorescein angiography and optical coherence tomography, and stabilizes diabetic macular edema [35]. On the contrary, Jeon and Lee reported that continuous intravitreal bevacizumab monotherapy had no beneficial effect on visual acuity and the number of hard exudates 6 months after the patients with DME with subfoveal and perifoveal hard exudates completed the treatment. In that study, anti-VEGF treatment did not facilitate lipid or proteinaceous material resorption, which would be the expected effect of treatment, as hard exudates are related to photoreceptor and neuronal degeneration in the outer plexiform layer and their presence increases the risk of visual impairment [36].

DME occurs when the barrier between the blood and the retina is damaged and vascular fluid and proteins leak and accumulate in the macula. Studies show that DME is related to microaneurysm (MA) and retinal leakage presence. It is known that both changes present similar spatial distribution in the retina. This indicates that leakage emerges from strongly hyperpermeable microaneurysms in the course of diabetic retinopathy [37]. Our results showed that the size of NPA was related to the total microaneurysm (MA) count and MA count in the posterior zone of the retina. The total MA count in both groups of patients was related to the treatment duration, nonperfusion presence, and interaction between those two factors. We observed a significant reduction in the total MA count before and after therapy. The effect of bevacizumab treatment was significantly stronger in patients with retinal nonperfusion than in patients without it. However, when it comes to MA count in the posterior zone of the retina, we can conclude that the bevacizumab treatment was equally effective for patients with and without retinal nonperfusion.

Additionally, we noted that an increase in the total nonperfusion area (NPA) had an impact on the increase in the total leakage, far-periphery leakage, and midperiphery

leakage areas. We found that retinal nonperfusion was related to peripheral and posterior vascular leakage. Feng et al. reported that the nonproliferative diabetic retinopathy with leakage (expressed with leakage index) varied depending on the region of the retina and between them. They also noted that the leakage index decreased as the distance from the fovea increased. The highest leakage was observed in the posterior and midperiphery zones of the retina [38]. Silva et al. observed the greatest amount of nonperfusion in the midperiphery zone of the retina [4]. On the contrary, Kristinsson et al. [39] observed that nonproliferative retinopathy with leakage was more extensive in the posterior zone of the retina than in its peripheral zones. The posterior part of the retina has the highest vascular density which translates to higher overall metabolic activity. These features make this region of the retina more susceptible to leakage [39]. In our study, the leakage was higher in the group of patients with nonperfusion than in the group of patients without it. Bevacizumab treatment significantly reduced vascular leakage, which acknowledged the efficiency of anti-VEGF treatment in patients with DME. Niki et al. also reported that an early stage of diabetic retinopathy, which in this case is nonproliferative diabetic retinopathy without leakage, was more extensive in the midperiphery than in other regions of the retina [5]. This finding agreed with previous analyses of overall nonproliferative diabetic retinopathy. The analyses showed that the condition is usually first recognized in the midperiphery zone of the retina. The authors suggested that the midperipheral retina in diabetic eyes may be more prone to develop capillary closure than its posterior part [5, 40].

Our analyses of UWFFA images showed that diffuse macular edema was more frequent in patients with retinal nonperfusion, while focal macular edema was more frequent in patients without retinal nonperfusion. This explains the fact that both the leakage area and the MA count were higher in patients with retinal nonperfusion than in patients without it. The diffuse macular edema was responding well to bevacizumab treatment. Bevacizumab treatment reduced vascular leakage in patients with retinal nonperfusion; thus, it can be considered an effective treatment in this group of patients.

Our study showed that diabetic retinopathy did not progress in patients with diagnosed DME after 9 injections (12 months) of bevacizumab treatment. We can conclude that patients with retinal nonperfusion present faster progress of the disease when compared to patients without retinal nonperfusion. In our study, the retinal nonperfusion was related to the diabetic retinopathy severity, but bevacizumab treatment stabilized it or even reversed it. This agrees with other studies that reported the usefulness of bevacizumab intravitreal injection in DME reduction. The studies reported that consecutive bevacizumab monotherapy, or combined with intravitreal triamcinolone, resulted in anatomic and functional improvement of the retina, and the results were compared with macular focal or grid laser photocoagulation [33, 41]. Another semiquantitative study, in a small series of patients with DR, showed that unselective intravitreal bevacizumab treatment improved peripheral nonperfusion in the short term [42]. Cataract surgery combined with bevacizumab injections seems to be an effective treatment option in

patients with coexisting diabetic retinopathy [38]. Bevacizumab treatment administered immediately after cataract surgery represents a safe and effective strategy: it prevents postoperative macular thickening or reduces macular edema, and it improves average visual acuity in diabetic patients [43].

In this study, we used UWFFA to evaluate the effectiveness of bevacizumab treatment in two groups of patients suffering from diabetic retinopathy and diabetic macular edema (DME): one group with retinal nonperfusion and another group without. The strict regimen of intravitreal injections was equally effective in both analyzed groups of patients, which is very important for proper ophthalmic management. Many reports compared therapeutic bevacizumab injections with retina laser therapy and injections combined or laser therapy alone. Peripheral retinal laser photocoagulation may be performed only if the nonperfusion areas are present. The procedure significantly reduces retinal nonperfusion but leaves the retina with many coagulated spots after laser application, which causes local destruction of the retina. In this study, the strict regimen of bevacizumab injections decreased DME and diabetic retinopathy severity in both groups of patients, one with retinal nonperfusion and the other without. Additionally, no macular grid laser photocoagulation was needed during this intensive course of treatment. However, it can be expected that some patients would need it in the future. UWFFA, as a modern diagnostic method, allowed us to give a better prognosis to patients treated with anti-VEGF with retinal nonperfusion. The main limitations of this study are connected to the number of patients qualified for the study and the lack of information about the long-term effects of the treatment.

5. Conclusions

The strict regimen of bevacizumab injections decreased diabetic macular edema (DME) and the severity of diabetic retinopathy in two groups of patients, one with retinal nonperfusion and the other without. The applied protocol of bevacizumab reduced the retinal nonperfusion areas. Patients without retinal nonperfusion showed no progression in diabetic retinopathy. UWFFA allowed us to determine a satisfactory prognosis for patients with retinal nonperfusion. For this group of patients, bevacizumab treatment was as effective as in patients without nonperfusion. Our study confirmed that patients with DME could be successfully treated with bevacizumab independently from nonperfusion status.

Data Availability

The numerical data is available after contact with the corresponding author.

Disclosure

This research was performed as part of the employment of the authors at Medical University of Silesia, Katowice, Poland.

Conflicts of Interest

The authors declare no conflict of interest.

Authors' Contributions

B.S.-M. and S.T. contributed in conceptualization. B.S.-M., S.T., M.B., M.M., and E.C. contributed in methodology. B.S.-M. and M.B. contributed software. B.S.-M., E.W., A.W., M.M., and S.T. contributed in validation. B.S.-M., E.W., A.W., and S.T. contributed in formal analysis. B.S.-M. and S.T. contributed resources. B.S.-M. contributed in the investigation. B.S.-M., E.C., and M.B. contributed in data curation. B.S.-M., S.T., E.C., A.W., M.M., and E.W. contributed in writing the original draft. B.S.-M., S.T., E.C., M.M., and A.W. contributed in writing, reviewing, and editing. B.S.-M. contributed in visualization. B.S.-M., S.T., and E.W. contributed in supervision. B.S.-M. and S.T. contributed in project administration. All authors have read and agreed to the published version of the manuscript.

References

- [1] D. A. Antonetti, R. Klein, and T. W. Gardner, "Diabetic retinopathy," *New England Journal of Medicine*, vol. 366, no. 13, pp. 1227–1239, 2012.
- [2] R. Klein, B. E. Klein, and S. E. Moss, "The Wisconsin epidemiological study of diabetic retinopathy: a review," *Diabetes Metabolism Reviews*, vol. 5, no. 7, pp. 559–570, 1989.
- [3] P. Romero-Aroca, R. Sagarra-Alamo, J. Basora-Gallisa, T. Basora-Gallisa, M. Baget-Bernaldiz, and A. Bautista-Perez, "Prospective comparison of two methods of screening for diabetic retinopathy by nonmydriatic fundus camera," *Clinical Ophthalmology*, vol. 4, pp. 1481–1488, 2010.
- [4] P. S. Silva, A. J. dela Cruz, M. G. Ledesma et al., "Diabetic retinopathy severity and peripheral lesions are associated with nonperfusion on ultrawide field angiography," *Ophthalmology*, vol. 122, no. 12, pp. 2465–2472, 2015.
- [5] T. Niki, K. Muraoka, and K. Shimizu, "Distribution of capillary nonperfusion in early-stage diabetic retinopathy," *Ophthalmology*, vol. 91, no. 12, pp. 1431–1439, 1984.
- [6] F. Bandello, M. Battaglia Parodi, P. Lanzetta et al., "Diabetic macular edema," in (*Developmental Ophthalmology*) *Macular Edema. 2nd, revised and extended edition*, G. Coscas, A. Loewenstein, J. Cunha-Vaz, and G. Soubrane, Eds., vol. 58, no. 9, pp. 102–138, Karger, Basel, Switzerland, 2017.
- [7] D. J. Browning, M. W. Stewart, and C. Lee, "Diabetic macular edema: evidence-based management," *Indian Journal of Ophthalmology*, vol. 66, no. 12, pp. 1736–1750, 2018.
- [8] E. L. Ross, D. W. Hutton, J. D. Stein et al., "Cost-effectiveness of aflibercept, bevacizumab, and ranibizumab for diabetic macular edema treatment: analysis from the Diabetic Retinopathy Clinical Research Network comparative effectiveness trial," *JAMA Ophthalmology*, vol. 134, no. 8, pp. 888–896, 2016.
- [9] T. Bro, M. Derebecka, Ø. K. Jørstad, and A. Grzybowski, "Off-label use of bevacizumab for wet age-related macular degeneration in Europe," *Graefes' Archive for Clinical and Experimental Ophthalmology*, vol. 258, no. 3, pp. 503–511, 2020.
- [10] F. R. Stefanini, J. F. Arevalo, and M. Maia, "Bevacizumab for the management of diabetic macular edema," *World Journal of Diabetes*, vol. 4, no. 2, pp. 19–26, 2013.
- [11] Diabetic Retinopathy Clinical Research Network, J. A. Wells, A. R. Glassman et al., "Aflibercept, bevacizumab, or ranibizumab for diabetic macular edema," *New England Journal of Medicine*, vol. 372, no. 13, pp. 1193–1203, 2015.
- [12] A. Wylęgała, B. Bolek, and E. Wylęgała, "Trends in optical coherence tomography angiography use in university clinic and private practice setting between 2014-2018," *Expert Review of Medical Devices*, vol. 17, no. 10, pp. 1109–1113, 2020.
- [13] M. Sagong, J. van Hemert, L. C. Olmos de Koo, C. Barnett, and S. V. R. Sadda, "Assessment of accuracy and precision of quantification of ultra-widefield images," *Ophthalmology*, vol. 122, no. 4, pp. 864–866, 2015.
- [14] D. E. Croft, J. van Hemert, C. C. Wykoff et al., "Precise montaging and metric quantification of retinal surface area from ultrawidefield fundus photography and fluorescein angiography," *Ophthalmic Surgery, Lasers and Imaging Retina*, vol. 45, no. 4, pp. 312–317, 2014.
- [15] C. S. Tan, M. C. Chew, J. van Hemert, M. A. Singer, D. Bell, and S. V. R. Sadda, "Measuring the precise area of peripheral retinal non-perfusion using ultra-widefield imaging and its correlation with the ischaemic index," *British Journal of Ophthalmology*, vol. 100, no. 2, pp. 235–239, 2016.
- [16] M. Ekinci, E. Ceylan, Ö. Çakıcı, B. Tanyıldız, O. Olcaysu, and H. H. Çağatay, "Treatment of macular edema in diabetic retinopathy: comparison of the efficacy of intravitreal bevacizumab and ranibizumab injections," *Expert Review of Ophthalmology*, vol. 9, no. 2, pp. 139–143, 2014.
- [17] M. Michaelides, A. Kaines, R. D. Hamilton et al., "A prospective randomized trial of intravitreal bevacizumab or laser therapy in the management of diabetic macular edema (BOLT Study) 12-month data: report 2," *Ophthalmology*, vol. 117, no. 6, pp. 1078–1086.e2, 2010.
- [18] S. Cai and N. M. Bressler, "Aflibercept, bevacizumab or ranibizumab for diabetic macular edema," *Current Opinion in Ophthalmology*, vol. 28, no. 6, pp. 636–643, 2017.
- [19] W. Fan, K. Wang, K. Ghasemi Falavarjani et al., "Distribution of nonperfusion area on ultra-widefield fluorescein angiography in eyes with diabetic macular edema: DAVE Study," *American Journal of Ophthalmology*, vol. 180, pp. 110–116, 2017.
- [20] M. Fang, W. Fan, Y. Shi et al., "Classification of regions of non-perfusion on ultra-widefield fluorescein angiography in patients with diabetic macular edema," *American Journal of Ophthalmology*, vol. 206, pp. 74–81, 2019.
- [21] F. Pham and L. Akduman, "Treatment of focal vs diffuse diabetic macular edema," *Retinal Physician*, vol. 14, pp. 19–23, 2017.
- [22] C. Wilkinson, Ferris FL 3rd, R. E. Klein et al., "Proposed international clinical diabetic retinopathy and diabetic macular edema disease severity scales," *Ophthalmology*, vol. 110, no. 9, pp. 1677–1682, 2003.
- [23] M. M. Wessel, G. D. Aaker, G. Parlitsis, M. Cho, D. J. D'Amico, and S. Kiss, "Ultra-wide-field angiography improves the detection and classification of diabetic retinopathy," *Retina*, vol. 32, no. 4, pp. 785–791, 2012.
- [24] M. M. Wessel, N. Nair, G. D. Aaker, J. R. Ehrlich, D. J. D'Amico, and S. Kiss, "Peripheral retinal ischaemia, as

- evaluated by ultra-widefield fluorescein angiography, is associated with diabetic macular oedema,” *British Journal of Ophthalmology*, vol. 96, no. 5, pp. 694–698, 2012.
- [25] K. Xue, E. Yang, and V. N. Chong, “Classification of diabetic macular oedema using ultra-widefield angiography and implications for response to anti-VEGF therapy,” *British Journal of Ophthalmology*, vol. 101, no. 5, pp. 559–563, 2017.
- [26] C. C. Wykoff, C. Shah, D. Dhoot et al., “Longitudinal retinal perfusion status in eyes with diabetic macular edema receiving intravitreal aflibercept or laser in VISTA Study,” *Ophthalmology*, vol. 126, no. 8, pp. 1171–1180, 2019.
- [27] J. H. Yoo, J. Ahn, J. Oh, J. Cha, and S. W. Kim, “Risk factors of recurrence of macular oedema associated with branch retinal vein occlusion after intravitreal bevacizumab injection,” *British Journal of Ophthalmology*, vol. 101, no. 10, pp. 1334–1339, 2017.
- [28] E. J. Chung, M. I. Roh, O. W. Kwon, and H. J. Koh, “Effects of macular ischemia on the outcome of intravitreal bevacizumab therapy for diabetic macular edema,” *Retina*, vol. 28, no. 7, pp. 957–963, 2008.
- [29] C. C. Wykoff, D. E. Croft, D. M. Brown et al., “Prospective trial of treat-and-extend versus monthly dosing for neovascular age-related macular degeneration: TREX-AMD 1-year results,” *Ophthalmology*, vol. 122, no. 12, pp. 2514–2522, 2015.
- [30] R. K. Reddy, D. J. Pieramici, S. Gune et al., “Efficacy of ranibizumab in eyes with diabetic macular edema and macular non-perfusion in RIDE and RISE,” *Ophthalmology*, vol. 125, no. 10, pp. 1568–1574, 2018.
- [31] S. G. Karst, G. G. Deak, B. S. Gerendas et al., “Association of changes in macular perfusion with ranibizumab treatment for diabetic macular edema: a subanalysis of the RESTORE (extension) study,” *JAMA Ophthalmology*, vol. 136, no. 4, pp. 315–321, 2018.
- [32] B. Mushtaq, N. J. Crosby, A. T. Dimopoulos et al., “Effect of initial retinal thickness on outcome of intravitreal bevacizumab therapy for diabetic macular edema,” *Clinical Ophthalmology*, vol. 8, pp. 807–812, 2014.
- [33] M. Soheilian, A. Ramezani, M. Yaseri, S. A. Mirdehghan, A. Obudi, and B. Bijanzadeh, “Initial macular thickness and response to treatment in diabetic macular edema,” *Retina*, vol. 31, no. 8, pp. 1564–1573, 2011.
- [34] H. Ahmadi, R. Nourinia, A. Hafezi-Moghadam et al., “Intravitreal injection of a rho-kinase inhibitor (fasudil) combined with bevacizumab versus bevacizumab monotherapy for diabetic macular oedema: a pilot randomised clinical trial,” *British Journal of Ophthalmology*, vol. 103, no. 7, pp. 922–927, 2019.
- [35] J. F. Arevalo, J. G. Sanchez, A. F. Lasave et al., “Intravitreal bevacizumab (Avastin) for diabetic retinopathy: the 2010 GLA-DAOF lecture,” *Journal of Ophthalmology*, vol. 2011, Article ID 584238, 13 pages, 2011.
- [36] S. Jeon and W. K. Lee, “Effect of intravitreal bevacizumab on diabetic macular edema with hard exudates,” *Clinical Ophthalmology*, vol. 12, no. 8, pp. 1479–1486, 2014.
- [37] B. Haj Najeeb, C. Simader, G. Deak et al., “The distribution of leakage on fluorescein angiography in diabetic macular edema: a new approach to its etiology,” *Investigative Ophthalmology and Visual Sciences*, vol. 58, no. 10, pp. 3986–3990, 2017.
- [38] Y. Feng, S. Zhu, E. Skiadaresi et al., “Phacoemulsification cataract surgery with prophylactic intravitreal bevacizumab for patients with coexisting diabetic retinopathy,” *Retina*, vol. 39, no. 9, pp. 1720–1731, 2019.
- [39] J. K. Kristinsson, M. S. Gottfredsdottir, and E. Stefansson, “Retinal vessel dilatation and elongation precedes diabetic macular oedema,” *British Journal of Ophthalmology*, vol. 81, no. 4, pp. 274–278, 1997.
- [40] K. Shimizu, Y. Kobayashi, and K. Muraoka, “Midperipheral fundus involvement in diabetic retinopathy,” *Ophthalmology*, vol. 88, no. 7, pp. 601–612, 1981.
- [41] J. F. Arevalo, J. G. Sanchez, L. Wu et al., “Primary intravitreal bevacizumab for diffuse diabetic macular edema: the Pan-American Collaborative Retina Study Group at 24 months,” *Ophthalmology*, vol. 116, no. 8, pp. 1488–1497.e1, 2009.
- [42] A. S. Neubauer, D. Kook, C. Haritoglou et al., “Bevacizumab and retinal ischemia,” *Ophthalmology*, vol. 114, no. 11, pp. 2096–2096.e2, 2007.
- [43] L.-Q. Zhao and J.-W. Cheng, “A systematic review and meta-analysis of clinical outcomes of intravitreal anti-VEGF agent treatment immediately after cataract surgery for patients with diabetic retinopathy,” *Journal of Ophthalmology*, vol. 2019, Article ID 2648267, 10 pages, 2019.

Research Article

miR-126 Mimic Counteracts the Increased Secretion of VEGF-A Induced by High Glucose in ARPE-19 Cells

Roberta Sanguineti ¹, Alessandra Puddu ¹, Massimo Nicolò ^{2,3}, Carlo Enrico Traverso,²
Renzo Cordera ¹, Giorgio L. Viviani ¹ and Davide Maggi ¹

¹Department of Internal Medicine and Medical Specialties, Viale Benedetto XV XV, Genova, Italy

²Department of Neuroscience, Ophthalmology and Genetics, Viale Benedetto, Genova, Italy

³Fondazione per la Macula Onlus-Genova, Piazza della Vittoria, Genova, Italy

Correspondence should be addressed to Alessandra Puddu; alep100@hotmail.com

Received 13 November 2020; Revised 25 January 2021; Accepted 3 February 2021; Published 25 February 2021

Academic Editor: Maria Vittoria Cicinelli

Copyright © 2021 Roberta Sanguineti et al. This is an open access article distributed under the Creative Commons Attribution License, which permits unrestricted use, distribution, and reproduction in any medium, provided the original work is properly cited.

Vascular endothelial growth factor-A (VEGF-A) has a pathologic role in microvascular diabetic complication, such as diabetic retinopathy (DR). miR-126 plays an important role in vascular development and angiogenesis by regulating the expression of VEGF-A. Since levels of miR-126 have been found downregulated in diabetes, this study is aimed at investigating whether hyperglycemia affects expression of miR-126 in a retinal pigment epithelium cell line. ARPE-19 cells were transfected with miR-126 inhibitor or with miR-126 mimic and the respective scramble negative control. After 24 hours, medium was replaced and cells were cultured for 24 hours in normal (CTR) or diabetic condition (HG). Then, we analyzed mRNA levels of miR-126, VEGF-A, PI3KR2, and SPRED1. We also evaluated protein amount of HIF-1 α , PI3KR2, and SPRED1 and VEGF-A secretion. The results showed that exposure of ARPE-19 cells to HG significantly decreased miR-126 levels; mRNA levels of VEGF-A and PI3KR2 were inversely correlated with those of miR-126. Overexpression of miR-126 under HG restored HIF-1 α expression and VEGF-A secretion to the level of CTR cells. These results indicate that reduced levels of miR-126 may contribute to DR progression by increasing expression of VEGF-A in RPE cells. In addition, we provide evidence that upregulation of miR-126 in RPE cells counteracts the rise of VEGF-A secretion induced by hyperglycemia. In conclusion, our data support a role of miR-126 mimic-approach in counteracting proangiogenic effects of hyperglycemia.

1. Introduction

Diabetic retinopathy (DR) is one of the most important microvascular complications of diabetes and the primary cause of visual loss in working age adults [1–3]. Prolonged hyperglycemia is a significant risk factor in the DR progression and could cause ocular neovascularization with aberrant formation of immature blood vessels [4, 5]. Indeed, it leads to progressive alterations of the retinal microvasculature, which start with pericyte dropout, pass through vasoregression and increased vasopermeability, and lead to pathological neovascularization in response to hypoxia [6].

Vascular endothelial growth factor-A (VEGF-A), a key mediator of blood vessel formation, plays an important role in the homeostasis of the retinal and choroidal vasculature,

by mediating both angiogenesis and inflammation [7]. Hyperglycemia induces aberrant levels of VEGF-A in the retina, which have been related to structural and functional changes that lead to DR [8, 9]. Indeed, VEGF-A activates quiescent endothelial cells, promotes cell proliferation and migration with the subsequent formation of new blood vessels, and increases vascular permeability [10].

The retinal pigment epithelium (RPE) is a monolayer of highly specialized cells located between the choroid and photoreceptors, which form the outer blood-retinal barrier (BRB) [11]. RPE cells play an important role in retinal homeostasis, by affecting the function and maintenance of both the photoreceptors and capillary endothelium. Consequently, RPE barrier dysfunction and altered secretion of growth factors and cytokines by RPE cells contribute to diabetic retinopathy worsening.

In particular, RPE cells are one of the main source of VEGF-A in the retina. During homeostasis, VEGF-A is secreted in low concentrations to the basal side of the RPE, where it contributes in maintaining endothelial cell survival and choriocapillaris fenestrations. Under diabetic conditions, VEGF-A is overproduced and released also toward the apical side [12], thus increasing the permeability of the choroidal vessels in diabetic eyes and compromising the maintenance of the structural integrity of the retina.

It is well known that transcription of VEGF-A is regulated by hypoxia-inducible factor 1- α (HIF-1 α), a transcription factor that is the master regulator of cellular response to hypoxia and hyperglycemia [9, 13]. Briefly, HIF-1 is a heterodimeric transcription factor consisting of a constitutively expressed β -subunit and an oxygen-regulated α -subunit [14]. Under normoxic conditions, HIF-1 α is degraded by proteasomes; on the contrary, in hypoxic conditions and during hyperglycemia, HIF-1 α is stabilized and able to interact with its coactivators and the β -subunit to increase expression of genes involved in energy metabolism and angiogenesis, including VEGF-A.

Expression of VEGF-A may be also regulated by microRNAs, small noncoding RNAs that regulate gene expression at posttranscriptional level [15]. In particular, miR-126, an endothelial specific microRNA, has been reported to have a central role in neovascularization process by regulating VEGF-A signaling [16]. Indeed, miR-126 targets to a binding site in 3'UTR of VEGF-A mRNA; therefore, reduced levels of miR-126 lead to increased expression of VEGF-A and may promote vascular permeability and pathological vascularization; on the contrary, miR-126 overexpression decreases the levels of VEGF-A [17]. In addition, miR-126 may affect the VEGF/PI3K/AKT signaling pathway targeting the expression of Sprouty-related protein (SPRED1) and phosphoinositol-3 kinase regulatory subunit 2 (PI3KR2), which are two negative regulators of VEGF-A expression [16, 18, 19].

Since the RPE cell dysfunction is involved in the early stages of the DR damage and miR-126 represents a promising target for novel antiangiogenic therapies, this study is aimed at investigating whether hyperglycemia affects expression of miR-126 and characterizing the molecular mechanisms through which miR-126 regulates VEGF-A expression in RPE cells.

2. Materials and Methods

2.1. Cell Culture and Experimental Conditions. The human cell line ARPE-19 (American Type Culture Collection, Manassas, VA, USA) from passages 22 to 28 were grown in DMEM/F12 1:1 medium (Euroclone, Milan, Italy) supplemented with 10% fetal bovine serum and 2 mmol/L glutamine (Euroclone, Milan, Italy) at 37°C in 5% CO₂. The cell medium was replaced every 2 days. Cells were grown to confluence, removed with trypsin-EDTA (Euroclone, Milan, Italy), and then seeded in multiwell plates for all experiments. Before each experiment, confluent cells were washed with phosphate-buffered saline (PBS) (Euroclone, Milan, Italy) and cultured in control medium (DMEM low glucose/F12, CTR).

2.2. miR-126 Mimics/Inhibitor Transfection. ARPE-19 cells were plated into 12-well plates with 8 × 10⁴ cells/well and cultured in normal glucose condition. Once the cells were 70% confluent, has-miR-126-3p miRCURY LNA Power inhibitor (miR-126 inhib), has-miR-126-3p miRCURY LNA Mimic (miR-126 mimic), and the respective scramble negative controls (all from Exiqon-Qiagen, Milan, Italy) were transfected into ARPE-19 cells using jetPRIME transfection reagent (Polyplus-transfection, New York, USA). After 24 hours of the transfection, medium was changed and replaced with fresh CTR or high glucose (HG, 25 mM glucose) medium for 24 hours.

2.3. Quantitative RT-PCR. RNA was extracted from ARPE-19 cells cultured under different conditions using the Quick-RNA Mini prep Kit (Zymo Research, Irvine, CA) according to the manufacturer's instructions. The amount and quality of RNA were determined spectrophotometrically. RNA samples featuring an A260/A280 value of at least 2.0 were generally used for further analysis. To analyze miRNA-expression level, 5 ng/ μ L of total RNA was reversed-transcribed using miRCURY LNA RT kit (Exiqon-Qiagen, Milan, Italy). The obtained cDNA was then diluted for further quantitative real-time polymerase chain reaction (qRT-PCR). miRNA levels were measured using miRCURY LNA miRNA PCR Assay (Exiqon-Qiagen, Milan, Italy) with specific primers: has-miR-126-3p and U6 snRNA(has, mmu) used as a normalization control for miRNA expression. All measurements were performed in triplicate on an ABI PRISM 7900 HT Fast Real-Time PCR System (Applied Biosystems Monza, Italy). Comparisons in gene expression were done using the $2^{-\Delta\Delta C_t}$ method [20].

For mRNA analysis, one microgram of RNA was reverse-transcribed to cDNA using Wonder RT-cDNA Synthesis kit (Euroclone, Milan, Italy). The expression levels of the target gene VEGF-A (Applied Biosystems assay ID: Hs00900055_m1) were measured by qRT-PCR amplification, performed using Luna Universal Probe qPCR Master Mix (New England Biolabs, NEB, Massachusetts, USA) in an ABI PRISM 7900 HT Fast Real-Time PCR System (Applied Biosystems Monza, Italy). All measurements were performed in triplicate with the following qRT-PCR run protocol: initial denaturation program (95°C 1 min), denaturation (95°C 15 sec), and extension program (60°C 30 sec) repeated 43 times (95°C 15 s and 60°C 1 min). Gene expression was normalized using the housekeeping as control gene (β -actin, Applied Biosystems assay ID: Hs01060665_g1). Comparisons in gene expression were done using the $2^{-\Delta\Delta C_t}$ method [20].

2.4. Secretion of VEGF-A. ARPE-19 cells were treated with miRNA mimic or miRNA inhibitor for 48 hours. At the end of incubation, fresh CTR or HG medium was added for 24 h. To quantify VEGF-A secretion, the conditioned media were collected and stored at -80°C until the assay was performed. Cells were then washed with PBS and lysed in radioimmunoprecipitation assay (RIPA) buffer, and protein content was determined with the BCA Protein Assay Kit (Pierce, Rockford, MD) according to the manufacturer's instructions. Secretion of VEGF-A was assessed with

enzyme-linked immunosorbent assay (ELISA; Raybiotech, Norcross, GA, USA), and concentrations were calculated from the standard curve and normalized to the total protein concentration of the respective lysate.

2.5. Immunoblot. At the end of the experiments, ARPE-19 cells were lysed in RIPA buffer supplemented with protease and phosphatase inhibitors, and protein concentrations were determined using the BCA Protein Assay Kit. Thirty micrograms of total cell lysate were separated on a SDS-PAGE and transferred onto nitrocellulose. Filters were blocked in 5% nonfat dried milk and incubated overnight at 4°C with primary specific antibodies (HIF-1 α , PI3KR2, and SPRED1 from Cell Signaling Technology, Beverly, MA, USA). Secondary specific horseradish peroxidase-linked antibodies were added for 1 h at room temperature. Bound antibodies were detected using the enhanced chemiluminescence lighting system (ECL Plus), according to the manufacturer's instructions. Each membrane was stripped (Restore PLUS Western Blot Stripping Buffer, Pierce Biotechnology, Rockford, IL, USA) and probed for β -actin (Cell Signaling Technology, Beverly, MA, USA) to verify equal protein loading. Bands of interest were quantified by densitometry using the Alliance software. Results were expressed as percentages of CTR (defined as 100%).

2.6. Statistical Analysis. All statistical analyses were performed using the GraphPad Prism 4.0 software (GraphPad Software, San Diego, CA, USA). Data were expressed as the mean \pm SEM and then analyzed using one-way ANOVA followed by Dunnett's multiple comparison test and *t*-test. A *p* value of <0.05 was considered statistically significant. The results are representative of at least 3 experiments.

3. Results

3.1. Hyperglycemia Decreased miR-126 Expression. First, we performed RT-qPCR to confirm the presence of miR-126 in ARPE-19 cells and the efficiency of transfection with miR-126 inhibitor and mimic.

As expected, miR-126 was expressed by ARPE-19 cells (Figure 1(a)). Hyperglycemia significantly reduced miR-126 levels compared to control conditions (Figure 1(a)). Addition of miR-126 inhibitor completely abrogated the detection of miR-126 in the samples. On the contrary, transfection of miR-126 mimic significantly increased miR-126 levels.

3.2. mRNA Levels of VEGF-A Are Inversely Correlated to Those of miR-126 under Standard and Diabetic Conditions. Addition of miR-126 inhibitor or mimic resulted, respectively, in a significant upregulation or downregulation of VEGF-A gene expression under control conditions.

In presence of high glucose, the VEGF-A gene expression was significantly increased (Figure 1(b)). Treatment with miR-126 inhibitor did not further increase the effect of hyperglycemia on VEGF-A expression (Figure 1(b)). Transfection of miR-126 mimic prevented the rise of VEGF-A expression levels induced by HG.

3.3. HIF-1 α Protein Expression Is Not Affected by Levels of miR-126. HIF-1 α is the main regulator of VEGF-A. To determine its contribution on VEGF-A expression when miR-126 is down- or upregulated, we evaluated HIF-1 α protein expression.

Treatment with HG significantly increased HIF-1 α protein level. Under control condition, no differences in HIF-1 α protein expression were observed in ARPE-19 cells transfected either with miR-126 inhibitor or miR-126 mimic (Figure 2). Transfection with miR-126 inhibitor did not affect HG-induced upregulation of HIF-1 α . On the contrary, transfection with miR-126 mimic caused a significant downregulation of HIF-1 α expression compared to HG cultures (Figure 2).

3.4. miR-126 Targeted SPRED1 and PI3KR2 in ARPE-19 Cells. In endothelial cells, miR-126 may regulate VEGF-A levels by directly repressing SPRED1 and PI3KR2, two negative regulators of the VEGF pathway [16, 18, 19]. To investigate whether SPRED1 and PI3KR2 are targets of miR-126 in ARPE-19 cells, we performed RT-qPCR and Western blot analysis in ARPE-19 cells transfected with miR-126 inhibitor or miR-126 mimic at normal and high-glucose conditions.

SPRED1 gene and protein expression were not affected by hyperglycemia (Figures 3(a) and 3(b)). The inhibition of miR-126 did not alter SPRED1 gene and protein expression under control conditions, but induced a significant increase of SPRED1 mRNA level under hyperglycemic conditions. Transfection with miR-126 mimic significantly downregulated SPRED1 gene and protein expression.

High glucose significantly enhanced PI3KR2 gene and protein expression compared to control (Figures 4(a) and 4(b)). When miR-126 was inhibited, PI3KR2 gene and protein expression were upregulated in comparison to control cultures. On the contrary, overexpression of miR-126 significantly reduced the mRNA and protein levels of PI3KR2 and prevented the rise induced by HG.

3.5. Overexpression of miR-126 Restores VEGF-A Secretion under HG to the Level of CTR Cells. Finally, we investigated whether the potential of therapeutic strategy based on miR-126 enrichment may counteract the increased secretion of VEGF-A induced by hyperglycemia. VEGF-A release was not affected neither by inhibition nor by overexpression of miR-126. Treatment with HG alone or in combination with miR-126 inhibitor increased VEGF-A secretion compared with control culture (Figure 5). miR-126 mimic transfection prevented the rise of VEGF-A secretion induced by HG, maintaining the release to the levels observed in control culture.

4. Discussion

Chronic hyperglycemia is a major long-term determinant of vascular changes in DR. Retinal neovascularization is primarily due to uncontrolled VEGF-A expression and secretion by the RPE [8, 11]. It is well known that the expression of VEGF-A is regulated by the activity of HIF-1 α , which is stabilized under hypoxia and diabetes [9, 13]. VEGF-A expression is also controlled by miR-126 [16].

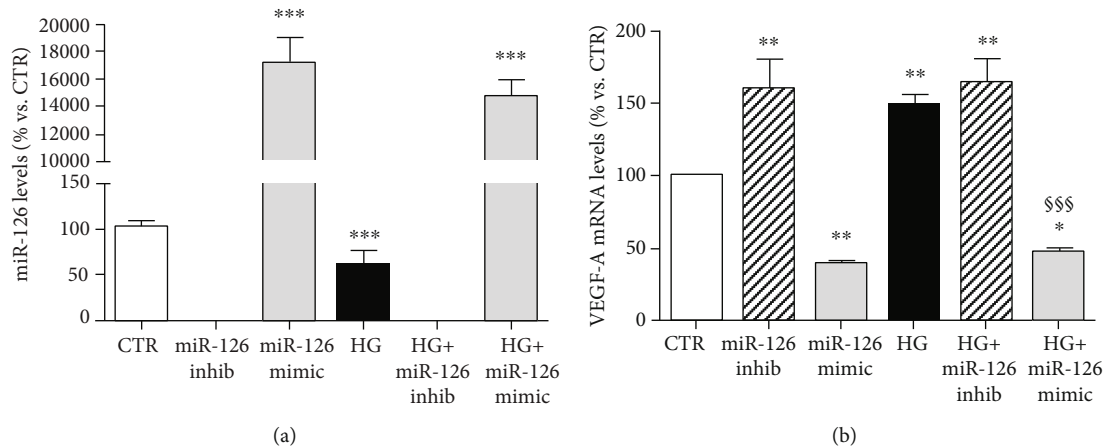


FIGURE 1: (a) Levels of miR-126 in ARPE-19 cells cultured for 24 hours in standard medium (CTR), silencing (inhib) and upregulating (mimic) miR-126 in control condition and in presence of high glucose (HG). Gene expression was normalized vs. U6 housekeeping gene. (b) mRNA levels of VEGF-A in ARPE-19 cells cultured for 24 hours in standard medium (CTR), silencing (inhib) and upregulating (mimic) miR-126 in control condition and in presence of high glucose (HG). VEGF-A gene expression was normalized vs. β -actin as housekeeping gene. Data are presented as the mean \pm SEM of three experiments ($n = 3$). * $p < 0.05$, ** $p < 0.01$, and *** $p < 0.001$ vs. CTR; \$\$\$ $p < 0.001$ HG+mimic vs. HG.

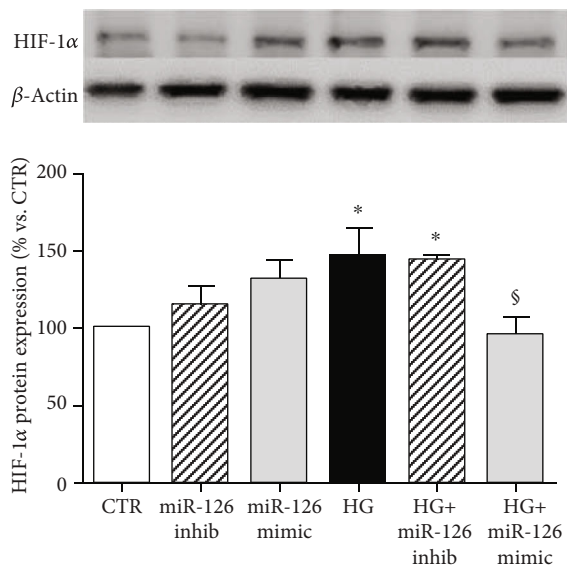


FIGURE 2: Western blot analysis of HIF-1 α protein levels in ARPE-19 cells cultured for 24 hours in standard medium (CTR), silencing (inhib) and upregulating (mimic) miR-126 in control condition and in presence of high glucose (HG). Representative Western blot analysis and quantification of densitometries of Western blot band. Data were expressed as mean \pm SEM of fold induction relative to β -actin of three independent experiments ($n = 3$). * $p < 0.05$ vs. CTR; § $p < 0.05$ HG+mimic vs. HG.

Therefore, it is important to determine whether glucose may affect levels of miR-126 in RPE cells.

The mechanisms through which miR-126 regulates angiogenesis have been deeply investigated in endothelial cells and are mainly related to modulation of VEGF-A expression [16]. Recently, Zhou et al. showed that miR-126 is involved in the regulation of VEGF-A expression and also

in RPE cells suggesting that VEGF-A is a miR-126-3p target [21]. Consistent with this report, we found that levels of miR-126 are inversely correlated with VEGF-A expression in ARPE-19 cells. To further explore whether altered expression of VEGF-A is due to a direct action of miR-126 on its mRNA transcript, we investigated the expression of HIF-1 α . Under physiologic condition, treatment with miR-126 inhibitor or mimic, respectively, increased or reduced mRNA levels of VEGF-A without affecting protein expression of HIF-1 α . Usually, the expression of HIF-1 α correlates with mRNA levels of VEGF-A. However, we found that in normal condition, the amount of HIF-1 α does not affect mRNA levels of VEGF-A. This suggests that reduction of VEGF-A mRNA in ARPE-19 cells is due to mRNA degradation induced by interaction with miR-126. On the contrary, the rise of VEGF-A expression may be related to lack of induction of degradation. Taken together, our results confirm that VEGF-A is a target of miR-126 in ARPE-19 cells.

The presence of a relationship between miR-126 levels and diabetes has been suggested by several studies. Plasma levels of miR-126 are lower in patients with DM in comparison with healthy subjects. [22]. Furthermore, levels of miR126 have been found downregulated in the retinal tissue of streptozotocin-induced diabetic rat [23]. Consistent with this evidence, we found that hyperglycemia decreased levels of miR-126, demonstrating that glucose may regulate miR-126 expression in RPE cells. Moreover, under hyperglycemia, reduced levels of miR-126 are coupled to rise of VEGF-A mRNA levels and increased the expression of HIF-1 α . Taken together, these findings suggest that both reduced degradation of VEGF-A mRNA and increased transcription of its gene contribute to upregulate VEGF-A mRNA levels. Use of miR-126 inhibitor did not further increase the levels of VEGF-A, reached when cells are cultured under diabetic condition, suggesting that hyperglycemia induced the maximum

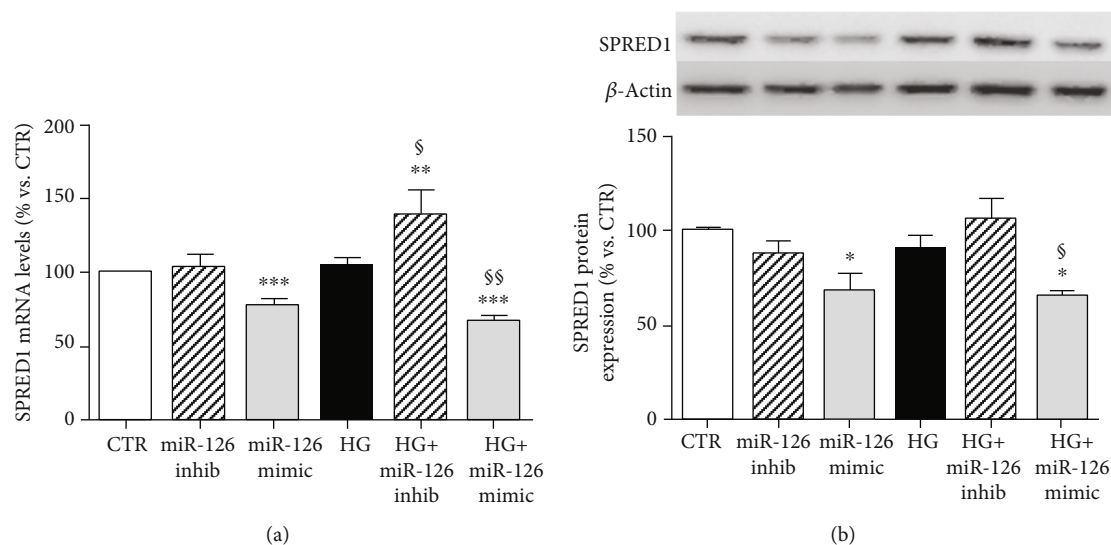


FIGURE 3: Expression of SPRED1 in ARPE-19 cells cultured for 24 hours in standard medium (CTR), silencing (inhib) and upregulating (mimic) miR-126 in control condition and in presence of high glucose (HG). (a) SPRED1 gene expression normalized vs. β -actin as housekeeping gene. (b) Representative Western blot analysis of SPRED1 protein expression with quantification of densitometries of relative bands. Data were expressed as mean \pm SEM of fold induction relative to β -actin of three independent experiments ($n = 3$). * $p < 0.05$, ** $p < 0.01$, and *** $p < 0.001$ vs. CTR; § $p < 0.05$ and §§ $p < 0.01$ HG+mimic vs. HG.

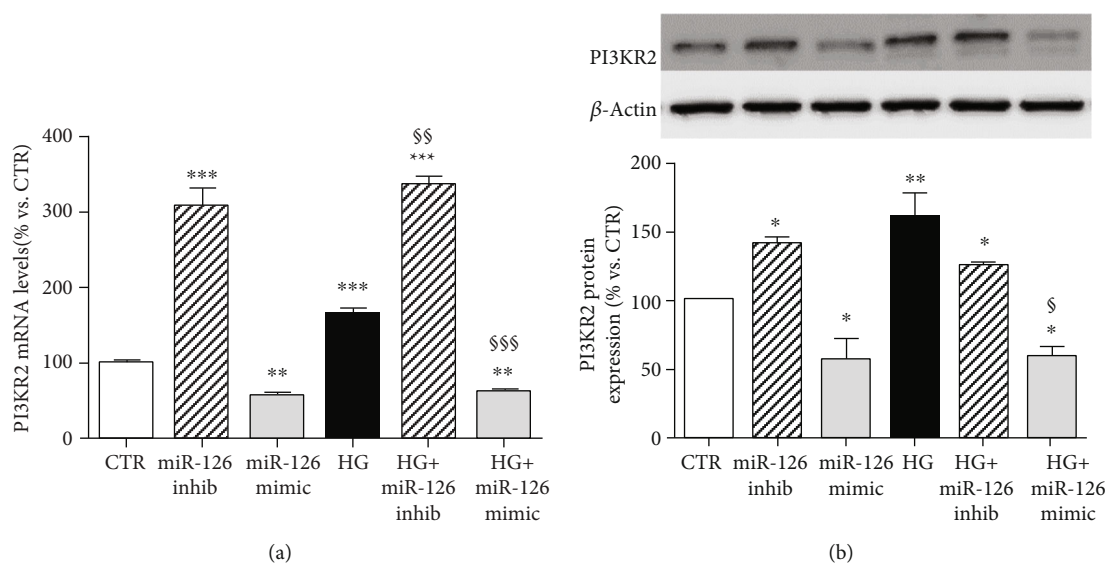


FIGURE 4: Expression of PI3KR2 in ARPE-19 cells cultured for 24 hours in standard medium (CTR), silencing (INHIB) and upregulating (MIMIC) miR-126 in control condition and in presence of high glucose (HG). (a) PI3KR2 gene expression normalized vs. β -actin as housekeeping gene. Representative Western blot analysis of (b) PI3KR2 protein expression with quantification of densitometries of relative bands. Data were expressed as mean \pm SEM of fold induction relative to β -actin of three independent experiments ($n = 3$). * $p < 0.05$, ** $p < 0.01$, and *** $p < 0.001$ vs. CTR; § $p < 0.05$, §§ $p < 0.01$, and §§§ $p < 0.001$ HG+mimic vs. HG.

levels of VEGF-A expression. On the contrary, miR-126 mimic prevented the upregulation of HIF-1 α expression and counteracted the increased levels of VEGF-A induced by hyperglycemia, suggesting that HIF-1 α may be an indirect target of miR-126 in ARPE-19 cells.

It has been shown that miR-126 regulates VEGF-A expression not only by directly targeting VEGF-A, but also by regulating the levels of SPRED1 and PI3KR2 [16, 18, 19]. Yang

et al. demonstrated that miR-126 regulated VEGF-A and PI3KR2 in retinal vascular endothelial cells under diabetic condition, and that miR-126 overexpression blocked the cell migration and sprouting induced by high glucose by inhibiting VEGF-A expression [19]. In addition, Wang et al. showed that transfection with miR-126 mimic prevented the increased mRNA and protein levels of VEGF-A and SPRED1 under diabetic condition [24]. Consistent with these findings, we

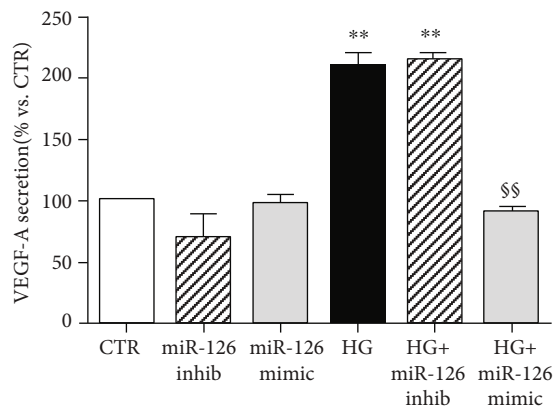


FIGURE 5: VEGF-A secretion measured by ELISA analysis. Data are presented as the mean \pm SEM of three experiments ($n = 3$). ** $p < 0.01$ vs. CTR; §§ $p < 0.01$ HG+mimic vs. HG.

observed an inverse correlation between levels of miR-126 and those of SPRED1 when cells are transfected with miR-126 mimic, both under control and high-glucose conditions, confirming that SPRED1 is a target of miR-126 in ARPE-19 cells. Since depletion of miR-126 did not result in upregulation of SPRED1 protein expression, it is likely that this is the maximum amount of SPRED1 produced by ARPE-19 cells. Furthermore, our results showed that miR-126 levels are inversely correlated with expression of PI3KR2 in all experimental conditions, demonstrating that in ARPE-19 cells, miR-126 directly targets PI3KR2. Taken together, these data suggest that SPRED1 and PI3KR2 are regulated by miR-126 and also in ARPE-19 cells. However, different from findings in other cell types [18, 25], the downregulation of SPRED1 and PI3KR2 expression did not result in increased levels of VEGF-A, suggesting that these two factors are not involved in the regulation of VEGF-A expression in ARPE-19 cells, and that miR-126 function is highly tissue specific. Reduced levels of miR-126 due to hyperglycemia play a crucial role in the pathogenesis and progression of DR [26]. VEGF-A is the main target of most pharmacological interventions to prevent the DR progression. However, the increased expression of VEGF-A in RPE cells could be also countered through an innovative therapeutic strategy represented by miR-126 enrichment. In this regard, several studies are underway to define a role for miR-126 overexpression as a future gene therapy to counteract the abnormal VEGF-A expression levels, thus offering new prospective in clinical application [26, 27]. Here, we found that overexpression of miR-126 counteracts the rise in VEGF-A secretion induced by hyperglycemia. To our knowledge, this is the first evidence that miR-126 overexpression may reduce secretion of VEGF-A in diabetic condition in RPE cells. Of importance, miR-126 mimic did not affect VEGF-A secretion under control condition, suggesting that this approach did not alter homeostasis in normoglycemic environment. Furthermore, this result suggests that downregulation of VEGF-A secretion under diabetic condition may be related to the decrease production of VEGF-A due to a reduced mRNA expression rather than to a defect in its release. Secretion of VEGF-A has not changed even in the presence of

increased expression of VEGF-A due to the effect of miR-126 inhibitor, confirming that the secretory machine of ARPE-19 cells is not affected neither by the levels of miR-126 nor by those of VEGF-A.

5. Conclusions

In conclusion, we demonstrated that miR-126 overexpression may be useful in reducing VEGF-A secretion from RPE cells under diabetic condition. This, in turns, may prevent progressive alterations of the retinal microvasculature by reducing both vascular permeability and activation of endothelial cells. Considering that RPE cell dysfunction is one of the early changes in the onset of diabetic retinopathy, miR-126 mimic-approach may represent a new therapeutic strategy in the prevention and treatment of DR and offer interesting prospects in future clinical application.

The main limitation of our findings is the absence of an animal model to extend the results obtained in vitro. However, the results of this study may contribute to develop clinical approach to counteract VEGF-A rise in response to hyperglycemia.

Data Availability

The data used to support the findings of this study are included within the article.

Conflicts of Interest

The authors declare that there is no conflict of interest regarding the publication of this paper.

References

- [1] R. Lee, T. Y. Wong, and C. Sabanayagam, "Epidemiology of diabetic retinopathy, diabetic macular edema and related vision loss," *Eye Vision*, vol. 2, 2015.
- [2] T. Y. Wong, C. M. Cheung, M. Larsen, S. Sharma, and R. Simo, "Diabetic retinopathy," *Nature Reviews Disease Primers*, vol. 2, no. 1, 2016.
- [3] Y. Zheng, M. He, and N. Congdon, "The worldwide epidemic of diabetic retinopathy," *Indian Journal of Ophthalmology*, vol. 60, no. 5, pp. 428–431, 2012.
- [4] R. Klein, B. E. Klein, S. E. Moss, and K. J. Cruickshanks, "Relationship of hyperglycemia to the long-term incidence and progression of diabetic retinopathy," *Archives of Internal Medicine*, vol. 154, no. 19, pp. 2169–2178, 1994.
- [5] E. S. Shin, C. M. Sorenson, and N. Sheibani, "Diabetes and retinal vascular dysfunction," *J. Ophthalmic Vis. Res.*, vol. 9, no. 3, pp. 362–373, 2014.
- [6] H. P. Hammes, Y. Feng, F. Pfister, and M. Brownlee, "Diabetic retinopathy: targeting vasoregression," *Diabetes*, vol. 60, no. 1, pp. 9–16, 2010.
- [7] R. S. Apte, D. S. Chen, and N. Ferrara, "VEGF in signaling and disease: beyond discovery and development," *Cell*, vol. 176, no. 6, pp. 1248–1264, 2019.
- [8] T. Behl and A. Kotwani, "Exploring the various aspects of the pathological role of vascular endothelial growth factor (VEGF)

- in diabetic retinopathy," *Pharmacology Research*, vol. 99, pp. 137–148, 2015.
- [9] M. L. Chang, C. J. Chiu, F. Shang, and A. Taylor, "High glucose activates ChREBP-mediated HIF-1 α and VEGF expression in human RPE cells under normoxia," *Advances in Experimental Medicine and Biology*, vol. 801, pp. 609–621, 2014.
- [10] H. Takahashi and M. Shibuya, "The vascular endothelial growth factor (VEGF)/VEGF receptor system and its role under physiological and pathological conditions," *Clinical Science (London, England)*, vol. 109, no. 3, pp. 227–241, 2005.
- [11] O. Strauss, "The retinal pigment epithelium in visual function," *Physiological Reviews*, vol. 85, no. 3, pp. 845–881, 2005.
- [12] R. Kannan, N. Zhang, P. G. Sreekumar et al., "Stimulation of apical and basolateral VEGF-A and VEGF-C secretion by oxidative stress in polarized retinal pigment epithelial cells," *Molecular Vision*, vol. 12, pp. 1649–1659, 2006.
- [13] Q. Xiao, S. Zeng, S. Ling, and M. Lv, "Up-regulation of HIF-1 α and VEGF expression by elevated glucose concentration and hypoxia in cultured human retinal pigment epithelial cells," *Journal of Huazhong University of Science and Technology. Medical Sciences*, vol. 26, no. 4, pp. 463–465, 2006.
- [14] Q. Ke and M. Costa, "Hypoxia-inducible factor-1 (HIF-1)," *Molecular Pharmacology*, vol. 70, no. 5, pp. 1469–1480, 2006.
- [15] D. P. Bartel, "MicroRNAs: genomics, biogenesis, mechanism, and function," *Cell*, vol. 116, no. 2, pp. 281–297, 2004.
- [16] J. E. Fish, M. M. Santoro, S. U. Morton et al., "miR-126 regulates angiogenic signaling and vascular integrity," *Developmental Cell*, vol. 15, no. 2, pp. 272–284, 2008.
- [17] B. Liu, X. C. Peng, X. L. Zheng, J. Wang, and Y. W. Qin, "MiR-126 restoration down-regulate VEGF and inhibit the growth of lung cancer cell lines in vitro and in vivo," *Lung Cancer*, vol. 66, no. 2, pp. 169–175, 2009.
- [18] S. Meng, J. T. Cao, B. Zhang, Q. Zhou, C. X. Shen, and C. Q. Wang, "Downregulation of microRNA-126 in endothelial progenitor cells from diabetes patients, impairs their functional properties, via target gene Spred-1," *Journal of Molecular and Cellular Cardiology*, vol. 53, no. 1, pp. 64–72, 2012.
- [19] W. Z. Yang, J. Yang, L. P. Xue, L. B. Xiao, and Y. Li, "MiR-126 overexpression inhibits high glucose-induced migration and tube formation of rhesus macaque choroid-retinal endothelial cells by obstructing VEGFA and PIK3R2," *Journal of Diabetes and its Complications*, vol. 31, no. 4, pp. 653–663, 2017.
- [20] K. J. Livak and T. D. Schmittgen, "Analysis of relative gene expression data using real-time quantitative PCR and the 2(-delta delta C(T)) method," *Methods*, vol. 25, no. 4, pp. 402–408, 2001.
- [21] Q. Zhou, C. Anderson, J. Hanus et al., "Strand and cell type-specific function of microRNA-126 in angiogenesis," *Molecular Therapy*, vol. 24, no. 10, pp. 1823–1835, 2016.
- [22] A. Zampetaki, S. Kiechl, I. Drozdov et al., "Plasma microRNA profiling reveals loss of endothelial miR-126 and other microRNAs in type 2 diabetes," *Circulation Research*, vol. 107, no. 6, pp. 810–817, 2010.
- [23] P. Ye, J. Liu, F. He, W. Xu, and K. Yao, "Hypoxia-induced deregulation of miR-126 and its regulative effect on VEGF and MMP-9 expression," *International Journal of Medical Sciences*, vol. 11, no. 1, pp. 17–23, 2014.
- [24] L. Wang, A. Y. W. Lee, J. P. Wigg, H. Peshavariya, P. Liu, and H. Zhang, "miR-126 regulation of angiogenesis in age-related macular degeneration in CNV mouse model," *International Journal of Molecular Sciences*, vol. 17, no. 6, p. 895, 2016.
- [25] J. J. Chen and S. H. Zhou, "Mesenchymal stem cells overexpressing MiR-126 enhance ischemic angiogenesis via the AKT/ERK-related pathway," *Cardiology Journal*, vol. 18, no. 6, pp. 675–681, 2011.
- [26] S. Fang, X. Ma, S. Guo, and J. Lu, "MicroRNA-126 inhibits cell viability and invasion in a diabetic retinopathy model via targeting IRS-1," *Oncology Letters*, vol. 14, no. 4, pp. 4311–4318, 2017.
- [27] E. Pishavar and J. Behravan, "miR-126 as a therapeutic agent for diabetes mellitus," *Current Pharmaceutical Design*, vol. 23, no. 22, pp. 3309–3314, 2017.

Research Article

Multifocal Electroretinogram Can Detect the Abnormal Retinal Change in Early Stage of type2 DM Patients without Apparent Diabetic Retinopathy

Jiang Huang¹, Yi Li², Yao Chen¹, Yuhong You¹, Tongtong Niu¹, Weijie Zou¹,
and Weifeng Luo³

¹Department of Ophthalmology, Second Affiliated Hospital of Soochow University, China

²Department of Ophthalmology, Huashan Hospital North, Fudan University, China

³Department of Neurology, Second Affiliated Hospital of Soochow University, China

Correspondence should be addressed to Weifeng Luo; luoweifengsz@sohu.com

Received 29 December 2020; Revised 6 February 2021; Accepted 12 February 2021; Published 23 February 2021

Academic Editor: Irini Chatziralli

Copyright © 2021 Jiang Huang et al. This is an open access article distributed under the Creative Commons Attribution License, which permits unrestricted use, distribution, and reproduction in any medium, provided the original work is properly cited.

Purpose. To study retinal function defects in type 2 diabetic patients without clinically apparent retinopathy using a multifocal electroretinogram (mf-ERG). **Methods.** Seventy-six eyes of thirty-eight type 2 diabetes mellitus (DM) patients without clinically apparent retinopathy and sixty-four normal eyes of thirty-two healthy control (HC) participants were examined using mf-ERG. **Results.** Patients with type 2 DM without apparent diabetic retinopathy demonstrated an obvious implicit time delay of P1 in ring 1, ring 3, and ring 5 compared with healthy controls ($t = 5.184, p \leq 0.001$; $t = 8.077, p \leq 0.001$; $t = 2.000, p = 0.047$, respectively). The implicit time (IT) in ring 4 of N1 wave was significantly delayed in the DM group ($t = 2.327, p = 0.021$). Compared with the HC group, the implicit time of the P1 and N1 waves in the temporal retina zone was significantly prolonged ($t = 3.66, p \leq 0.001$; $t = 2.187, p = 0.03$, respectively). And the amplitude of P1 in the temporal retina decreased in the DM group, which had a significantly statistical difference with the healthy controls ($t = -6.963, p \leq 0.001$). However, there were no differences in either the amplitude of the response or the implicit time of the nasal retina zone between DM and HC. The AUC of multiparameters of mf-ERG was higher in the diagnosis of DR patients. **Conclusions.** Patients with type 2 DM without clinically apparent retinopathy had a delayed implicit time of P1 wave in temporal regions of the postpole of the retina compared with HC subjects. It demonstrates that mf-ERG can detect the abnormal retinal change in the early stage of type 2 DM patients without apparent diabetic retinopathy. Multiparameters of mf-ERG can improve the diagnostic efficacy of DR, and it may be a potential clinical biomarker for early diagnosis of DR.

1. Introduction

Diabetic retinopathy (DR) is one of the irreversible blindness in working-age people in mainland China [1, 2]. Laser photocoagulation, intraocular drug injections (including anti-VEGF), and vitrectomy are the major therapies used to treat DR. All these therapies slow the progression of retinopathy; however, they are unlikely to reverse the loss of vision, and the effective methods for saving vision in the late stages of diabetic retinopathy are still lacking. Moreover, during the stage of proliferative diabetic retinopathy, patients often experience great difficulty in performing daily life activities,

and vision-related quality of life shows a particularly dramatic decline.

Previous studies [3–6] have shown that the mf-ERG is a noninvasive and specific method for detecting the changes of the retinal function in diabetic retinopathy. The delayed implicit time of mf-ERG is locally predictive of nonproliferative retinopathy [7–9]. Additionally, a large amount of research has suggested that neural damage occurs in the retina before the retinal vascular changes become apparent [10–12].

The detection of changes in the retinal function before the occurrence of diabetic damage to the retina would

provide significant clinical evidence for early intervention. The purpose of this study was to identify abnormalities in the retinal function in Chinese type 2 diabetic patients without clinically apparent retinopathy by mf-ERG examination.

2. Methods

2.1. Study Subjects. The study design complied with the principles of the Declaration of Helsinki and all procedures were approved by the Committee on Human Studies of The Second Affiliated Hospital of Soochow University. Written consent was obtained from the participants regarding the use of their clinical records. Seventy-six eyes of thirty-eight type 2 diabetes mellitus (DM) patients without clinically apparent retinopathy (mean age, 64.08 ± 8.53 years) based on several ocular examinations, including slit-lamp, ophthalmoscopy, noncontact intraocular pressure and fundus photography, and sixty-four normal eyes from thirty-two healthy control (HC) participants (mean age, 65.19 ± 5.46 years), were randomly examined using multifocal electroretinogram. The duration of diabetes ranged from 5 to 10 years (mean = 7.13 ± 1.63 years). All eyes had a visual acuity above 16/20 without apparent microaneurysm or exudation in the retina. Patients with glaucoma, hypermyopia, macular disease, and other fundus diseases were excluded from the study.

A review of medical records and an ocular examination revealed that all normal subjects were free of ocular and systemic disease and had a corrected visual acuity of 16/20 or better with a refractive error range from +1.00D to -2.50D. The potential risks and purposes of the study were explained to the subjects, and informed consent was obtained from all subjects before testing. The procedures followed the tenets of the Second Affiliated Hospital of Soochow University Committee for the protection of human subjects.

2.2. mf-ERG Recording. mf-ERG was performed followed by the International Society for Clinical Electrophysiology of Vision guidelines with the test system (VETS V8.1; GOTECH, Chongqing). Pupils of participants were dilated (≥ 7 mm) using 1.0% tropicamide and 2.5% phenylephrine. After topical corneal anesthesia (0.5% proparacaine), a monopolar Jet contact lens electrode was used. Patients were positioned in front of a 19-inch CRT monitor with a distance of 33 cm. A scaled 103-hexagon stimulus pattern with a frame rate of 75 Hz was shown on the CRT monitor. With an m-sequence in every 8-minute recording cycle, the hexagons were regulated between white (200 cd/m^2) and black ($< 2 \text{ cd/m}^2$). The stimulus area was focused on the fovea of the posterior retina (Figure 1), and the data recording was collected in approximately 25 seconds. A Burian-Allen contact lens electrodes were placed on the anesthetized (0.4% hydrochloride Oxybutyprocaine) cornea surface of both eyes. The ground contact electrode was placed on the right earlobe, and the electrode impedance was kept below $5 \text{ k}\Omega$. Fixation was controlled using an "x" target in the center of the stimulus [13]. Contaminated segments were discarded and reevaluated. The amplitude density (AD) and implicit time (IT) were used to analyze general information.

2.3. Statistical Analysis. The Mann-Whitney *U* test was used to identify significant differences between the diabetes mellitus (DM) group and the healthy control (HC) group for all measurements (AD and IT). The results are presented as mean \pm SD. Student's two-tailed *t*-test was used to compare age. The statistical analyses were performed with the SPSS21.0 (SPSS Inc., Chicago, USA). All statistical tests were two-tailed, and a $p < 0.05$ was considered statistically significant. The Pearson chi-square test was used for comparison of sex.

3. Results

3.1. General Demographic Analysis. The demographic data of all participants are shown in Table 1. There were no statistically significant differences for age, sex, BCVA, and intraocular pressure (IOP) between the HC and DM group. However, compared with the HC group, the glycosylated hemoglobin (HbA1c) in the DM group was significantly higher in the DM group ($p < 0.01$).

3.2. Multifocal Electroretinography in Rings. The amplitude density (AD) of P1 wave did not differ significantly between the healthy controls and the diabetic patients for all rings (Table 2). And there was no statistically significant difference in the amplitude of N1 wave. Compared with the HC group, the implicit time (IT) in ring 1, ring 3, and ring 5 of the P1 wave was significantly prolonged in type 2 diabetic patients ($t = 5.184, p \leq 0.001$; $t = 8.077, p \leq 0.001$; $t = 2.000, p = 0.047$, respectively). The implicit time (IT) in ring 4 of N1 wave was significantly delayed in the DM group ($t = 2.327, p = 0.021$).

3.3. Multifocal Electroretinography in the Temporal and Nasal Retina Zone. Compared with the control group, the implicit time of the P1 and N1 waves, which reflected the function of the temporal retina zone, was significantly prolonged ($t = 3.66, p \leq 0.001$; $t = 2.187, p = 0.03$, respectively) (Figure 2). And the amplitude of P1 in temporal retina decreased in the DM group, which had a significant statistical difference with the healthy control ($t = -6.963, p \leq 0.001$) (Figure 3). However, there were no differences in either the amplitude of the response or the implicit time of the nasal retina zone between the patient group and the control group (Figures 2 and 3).

3.4. The ROC Curve Analyses of mf-ERG Examination Results to Test the Predictive Ability of Diabetic Retinopathy. The ROC curves of a single indicator of mf-ERG were represented in Figures 4(a)–4(c). The ROC curves of P1 in ring 1, ring 3, and ring 5 to detect DM were 0.745, 0.876, and 0.690, respectively.

The ROC curves of combinative indicators were plotted in Figures 4(d)–4(f). The AUC of a combination of the IT of P1 in ring 1 and that in ring 3 to detect DM diagnosis DM was 0.912. A combination of the IT of P1 in ring 1 and that in ring 5 revealed an AUC of 0.809. The AUC of the IT of P1 in ring 3 combined with that in ring 5 was 0.887.

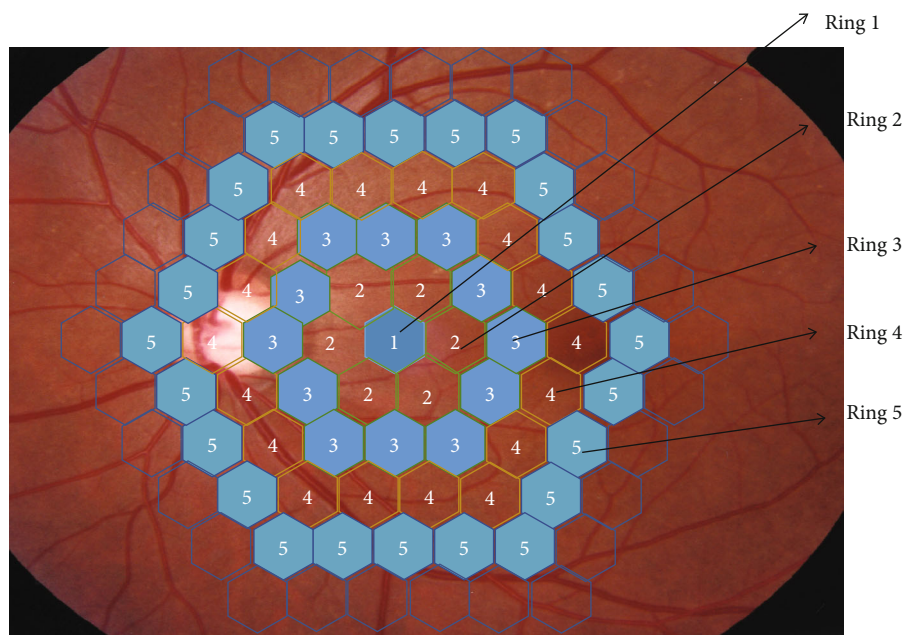


FIGURE 1: shows a fundus photo of the retina with the five rings regions where the mf-ERG can detect the retinal function in the relevant area by extraction of signal in posterior retina.

TABLE 1: Epidemiologic and disease characteristics of all participants in this study.

Number of subjects	HC <i>n</i> = 32	DM <i>n</i> = 38	<i>p</i>
Age (years)	65.19 ± 5.46	64.08 ± 8.35	0.522 ^a
Male/female	17/15	25/13	0.157 ^b
DM duration (years)	—	7.13 ± 1.63	—
HbA1c (%)	4.9 ± 0.70	5.5 ± 0.80	0.005 ^{a**}
BCVA	4.97 ± 0.06	4.96 ± 0.71	0.245 ^c
IOP (mmHg)	15.09 ± 2.57	14.29 ± 2.87	0.086 ^c

Values expressed as mean ± SD (unless otherwise stated). Statistical tests: ^a*t*-test, ^bPearson χ^2 test, and ^cMann-Whitney *U* test. ***p* < 0.01. BCVA: best corrected visual acuity; IOP: intraocular pressure.

4. Discussion

Diabetic retinopathy is one of the leading causes of blindness in developed countries. Pathophysiological studies have demonstrated that diabetic retinopathy is a disease of the small retinal vessels that develops even before the appearance of visible fundus lesions. Typical early changes in the retinal vasculature of diabetic eyes are pericyte loss, basement membrane thickening, microaneurysms, and hyperglycemia [14–16]. Local glucose levels regulate some factors associated with diabetic retinopathy that modulate the activity of smooth muscle cells and pericytes. Hyperglycemia does not lead to visible pathological changes in the retina within the first six weeks. However, even blood glucose levels return to normal, and pericyte apoptosis, basement membrane swelling, vascular endothelial cell proliferation, retinal neurons damage, and vessel lesions are observed. These processes are collectively called “metabolic memory.” Thus, the identification of reti-

nal abnormalities during the early disease stages of diabetic patients is critically important.

There is considerable evidence for defects in the retinal function in diabetic patients even at very early stage of diabetic retinopathy, before the appearance of pathological changes [17–19]. A characteristic example is an observed decline in the visual function, including color vision and contrast sensitivity, in diabetic patients, including those without the clinical manifestation of retinopathy. Microstructurally, the function of the retinal vasculature is also slowly damaged during the diabetes. Previous studies have reported an increase in retinal blood flow and heterogeneity in the distribution of retinal blood flow [20–22]. So, the diagnosis of DR is not simple, especially when it is in the early stage. Recently, Kim et al. [23] concluded that the retinal neurodegeneration and microvascular change may have high association in the early stage of DM. They identified the macular ganglion cell/inner plexiform layer (mGCIPL) thinning prior to the microvascular impairment in DR by optical coherence tomography angiography. That is the morphological evidence. And our research has illustrated this conclusion in the retinal function in DM patients.

Previous research has demonstrated changes in the implicit time and/or amplitude response in diabetic patients with or without retinopathy. Some studies have reported a decrease in mf-ERG amplitudes in diabetic patients [24, 25]. However, other groups have also described higher amplitudes of the first- and second-order components in diabetic patients, a phenomenon that is believed to depend on the higher retinal blood flow resulting from vascular abnormalities in diabetic patients [26, 27]. In the present study, we found that the amplitude response of the P1 wave tended to decrease in all rings; however, these changes had not a statistically significant difference (*p* > 0.05). This observation is

TABLE 2: Retinal function analysis of DM patients and healthy subjects using mf-ERG examinations in healthy controls and DM patients.

Number of eyes tested	HC <i>n</i> = 64	DM <i>n</i> = 76	<i>p</i>
AD of P1 in ring 1	121.88 ± 16.46	116.70 ± 22.90	0.133
AD of P1 in ring 2	40.87 ± 13.95	37.59 ± 12.30	0.142
AD of P1 in ring 3	18.68 ± 3.31	18.56 ± 4.38	0.861
AD of P1 in ring 4	14.17 ± 4.70	12.96 ± 4.59	0.127
AD of P1 in ring 5	8.64 ± 2.00	7.94 ± 2.21	0.053
IT of P1 in ring 1	45.42 ± 4.74	48.85 ± 3.00	≤0.001**
IT of P1 in ring 2	43.20 ± 5.26	44.22 ± 4.25	0.206
IT of P1 in ring 3	40.63 ± 3.53	44.81 ± 2.56	≤0.001**
IT of P1 in ring 4	43.64 ± 3.29	44.75 ± 4.50	0.102
IT of P1 in ring 5	39.97 ± 4.04	41.05 ± 2.26	0.047*
AD of N1 in ring 1	0.78 ± 0.26	0.78 ± 0.26	0.880
AD of N1 in ring 2	0.36 ± 0.16	0.34 ± 0.12	0.349
AD of N1 in ring 3	0.24 ± 0.07	0.23 ± 0.04	0.079
AD of N1 in ring 4	0.23 ± 0.05	0.24 ± 0.08	0.461
AD of N1 in ring 5	0.16 ± 0.12	0.16 ± 0.07	0.754
IT of N1 in ring 1	19.41 ± 4.85	18.59 ± 6.60	0.412
IT of N1 in ring 2	21.71 ± 3.79	23.25 ± 5.86	0.072
IT of N1 in ring 3	19.44 ± 5.28	19.40 ± 6.56	0.970
IT of N1 in ring 4	21.82 ± 7.07	23.92 ± 3.20	0.021*
IT of N1 in ring 5	25.84 ± 4.69	24.12 ± 6.13	0.069

Values expressed as mean ± SD. Statistical tests: Mann-Whitney *U* test. AD: amplitude density (nV/deg²); IT: implicit time (ms). **p* < 0.05, ***p* < 0.01.

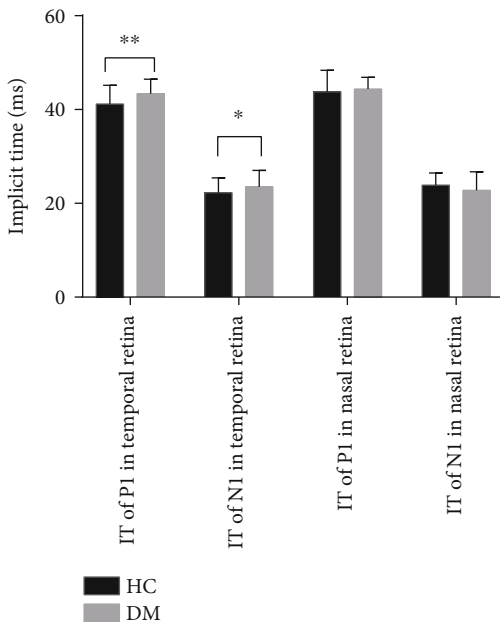


FIGURE 2: The implicit time of P1 and N1 waves in temporal and nasal retina between HC and DM patients.

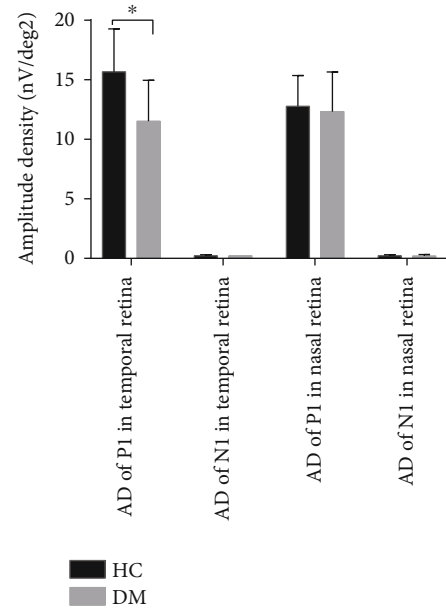


FIGURE 3: The amplitude of P1 and N1 waves in temporal and nasal retina between HC and DM patients, **p* < 0.05.

consistent with previous research [28]. One possible explanation for our findings is that the recruited patients in this research have a steady, normal blood sugar level for a long duration, and their retinal functions were similar to that of a healthy person. Furthermore, in the early stage of diabetes without visible retinopathy, the mf-ERG results showed only selective neurosensory deficits in the inner layers of the retina. Another consideration is that measurement of the amplitude response reflects the strength of the summed responses generated by retinal cells, and changes in the amplitude response failed to reflect abnormalities in the retinal function within only a certain ring zone.

We found that the implicit time of the P1 and N1 waves was significantly prolonged in some regions of the retina in type 2 diabetic patients. The delayed implicit time in diabetic patients without clinically apparent retinopathy may be a consequence of early or undetected perfusion or retinal hypoxia defects associated with choriocapillary degeneration [29].

Additionally, in the present study, we also found that the function of temporal retina was more frequently affected than that in the nasal retina. It suggests that before the appearance of retinopathy, the function of the retina is more susceptible to be damaged. We also found that the greater susceptibility of the temporal retina may be attributed to the reduced retinal vasodilator reserve and the potentially associated risk of ischemic damage in comparison to the nasal retina [30–33]. And another possible reason is, as Curcio et al. reported, a higher density of cones and ganglion cells in the nasal macular area compared with the temporal area [32]. The mf-ERG recordings reflect the electrical activity of bipolar and photoreceptor cells. Our findings suggest that high blood sugar results in greater damage to the temporal retina in diabetic patients, even those without clinically

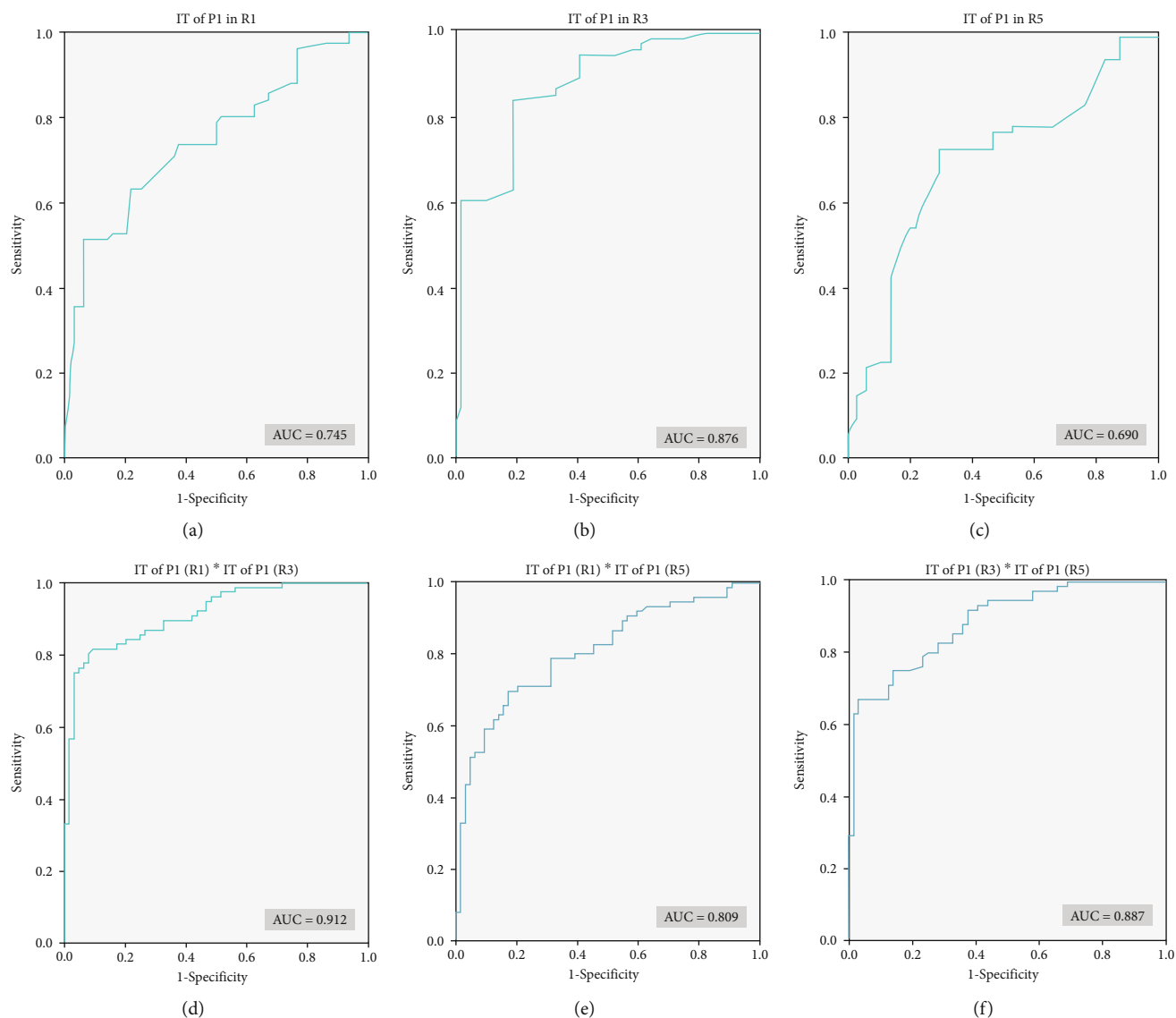


FIGURE 4: (a)–(c) shows ROC curves of the single parameter of mf-ERG for diagnosing diabetic retinopathy. (d)–(f) shows ROC curves of multiparameters of mf-ERG for diagnosing diabetic retinopathy. IT: implicit time; R1: ring 1; R3: ring 3; R5: ring 5.

apparent retinopathy, because the low density of cones and ganglion cells in the temporal area is associated with less compensatory function.

Interestingly, the mf-ERG amplitude measurements were not significantly decreased in rings compared with the implicit times, which is consistent with previous findings [28]. One possible explanation for this result is that focal ERG revealed selective neurosensory deficits of the inner retinal layers in patients with early-stage diabetes without visible retinopathy. So, these results are suggested that only one parameter in certain ring could not reflect the retinal dysfunction especially in the early stage of DM, and it should be combined with multiparameters to detect the abnormal change of retina. This is the new perspectives of our research.

The ROC analysis illustrated that although the IT in ring 1, ring 3, and ring 5 of the P1 wave had significant difference

in DM patients, compared with the health control group, and the single parameter ROC curve analysis showed the low AUC, respectively.

Multiparameter ROC curve analysis demonstrated that it can increase the diagnostic efficacy of diabetic retinopathy. The combination of multiparameter mf-ERG could get a higher diagnosis effectiveness to identify diabetic retinopathy in DM patients without clinically visible DR in the early stage. It indicated that the IT in P1 combined with IT in P3 had the highest efficacy in diagnosis of DR. It reveals that the abnormal results of mf-ERG test in multiregions of the posterior retina may suggest the prominently decreased retinal function of DM patients even without apparent clinical diabetic retinopathy.

In summary, before the onset of clinically apparent diabetic retinopathy, there is a prolonged period of pathological

changes. The mf-ERG is well suited to study retinal diseases that are confined to local lesions, especially those in the posterior pole such as diabetic retinopathy and age-related macular degeneration, among others. The mechanism underlying the mf-ERG implicit time delay in diabetic patients remains unknown. Hypoxia, modifications of local blood flow, or changes in local metabolism may be responsible for the observed effects. The mf-ERG implicit time is sufficiently sensitive to reflect the retinal function and can be employed to evaluate diabetic patients without apparent clinical retinopathy or those in very early stages of diabetes.

Data Availability

The data used to support the findings of this study are available from the corresponding author upon request.

Ethical Approval

The study was approved by the Second affiliated Hospital of Soochow University. All procedures conformed to the tenets of the Declaration of Helsinki. Written informed consent was obtained.

Conflicts of Interest

The authors do not have a conflict of interest.

Authors' Contributions

Jiang Huang and Yi Li You have contributed equally to this work, and they are the co-first authors.

Acknowledgments

We are especially grateful to the participants in this study. This work was supported by the Second Affiliated Hospital of Soochow University Research Fund Project (SDFEYBS1903 and SDFEYBS1914), National Natural Science Foundation of China (No. 81671270), and the Second Affiliated Hospital of Soochow University Preponderant Clinic Discipline Group Project Funding (XKQ2015002).

References

- [1] M. Yang, Y. Liu, C. Wen et al., "Association between spousal diabetes status and diabetic retinopathy in Chinese patients with type 2 diabetes," *Diabetes & Vascular Disease Research*, vol. 16, no. 5, pp. 474–477, 2019.
- [2] P. Song, J. Yu, K. Y. Chan, E. Theodoratou, and I. Rudan, "Prevalence, risk factors and burden of diabetic retinopathy in China: a systematic review and meta-analysis," *Journal of Global Health*, vol. 8, no. 1, article 010803, 2018.
- [3] N. Goel, A. Prakash, and A. K. Gupta, "Multifocal electroretinography in diabetic retinopathy with and without macular edema," *Ophthalmic Surgery, Lasers & Imaging Retina*, vol. 49, no. 10, pp. 780–786, 2018.
- [4] P. Adhikari, S. Marasini, R. P. Shah, S. N. Joshi, and J. K. Shrestha, "Multifocal electroretinogram responses in Nepalese diabetic patients without retinopathy," *Documenta Ophthalmologica*, vol. 129, no. 1, pp. 39–46, 2014.
- [5] A. R. Santos, L. Ribeiro, F. Bandello et al., "Functional and structural findings of neurodegeneration in early stages of diabetic retinopathy: cross-sectional analyses of baseline data of the EUROCONDOR project," *Diabetes*, vol. 66, no. 9, pp. 2503–2510, 2017.
- [6] H. Safi, S. Safi, A. Hafezi-Moghadam, and H. Ahmadi, "Early detection of diabetic retinopathy," *Survey of Ophthalmology*, vol. 63, no. 5, pp. 601–608, 2018.
- [7] W. W. Harrison, M. A. Bearse, J. S. Ng et al., "Multifocal electroretinograms predict onset of diabetic retinopathy in adult patients with diabetes," *Investigative Ophthalmology & Visual Science*, vol. 52, no. 2, pp. 772–777, 2011.
- [8] M. A. Bearse Jr. and G. Y. Ozawa, "Multifocal electroretinography in diabetic retinopathy and diabetic macular edema," *Current Diabetes Reports*, vol. 14, no. 9, p. 526, 2014.
- [9] W. W. Harrison, M. A. Bearse Jr., M. E. Schneck et al., "Prediction, by retinal location, of the onset of diabetic edema in patients with nonproliferative diabetic retinopathy," *Investigative Ophthalmology & Visual Science*, vol. 52, no. 9, pp. 6825–6831, 2011.
- [10] C. Rapino, D. Tortolani, L. Scipioni, and M. Maccarrone, "Neuroprotection by (endo)cannabinoids in glaucoma and retinal neurodegenerative diseases," *Current Neuropharmacology*, vol. 16, no. 7, pp. 959–970, 2018.
- [11] M. A. Zorrilla-Zubilete, A. Yeste, F. J. Quintana, D. Toiber, R. Mostoslavsky, and D. M. Silberman, "Epigenetic control of early neurodegenerative events in diabetic retinopathy by the histone deacetylase SIRT6," *Journal of Neurochemistry*, vol. 144, no. 2, pp. 128–138, 2018.
- [12] R. Mastropasqua, R. D'Aloisio, C. De Nicola et al., "Widefield swept source OCTA in retinitis pigmentosa," *Diagnostics*, vol. 10, no. 1, p. 50, 2020.
- [13] J. Huang, Y. Li, J. Xiao et al., "Combination of Multifocal Electroretinogram and Spectral-Domain OCT Can Increase Diagnostic Efficacy of Parkinson's Disease," *Parkinson's Disease*, vol. 2018, Article ID 4163239, 7 pages, 2018.
- [14] B. Molins, A. Mora, S. Romero-Vázquez et al., "Shear stress modulates inner blood retinal barrier phenotype," *Experimental Eye Research*, vol. 187, p. 107751, 2019.
- [15] K. D. Rochfort, L. S. Carroll, P. Barabas et al., "COMP-Ang1 stabilizes hyperglycemic disruption of blood-retinal barrier phenotype in human retinal microvascular endothelial cells," *Investigative Ophthalmology & Visual Science*, vol. 60, no. 10, pp. 3547–3555, 2019.
- [16] M. G. Rossino, M. D. Monte, and G. Casini, "Relationships between neurodegeneration and vascular damage in diabetic retinopathy," *Frontiers in Neuroscience*, vol. 13, p. 1172, 2019.
- [17] Y. Zeng, D. Cao, H. Yu et al., "Early retinal neurovascular impairment in patients with diabetes without clinically detectable retinopathy," *The British Journal of Ophthalmology*, vol. 103, no. 12, pp. 1747–1752, 2019.
- [18] K. A. Joltikov, V. M. de Castro, J. R. Davila et al., "Multidimensional functional and structural evaluation reveals Neuroretinal impairment in early diabetic retinopathy," *Investigative Ophthalmology & Visual Science*, vol. 58, no. 6, pp. BIO277–BIO290, 2017.
- [19] S. Neriyani, S. Pardhan, L. Gella et al., "Retinal sensitivity changes associated with diabetic neuropathy in the absence of diabetic retinopathy," *The British Journal of Ophthalmology*, vol. 101, no. 9, pp. 1174–1178, 2017.

- [20] H. Kremer, J. Gebauer, S. Elvers-Hornung et al., "Pro-angiogenic activity discriminates human adipose-derived stromal cells from retinal pericytes: considerations for cell-based therapy of diabetic retinopathy," *Frontiers in Cell and Developmental Biology*, vol. 8, p. 387, 2020.
- [21] N. S. Sahajpal, R. K. Goel, A. Chaubey, R. Aurora, and S. K. Jain, "Pathological perturbations in diabetic retinopathy: hyperglycemia, AGEs, oxidative stress and inflammatory pathways," *Current Protein & Peptide Science*, vol. 20, no. 1, pp. 92–110, 2018.
- [22] S. A. Madsen-Bouterse and R. A. Kowluru, "Oxidative stress and diabetic retinopathy: pathophysiological mechanisms and treatment perspectives," *Reviews in Endocrine & Metabolic Disorders*, vol. 9, no. 4, pp. 315–327, 2008.
- [23] K. Kim, E. S. Kim, D. G. Kim, and S. Y. Yu, "Progressive retinal neurodegeneration and microvascular change in diabetic retinopathy: longitudinal study using OCT angiography," *Acta Diabetologica*, vol. 56, no. 12, pp. 1275–1282, 2019.
- [24] U. Frydkjaer-Olsen, R. S. Hansen, K. Pedersen, T. Peto, and J. Grauslund, "Retinal vascular fractals correlate with early neurodegeneration in patients with type 2 diabetes mellitus," *Investigative Ophthalmology & Visual Science*, vol. 56, no. 12, pp. 7438–7443, 2015.
- [25] Y. Fu, P. Wang, X. Meng, Z. Du, and D. Wang, "Structural and functional assessment after intravitreal injection of ranibizumab in diabetic macular edema," *Documenta Ophthalmologica*, vol. 135, no. 3, pp. 165–173, 2017.
- [26] T. Bek, "Diameter changes of retinal vessels in diabetic retinopathy," *Current Diabetes Reports*, vol. 17, no. 10, 2017.
- [27] K. B. Schaal, M. R. Munk, I. Wyssmueller, L. E. Berger, M. S. Zinkernagel, and S. Wolf, "Vascular abnormalities in diabetic retinopathy assessed with swept-source optical coherence tomography angiography widefield IMAGING," *Retina*, vol. 39, no. 1, pp. 79–87, 2019.
- [28] K. B. Jonsson, U. Frydkjaer-Olsen, and J. Grauslund, "Vascular changes and neurodegeneration in the early stages of diabetic retinopathy: which comes first?," *Ophthalmic Research*, vol. 56, no. 1, pp. 1–9, 2016.
- [29] J. Mesquita, J. P. Castro-de-Sousa, S. Vaz-Pereira, A. Neves, L. A. Passarinha, and C. T. Tomaz, "Vascular endothelial growth factors and placenta growth factor in retinal vasculopathies: current research and future perspectives," *Cytokine & Growth Factor Reviews*, vol. 39, pp. 102–115, 2018.
- [30] D. van Norren and J. J. Vos, "Light damage to the retina: an historical approach," *Eye (London, England)*, vol. 30, no. 2, pp. 169–172, 2016.
- [31] V. Baksheeva, V. Tiulina, N. Tikhomirova et al., "Suppression of light-induced oxidative stress in the retina by mitochondria-targeted antioxidant," *Antioxidants*, vol. 8, no. 1, p. 3, 2019.
- [32] C. A. Curcio, K. R. Sloan, R. E. Kalina, and A. E. Hendrickson, "Human photoreceptor topography," *The Journal of Comparative Neurology*, vol. 292, no. 4, pp. 497–523, 1990.
- [33] U. Frydkjaer-Olsen, R. S. Hansen, T. Peto, and J. Grauslund, "Structural neurodegeneration correlates with early diabetic retinopathy," *International Ophthalmology*, vol. 38, no. 4, pp. 1621–1626, 2018.

Research Article

The Risk Factors for Diabetic Retinopathy in a Chinese Population: A Cross-Sectional Study

Qingmin Sun,^{1,2} Yali Jing,³ Bingjie Zhang,³ Tianwei Gu,³ Ran Meng,³ Jie Sun,³
Dalong Zhu ,³ and Yaping Wang ^{1,4}

¹Department of Medical Genetics, Nanjing University School of Medicine, Nanjing 210093, China

²Department of Pharmacy, Jiangsu Province Hospital of Chinese Medicine, Affiliated Hospital of Nanjing University of Chinese Medicine, Nanjing 210029, China

³Department of Endocrinology, Drum Tower Hospital Affiliated to Nanjing University Medical School, No321 Zhongshan Road, Nanjing 210008, China

⁴Jiangsu Key Laboratory of Molecular Medicine, Nanjing University, Nanjing 210093, China

Correspondence should be addressed to Dalong Zhu; zhu_dalong@126.com and Yaping Wang; wangyap@nju.edu.cn

Received 22 July 2020; Revised 21 December 2020; Accepted 22 January 2021; Published 28 January 2021

Academic Editor: Irini Chatziralli

Copyright © 2021 Qingmin Sun et al. This is an open access article distributed under the Creative Commons Attribution License, which permits unrestricted use, distribution, and reproduction in any medium, provided the original work is properly cited.

Aims. Epidemiological data on diabetic retinopathy (DR) in Chinese population is still rather scarce, and risk factors for diabetic retinopathy are inconsistent because of study designs, grading standards, and population samples. **Materials and Methods.** This hospital-based retrospective study included 1052 type 2 diabetes patients. Diabetic retinopathy was diagnosed by nonmydriatic fundus photography and/or fundus examination apparatus. Logistic regression analysis was performed to evaluate the risk of diabetic retinopathy. **Results.** A total of 352 (33.5% prevalence) subjects were diagnosed with diabetic retinopathy based on our population. The patients in the DR group not only had significantly higher hemoglobin A1c (HbA1c), fasting plasma glucose (FPG), urinary microalbumin-creatinine ratio (ACR), and systolic blood pressure but also had higher follicle-stimulating hormone (FSH), luteinizing hormone (LH), and sex hormone-binding globulin (SHBG) levels compared to those in the non-DR group. Moreover, we confirmed that diabetes duration and HbA1c are strongly associated with DR risk. We also found that serum LH was an independent risk factor in male diabetic retinopathy patients (OR = 1.086, 95% CI 1.024–1.152), and the levels of LH were significantly associated with diabetic retinopathy prevalence ($P = 0.018$). **Conclusions.** Our study strengthens the argument that diabetes duration and HbA1c are risk factors for patients with DR. Additionally; we firstly confirmed that serum LH was an independent risk factor in male diabetic retinopathy patients.

1. Introduction

Diabetic retinopathy (DR) is a common microvascular complication of diabetes and is the first leading cause of irreversible vision loss in people of working age. A global meta-analysis reported that nearly one-third of diabetic patients have been diagnosed with diabetic retinopathy [1]. Diabetic retinopathy has been considered to be correlated with a higher risk of systemic vascular complications, such as nephropathy, peripheral neuropathy, and cardiovascular events, all of which lead to poor quality of life [2]. Therefore, the study of related risk factors is conducive to predict the condition of diabetic retinopathy in clinic.

Several epidemiological studies have reported the risk factors of diabetic retinopathy and aiming at the prevention and management of the disease, including a series of cross-sectional studies or cohort studies [3–5]. However, epidemiological data on diabetic retinopathy in Chinese population is still rather scarce, and risk factors for diabetic retinopathy are inconsistent because of study designs, grading standards, and population samples. Previous studies had confirmed that a variety of risk factors are associated with the development of diabetic retinopathy, including the history of diabetes, glycosylated hemoglobin A1c (HbA1c) levels, hyperglycemia, dyslipidemia, hypertension, and obesity [6, 7]. Especially, the longer diabetes duration and higher levels of HbA1c have

been recognized as the key risk factors for diabetic retinopathy in a global diabetic retinopathy study [1].

There is a growing body of evidence indicating that multiplicity and complexity of sex hormone action target organs, particularly in the diabetic setting [8]. Some evidence suggested sex hormones appear to play an important role in optic nerve pathologies and other eye diseases [9]. Moreover, recent findings showed women seem to be at a higher risk for diabetic macrovascular complications, but the consequences of microvascular complications may be greater in men [8]. Therefore, in our cross-sectional study, multiple regression analysis was used to investigate the independently risk factor of diabetic retinopathy either including gender, age, diabetes duration, hyperglycemia, body mass index (BMI), blood pressure, HbA1c, and sex hormones in patients of type 2 diabetes. In this study, we sought to explore the special risk factors associated with diabetic retinopathy in a Chinese population.

2. Materials and Methods

2.1. Subjects. Clinical data of 1052 patients with type 2 diabetes were collected retrospectively during a period between January 2016 and January 2018 in the department of endocrinology, Nanjing Drum Tower Hospital, including 724 males and 328 females, aged between 18 and 70 years. Diagnostic of type 2 diabetes were considered according to 2003 American Diabetes Association criteria [10]. International clinical diabetic retinopathy disease severity scale was adopted to grade the retinopathy [11]. Subjects who combined with acute complications of diabetes, serious infections and important viscera, organ (heart, liver, kidney, etc.) dysfunction, and malignant tumor were excluded. Patients who have taken drugs affecting sexual hormone levels in the past three months were also excluded. This study has been approved by the Ethics Committee of the Nanjing Drum Tower Hospital.

2.2. Demographic Data. Anthropometric data on the height, weight, body mass index (BMI), waist circumference, hip circumference, and waist to hip ratio (WHR) were obtained from each subject. BMI was estimated based on the formula: $BMI = \text{weight (kg)}/\text{height (m}^2\text{)}$ [2]. WHR was determined according to the ratio between the standing waist and hip circumference. Patients' diabetes duration, blood pressure, and smoking and drinking history were collected.

2.3. Biochemical Measurements. Biochemical measurements were performed after fasting for at least 10 hours. Fasting plasma glucose (FPG) was tested using a hexokinase method (TBA-200FR, Tokyo, Japan). Fasting plasma C-peptide (FCP), follicle-stimulating hormone (FSH), luteinizing hormone (LH), serum testosterone, sulfated dehydroepiandrosterone (DHEAS), and hormone-binding globulin (SHBG) were determined by chemiluminescence analysis (Siemens, Bad Nauheim, Germany). The method of high-pressure liquid chromatography is using for determining HbA1c. Triglycerides (TG), high-density lipoprotein cholesterol (HDL-c), low-density lipoprotein cholesterol (LDL-c), total cholesterol (TC), creatinine, and urea nitrogen were

TABLE 1: Characteristics of subjects with or without diabetic retinopathy.

	Non-DR	DR	P value
<i>n</i>	700	352	—
Age (y)	52.7 ± 11.5	55.3 ± 9.8	<0.001
BMI (kg/m ²)	25.4 ± 3.8	25.0 ± 3.7	0.144
Waist circumference (cm)	91.7 ± 9.5	91.3 ± 9.8	0.568
Waist-to-hip ratio	0.9 ± 0.1	0.9 ± 0.1	0.275
Systolic BP (mmHg)	132.4 ± 16.4	136.5 ± 19.2	0.001
Diastolic BP (mmHg)	80.7 ± 11.8	81.0 ± 11.5	0.672
Smoking (%)	230 (32.9)	112 (31.8)	0.780
Drinking (%)	128 (18.3)	56 (15.9)	0.390
Diabetes duration (y)	7.1 ± 6.3	10.5 ± 6.4	<0.001
HbA1c (%)	8.7 ± 2.3	9.3 ± 2.2	<0.001
FPG (mmol/L)	8.4 ± 2.7	8.8 ± 3.1	0.037
FCP (pmol/L)	688.1 ± 371.1	617.7 ± 414.8	0.006
BUN (mmol/L)	6.2 ± 16.9	5.8 ± 3.1	0.711
Creatinine (μmol/L)	60.9 ± 14.8	61.5 ± 15.2	0.488
ACR (mg/g)	42.0 ± 120.7	176.4 ± 538.2	<0.001
Triglycerides (mmol/L)	1.9 ± 2.4	1.8 ± 2.0	0.538
Total cholesterol (mmol/L)	5.0 ± 15.5	4.4 ± 1.2	0.485
HDL cholesterol (mmol/L)	1.3 ± 4.6	1.1 ± 0.3	0.493
LDL cholesterol (mmol/L)	2.6 ± 0.9	2.5 ± 0.9	0.425
FSH (mIU/mL)	18.1 ± 21.6	23.9 ± 25.2	<0.001
LH (mIU/mL)	9.0 ± 10.8	11.4 ± 10.6	0.001
Estradiol (pmol/L)	151.6 ± 125.2	153.2 ± 186.5	0.875
Testosterone (nmol/L)	8.5 ± 6.9	8.7 ± 10.9	0.770
DHEAS (μg/dL)	165.1 ± 94.4	144.0 ± 80.7	0.006
SHBG (nmol/L)	30.8 ± 17.3	36.2 ± 19.9	0.001

Abbreviation: DR: diabetic retinopathy; BMI: body mass index; BP: blood pressure; FPG: fasting plasma glucose; FCP: fasting plasma C-peptide; BUN: blood urea nitrogen; ACR: urinary microalbumin-creatinine ratio; FSH: follicle-stimulating hormone; LH: luteinizing hormone; DHEAS: sulfated dehydroepiandrosterone; SHBG: sex hormone-binding globulin. Data are shown as mean ± SD or number (percentage).

detected by automatic biochemical analyzer. The urine microalbumin-creatinine ratio (ACR) is determined by immunoturbidimetry.

2.4. Study Design. Based on international clinical diabetic retinopathy disease severity scale, the patients were divided into the diabetic retinopathy group (DR group) and nondiabetic retinopathy group (non-DR group) by nonmydriatic fundus photography and/or fundus examination apparatus. Patients in the diabetic retinopathy group are all nonproliferative diabetic retinopathy. We divided the diabetic retinopathy group into the mild nonproliferative diabetic retinopathy group (mild NPDR), moderate nonproliferative diabetic retinopathy group (moderate NPDR), and severe nonproliferative diabetic retinopathy group (severe NPDR) according to disease severity.

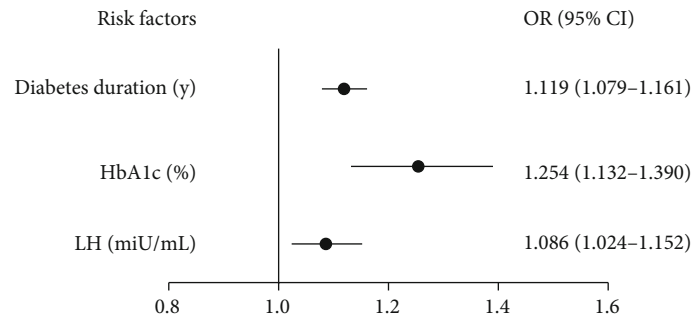


FIGURE 1: Independent risk factors for male diabetic retinopathy patients. Binary logistic regression analysis was performed by adjusting for age, smoking, drinking, systolic BP, BMI, HbA1c, TG, TC, FSH, T, DHEAS, and SHBG.

TABLE 2: Characteristics of male subjects by the severity of diabetic retinopathy.

	Mild NPDR	Moderate NPDR	Severe NPDR	P value
<i>n</i>	169	51	13	—
Age (y)	54.8 ± 10.3	53.3 ± 8.8	50.7 ± 13.8	0.274
Systolic BP (mmHg)	135.2 ± 19.3	136.6 ± 16.9	135.5 ± 18.7	0.904
Diabetes duration (y)	9.9 ± 6.5	11.3 ± 5.4	15.1 ± 7.5*	0.011
HbA1c (%)	9.2 ± 2.2	9.3 ± 2.0	9.3 ± 2.2	0.963
FPG (mmol/L)	8.7 ± 3.0	9.3 ± 4.1	8.1 ± 3.2	0.360
ACR (mg/g)	171.0 ± 538.7	295.4 ± 767.2	159.2 ± 167.8	0.428
LDL cholesterol (mmol/L)	2.4 ± 0.8	2.6 ± 0.9	2.3 ± 0.6	0.398
LH (mIU/mL)	6.3 ± 4.3	5.7 ± 3.0	6.1 ± 4.3	0.706

Abbreviation: NPDR: nonproliferative diabetic retinopathy; BP: blood pressure; ACR: urinary microalbumin-creatinine ratio; LH: luteinizing hormone. Data are shown as mean ± SD or number (percentage). * $P < 0.05$ versus the mild NPDR group; # $P < 0.05$ versus the moderate NPDR group.

2.5. Statistical Analyses. All statistical analyses were performed using SPSS software, version 22.0 (SPSS Inc., Chicago, IL, USA). A value of $P < 0.05$ was considered statistically significant. Continuous variables are represented by mean ± standard deviation (SD), and categorical variables are represented by percentage. According to different types of variables, independent sample *t*-test, rank sum test (Mann–Whitney *U* test), or chi square test was used to compare outcomes between two independent groups. The Cochran–Armitage trend test was used to analyze the difference of incidence rate of diabetic retinopathy in different LH levels. Binary logistic regression analysis was performed to evaluate the risk of LH and diabetic retinopathy, adjusted for confounding factors including age, BMI, systolic blood pressure, diabetes durations, HbA1c, FPG, FCP, urinary ACR, FSH, LH, DHEAS, and SHBG, to clarify the relationship between serum LH level and diabetic retinopathy.

3. Results

3.1. Characteristics of Participants. A total of 1052 type 2 diabetes patients (328 females, 724 males) were included in this study, and 352 (33.5%, 352/1052) subjects were diagnosed with diabetic retinopathy (DR group), the other 700 (66.5%, 700/1052) patients without diabetic retinopathy (non-DR group). The mean ages and diabetes durations of the patients

were 55.3 ± 9.8 years and 10.5 ± 6.4 years in the DR group and 52.7 ± 11.5 years and 7.1 ± 6.3 years in the non-DR group. As expected, the patients in the diabetic retinopathy group had significantly higher HbA1c ($P < 0.001$), FPG ($P = 0.037$), urinary ACR ($P < 0.001$), and systolic blood pressure ($P = 0.001$) compared to those in the non-DR group. Compared with the non-DR group, FCP was lower in the diabetic retinopathy group ($P = 0.006$). No difference was observed in BMI, WHR, smoking and drinking situation, TC, TG, HDL-c, LDL-c, BUN, and creatinine between the two groups. However, higher FSH ($P < 0.001$), LH ($P = 0.001$), and SHBG ($P = 0.001$) levels were observed in the diabetic retinopathy group. These results indicated that sex hormones may be associated with progress of diabetic retinopathy. All characteristics of subjects were summarized in Table 1.

3.2. Risk Factors for Diabetic Retinopathy. In regression analysis, diabetes duration (OR = 1.098, 95% CI 1.068–1.129) and HbA1c (OR = 1.195, 95% CI 1.103–1.295) were significantly associated with diabetic retinopathy for all the included subjects in this study. In further binary logistic regression analysis for males and females, diabetes duration (OR = 1.119, 95% CI 1.079–1.161), HbA1c (OR = 1.254, 95% CI 1.132–1.390), and LH (OR = 1.086, 95% CI 1.024–1.152) showed being independent risk factors for male

TABLE 3: Characteristics of male subjects with or without diabetic retinopathy.

	Non-DR	DR	<i>P</i> value
<i>n</i>	491	233	—
Age (y)	51.3 ± 11.7	54.3 ± 10.3	<0.001
BMI (kg/m ²)	25.5 ± 3.7	24.8 ± 3.3	0.014
Waist circumference (cm)	92.9 ± 8.7	91.7 ± 8.9	0.141
Waist-to-hip ratio	0.9 ± 0.1	0.9 ± 0.1	0.991
Systolic BP (mmHg)	131.7 ± 15.6	135.6 ± 18.7	0.004
Diastolic BP (mmHg)	81.5 ± 11.5	81.9 ± 10.8	0.643
Smoking (%)	230 (46.8)	112 (48.1)	0.811
Drinking (%)	128 (26.1)	56 (24.0)	0.584
Diabetes duration (y)	6.7 ± 6.1	10.5 ± 6.4	<0.001
HbA1c (%)	8.7 ± 2.4	9.2 ± 2.2	0.003
FPG (mmol/L)	8.3 ± 2.7	8.8 ± 3.3	0.045
FCP (pmol/L)	698.1 ± 383.7	588.9 ± 309.8	<0.001
BUN (mmol/L)	6.5 ± 20.0	5.8 ± 1.4	0.605
Creatinine (μmol/L)	66.2 ± 12.8	66.1 ± 13.2	0.958
ACR (mg/g)	37.3 ± 90.0	199.6 ± 587.8	<0.001
Triglycerides (mmol/L)	2.0 ± 2.8	1.9 ± 2.2	0.557
Total cholesterol (mmol/L)	4.3 ± 1.4	4.4 ± 1.3	0.772
HDL cholesterol (mmol/L)	1.3 ± 5.5	1.0 ± 0.3	0.525
LDL-cholesterol (mmol/L)	2.5 ± 0.9	2.5 ± 0.9	0.696
FSH (mIU/mL)	7.9 ± 6.3	10.5 ± 9.6	<0.001
LH (mIU/mL)	4.8 ± 3.3	6.1 ± 4.1	<0.001
Estradiol (pmol/L)	144.5 ± 49.8	158.7 ± 172.6	0.109
Testosterone (nmol/L)	12.1 ± 5.3	13.2 ± 11.5	0.177
DHEAS (μg/dL)	189.5 ± 93.9	164.9 ± 80.4	0.009
SHBG (nmol/L)	28.8 ± 14.5	34.7 ± 17.2	<0.001

Abbreviation: DR: diabetic retinopathy; BMI: body mass index; BP: blood pressure; FPG: fasting plasma glucose; FCP: fasting plasma C-peptide; BUN: blood urea nitrogen; ACR: urinary microalbumin-creatinine ratio; FSH: follicle-stimulating hormone; LH: luteinizing hormone; DHEAS: sulfated dehydroepiandrosterone; SHBG: sex hormone-binding globulin. Data are shown as mean ± SD or number (percentage).

diabetic retinopathy patients, after controlling for age, smoking, drinking, systolic BP, BMI, HbA1c, TG, TC, FSH, T, DHEAS, and SHBG (Figure 1). Interestingly, there was no risk association between the DR group and non-DR group in LH levels among female patients. Furthermore, we divide the female group into the premenopausal and postmenopausal groups; there was still no difference between the two groups. Additionally, according to the severity of diabetic retinopathy, we divided all the male diabetic retinopathy patients into three groups: the mild NPDR group, moderate NPDR group, and severe NPDR group. Table 2 showed that only the duration of diabetes were positively associated with the degrees of diabetic retinopathy ($P = 0.011$), and no correlation between LH and diabetic retinopathy severity was found. Therefore, similar to previous studies, the present study confirmed that diabetes duration and HbA1c are

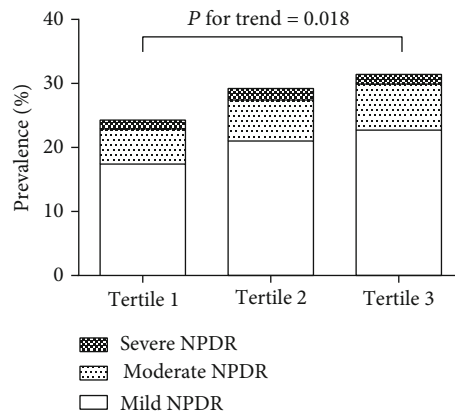


FIGURE 2: Prevalence of diabetic retinopathy by tertiles of LH. The Cochran-Armitage trend test was used to analyze the difference of incidence rate of diabetic retinopathy in different LH levels. With increasing levels of LH, there was a trend accompanied with higher prevalence of diabetic retinopathy.

strongly associated with diabetic retinopathy. Additionally, we also confirmed that serum LH was an independent risk factor in male diabetic retinopathy patients.

3.3. The Association of LH Levels and Diabetic Retinopathy Prevalence. Given that serum LH can have a role on male diabetic retinopathy, we further compared the levels of LH in the DR group and non-DR group in the male patients and found that the level of LH in the DR group was significantly higher ($P < 0.001$). Unexpectedly, a much less BMI was observed in the male DR group ($P = 0.014$). Similar to the results from all subjects, HbA1c, FPG, urinary ACR, and systolic blood pressure levels were also higher in the male DR group than those in the non-DR group ($P < 0.050$ for each) (Table 3). Furthermore, LH was divided into tertiles according to the expression levels in male diabetic retinopathy patients. We found that increasing levels of LH were accompanied with higher prevalence of diabetic retinopathy ($P = 0.018$, Figure 2). With increasing tertiles of LH, systolic BP, creatinine, and ACR was increased as well. Moreover, TC and LDL-c levels showed downtrends accompanied with LH tertiles (Table 4). These results showed that the levels of LH were significantly associated with diabetic retinopathy prevalence.

4. Discussion

In the present study, we found that 33.5% subjects were diagnosed with diabetic retinopathy in type 2 diabetes patients based on a Chinese population. The patients in the diabetic retinopathy group not only had significantly higher HbA1c, FPG, urinary ACR, and systolic blood pressure but also had higher FSH, LH, and SHBG levels compared to those in the non-DR group. Moreover, we confirmed that diabetes duration and HbA1c are strongly associated with diabetic retinopathy risk. Additionally; we firstly suggested that serum LH was an independent risk factor in male diabetic retinopathy patients, and the levels of LH were significant associated with diabetic retinopathy prevalence. It is suggested that LH can be used as a risk predictor of diabetic retinopathy in men.

TABLE 4: Characteristics of male subjects by tertiles of LH.

	T1 (0.1-3.6)	T2 (3.6-5.38)	T3 (5.38-40.0)	P value
Age (y)	46.4 ± 11.5	52.8 ± 10.4*	57.2 ± 9.3*#	<0.001
BMI (kg/m ²)	26.0 ± 4.5	25.4 ± 3.3	24.6 ± 2.7*#	<0.001
Systolic BP (mmHg)	130.6 ± 17.0	132.4 ± 17.5	136.5 ± 16.3*#	0.001
Diabetes duration (y)	5.1 ± 5.2	8.3 ± 6.1*	10.1 ± 6.7*#	<0.001
HbA1c (%)	9.2 ± 2.3	8.6 ± 2.2*	8.9 ± 2.3	0.026
FPG (mmol/L)	8.9 ± 3.3	8.2 ± 2.5*	8.4 ± 2.9	0.041
FCP (pmol/L)	707.1 ± 457.6	666.9 ± 321.2	627.3 ± 328.1	0.088
Creatinine (μmol/L)	62.8 ± 11.5	66.4 ± 12.4*	68.6 ± 14.1*	<0.001
ACR (mg/g)	55.8 ± 203.4	53.3 ± 141.3	165.9 ± 564.6*#	0.001
TC (mmol/L)	4.5 ± 1.3	4.3 ± 1.2*	4.2 ± 1.1*	0.021
LDL-c (mmol/L)	2.6 ± 0.9	2.5 ± 0.8	2.4 ± 0.9*	0.032

Abbreviation: LH: luteinizing hormone; T1: tertile 1; T2: tertile 2; T3: tertile 3; BMI: body mass index; BP: blood pressure; FPG: fasting plasma glucose; FCP: fasting plasma C-peptide; ACR: urinary microalbumin-creatinine ratio; TC: total cholesterol; LDL-c, low-density lipoprotein cholesterol. Data are shown as mean ± SD or number (percentage). **P* < 0.05 versus the T1 group; #*P* < 0.05 versus the T2 group.

Epidemiological data show that there are about 3.82 billion people diagnosed with diabetes globally at present, of which 1.26 billion people are suffering from diabetic retinopathy and about 370 million people have serious vision-threatening complications, which seriously affects the patient's daily activities and quality of life and overburdening the global health care system [12, 13]. Diabetic chronic microvascular complications mainly refer to vascular damage of the retina and kidney, which can also accelerate the occurrence of cardiovascular disease [14, 15]. Therefore, it is very important to find more risk factors for diabetic retinopathy. Previous studies have confirmed that the duration of diabetes, age, plasma glucose, blood lipid, blood pressure, HbA1c, and obesity are risk factors for diabetic retinopathy [7, 16]. Similarly, our results showed that compared with the non-DR group, the duration of diabetes in the diabetic retinopathy group was longer, and the systolic blood pressure, HbA1c, FPG, and urine ACR were significantly higher in the diabetic retinopathy group. The latest study showed that the concentrations of serum uric acid and urinary albumin are associated with the severity of DR in individuals with T2DM [17]. Moreover, our regression analysis also showed that diabetes duration and HbA1c were risk factors for diabetic retinopathy patients. Other risk factors of DR include nephropathy, dyslipidemia, smoking, and higher body mass index, which are revealed in previous studies [18]. Additionally, we firstly confirmed that serum LH was an independent risk factor in male diabetic retinopathy patients.

LH is included in the family of glycoprotein hormones. It is generated in the anterior pituitary gland and plays a very important role in gonad function [19]. As early as 1986, researchers detected LH exists in the vitreous humor of cadavers using radioimmunoassay. However, whether the quantification of LH in cadaveric eyes can reflect the physiological level of living eyes is still uncertain [20]. Until 1998, Thompson et al. discovered the expression of the luteinizing hormone receptor (LHR) gene in the neural retina and subsequently found that LHR was expressed in various organs

such as the brain, placenta, skin, and kidney [10, 21]. The LHR transcription level in the retina is roughly equivalent to the LHR transcription level in the cerebral cortex. The density of LHR receptor transcripts and LHR protein is highest in retinal cone cells [21, 22]. It can be seen that the LH level in the eyes is correlated with the occurrence of retinal diseases. Movsas et al. collected vitreous samples from 40 adults (23 diabetics, 17 nondiabetics) and confirmed LH is present in the adult human eye. They also found that a diminution in LH receptor signaling negatively affects visual processing of the cone photoreceptors in adult mice [19]. Previous study showed that subjects with diabetic neuropathy had less testosterone and high LH and FSH levels [23]. In the present study, we detected that serum LH is an independent risk factor for male diabetic retinopathy patients. With the increasing of the LH level, the prevalence of diabetic retinopathy was increased as well.

As we all know, LH, the placental hormone, human chorionic gonadotropin, and the pituitary hormone can stimulate the same LH receptor (LHR) in the human body, including gonadal tissue and nongonadal organs containing the eyes. These hormones are known to promote vascular endothelial growth factor (VEGF) expression [22, 24]. Recently, a study found a strong correlation between LH and VEGF in mammalian eyes [25]. Previous studies demonstrated that VEGF dysregulation is a key factor in the pathogenesis of retinopathy of prematurity [26, 27]. In vivo, researchers certified that LHR signaling has an important action in VEGF regulation and vascularization in the developing eye [28]. Therefore, the possible mechanisms that LH correlated to diabetic retinopathy could be explained by serum LH activating the LHR in the retina and induce VEGF expression, which leads to the occurrence of diabetic retinopathy. Certainly, the exact mechanisms between LH and diabetic retinopathy need to be further elucidated.

Several potential limitations of the present study should be clarified. Firstly, the current study is an observational study that needs long-term follow-up to support. Secondly,

the study sample size is relatively small, especially in stratified analysis; subjects in the severe NPDR group are small, which may cause some bias although it does not affect the overall research results. Thirdly, this study lacks patients' eye samples to detect the LH and LHR expressions in eyes. The main reason is that none of the patients included in this study need surgical treatment. Lastly, our study only found correlation between LH and diabetic retinopathy incidence in men, which may depend on the sex hormone differences. Large sample study is still needed to further certify the phenotype. Therefore, we will continue to follow up these patients.

In summary, our present study confirmed that diabetes duration and HbA1c are strongly associated with diabetic retinopathy risk. Moreover, we firstly suggested that serum LH is significantly related to the occurrence of diabetic retinopathy in men, which provides a new starting point for predicting the incidence of the disease in male. Further studies with large sample and long-term follow-up are still needed to verify a more persuasive conclusion in all the population.

Data Availability

The data used to support the findings of this study are available from the corresponding author upon request.

Conflicts of Interest

The authors declare that they have no conflicts of interest.

Authors' Contributions

Dr. Qingmin Sun and Yali Jing are co-first authors. Qingmin Sun and Yali Jing contributed equally to this work.

Acknowledgments

This study was supported by the National Natural Science Foundation of China (Grant Awards 81970689, 81970704, 81770819, 81703294, 81800752, 81900787, and 81800719), the National Key Research and Development Program of China (2016YFC1304804 and 2017YFC1309605), the Jiangsu Provincial Key Medical Discipline (ZDXKB2016012), the Key Project of Nanjing Clinical Medical Science, the Jiangsu Provincial Key Research and Development Program of China (BE2015604 and BE2016606), the Natural Science Foundation of Jiangsu Province of China (BK20170125 and BK20181116), the Jiangsu Provincial Medical Talent (ZDRCA2016062), the Jiangsu Provincial Medical Youth Talent (QNRC2016020, QNRC2016019, and QNRC2016018), the Six Talent Peaks Project in Jiangsu Province of China (SWYY-091, YY-086), the Scientific Research Project of the Fifth Phase of "333 Project" of Jiangsu Province of China, the Fundamental Research Funds for the Central Universities (021414380444), the Nanjing Science and Technology Development Project (YKK16105, YKK18067), and the Nanjing Health Youth Talent (QRX17123).

References

- [1] J. W. Yau, S. L. Rogers, R. Kawasaki et al., "Global prevalence and major risk factors of diabetic retinopathy," *Diabetes Care*, vol. 35, no. 3, pp. 556–564, 2012.
- [2] Y. Liu, J. Yang, L. Tao et al., "Risk factors of diabetic retinopathy and sight-threatening diabetic retinopathy: a cross-sectional study of 13 473 patients with type 2 diabetes mellitus in mainland China," *BMJ Open*, vol. 7, no. 9, article e016280, 2017.
- [3] X. Zhang, J. B. Saaddine, C. F. Chou et al., "Prevalence of diabetic retinopathy in the United States, 2005–2008," *Journal of the American Medical Association*, vol. 304, no. 6, pp. 649–656, 2010.
- [4] Y. Wang, Z. Lin, G. Zhai et al., "Prevalence of and risk factors for diabetic retinopathy and diabetic macular edema in patients with early and late onset diabetes mellitus," *Ophthalmic Research*, 2020.
- [5] H. Jammal, Y. Khader, S. Alkhatib, M. Abujbara, M. Alomari, and K. Ajlouni, "Diabetic retinopathy in patients with newly diagnosed type 2 diabetes mellitus in Jordan: prevalence and associated factors," *Journal of Diabetes*, vol. 5, no. 2, pp. 172–179, 2013.
- [6] D. S. Ting, G. C. Cheung, and T. Y. Wong, "Diabetic retinopathy: global prevalence, major risk factors, screening practices and public health challenges: a review," *Clinical & Experimental Ophthalmology*, vol. 44, no. 4, pp. 260–277, 2016.
- [7] J. Z. Kuo, T. Y. Wong, and J. I. Rotter, "Challenges in elucidating the genetics of diabetic retinopathy," *JAMA Ophthalmology*, vol. 132, no. 1, pp. 96–107, 2014.
- [8] C. Maricbilkan, "Sex differences in micro- and macro-vascular complications of diabetes mellitus," *Clinical Science*, vol. 131, no. 9, pp. 833–846, 2017.
- [9] R. Nuzzi, S. Scalabrin, A. Becco, and G. Panzica, "Sex hormones and optic nerve disorders: a review," *Frontiers in Neuroscience*, vol. 13, p. 57, 2019.
- [10] S. Genuth, K. G. Alberti, P. Bennett et al., "Follow-up report on the diagnosis of diabetes mellitus," *Diabetes Care*, vol. 26, no. 11, pp. 3160–3167, 2003.
- [11] C. P. Wilkinson, Ferris FL 3rd, R. E. Klein et al., "Proposed international clinical diabetic retinopathy and diabetic macular edema disease severity scales," *Ophthalmology*, vol. 110, no. 9, pp. 1677–1682, 2003.
- [12] K. Ogurtsova, J. D. da Rocha Fernandes, Y. Huang et al., "IDF diabetes atlas: global estimates for the prevalence of diabetes for 2015 and 2040," *Diabetes Research and Clinical Practice*, vol. 128, pp. 40–50, 2017.
- [13] R. A. Gangwani, J. X. Lian, S. M. McGhee, D. Wong, and K. K. Li, "Diabetic retinopathy screening: global and local perspective," *Hong Kong medical journal = Xianggang yi xue za zhi*, vol. 22, no. 5, pp. 486–495, 2016.
- [14] J. E. Grunwald, G. S. Ying, M. Maguire et al., "Association between retinopathy and cardiovascular disease in patients with chronic kidney disease (from the Chronic Renal Insufficiency Cohort [CRIC] Study)," *The American Journal of Cardiology*, vol. 110, no. 2, pp. 246–253, 2012.
- [15] J. Son, E. Jang, M. Kim et al., "Diabetic retinopathy is associated with subclinical atherosclerosis in newly diagnosed type 2 diabetes mellitus," *Diabetes Research and Clinical Practice*, vol. 91, no. 2, pp. 253–259, 2011.

- [16] J. Cunhavaz, L. Ribeiro, and C. Lobo, "Phenotypes and biomarkers of diabetic retinopathy," *Progress in Retinal and Eye Research*, vol. 41, pp. 90–111, 2014.
- [17] D. Chen, X. Sun, X. Zhao, and Y. Liu, "Associations of serum uric acid and urinary albumin with the severity of diabetic retinopathy in individuals with type 2 diabetes," *BMC Ophthalmology*, vol. 20, no. 1, p. 467, 2020.
- [18] K. Y. Lin, W. H. Hsieh, Y. B. Lin, C. Y. Wen, and T. J. Chang, "Update in the epidemiology, risk factors, screening, and treatment of diabetic retinopathy," *Journal of Diabetes Investigation*, 2021.
- [19] T. Z. Movsas, K. Y. Wong, M. D. Ober, R. E. Sigler, Z. M. Lei, and A. Muthusamy, "Confirmation of luteinizing hormone (LH) in living human vitreous and the effect of LH receptor reduction on murine electroretinogram," *Neuroscience*, vol. 385, pp. 1–10, 2018.
- [20] A. P. Chong and S. E. Aw, "Postmortem endocrine levels in the vitreous humor," *Annals Academy of Medicine Singapore*, vol. 15, no. 4, pp. 606–609, 1986.
- [21] D. A. Thompson, M. I. Othman, Z. M. Lei et al., "Localization of receptors for luteinizing hormone/chorionic gonadotropin in neural retina," *Life Sciences*, vol. 63, no. 12, pp. 1057–1064, 1998.
- [22] S. Dukic-Stefanovic, J. Walther, S. Wosch et al., "Chorionic gonadotropin and its receptor are both expressed in human retina, possible implications in normal and pathological conditions," *PloS one*, vol. 7, no. 12, 2012.
- [23] S. T. Ali, R. N. Shaikh, N. Ashfaqiddiqi, and P. Q. R. Siddiqi, "Serum and urinary levels of pituitary-gonadal hormones in insulin-dependent and non-insulin-dependent diabetic males with and without neuropathy," *Archives of Andrology*, vol. 30, no. 2, pp. 117–123, 2009.
- [24] H. A. Trau, J. S. Davis, and D. M. Duffy, "Angiogenesis in the primate ovulatory follicle is stimulated by luteinizing hormone via prostaglandin E₂," *Biology of Reproduction*, vol. 92, no. 1, pp. 15–15, 2015.
- [25] T. Z. Movsas, R. E. Sigler, and A. Muthusamy, "Vitreous levels of luteinizing hormone and VEGF are strongly correlated in healthy mammalian eyes," *Current Eye Research*, vol. 43, no. 8, pp. 1041–1044, 2018.
- [26] M. E. Hartnett, "Pathophysiology and mechanisms of severe retinopathy of prematurity," *Ophthalmology*, vol. 122, no. 1, pp. 200–210, 2015.
- [27] M. E. Hartnett and J. S. Penn, "Mechanisms and management of retinopathy of prematurity," *The New England Journal of Medicine*, vol. 367, no. 26, pp. 2515–2526, 2012.
- [28] T. Z. Movsas, R. E. Sigler, and A. Muthusamy, "Elimination of signaling by the luteinizing hormone receptor reduces ocular VEGF and retinal vascularization during mouse eye development," *Current Eye Research*, vol. 43, no. 10, pp. 1286–1289, 2018.

Research Article

Tangeretin Inhibition of High-Glucose-Induced IL-1 β , IL-6, TGF- β 1, and VEGF Expression in Human RPE Cells

Dong Qin ¹ and Yan-rong Jiang²

¹Henan Eye Institute, Henan Provincial Eye Hospital, People's Hospital of Zhengzhou University, Zhengzhou, China

²Department of Ophthalmology, People's Hospital, Peking University, Beijing, China

Correspondence should be addressed to Dong Qin; drqd888@163.com

Received 18 May 2020; Revised 9 September 2020; Accepted 25 November 2020; Published 7 December 2020

Academic Editor: Maria Vittoria Cicinelli

Copyright © 2020 Dong Qin and Yan-rong Jiang. This is an open access article distributed under the Creative Commons Attribution License, which permits unrestricted use, distribution, and reproduction in any medium, provided the original work is properly cited.

Tangeretin, a natural compound extracted from citrus plants, has been reported to have antiproliferative, antidiabetic, anti-invasive, and antioxidant properties. However, the role of tangeretin in diabetic retinopathy (DR) is unknown. In the present study, we investigated whether tangeretin had any effect on the expression of interleukin 1 beta (IL-1 β), interleukin 6 (IL-6), transforming growth factor beta 1 (TGF- β 1), and vascular endothelial growth factor (VEGF) in human retinal pigment epithelial (RPE) cells under high-glucose (HG) conditions. Our results illustrated that HG levels induced IL-1 β , IL-6, TGF- β 1, and VEGF expression and that tangeretin significantly reduced HG-induced IL-1 β , IL-6, TGF- β 1, and VEGF expression in human RPE cells. Moreover, tangeretin efficiently inhibited the activation of the protein kinase B (Akt) signalling pathway in HG-stimulated RPE cells. Therefore, tangeretin may serve a role in the treatment of DR.

1. Introduction

Diabetic retinopathy (DR) is the leading cause of visual impairment and blindness among adults of working age [1]. Sustained hyperglycaemia plays an important role in the development of DR. The retinal pigment epithelial (RPE) cell is believed to contribute to the pathogenesis of DR. Proinflammatory cytokines, inflammatory mediators, and chemokines are also involved in the pathogenesis of DR. Previous studies have shown that high levels of interleukin 1 beta (IL-1 β) are detected in the retinas of diabetic animals [2] and in the vitreous of patients with proliferative DR (PDR) [3]. In addition, high levels of interleukin 6 (IL-6) are also detected in the vitreous of patients with PDR or diabetic macular oedema [4–6].

Transforming growth factor beta (TGF- β) is reported to be involved in the differentiation, migration, proliferation, apoptosis, and accumulation of extracellular matrix molecules in various cell types [7]. TGF- β , a critical mediator

and regulator, is associated with the pathophysiological processes of ocular tissue development or repair [8–11]. TGF- β is also believed to be involved in the development of DR. The TGF- β induction of vascular endothelial growth factor (VEGF) secretion by human RPE cells has a key role in neovascularisation in diabetic eye disease [12]. VEGF is a multifunctional molecule that is produced by some cell types in the retina in diabetes [13]. VEGF can trigger many retinal vascular changes caused by diabetes, including vascular leakage, capillary nonperfusion, and retinal neovascularisation [12, 13]. Hyperglycaemia in DR has been linked to the upregulation of VEGF.

Tangeretin, extracted from the peel of citrus fruits, has multiple pharmacological properties, including antioxidant, antiasthmatic, anti-inflammatory, and neuroprotective properties [14–16]. It was reported that tangeretin had potent neuroprotective effects against pilocarpine-induced seizures [17] and attenuated brain injury in a rat model [18]. However, the effect of tangeretin on DR has not been investigated.

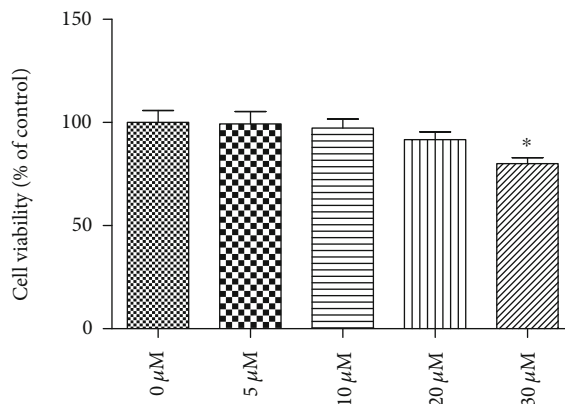


FIGURE 1: Effect of tangeretin on human RPE cell viability. The cells were incubated with different concentrations of tangeretin (0, 5, 10, 20, and 30 μM) for 24 h. The MTT assay was then performed to measure cell viability of human RPE cells. * $p < 0.05$ vs. control group (0 μM).

Therefore, the present study shows that high-glucose (HG) levels induce the expression of IL-1 β , IL-6, TGF- β 1, and VEGF in human RPE cells. HG also activates the phosphorylation of protein kinase B (Akt) in human RPE cells, and tangeretin can inhibit the phosphorylation of Akt under HG conditions. In addition, tangeretin significantly inhibits the HG-induced expression of IL-1 β , IL-6, TGF- β 1, and VEGF in human RPE cells. Thus, tangeretin may serve a role in the treatment of DR.

2. Materials and Methods

2.1. Reagents. Anti-Akt was obtained from Cell Signaling Technology (Danvers, MA, USA). IL-1 β , IL-6, TGF- β 1, and VEGF enzyme-linked immunosorbent assay (ELISA) kits were purchased from Abcam (Cambridge, MA, USA). LY294002 was obtained from Sigma-Aldrich/Merck KGaA.

2.2. Cell Culture. Human RPE cell line (ARPE-19; CRL-2302) was obtained from the American Type Culture Collection (Manassas, VA, USA). The cells were cultured in Dulbecco's Modified Eagle Medium (DMEM, Gibco, Grand Island, NY, USA); the medium was supplemented with 10% foetal bovine serum, 100 ng/ml streptomycin, and 100 U/ml penicillin. The cells were maintained at 37°C in a humidified incubator of 5% CO₂.

2.3. MTT Assay. The MTT assay was performed for cell viability. The human RPE cells were plated into 96-well plates at a density of 1×10^4 /well. After treatment with different concentrations of tangeretin (0, 5, 10, 20, and 30 μM) for 24 h, the MTT reagents were added to each well and incubated for 4 h. Then, the medium was removed, and dimethyl sulfoxide (DMSO) was added to dissolve the formazan crystals. The absorbance was read at 490 nm using a microplate reader.

2.4. Real-Time Polymerase Chain Reaction (PCR) Analysis. Total RNAs were extracted from human RPE cells using a TRIzol reagent kit. The cDNA was prepared using a RevertAid First Strand cDNA Synthesis Kit (Fermentas, St. Leon-Roth, Germany). Real-time PCR was performed

in triplicates on a Real-Time System (Bio-Rad, Munich, Germany). Each reaction contained 2.5 μl cDNA, 12.5 μl Maxima SYBR Green qPCR Master Mix (Fermentas, Waltham, MA, USA), and specific primers (0.3 μM each), with a final volume of 25 μl . The primers were as follows: human IL-1 β , forward 5'-GGA CAA GCT GAG GAA GAT GC-3' and reverse 5'-TCC ATA TCC TGT CCC TGG AG-3'; human IL-6, forward 5'-TGG CTG AAA AAG ATG GAT GCT-3' and reverse 5'-TCT GCA CAG CTC TGG CTT GT-3'; human TGF- β 1, forward 5'-GCC AGG ATA TGA GTT TGG GA-3' and reverse 5'-GGG TGC ATG TCT GCT CCT GT-3'; and human VEGF, forward 5'-AAG GAG GAG GGC AGA ATC AT-3' and reverse 5'-ATC TGC ATG GTG ATG TTG GA-3'. The reaction conditions were 95°C for 30 s, followed by 39 cycles of 95°C for 5 s and 60°C for 30 s. The RNA expression was normalized to the level of GAPDH mRNA.

2.5. Western Blot Analysis. After treatment, human RPE cells were lysed in radioimmunoprecipitation assay (RIPA) buffer supplemented with phenylmethylsulphonyl fluoride (PMSF) protease inhibitors. The protein concentration was quantified using a bicinchoninic acid assay (BCA). The protein samples were loaded on 10% SDS-PAGE gels and transferred to polyvinylidene fluoride (PVDF) membranes (Millipore, Billerica, MA, USA). They were processed for analysis using an enhanced chemiluminescence (ECL) detection system (Amersham, Arlington Heights, IL, USA). The dilutions for the primary antibodies were as follows: the anti-p-Akt was diluted at 1:2000, and the antitotal Akt was diluted at 1:1000.

2.6. ELISA Analysis. After treatment, the samples were collected. The protein levels of IL-1 β , IL-6, TGF- β 1, and VEGF in the culture supernatants were determined using IL-1 β , IL-6, TGF- β 1, and VEGF ELISA kits according to the manufacturer's instructions.

2.7. Statistical Analysis. Statistical analysis was performed using a one-way analysis of variance (ANOVA) followed by

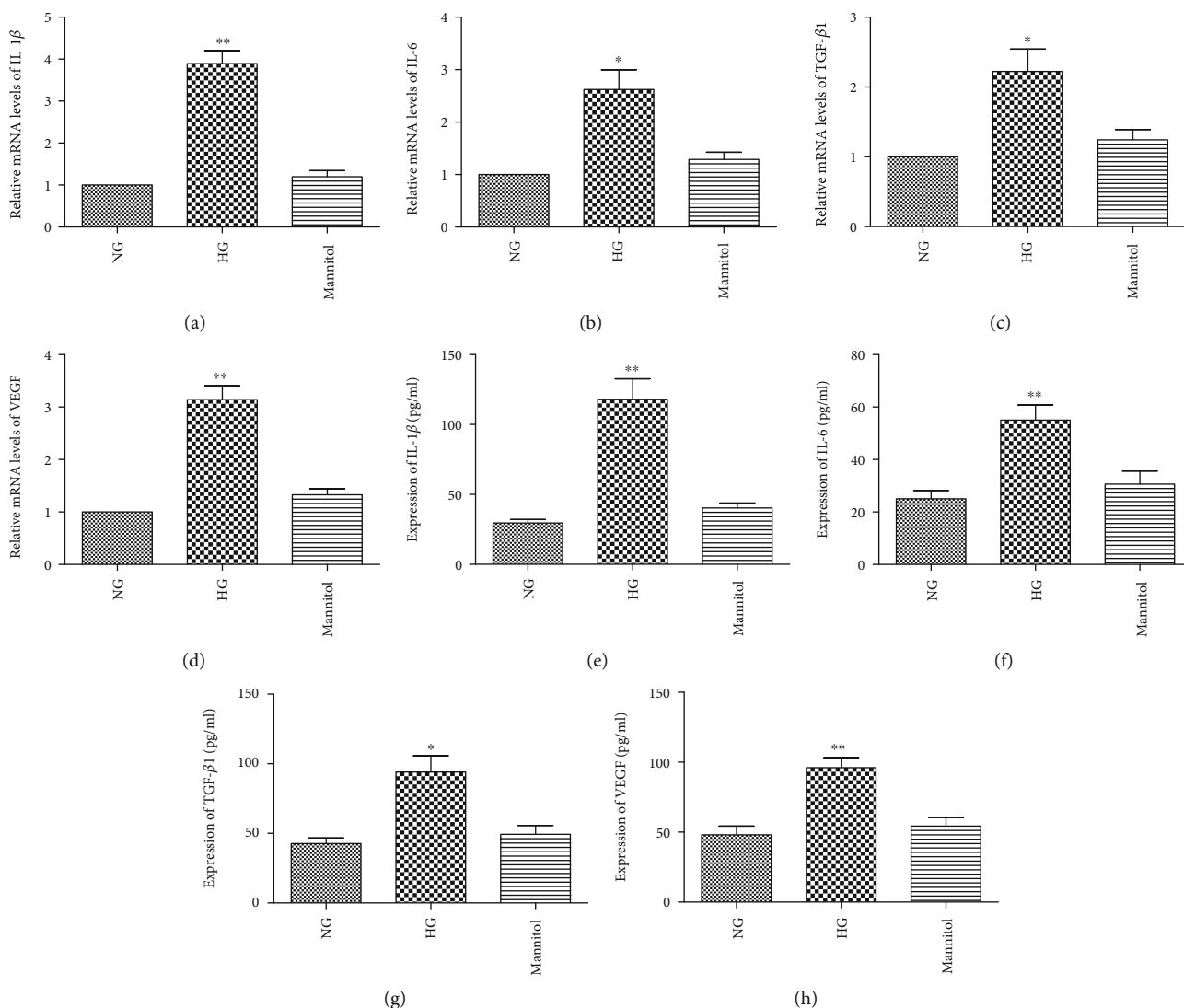


FIGURE 2: HG levels induced the expression of IL-1β, IL-6, TGF-β1, and VEGF in RPE cells. RPE cells were exposed to NG (5.5 mM), HG (30 mM), and mannitol (24.4 mM) for 24 h before the expressions of IL-1β, IL-6, TGF-β1, and VEGF were measured. When compared with NG, a real-time PCR and an ELISA kit analysis showed that the mRNA (a-d) and protein (e-h) levels of IL-1β, IL-6, TGF-β1, and VEGF were upregulated in response to HG. The data shown represents the mean ± SD of three independent experiments. *p < 0.05 versus NG; **p < 0.01 versus NG.

Tukey's test. All data are expressed as mean ± standard deviation (SD). They were analysed using SPSS 17.0 (SPSS, Chicago, IL, USA). A p value < 0.05 was considered statistically significant.

3. Results

3.1. Effect of Tangeretin on RPE Cell Viability. To evaluate the cytotoxicity effect of tangeretin on RPE cells, the cells were incubated with different concentrations of tangeretin (0, 5, 10, 20, and 30 μM) for 24 h. The MTT assay showed that tangeretin (30 μM) caused the decrease in cell viability; however, tangeretin at a concentration of 5, 10, and 20 μM did not affect the viability of RPE cells (Figure 1).

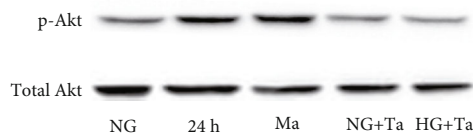


FIGURE 3: The effect of HG and tangeretin activated the phosphorylation of Akt in RPE cells. RPE cells were stimulated with HG (30 mM) or 24.4 mmol/l mannitol for 24 h. Cell lysates were immunoblotted with anti-p-Akt and anti-Akt antibodies. RPE cells were pretreated with 20 μM tangeretin for 1 h and then incubated with HG for 24 h for the assay of Akt phosphorylation. Ta: tangeretin; Ma: mannitol.

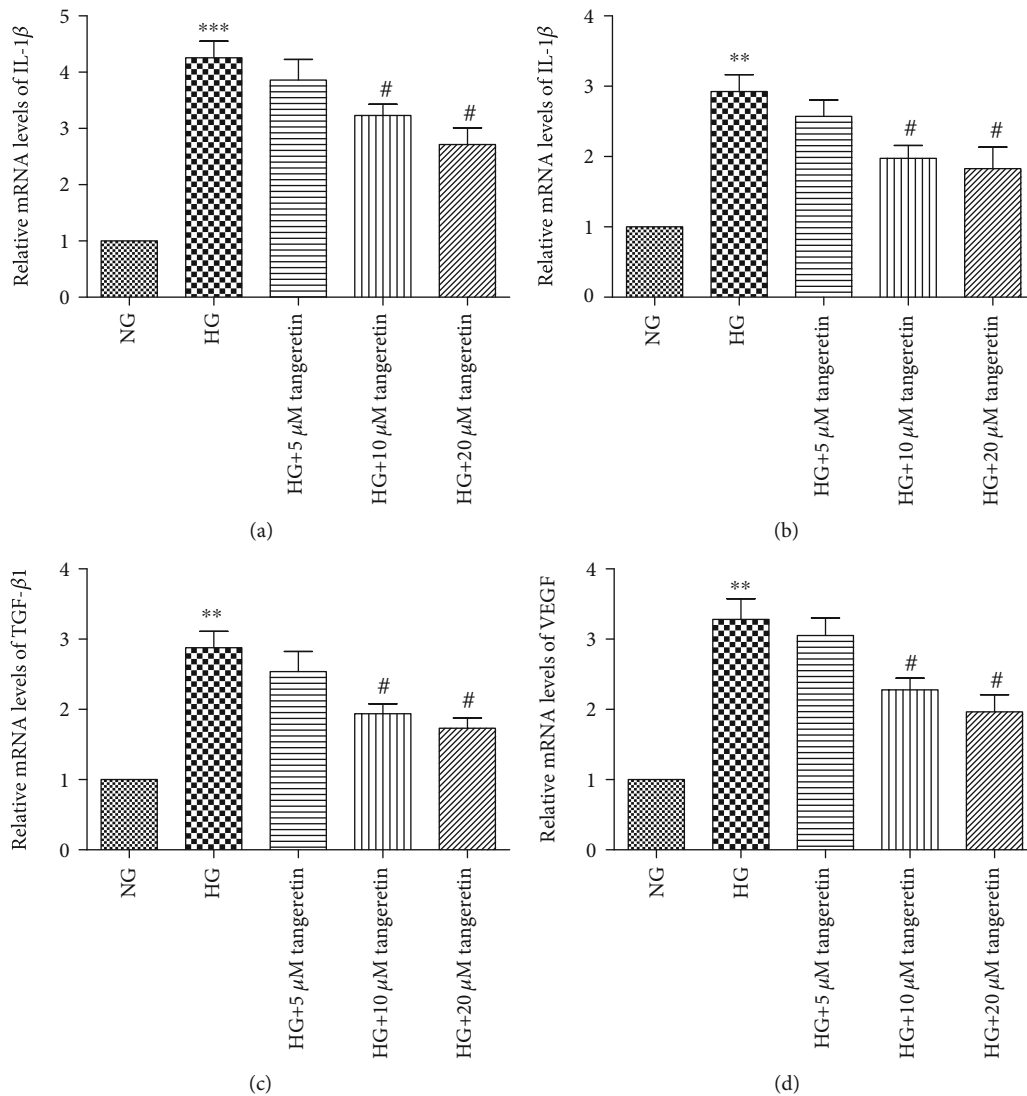


FIGURE 4: Tangeretin inhibited the mRNA expression of IL-1 β , IL-6, TGF- β 1, and VEGF in RPE cells. RPE cells were pretreated with various concentrations of tangeretin (5 μ M, 10 μ M, and 20 μ M) for 1 h and then stimulated by the addition of HG (30 mM) for 24 h. A real-time PCR analysis was performed to assess the expression of IL-1 β , IL-6, TGF- β 1, and VEGF. Tangeretin significantly decreased the HG-induced mRNA (a–d) level of IL-1 β , IL-6, TGF- β 1, and VEGF in RPE cells in a dose-dependent manner. Values are expressed as the mean \pm SD of three independent experiments. ** p < 0.01 versus NG; *** p < 0.001 versus NG; # p < 0.05 versus HG.

3.2. Induction of IL-1 β , IL-6, TGF- β 1, and VEGF in HG Conditions in RPE Cells. We examined the expression of IL-1 β , IL-6, TGF- β 1, and VEGF in HG conditions. The human RPE cells were cultured in DMEM containing normal glucose (NG; 5.5 mM) and high glucose (30 mM) and were exposed for 24 h. Real-time PCR and ELISA kit data revealed an increased mRNA level in IL-1 β , IL-6, TGF- β 1, and VEGF in the cells under the HG condition (Figures 1(a)–1(d)). An increased protein level in IL-1 β , IL-6, TGF- β 1, and VEGF was also observed in the cells under the HG condition (Figures 2(e)–2(h)).

3.3. Effect of HG and Tangeretin on Akt Signalling Pathways in Human RPE Cells. To examine the effect of HG and tan-

geretin on Akt signalling pathways, the human RPE cells were cultured in DMEM containing either NG (5.5 mM) or HG (30 mM) and were exposed for 10 min or 20 min, with or without pretreatment with 20 μ M tangeretin for 30 min. A western blot analysis showed that HG can activate the phosphorylation of Akt in RPE cells. The phosphorylation of Akt was blocked by pretreatment with tangeretin under HG conditions for 20 min (Figure 3).

3.4. Tangeretin and Akt Inhibitor LY294002 Suppress the HG-Induced Expression of IL-1 β , IL-6, TGF- β 1, and VEGF in Human RPE Cells. Having found that HG promoted the expression of IL-1 β , IL-6, TGF- β 1, and VEGF and induced the phosphorylation of Akt in human RPE

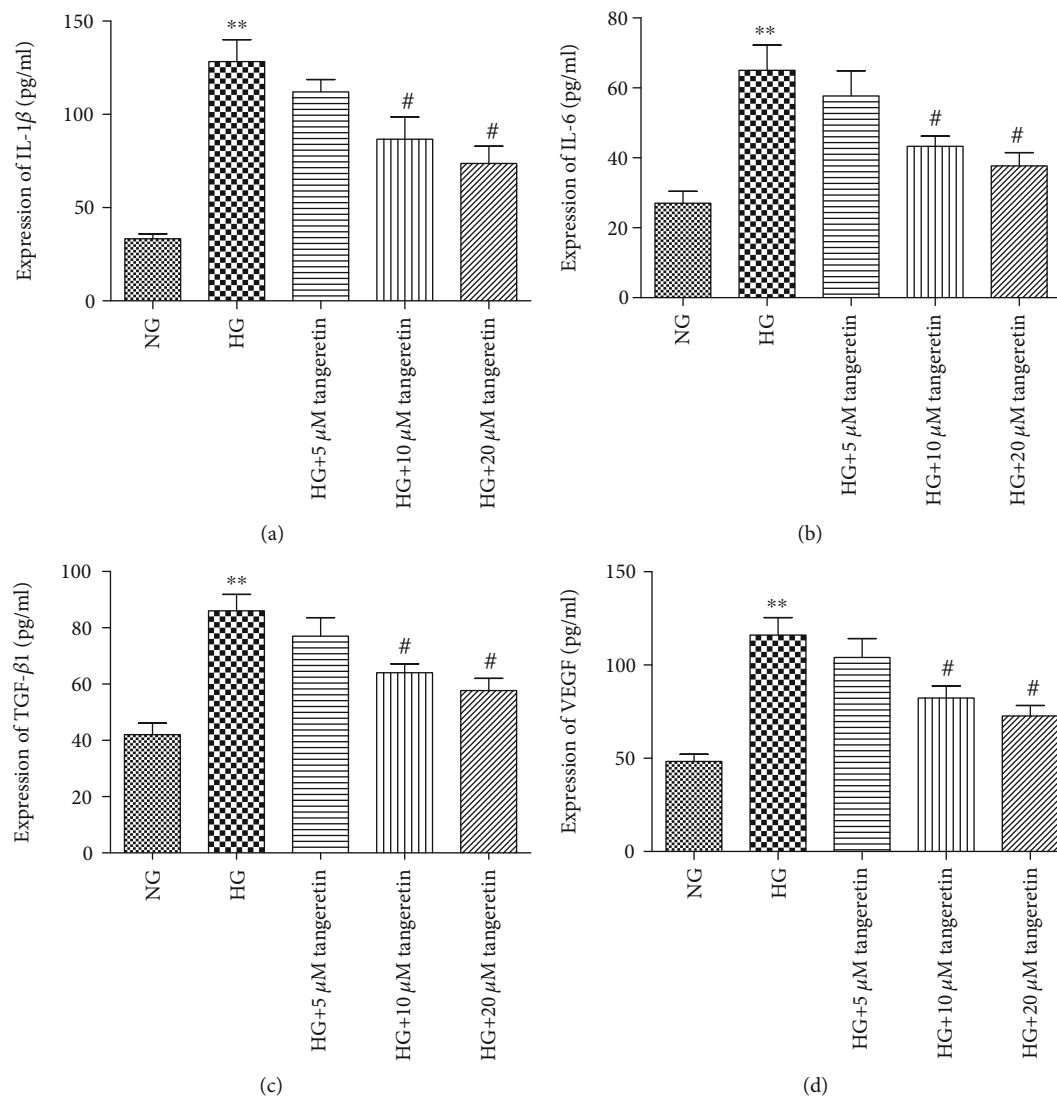


FIGURE 5: Tangeretin decreased the protein level of IL-1 β , IL-6, TGF- β 1, and VEGF in RPE cells. After pretreatment with various concentrations of tangeretin (5 μ M, 10 μ M, and 20 μ M) for 1 h, RPE cells were stimulated by the addition of HG (30 mM) for 24 h. An ELISA kit analysis was performed to assess the protein level of IL-1 β , IL-6, TGF- β 1, and VEGF. Tangeretin significantly decreased the HG-induced protein (a–d) levels of IL-1 β , IL-6, TGF- β 1, and VEGF in RPE cells in a dose-dependent manner. Values are expressed as the mean \pm SD of three independent experiments. ** p < 0.01 versus NG; # p < 0.05 versus HG.

cells, we then examined whether tangeretin had any effect on the HG-induced expression of IL-1 β , IL-6, TGF- β 1, and VEGF. In addition, we examined whether the activation of the phosphorylation of Akt plays a vital role in the HG-induced expression of IL-1 β , IL-6, TGF- β 1, and VEGF in RPE cells. Using an ELISA kit and a real-time PCR assay, the HG-induced expression of IL-1 β , IL-6, TGF- β 1, and VEGF was shown to be inhibited by tangeretin in a dose-dependent manner in human RPE cells (Figures 4 and 5). Meanwhile, the pretreatment of RPE cells with LY294002 inhibited the HG-induced expression of IL-1 β , IL-6, TGF- β 1, and VEGF (Figures 6 and 7).

4. Discussion

Hyperglycaemia is one of the most important initiators of the pathogenesis of DR. Sustained hyperglycaemia can

upregulate growth factors, cytokines, and other molecules. Studies have demonstrated that the levels of IL-1 β and IL-6 are upregulated in the vitreous of patients with PDR [2–6]. In this study, we chose IL-1 β and IL-6 as our target genes, examining whether tangeretin had any effect on the HG-induced expression of IL-1 β and IL-6. We demonstrated that HG significantly increased the induction of IL-1 β and IL-6 in RPE cells when they were exposed to 30 mM glucose for 24 h. Interestingly, tangeretin significantly decreased the expression of IL-1 β and IL-6 in human RPE cells under the condition of 30 mM glucose in a dose-dependent manner, which suggested that tangeretin could suppress cytokine secretion under the HG condition in human RPE cells.

TGF- β , a multifunctional cytokine, regulates critical cell biological actions, such as migration, differentiation, and apoptosis. TGF- β is reported to be one of the most

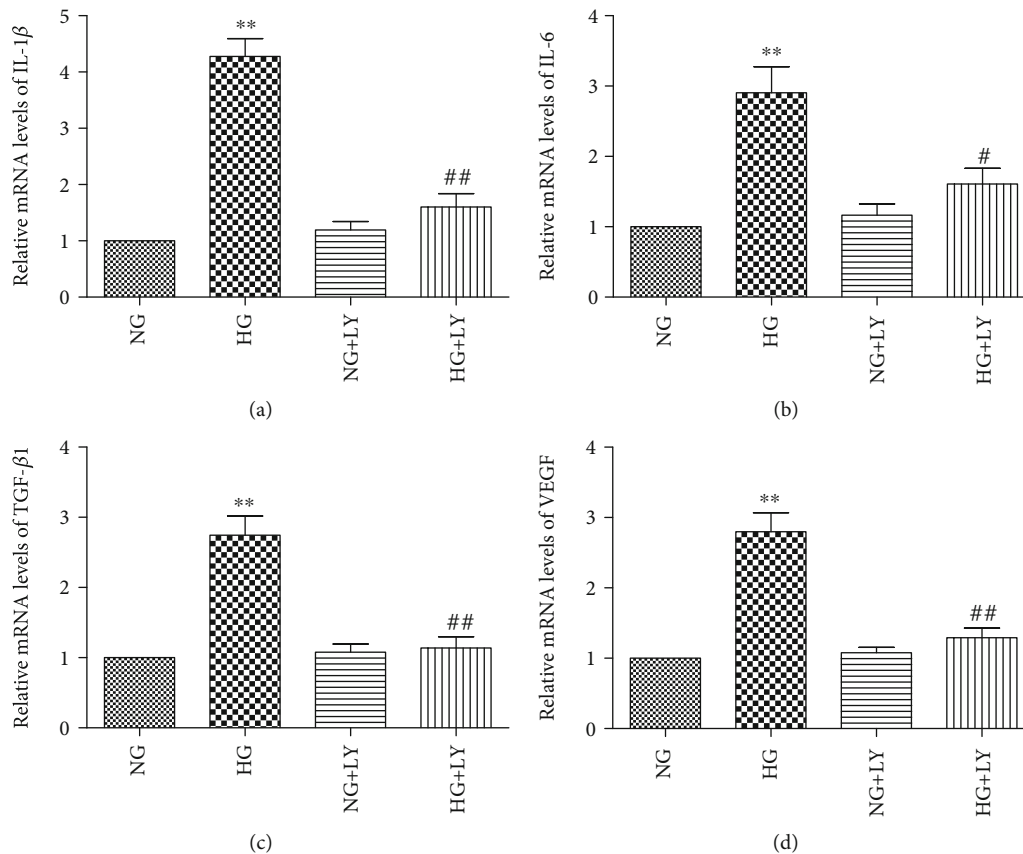


FIGURE 6: Inhibition of Akt signalling downregulated HG-induced IL-1 β , IL-6, TGF- β 1, and VEGF mRNA expression in RPE cells. RPE cells were preincubated for 1 h with 10 μ M of LY294002 and then stimulated by HG (30 mM) for 24 h. The IL-1 β , IL-6, TGF- β 1, and VEGF mRNA levels were determined using real-time PCR. LY294002 significantly decreased the HG-induced mRNA (a–d) levels of IL-1 β , IL-6, TGF- β 1, and VEGF in RPE cells. The data shown represent the mean \pm SD of three independent experiments. ** p < 0.01 versus NG; # p < 0.05 versus HG; ## p < 0.01 versus HG.

important ligands in the pathological processes of fibrotic diseases in the retina, including PDR, proliferative vitreoretinopathy (PVR), and retinopathy of prematurity (ROP) [19, 20]. In addition, TGF- β is believed to contribute to the contraction of subretinal and epiretinal membranes in patients with PVR and PDR [20]. VEGF is a potent angiogenic stimulator of neovascularisation, and it promotes vascular permeability. VEGF plays a vital role in the pathogenesis of DR [21–23]. High levels of VEGF in both human and animal samples are reported to be associated with the development and progression of DR [24–26]. Our data illustrated that the expression of TGF- β 1 and VEGF was upregulated in RPE cells when exposed to 30 mM glucose for 24 h. In addition, tangeretin significantly reduced the HG-induced expression of TGF- β 1 and VEGF in human RPE cells in a dose-dependent manner. The findings indicated that tangeretin could suppress the expression of TGF- β 1 and VEGF in the human RPE cell under the HG condition.

The phosphoinositide 3-kinase (PI3K)/Akt signalling pathway plays an important role in DR and in numerous cellular functions, including proliferation, migration, inva-

sion, adhesion, metabolism, and survival [27]. The PI3K pathway is associated with the formation of normal blood vessels [28]. Studies have reported that the inhibition of the Akt pathway could inhibit pathological vascularisation [29] and many tumour types [30]. Our previous study showed that HG activated the phosphorylation of Akt, and inhibition of the PI3K/Akt signalling pathway could inhibit the expression of extracellular matrix molecules under HG conditions in RPE cells [31]. In this study, we found that inhibition of Akt abolished HG-induced IL-1 β , IL-6, TGF- β 1, and VEGF expression in human RPE cells. The findings of the present study also showed that 30 mM glucose also activated the phosphorylation of Akt, and 20 μ M tangeretin significantly inhibited the phosphorylation of Akt in RPE cells under the HG condition. These findings indicated that tangeretin may inhibit the expression of IL-1 β , IL-6, TGF- β 1, and VEGF through the Akt signalling pathway.

In future research, the role of tangeretin should be investigated in animal models in vivo. In addition, oxidative stress and other pathways involved in inflammation and activated by high glucose such as JNK, P38 MAPK,

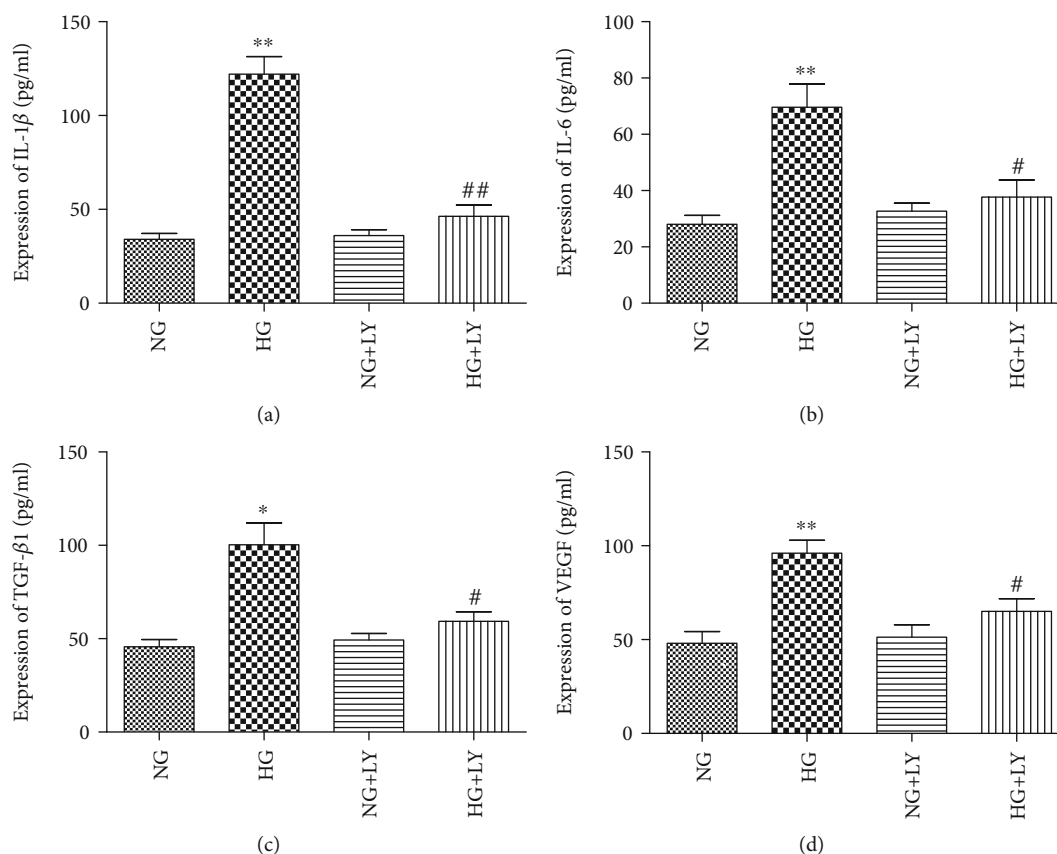


FIGURE 7: The PI3K/Akt signalling pathway mediated the protein level of IL-1 β , IL-6, TGF- β 1, and VEGF in RPE cells under high-glucose conditions. RPE cells were preincubated for 1 h with 10 μ M of LY294002 and then stimulated by HG (30 mM) for 24 h. The IL-1 β , IL-6, TGF- β 1, and VEGF protein levels were determined using the ELISA kit. LY294002 significantly decreased the HG-induced protein (a–d) levels of IL-1 β , IL-6, TGF- β 1, and VEGF in RPE cells. The data shown represent the mean \pm SD of three independent experiments. * p < 0.05 versus NG; ** p < 0.01 versus NG; # p < 0.05 versus HG; ## p < 0.01 versus HG. LY: LY294002.

and NF- κ B should be conducted. These are the limitations of the present study. In summary, it has been reported that tangeretin has multifunctional properties, including anti-invasive, antiproliferative, antimetastatic, antidiabetic, and antioxidative properties. However, the role of tangeretin in DR is unclear. The present study demonstrated that HG levels induced IL-1 β , IL-6, TGF- β 1, and VEGF expression and the phosphorylation of Akt and that tangeretin significantly reduced the HG-induced expression of IL-1 β , IL-6, TGF- β 1, and VEGF in human RPE cells. Thus, tangeretin significantly reduced cytokine secretion in HG environments and extends our knowledge in the treatment of diabetic retinopathy.

Data Availability

The data used to support the findings of this study are available from the corresponding author upon request.

Additional Points

Highlights. High glucose induced the expression of IL-1 β , IL-6, TGF- β 1, and VEGF in human RPE cells. Tangeretin inhibited

the activation of the protein kinase B (Akt) signalling pathway in high-glucose-stimulated human RPE cells. Tangeretin significantly inhibited high-glucose-induced IL-1 β , IL-6, TGF- β 1, and VEGF expression in human RPE cells.

Conflicts of Interest

All the authors declare that there are no conflicts of interest in this study.

Acknowledgments

The present study was supported by the Department of Science and Technology of Henan Province (No. 162300410112).

References

- [1] D. A. Antonetti, A. J. Barber, S. K. Bronson et al., "Diabetic retinopathy," *Diabetes*, vol. 55, no. 9, pp. 2401–2411, 2006.
- [2] J. A. Vincent and S. Mohr, "Inhibition of Caspase-1/Interleukin-1 Signaling Prevents Degeneration of retinal capillaries in diabetes and galactosemia," *Diabetes*, vol. 56, no. 1, pp. 224–230, 2006.

- [3] N. Demircan, B. G. Safran, M. Soyulu, A. A. Ozcan, and S. Sizmaz, "Determination of vitreous interleukin-1 (IL-1) and tumour necrosis factor (TNF) levels in proliferative diabetic retinopathy," *Eye*, vol. 20, no. 12, pp. 1366–1369, 2006.
- [4] A. M. Abu El-Asrar, D. Maimone, P. H. Morse, S. Gregory, and A. T. Reder, "Cytokines in the vitreous of patients with proliferative diabetic retinopathy," *American Journal of Ophthalmology*, vol. 114, no. 6, pp. 731–736, 1992.
- [5] A. M. Abu El-Asrar, J. Van Damme, W. Put et al., "Monocyte chemotactic protein-1 in proliferative vitreoretinal disorders," *American Journal of Ophthalmology*, vol. 123, no. 5, pp. 599–606, 1997.
- [6] H. Funatsu, H. Noma, T. Mimura, S. Eguchi, and S. Hori, "Association of vitreous inflammatory factors with diabetic macular edema," *Ophthalmology*, vol. 116, no. 1, pp. 73–79, 2009.
- [7] J. Massague and Y. G. Chen, "Controlling TGF-beta signaling," *Genes & Development*, vol. 14, no. 6, pp. 627–644, 2000.
- [8] W. A. Border and N. A. Noble, "Transforming growth factor-beta in tissue fibrosis," *The New England Journal of Medicine*, vol. 331, no. 19, pp. 1286–1292, 1994.
- [9] C. Gordon-Thomson, R. U. de Iongh, A. M. Hales, C. G. Chamberlain, and J. W. McAvoy, "Differential cataractogenic potency of TGF-beta1, -beta2, and -beta3 and their expression in the postnatal rat eye," *Investigative Ophthalmology & Visual Science*, vol. 39, pp. 1399–1409, 1998.
- [10] E. H. Lee and C. K. Joo, "Role of transforming growth factor-beta in transdifferentiation and fibrosis of lens epithelial cells," *Investigative Ophthalmology & Visual Science*, vol. 40, no. 9, pp. 2025–2032, 1999.
- [11] S. Saika, "TGFβ pathobiology in the eye," *Laboratory Investigation*, vol. 86, no. 2, pp. 106–115, 2006.
- [12] C. N. Nagineni, W. Samuel, S. Nagineni et al., "Transforming growth factor-beta induces expression of vascular endothelial growth factor in human retinal pigment epithelial cells: involvement of mitogen-activated protein kinases," *Journal of Cellular Physiology*, vol. 197, no. 3, pp. 453–462, 2003.
- [13] K. Miyamoto, S. Khosrof, S. E. Bursell et al., "Vascular endothelial growth factor (VEGF)-induced retinal vascular permeability is mediated by intercellular adhesion molecule-1 (ICAM-1)," *The American Journal of Pathology*, vol. 156, no. 5, pp. 1733–1739, 2000.
- [14] L. L. Liu, F. H. Li, Y. Zhang, X. F. Zhang, and J. Yang, "Tangeretin has antiasthmatic effects via regulating PI3K and Notch signaling and modulating Th1/Th2/Th17 cytokine balance in neonatal asthmatic mice," *Brazilian Journal of Medical and Biological Research*, vol. 50, no. 8, article e5991, 2017.
- [15] M. Wang, D. Meng, P. Zhang et al., "Antioxidant protection of nobiletin, 5-demethylnobiletin, tangeretin, and 5-demethyltangeretin from citrus peel in *Saccharomyces cerevisiae*," *Journal of Agricultural and Food Chemistry*, vol. 66, no. 12, pp. 3155–3160, 2018.
- [16] J. Wu, Y. M. Zhao, and Z. K. Deng, "Tangeretin ameliorates renal failure via regulating oxidative stress, NF-κB-TNF-α/iNOS signaling and improves memory and cognitive deficits in 5/6 nephrectomized rats," *Inflammopharmacology*, vol. 26, pp. 114, 2018.
- [17] X. Guo, Y. Cao, F. Hao, Z. Yan, M. Wang, and X. Liu, "Tangeretin alters neuronal apoptosis and ameliorates the severity of seizures in experimental epilepsy-induced rats by modulating apoptotic protein expressions, regulating matrix metalloproteases, and activating the PI3K/Akt cell survival pathway," *Advances in Medical Sciences*, vol. 62, no. 2, pp. 246–253, 2017.
- [18] E. J. Yang, S. H. Lim, K. S. Song, H. S. Han, and J. Lee, "Identification of active compounds from *Aurantii Immatri Pericarpium* attenuating brain injury in a rat model of ischemia-reperfusion," *Food Chemistry*, vol. 138, no. 1, pp. 663–670, 2013.
- [19] S. Saika, O. Yamanaka, T. Sumioka et al., "Fibrotic disorders in the eye: targets of gene therapy," *Progress in Retinal and Eye Research*, vol. 27, no. 2, pp. 177–196, 2008.
- [20] S. K. Paine, A. Basu, L. K. Mondal et al., "Association of vascular endothelial growth factor, transforming growth factor beta, and interferon gamma gene polymorphisms with proliferative diabetic retinopathy in patients with type 2 diabetes," *Molecular Vision*, vol. 18, pp. 2749–2757, 2012.
- [21] S. Ishida, T. Usui, K. Yamashiro et al., "VEGF164Is proinflammatory in the diabetic retina," *Investigative Ophthalmology & Visual Science*, vol. 44, no. 5, pp. 2155–2162, 2003.
- [22] G. D. Yancopoulos, S. Davis, N. W. Gale, J. S. Rudge, S. J. Wiegand, and J. Holash, "Vascular-specific growth factors and blood vessel formation," *Nature*, vol. 407, no. 6801, pp. 242–248, 2000.
- [23] R. Simom, A. Lecube, R. M. Segura, J. G. Arumi, and C. Hernandez, "Free insulin growth factor-I and vascular endothelial growth factor in the vitreous fluid of patients with proliferative diabetic retinopathy," *American Journal of Ophthalmology*, vol. 134, no. 3, pp. 376–382, 2002.
- [24] L. P. Aiello, R. L. Avery, P. G. Arrigg et al., "Vascular endothelial growth factor in ocular fluid of patients with diabetic retinopathy and other retinal disorders," *The New England Journal of Medicine*, vol. 331, no. 22, pp. 1480–1487, 1994.
- [25] A. B. El-Remessy, M. A. Behzadian, G. Abou-Mohamed, T. Franklin, R. W. Caldwell, and R. B. Caldwell, "Experimental diabetes causes breakdown of the blood-retina barrier by a mechanism involving tyrosine nitration and increases in expression of vascular endothelial growth factor and urokinase plasminogen activator receptor," *The American Journal of Pathology*, vol. 162, no. 6, pp. 1995–2004, 2003.
- [26] H. P. Hammes, J. Lin, R. G. Bretzel, M. Brownlee, and G. Breier, "Upregulation of the vascular endothelial growth factor/vascular endothelial growth factor receptor system in experimental background diabetic retinopathy of the rat," *Diabetes*, vol. 47, no. 3, pp. 401–406, 1998.
- [27] A. G. Bader, S. Kang, L. Zhao, and P. K. Vogt, "Oncogenic PI3K deregulates transcription and translation," *Nature Reviews. Cancer*, vol. 5, no. 12, pp. 921–929, 2005.
- [28] M. Graupera, J. Guillermet-Guibert, L. C. Foukas et al., "Angiogenesis selectively requires the p110α isoform of PI3K to control endothelial cell migration," *Nature*, vol. 453, no. 7195, pp. 662–666, 2008.
- [29] J. Karar and A. Maity, "PI3K/AKT/mTOR pathway in angiogenesis," *Frontiers in Molecular Neuroscience*, vol. 4, p. 51, 2011.
- [30] J. Polivka Jr. and F. Janku, "Molecular targets for cancer therapy in the PI3K/AKT/mTOR pathway," *Pharmacology & Therapeutics*, vol. 142, no. 2, pp. 164–175, 2014.
- [31] D. Qin, G.-m. Zhang, X. Xu, and L.-y. Wang, "The PI3K/Akt signaling pathway mediates the high glucose-induced expression of extracellular matrix molecules in human retinal pigment epithelial cells," *Journal of Diabetes Research*, vol. 2015, Article ID 920280, 11 pages, 2015.

Review Article

Widefield Optical Coherence Tomography Angiography in Diabetic Retinopathy

Alessia Amato ¹, Francesco Nadin ¹, Federico Borghesan ¹,
Maria Vittoria Cicinelli ^{1,2,3}, Irini Chatziralli ⁴, Saena Sadiq,³ Rukhsana Mirza,³
and Francesco Bandello ^{1,2}

¹Department of Ophthalmology, IRCCS San Raffaele Scientific Institute, Milan, Italy

²School of Medicine, Vita-Salute San Raffaele University, Milan, Italy

³Department of Ophthalmology, Feinberg School of Medicine, Northwestern University, Chicago, IL, USA

⁴2nd Department of Ophthalmology, National and Kapodistrian University of Athens, Athens, Greece

Correspondence should be addressed to Maria Vittoria Cicinelli; cicinelli.mariavittoria@hsr.it

Received 6 September 2020; Revised 6 November 2020; Accepted 7 November 2020; Published 24 November 2020

Academic Editor: Akira Sugawara

Copyright © 2020 Alessia Amato et al. This is an open access article distributed under the Creative Commons Attribution License, which permits unrestricted use, distribution, and reproduction in any medium, provided the original work is properly cited.

Purpose. To summarize the role of widefield optical coherence tomography angiography (WF-OCTA) in diabetic retinopathy (DR), extending from the acquisition strategies to the main clinical findings. **Methods.** A PubMed-based search was carried out using the terms “Diabetic retinopathy”, “optical coherence tomography angiography”, “widefield imaging”, and “ultra-widefield imaging”. All studies published in English up to August 2020 were reviewed. **Results.** WF-OCTA can be obtained with different approaches, offering advantages over traditional imaging in the study of nonperfusion areas (NPAs) and neovascularization (NV). Quantitative estimates and topographic distribution of NPA and NV are useful for treatment monitoring and artificial intelligence-based approaches. Curvature, segmentation, and motion artifacts should be assessed when using WF-OCTA. **Conclusions.** WF-OCTA harbors interesting potential in DR because of its noninvasiveness and capability of objective metrics of retinal vasculature. Further studies will facilitate the migration from traditional imaging to WF-OCTA in both the research and clinical practice fields.

1. Introduction

Diabetes mellitus (DM) is a major public health concern, with a global prevalence expected to rise from 8.8% in 2015 to 10.4% in 2040 [1]. Diabetic retinopathy (DR) is a microangiopathic complication of DM and, despite the latest diagnostic and therapeutic advancements, is still one of the leading causes of blindness worldwide, affecting about one-third of diabetic patients [2–6]. Considering its burden, efficient management of DR patients depends on proper classification and severity grading which, in turn, lay the foundations on the most appropriate imaging modality.

Until relatively recent times, the classification of DR has been relying on stereoscopic color fundus photography (CFP); the Early Treatment Diabetic Retinopathy Study

(ETDRS) grading system, a 13-level severity scale based on 7-field photography ranging from early changes to severe proliferative DR (PDR), has been the gold standard for years. Fundus fluorescein angiography (FFA) is another useful tool for the classification of DR, as it allows the detection of the blood-retinal barrier (BRB) breakdown, microaneurysms (MA), nonperfusion areas (NPAs), intraretinal microvascular abnormalities (IRMA), and neovascularization (NV). FFA is relatively invasive, and it might be associated with the risk of life-threatening allergic reactions to the intravenous dye. It is relatively contraindicated in the case of kidney disease, which is fairly common in diabetic patients, and pregnancy. FFA does not allow for a separate visualization of the different retinal vascular plexuses. Lastly, the FFA-based assessment of DR severity mainly relies on a qualitative approach.

With the introduction of optical coherence tomography angiography (OCTA) technology, a turning point was set in the management of DR [7–10]. OCTA is an OCT-derived technique that generates high-resolution angiographic images by using repeated B-scans to detect motion contrast from flowing erythrocytes. Currently available OCTA technologies acquire clusters of 2–4 B-scans on the “x” fast axis at each of the “y” slow scan axis points, and the software eventually extracts the moving image from each of such clusters. OCTA offers several advantages over traditional angiography, including avoidance of dye injection and the provision of depth-resolved information of the superficial and deep retinal vasculature. OCTA image resolution is higher compared to FFA and allows quantitative data processing, including measurement of vessel density (VD), vessel length density (VLD), perfusion density (PD), and the size and the shape of the foveal avascular zone (FAZ) [7, 11].

The OCTA field of view has been limited to 6×6 mm scans until recent times. Efforts to obtain a wider field of view have been pursued with increasing success; the results achieved have ushered in a new era in disease management. Widefield (WF) OCTA imaging represents the state of the art in retinal vascular diseases, including DR. This novel imaging technique has offered great advantages in the detection of NPAs and NV. The present review is aimed at summarizing the role of WF-OCTA in DR, extending from the acquisition strategies to the main clinical findings.

2. Technical Solutions to Achieve WF-OCTA

The WF-OCTA scan can be obtained with three main approaches:

- (I) Extended field imaging (EFI), which consists of the employment of trial frames fitted with a magnifying +20 D lens
- (II) Montage technique, including a variety of protocols aimed at merging multiple smaller scans
- (III) Single-shot widefield 12×12 mm scans or 15×9 mm scans

2.1. EFI. The interposition of a positive diopter lens between the OCTA probe and the eye results in an increased light incidence angle and thus an imaging field expansion [12].

Uji and Yoshimura compared the scan length measurements obtained with conventional imaging (spectral-domain Spectralis OCT, Spectralis HRA + OCT, Heidelberg Engineering, Heidelberg, Germany) and a swept-source OCT (DRI OCT-1, Topcon, Tokyo, Japan) with those of EFI-OCT applied to the two OCT systems. They reported a statistically significant difference in both the horizontal and the vertical direction, with a scan length corresponding to the nearly $60\text{--}70^\circ$ angle field when EFI was coupled with DRI OCT-1 [12].

When the EFI technique has been applied to SS-OCTA (Plex® Elite 9000, Carl Zeiss Meditec, Dublin, California, USA), it resulted in a larger scan size than both SS-OCTA images acquired without EFI and traditional HRA2 FFA

captured using a 55° Heidelberg lens. In eyes with DR, EFI-SS-OCTA had good sensitivity (96% and 79%, respectively) and specificity (100% and 96%, respectively) in detecting NPA and NV compared to FFA. WF-OCTA with EFI was significantly more comfortable for patients than conventional dye angiography [13]. Parallely, Pellegrini et al., using a similar study design, evaluated the extension of NPA and the presence and the number of NV. Aside from a larger captured fundus area, EFI SS-OCTA revealed a significantly larger extension of NPA compared to non-EFI SS-OCTA and FFA [14].

EFI is a simple and economic technique that can be carried out with readily available equipment. However, it covers a larger retinal territory with the same number of A-scans of non-EFI acquisitions; i.e., it extends the field of the image by magnifying each pixel, reducing the global slab resolution. This may lead to underestimation of VD and overestimation of NPA in DR evaluation; validation of this technique with regard to traditional imaging is still warranted.

2.2. Montage Technique. The montage technique consists of assembling multiple smaller scans to gather a wider OCTA image, while maintaining an adequate axial and lateral resolution. A variety of montage protocols have been adopted.

de Carlo et al. were among the first to use this approach to improve the visualization of the retinal vasculature in a small prospective case series [15]. The authors included one patient with unilateral branch retinal vein occlusion, one patient with bilateral severe PDR, and one healthy control. By combining nine adjacent 3×3 mm OCTA scans (AngioVue XR Avanti, Optovue, Fremont, CA), the authors managed to create a single WF montage OCTA of approximately 8×8 mm or 30° field, without moving the patient’s fixation point. The montage OCTA showed the retinal vasculature in the greatest details compared to a single 8×8 mm OCTA scan acquired using 304×304 A-scans. Once compared to 50° FFA, montage OCTA identified more pathology than FFA or single-scan 8×8 mm OCTA.

More recently, Lavia et al. got an advantage from the high resolution provided by the 3×3 mm OCTA scans of the 100 kHz PlexElite 9000 SS-OCTA to obtain WF images of the retina in healthy individuals [16]. The authors acquired an average of $25 \times 3 \times 3$ mm scans from the fovea to the retinal periphery to create a horizontal and a vertical band passing through the fovea. The scanning cursor was manually moved to the desired area ensuring an overlay of about 40% between adjacent volumes. Afterward, consecutive 3×3 mm volumes were manually superimposed using a single 12×12 mm scan as a reference. This method was able to limit low-signal artifacts, which are a major drawback of larger scans, and allowed for better segmentation and quantitative analyses.

Montage protocols are not rigidly standardized and can be customized by the operators. In a small prospective study aimed at quantifying the burden of microvascular disease in the eyes with PDR, Zhang et al. captured a 100-degree field of view using sixteen 6×6 mm scans. Montage WF-OCTA images provided a more accurate visualization of the retinal vascular plexuses than the traditional FFA, showing a higher burden of pathology in the retinal periphery [17].

Though allowing for high-quality images, the montage technique is time-consuming and labor-intensive, requiring optimal patients' cooperation to avoid misalignment; this may hinder the acquisition in subjects with low visual acuity and poor fixation. Due to these drawbacks, montage WF-OCTA is currently hard to export from the field of research to the clinical setting [17].

2.3. Single-Shot Scans. The newest generation of SS-OCTA is embedded with one-shot WF acquisition of 15×9 mm or 12×12 mm scans, corresponding to a 40° field of view [18], which can be further combined into greater composite images up to 80° of the retina [19, 20]. Single-shot acquisitions are faster to obtain compared to montage scans and provide information of the entire posterior pole, though sacrificing to some extent the image resolution.

Hirano et al. evaluated the vascular morphology in patients with varying severities of DR using different SS-OCTA image sizes and reported that 3×3 mm images had the best diagnostic performance in predicting DR eyes from a pool of healthy controls. The superior sensitivity of 3×3 mm macular scans for the detection of DR vascular abnormalities might seem contradictory at a first glance, since DR primarily affects the retinal periphery.

The lower resolution of larger scans as compared to a smaller field of view may partially explain these findings [21, 22]. Moreover, as the image size increases, so does the proportion occupied by larger blood vessels; as the pathogenesis of DR is dominated by microvascular damage, larger scans can occult or underestimate the entity of small vessel dropout [21]. Large vessel removal from VD quantification on WF-OCTA images has yielded improved diagnostic performance in terms of discriminating different stages of DR [23]. Some studies reported that the DR-related microvascular damage begins in the perimacular area (as suggested by the FAZ enlargement often observed in DR patients) [24], making the 3×3 mm scan the one with the best predictive value in DR. Finally, the 12×12 and 15×9 mm scans harbor peripheral and motion artifacts that can interfere with quantitative and qualitative analyses of the retinal vasculature [25].

WF-OCTA artifacts in DR patients fall into 3 categories: systemic artifacts (i.e., projection artifacts, masking, unmasking, and loss of signal), image processing errors (i.e., segmentation, duplication of vessels, and alignment errors), and motion artifacts (i.e., displacement, blink artifacts, and stretch artifacts). Because of the large dimension of the scans, the time necessary for acquisition, and the automated fusion operated by the instrument, OCTA montage images are susceptible to all these types of artifacts. Patients with higher-severity DR eyes with NV, epiretinal membrane, diabetic macular edema, and pigment epithelium detachment may be at particular risk for poor-quality imaging [26].

3. WF-OCTA and Nonperfusion Areas in DR

Capillary occlusion is the pivotal mechanism in DR progression [27–30]. Peripheral nonperfusion has been associated with visual deterioration and visual field damage progression

(Figure 1) [31]. The quantification of the extent of retinal ischemia might be a promising prognostic biomarker in DR, aiding in tailoring personalized treatment algorithms [32, 33].

3.1. Diagnostic Performance of WF-OCTA in NPA Detection. WF-OCTA has very high sensitivity and discretely high specificity for NPA detection, using UWF-FFA as a reference [34]. WF-OCTA 12×12 mm scans demonstrated good discriminating accuracy in classifying eyes with DR (any severity) versus diabetic eyes without retinopathy, with an area under the curve (AUC) of 0.93 [35]. When nonproliferative DR (NPDR) eyes were compared to diabetic eyes without retinopathy, OCTA yielded poorer results (AUC was 0.875).

As capillary dropout in NPDR initially occurs in the mid-periphery, wider scans are necessary to accurately determine the severity of DR, provided that peripheral NVs are carefully excluded as they can alter quantitative vascular metrics. Tan et al. [23] compared the diagnostic accuracy of the 12×12 mm with a 6×6 mm OCTA image. The authors cropped a 12×12 mm image into a central 6×6 mm field and a peripheral square annulus region and calculated four different vascular metrics (namely, the total perfusion density (TPD), the capillary perfusion density (CPD), the large vessel density (LVD), and the capillary dropout density (CDD)) in each subregion. They found a stepwise increase in CDD from no DR to severe DR; the CCD in the peripheral square annulus was the best parameter discriminating between mild NPDR and no DR groups. The TPD and CPD in the peripheral subfield had higher discriminative power for more advanced stages of DR than small-field images.

3.2. Further Characterization of Vascular Anatomy in DR. The introduction of projection-resolved (PR) OCTA algorithms [36, 37] and 3D visualization [38] systems has increased the quality of depth-resolved OCTA scans. Indeed, while in 2D reconstructions, retinal layers are segmented and reconstructed by two topographic axes (i.e., x and y), volume-rendered OCTA reconstructions integrate structural and angiographic data to create 3D images. By incorporating the z -axis to the OCTA slabs, the relationship between retinal vascular and morphological alterations can be further investigated, e.g., the association between flow voids and cystoid spaces in DME [39] or between flow voids and areas of disorganization of the retinal inner layers [40]. 3D OCTA, implemented with a rotational display mode, may also assess the distribution of microaneurysms in relation to macular ischemia [41].

The exact distribution of the capillary plexuses in the mid-to-far periphery has not been investigated to a similar extent. In healthy eyes, the capillary density of the intermediate capillary plexus (ICP) and the deep capillary plexus (DCP) progressively reduces from the fovea to the periphery, with the ICP ultimately disappearing at about 8–9 mm of eccentricity. Parallely, the ganglion cell complex and the inner nuclear layer thin with a centrifugal fashion [16].

Diabetic microangiopathy starts in the midperiphery and extends towards the perifoveal region with progressive severity of the disease [42]. Capillary dropout displays a sectorial

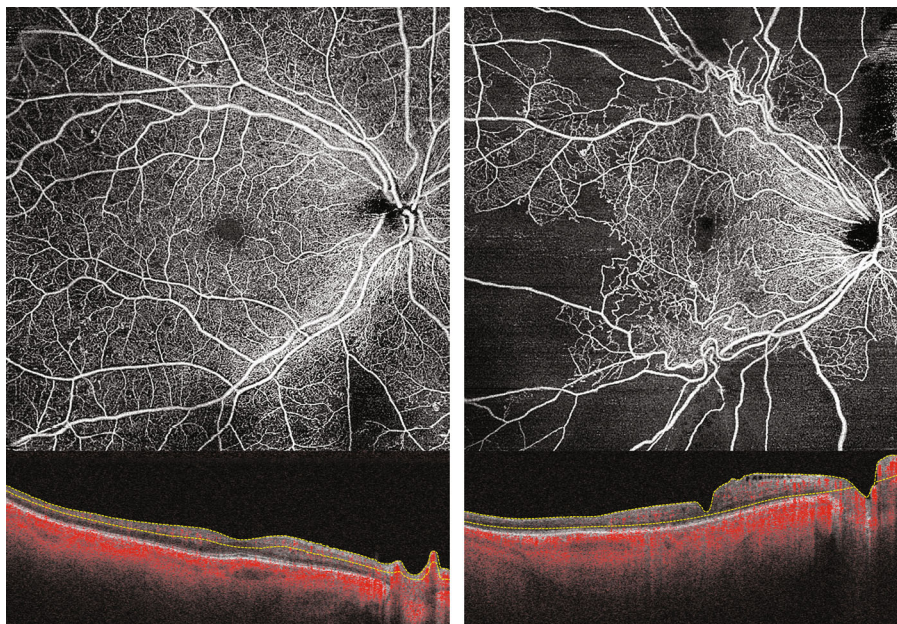


FIGURE 1: Two patients with diabetic retinopathy showing different degrees of capillary nonperfusion.

preference for the temporal quadrants, at least in the early stages of NPDR. The rarefaction of the vascular supply in the midperiphery (where the vascular plexuses merge from 3 into 2 networks) and the presence of radial peripapillary capillaries in the nasal quadrant, together with decreased retinal thickness temporally, might contribute to the topographic distribution of NPA in diabetic eyes [43, 44]. The macular area bears a less amount of NPAs as compared to the midperiphery, thanks to multiple overlappingly plexa into the superficial and the deeper retinal layers.

Yasukura and associates hypothesized the existence, in the extramacular region, of distinct lobules of retinal perfusion, separated by each other by large arterioles encompassing both the superficial and deep layers [45]. They also posed that extramacular retinal areas could be divided into two groups: those perfused by a singular arteriolar trunk and those dually nourished. By using 12×12 mm OCTA slabs, the authors found higher vulnerability of areas nourished by a single arteriole to diabetic microangiopathy. There were no differences in the extramacular NPAs between severe NPDR and PDR, while the eyes with PDR had significantly greater NPAs in the macular area than those with severe NPDR. The importance of the different vascular anatomic configurations between the macular and extramacular regions may have other clinical correlates, including the distribution and the extent of cotton wool spots [46]. Extramacular cotton wool spots (or white spots) have been mostly associated with NPAs encompassing all retinal layers, as opposed to macular cotton wool spots, which are more associated with NPAs in the superficial layer only [46].

Preferential localization of NPAs along the main retinal arteries has also been described [47]. Ishibazawa et al. examined 63 eyes from 44 patients with NPDR or PDR aided by a computer-based algorithm determining the shortest distance between nonperfusion and retinal vessels. The authors found

a larger rate of arterial-adjacent NPAs compared with venous-adjacent NPAs in all stages of DR. The authors hypothesized diabetic microangiopathy starting near the arterial side, with no regard to the level of DR severity, and then progressing towards the venous side.

Finally, WF-OCTA demonstrated more pronounced vascular involvement in the DCP, irrespective of the stage of DR. A recent study of 104 eyes with PDR showed a disproportion of lamellar capillary nonperfusion between the SCP and the DCP, the latter being more greatly involved in all the assessed quadrants [48]. The difference in the perfusion pressure between the SCP and the DCP could be a plausible explanation of this discrepancy [49].

In light of the above-described findings, OCTA provides additional clues of the vascular involvement in diabetic microangiopathy, as well as a quantitative estimate and topographic distribution of NPAs. These parameters could aid deep learning systems in the automatic detection of DR and estimation of its severity.

3.3. WF-OCTA and Vascular Reperfusion in DR Eyes. The possibility of vascular reperfusion in DR has been a matter of debate for many years. Some studies suggest that DR may spontaneously regress [50–52], and some older reports claim a rate of reperfusion as high as 69% [53]. It is not yet clear if anti-VEGF agents play a role in this process, and current pieces of evidence are contradictory. Some authors support reperfusion following anti-VEGF agents' injection [54], while others deny any vascular change in response to antiangiogenic treatment [55], despite an overall improvement in the DR severity score.

Couturier et al. noted additional areas of capillary dropouts on WF-OCTA compared to FFA [32]. Additional studies employing WF-OCTA may help in shedding further light on the possibility of capillary reperfusion in treated eyes.

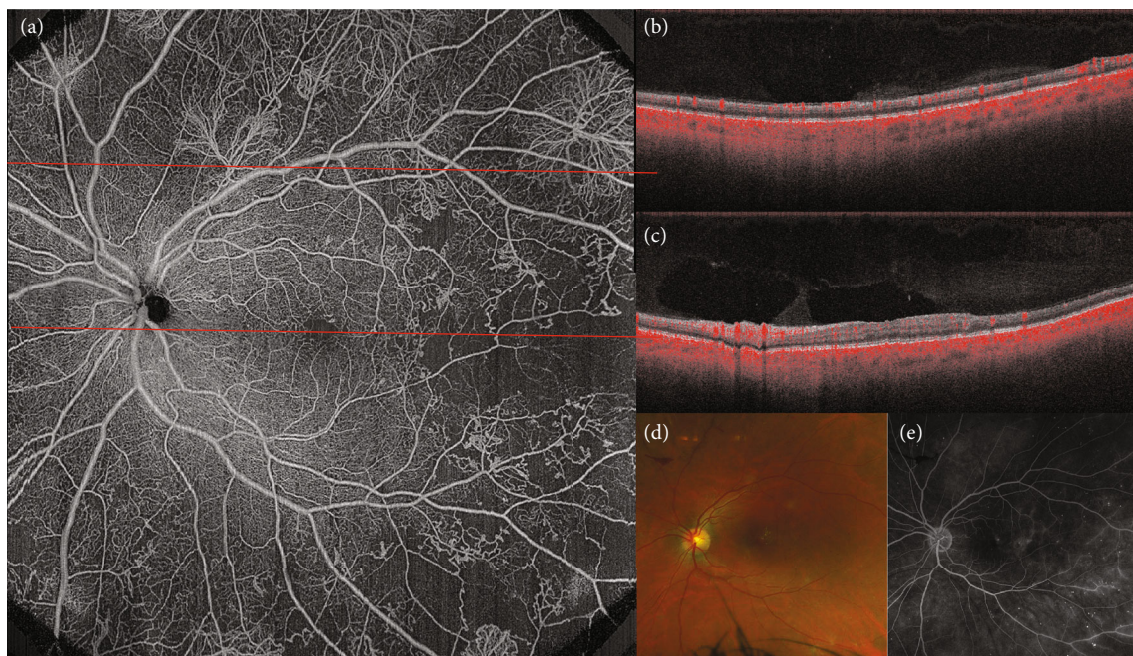


FIGURE 2: Multimodal imaging of proliferative diabetic retinopathy (PDR). (a) Widefield optical coherence tomography angiography (WF-OCTA) of the posterior pole, revealing multiple neovascularization elsewhere (NVEs) and capillary nonperfusion (NP) temporal to the macula. (b) Structural B-scan passing through the area corresponding to the upper red dashed line. Temporally, NVE is discernible on the B-scan. (c) Structural B-scan passing through the fovea, corresponding to the lower red dashed line and showing temporal retinal thinning secondary to retinal ischemia. (d) Color fundus picture of the same patient, revealing macular exudates, cotton wool spots, and preretinal hemorrhages. (e) Fundus fluorescein angiography shows microaneurysms, capillary nonperfusion, and NVE.

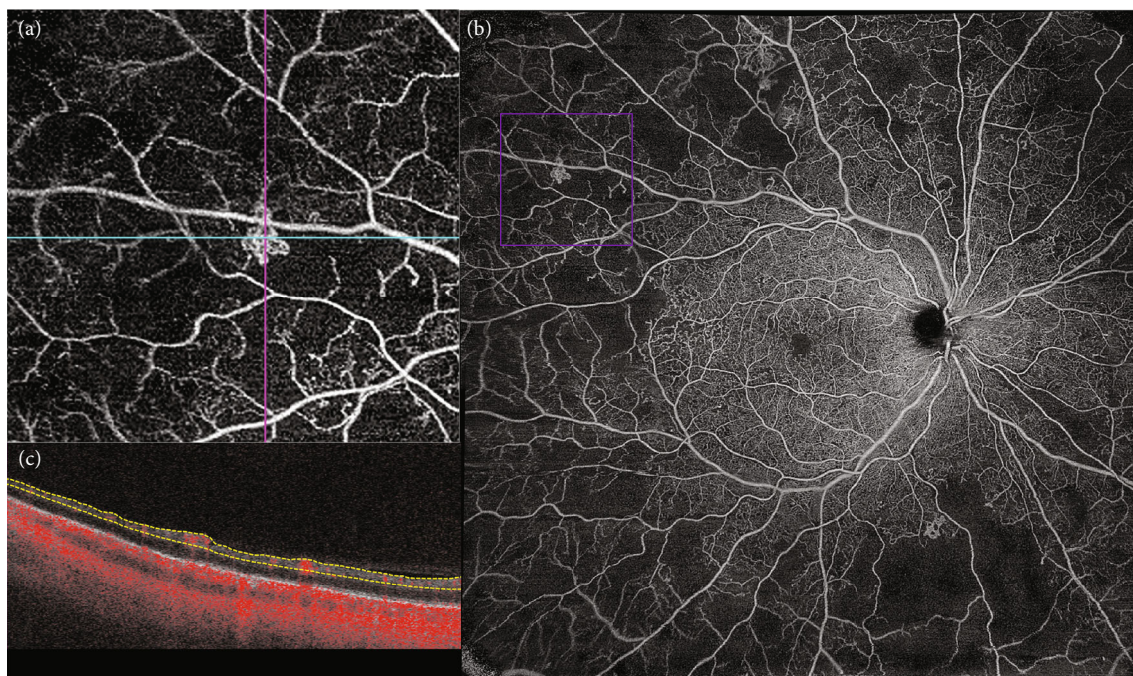


FIGURE 3: B-scan with slab boundaries and the corresponding flow *en face* image. (a) Widefield optical coherence tomography angiography (WF-OCTA) of the posterior pole, revealing multiple areas of capillary nonperfusion and intraretinal microvascular abnormality (IRMA), outlined in the purple box. (b) Magnification of the area outlined in the purple box, showing IRMA surrounded by capillary nonperfusion. (c) The intraretinal localization of the anomalous vascular network (i.e., the absence of protrusion into the vitreous) makes it possible to differentiate IRMA from neovascularization elsewhere.

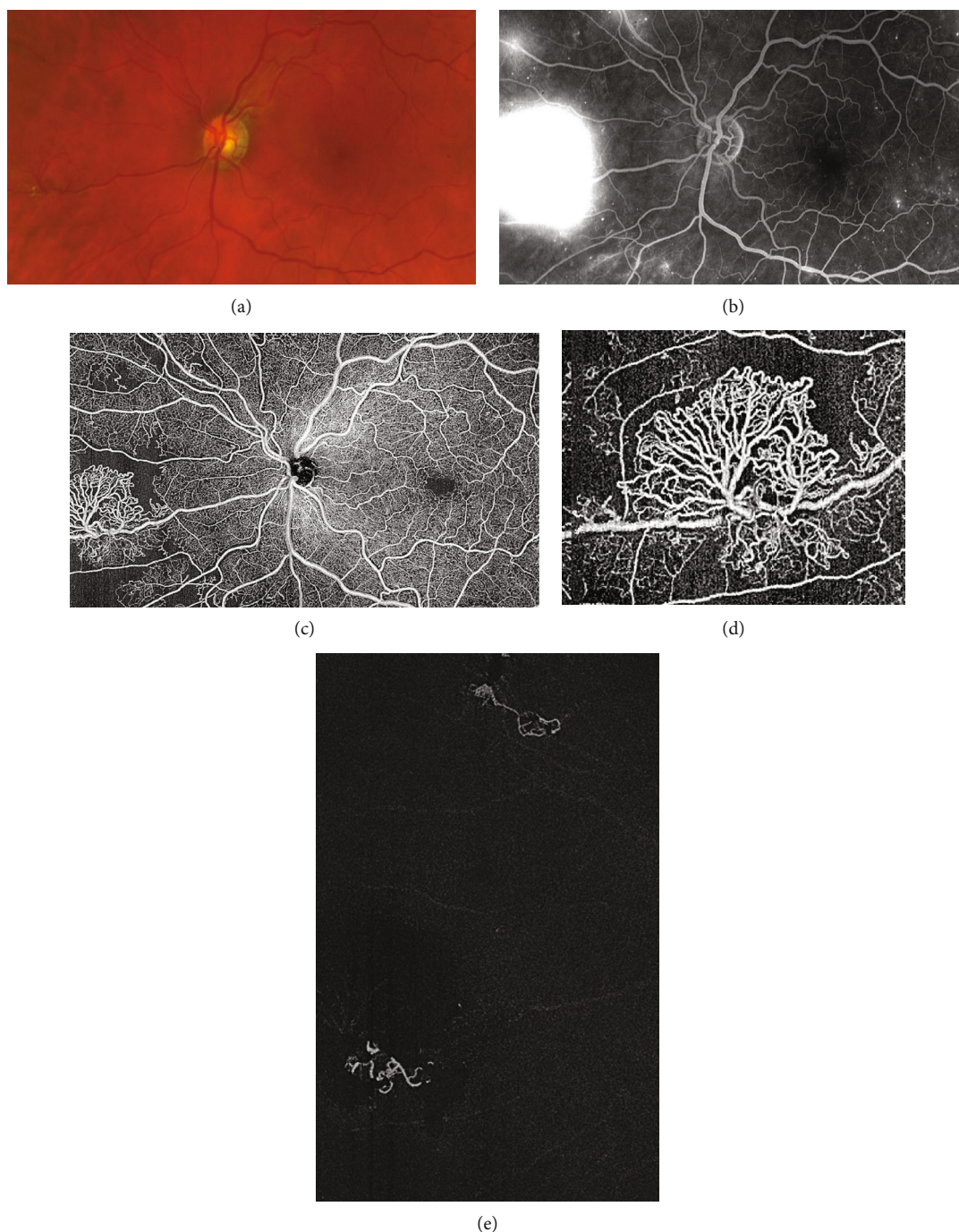


FIGURE 4: Proliferative diabetic retinopathy with neovascularization elsewhere. (a) Color fundus picture showing the neovascular epiretinal network in the nasal periphery. (b) Fundus fluorescein angiography (FFA) shows marked hyperfluorescence due to dye leakage in the late phase of the exam. Morphologic characterization of the neovascularization is not possible using FFA. (c) Widefield optical coherence tomography angiography of the same eye, depicting the neovascularization (NV) and its peripheral loops (d). (e) Vitreoretinal slab of OCTA, showing the NV protruding into the vitreous.

4. WF-OCTA and Proliferative Diabetic Retinopathy

Due to the absence of late dye leakage, OCTA allows a better morphologic characterization of IRMA and NV as compared to FFA (Figure 2).

IRMAs appear on WF-OCTA as tortuous intraretinal vascular segments not exceeding the inner limiting membrane boundaries; contrarily, neovascularization elsewhere (NVE) protrudes into the vitreous cavity (Figure 3) [19]. Some IRMA may be associated with small vascular tufts, i.e., small buds at their tip with a closed-end and a bulging

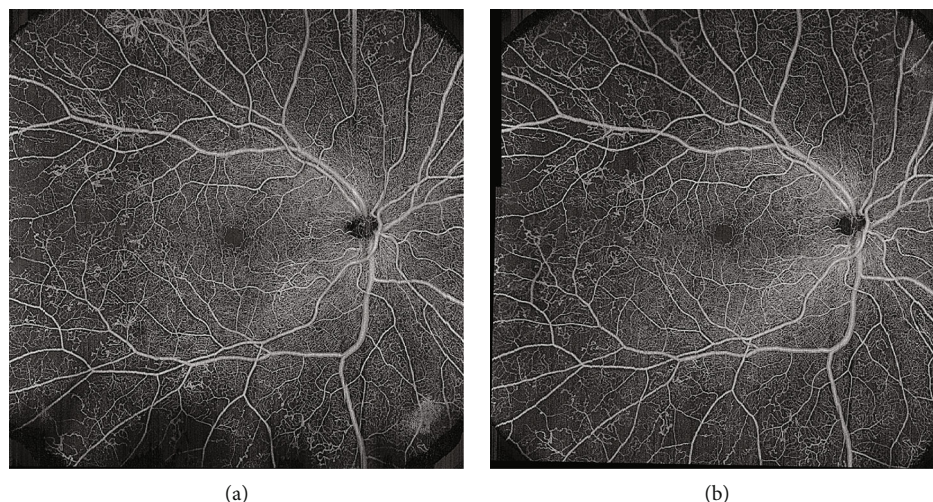


FIGURE 5: A 12×12 mm en face image of the same patient before (a) and after (b) treatment with a combination of panretinal photocoagulation and intravitreal anti-VEGF agents. Complete regression of epiretinal neovascularization is noted. The eyelashes may create masking artifacts (a), which can overestimate the extent of the nonperfusion areas.

shape [56]. IRMA shows heterogeneous behavior after panretinal photocoagulation (PRP) treatment: some remain unchanged, some show regression, some others may be worse. IRMA that regresses may be adjacent to areas of restored vascular perfusion after PRP [56].

Both NVE and NV of the disc (NVD) appear as irregular, convoluted masses of large- and small-caliber vessels, better visualized in the vitreoretinal interface (VRI) slab, which covers the most posterior portion of the vitreous body (the hyaloid) and the most anterior part of the retinal surface (Figure 4) [13, 19].

The presence of preretinal vessels can be confirmed by comparing the *en face* OCTA slab with the corresponding OCT B-scan image, which shows flow signal either laying on the retinal surface or protruding into the vitreous cavity in patients with NVE [57, 58]. Structural scans may help in differentiating active from inactive lesions: active NV appears as an exuberant proliferation of fine vessels, while inactive NV features pruned vascular loops of filamentous vessels [58].

Segmentation accuracy and sufficient signal detection are the mainstays for the identification of NV through *en face* OCTA [59]. Segmentation errors are one of the main sources of artifact in OCTA images [60, 61], and they occur more frequently in NVD than in NVE [59]. Furthermore, the difference in segmentation parameters between multiple SS-OCTA devices must be taken into account when considering the sensitivity of VRI slabs for detecting NVs.

4.1. Sensitivity and Specificity of WF-OCTA for NV. A growing body of evidence supports the use of WF-OCTA for the diagnosis and the management of PDR [62]. WF-OCTA may be superior to both indirect ophthalmoscopy and CFP in terms of NV detection [63, 64].

A comparison between UWF-FFA and simulated WF-OCTA in 651 eyes of 433 PDR patients found that the WF-OCTA was able to capture NV in 98% of cases, with a slightly higher sensitivity for treatment-naïve eyes (99%) than for

treated ones (97%) [62]. Recent studies using different strategies of WF-OCTA montage have confirmed these numbers [34]. WF-OCTA may be particularly advantageous in the case of small neovascular lesions, which could be missed by FFA or misdiagnosed as IRMA or MA.

NVD and NVE have a dissimilar distribution in PDR patients. The majority of the eyes feature both NVD and NVE (50%), 40% display NVE only, and 10% have NVD only [62]. NVE is most prevalent in the superotemporal quadrants and rarely occurs in the nasal quadrants. No significant difference in the NVE/NVD ratio and NVE location has been found between treatment-naïve eyes and those that had previously undergone PRP, macular grid laser, intravitreal anti-VEGF injections, or vitrectomy. This might suggest a reevaluation of the clinical significance of NVD in the setting of PDR eyes, which has been traditionally associated with increased severity of the disease. In this view, longitudinal observation is needed to clarify the natural history of NV on WF-OCTA.

The WF-OCTA detection rate of NVE might be limited by NVE located outside the field of view of the WF slab [65]. As predominantly peripheral disease has been associated with faster disease progression [44, 66, 67], adjustments in scan localization (e.g., image centered on the optic disc rather than on the fovea), segmentation, and size are warranted to optimize the sensitivity of noninvasive devices [59].

4.2. Role of WF-OCTA in Treated PDR Eyes. To date, only a few studies have investigated the role of WF-OCTA in PDR following PRP or anti-VEGF injections. *En face* OCTA is not inferior to UWF-FFA [68] and represents a reliable tool for defining NV regression, as well as its reactivation and resistance after treatment [69].

Pruning of new vessels and reduction in smaller-caliber vessel density within NV fronds are the most characteristic signs of NV regression, along with a marked reduction of the detected flow area (Figure 5) [58, 68]. Morphologic changes in NV shape and size in regressed NV have been

observed as early as 1 week after PRP. Conversely, NVE showing progression at 3 months showed a return to the baseline value in smaller-caliber vessel density at 1 month. Some NVs considered regressed on FFA due to a reduction in dye leakage were deemed as enlarged on OCTA.

5. Conclusion

The present review is aimed at exploring, with an evidence-based approach, the usefulness of WF-OCTA in DR patients. WF-OCTA harbors an interesting potential because of its noninvasiveness and high-resolution; moreover, it allows quantitative assessments and comparable metrics of retinal vasculature. Nevertheless, WF-OCTA is still not available in many centers and is susceptible to various types of artifacts. In the coming years, further studies will facilitate the migration of WF-OCTA tools from the research field to everyday clinical practice.

Data Availability

The data supporting this review are from previously reported studies and datasets, which have been cited. The processed data are available from the corresponding author upon request.

Conflicts of Interest

The authors declare that they have no conflicts of interest.

References








- [1] K. Ogurtsova, J. D. da Rocha Fernandes, Y. Huang et al., "IDF Diabetes Atlas: global estimates for the prevalence of diabetes for 2015 and 2040," *Diabetes Research and Clinical Practice*, vol. 128, pp. 40–50, 2017.
- [2] N. Cheung, P. Mitchell, and T. Y. Wong, "Diabetic retinopathy," *Lancet*, vol. 376, no. 9735, pp. 124–136, 2010.
- [3] T. Y. Wong, C. M. G. Cheung, M. Larsen, S. Sharma, and R. Simó, "Diabetic retinopathy," *Nature Reviews. Disease Primers*, vol. 2, no. 1, 2016.
- [4] R. R. A. Bourne, J. B. Jonas, A. M. Bron et al., "Prevalence and causes of vision loss in high-income countries and in Eastern and Central Europe in 2015: magnitude, temporal trends and projections," *The British Journal of Ophthalmology*, vol. 102, no. 5, pp. 575–585, 2018.
- [5] D. S. W. Ting, G. C. M. Cheung, and T. Y. Wong, "Diabetic retinopathy: global prevalence, major risk factors, screening practices and public health challenges: a review," *Clinical & Experimental Ophthalmology*, vol. 44, no. 4, pp. 260–277, 2016.
- [6] J. W. Y. Yau, S. L. Rogers, R. Kawasaki et al., "Global prevalence and major risk factors of diabetic retinopathy," *Diabetes Care*, vol. 35, no. 3, pp. 556–564, 2012.
- [7] Y. Jia, S. T. Bailey, T. S. Hwang et al., "Quantitative optical coherence tomography angiography of vascular abnormalities in the living human eye," *Proceedings of the National Academy of Sciences of the United States of America*, vol. 112, no. 18, pp. E2395–E2402, 2015.
- [8] A. S. Nam, I. Chico-Calero, and B. J. Vakoc, "Complex differential variance algorithm for optical coherence tomography angiography," *Biomedical Optics Express*, vol. 5, no. 11, pp. 3822–3832, 2014.
- [9] Y. Watanabe, Y. Takahashi, and H. Numazawa, "Graphics processing unit accelerated intensity-based optical coherence tomography angiography using differential frames with real-time motion correction," *Journal of Biomedical Optics*, vol. 19, no. 2, article 021105, 2014.
- [10] E. Moul, W. J. Choi, N. K. Waheed et al., "Ultrahigh-speed swept-source OCT angiography in exudative AMD," *Ophthalmic Surgery, Lasers & Imaging Retina*, vol. 45, no. 6, pp. 496–505, 2014.
- [11] R. F. Spaide, J. G. Fujimoto, N. K. Waheed, S. R. Sadda, and G. Staurengi, "Optical coherence tomography angiography," *Progress in Retinal and Eye Research*, vol. 64, pp. 1–55, 2018.
- [12] A. Uji and N. Yoshimura, "Application of extended field imaging to optical coherence tomography," *Ophthalmology*, vol. 122, no. 6, pp. 1272–1274, 2015.
- [13] T. Hirano, S. Kakiyama, Y. Toriyama, M. G. Nittala, T. Murata, and S. Sadda, "Wide-field en face swept-source optical coherence tomography angiography using extended field imaging in diabetic retinopathy," *The British Journal of Ophthalmology*, vol. 102, no. 9, pp. 1199–1203, 2018.
- [14] M. Pellegrini, M. Cozzi, G. Staurengi, and F. Corvi, "Comparison of wide field optical coherence tomography angiography with extended field imaging and fluorescein angiography in retinal vascular disorders," *PLoS One*, vol. 14, no. 4, article e0214892, 2019.
- [15] T. E. de Carlo, D. A. Salz, N. K. Waheed, C. R. Baumal, J. S. Duker, and A. J. Witkin, "Visualization of the retinal vasculature using wide-field montage optical coherence tomography angiography," *Ophthalmic Surgery, Lasers & Imaging Retina*, vol. 46, no. 6, pp. 611–616, 2015.
- [16] C. Lavia, P. Mecê, M. Nassisi et al., "Retinal capillary plexus pattern and density from fovea to periphery measured in healthy eyes with swept-source optical coherence tomography angiography," *Scientific Reports*, vol. 10, no. 1, p. 1474, 2020.
- [17] Q. Zhang, K. A. Rezaei, S. S. Saraf, Z. Chu, F. Wang, and R. K. Wang, "Ultra-wide optical coherence tomography angiography in diabetic retinopathy," *Quantitative Imaging in Medicine and Surgery*, vol. 8, no. 8, pp. 743–753, 2018.
- [18] R. K. Wang, A. Zhang, W. J. Choi et al., "Wide-field optical coherence tomography angiography enabled by two repeated measurements of B-scans," *Optics Letters*, vol. 41, no. 10, pp. 2330–2333, 2016.
- [19] K. B. Schaal, M. R. Munk, I. Wyssmueller, L. E. Berger, M. S. Zinkernagel, and S. Wolf, "Vascular abnormalities in diabetic retinopathy assessed with swept-source optical coherence tomography angiography widefield imaging," *Retina*, vol. 39, no. 1, pp. 79–87, 2019.
- [20] R. Mastropasqua, R. D'Aloisio, L. di Antonio et al., "Widefield optical coherence tomography angiography in diabetic retinopathy," *Acta Diabetologica*, vol. 56, no. 12, pp. 1293–1303, 2019.
- [21] T. Hirano, J. Kitahara, Y. Toriyama, H. Kasamatsu, T. Murata, and S. Sadda, "Quantifying vascular density and morphology using different swept-source optical coherence tomography angiographic scan patterns in diabetic retinopathy," *The British Journal of Ophthalmology*, vol. 103, no. 2, pp. 216–221, 2019.
- [22] A. Rabiolo, F. Gelormini, A. Marchese et al., "Macular perfusion parameters in different angiocube sizes: does the size

- matter in quantitative optical coherence tomography angiography?," *Investigative Ophthalmology & Visual Science*, vol. 59, no. 1, pp. 231–237, 2018.
- [23] B. Tan, J. Chua, E. Lin et al., "Quantitative microvascular analysis with wide-field optical coherence tomography angiography in eyes with diabetic retinopathy," *JAMA Network Open*, vol. 3, no. 1, article e1919469, 2020.
- [24] G. Di, Y. Weihong, Z. Xiao et al., "A morphological study of the foveal avascular zone in patients with diabetes mellitus using optical coherence tomography angiography," *Graefe's Archive for Clinical and Experimental Ophthalmology*, vol. 254, no. 5, pp. 873–879, 2016.
- [25] E. Borrelli, P. Viggiano, F. Evangelista, L. Toto, and R. Mastropasqua, "Eyelashes artifact in ultra-widefield optical coherence tomography angiography," *Ophthalmic Surgery, Lasers & Imaging Retina*, vol. 50, no. 11, pp. 740–743, 2019.
- [26] Y. Cui, Y. Zhu, J. C. Wang et al., "Imaging artifacts and segmentation errors with wide-field swept-source optical coherence tomography angiography in diabetic retinopathy," *Translational Vision Science & Technology*, vol. 8, no. 6, p. 18, 2019.
- [27] D. A. Sim, P. A. Keane, J. Zarranz-Ventura et al., "The effects of macular ischemia on visual acuity in diabetic retinopathy," *Investigative Ophthalmology & Visual Science*, vol. 54, no. 3, pp. 2353–2360, 2013.
- [28] S. H. Byeon, Y. K. Chu, H. Lee, S. Y. Lee, and O. W. Kwon, "Foveal ganglion cell layer damage in ischemic diabetic maculopathy: correlation of optical coherence tomographic and anatomic changes," *Ophthalmology*, vol. 116, no. 10, pp. 1949–1959.e8, 2009, e8.
- [29] Y. Dodo, T. Murakami, A. Uji, S. Yoshitake, and N. Yoshimura, "Disorganized retinal lamellar structures in nonperfused areas of diabetic retinopathy," *Investigative Ophthalmology & Visual Science*, vol. 56, no. 3, pp. 2012–2020, 2015.
- [30] N. Unoki, K. Nishijima, A. Sakamoto et al., "Retinal sensitivity loss and structural disturbance in areas of capillary nonperfusion of eyes with diabetic retinopathy," *American Journal of Ophthalmology*, vol. 144, no. 5, pp. 755–760.e1, 2007.
- [31] M. G. Maguire, D. Liu, A. R. Glassman et al., "Visual field changes over 5 years in patients treated with panretinal photocoagulation or ranibizumab for proliferative diabetic retinopathy," *JAMA Ophthalmol*, vol. 138, no. 3, pp. 285–293, 2020.
- [32] A. Couturier, P. A. Rey, A. Erginay et al., "Widefield OCT-angiography and fluorescein angiography assessments of non-perfusion in diabetic retinopathy and edema treated with anti-vascular endothelial growth factor," *Ophthalmology*, vol. 126, no. 12, pp. 1685–1694, 2019.
- [33] C. Lavia, S. Bonnin, M. Maule, A. Erginay, R. Tadayoni, and A. Gaudric, "Vessel density of superficial, intermediate, and deep capillary plexuses using optical coherence tomography angiography," *Retina*, vol. 39, no. 2, pp. 247–258, 2019.
- [34] O. Sawada, Y. Ichiyama, S. Obata et al., "Comparison between wide-angle OCT angiography and ultra-wide field fluorescein angiography for detecting non-perfusion areas and retinal neovascularization in eyes with diabetic retinopathy," *Graefe's Archive for Clinical and Experimental Ophthalmology*, vol. 256, no. 7, pp. 1275–1280, 2018.
- [35] A. Y. Alibhai, L. R. de Pretto, E. M. Moul et al., "Quantification of retinal capillary nonperfusion in diabetics using wide-field optical coherence tomography angiography," *Retina*, vol. 40, no. 3, pp. 412–420, 2020.
- [36] M. Zhang, T. S. Hwang, J. P. Campbell et al., "Projection-resolved optical coherence tomographic angiography," *Biomedical Optics Express*, vol. 7, no. 3, pp. 816–828, 2016.
- [37] J. X. Ong, C. C. Kwan, M. V. Cicinelli, and A. A. Fawzi, "Superficial capillary perfusion on optical coherence tomography angiography differentiates moderate and severe nonproliferative diabetic retinopathy," *PLoS One*, vol. 15, no. 10, article e0240064, 2020.
- [38] E. Borrelli, R. Sacconi, G. Klose, L. de Sisternes, F. Bandello, and G. Querques, "Rotational three-dimensional OCTA: a notable new imaging tool to characterize type 3 macular neovascularization," *Scientific Reports*, vol. 9, no. 1, p. 17053, 2019.
- [39] R. F. Spaide, "Volume-rendered angiographic and structural optical coherence tomography," *Retina*, vol. 35, no. 11, pp. 2181–2187, 2015.
- [40] R. F. Spaide, "Volume-rendered optical coherence tomography of diabetic retinopathy pilot study," *American Journal of Ophthalmology*, vol. 160, no. 6, pp. 1200–1210, 2015.
- [41] E. Borrelli, R. Sacconi, M. Brambati, F. Bandello, and G. Querques, "In vivo rotational three-dimensional OCTA analysis of microaneurysms in the human diabetic retina," *Scientific Reports*, vol. 9, no. 1, p. 16789, 2019.
- [42] T. Niki, K. Muraoka, and K. Shimizu, "Distribution of capillary nonperfusion in early-stage diabetic retinopathy," *Ophthalmology*, vol. 91, no. 12, pp. 1431–1439, 1984.
- [43] K. Shimizu, Y. Kobayashi, and K. Muraoka, "Midperipheral fundus involvement in diabetic retinopathy," *Ophthalmology*, vol. 88, no. 7, pp. 601–612, 1981.
- [44] P. S. Silva, A. J. dela Cruz, M. G. Ledesma et al., "Diabetic retinopathy severity and peripheral lesions are associated with nonperfusion on ultrawide field angiography," *Ophthalmology*, vol. 122, no. 12, pp. 2465–2472, 2015.
- [45] S. Yasukura, T. Murakami, K. Suzuma et al., "Diabetic nonperfused areas in macular and extramacular regions on wide-field optical coherence tomography angiography," *Investigative Ophthalmology & Visual Science*, vol. 59, no. 15, pp. 5893–5903, 2018.
- [46] K. Morino, T. Murakami, Y. Dodo et al., "Characteristics of diabetic capillary nonperfusion in macular and extramacular white spots on optical coherence tomography angiography," *Investigative Ophthalmology & Visual Science*, vol. 60, no. 5, pp. 1595–1603, 2019.
- [47] A. Ishibazawa, L. R. de Pretto, A. Y. Alibhai et al., "Retinal nonperfusion relationship to arteries or veins observed on widefield optical coherence tomography angiography in diabetic retinopathy," *Investigative Ophthalmology & Visual Science*, vol. 60, no. 13, pp. 4310–4318, 2019.
- [48] D. Uchitomi, T. Murakami, Y. Dodo et al., "Disproportion of lamellar capillary non-perfusion in proliferative diabetic retinopathy on optical coherence tomography angiography," *The British Journal of Ophthalmology*, vol. 104, no. 6, pp. 857–862, 2020.
- [49] D. Cabral, T. Pereira, G. Ledesma-Gil et al., "Volume rendering of dense B-scan optical coherence tomography angiography to evaluate the connectivity of macular blood flow," *Investigative Ophthalmology & Visual Science*, vol. 61, no. 6, p. 44, 2020.
- [50] E. M. Kohner, A. M. Hamilton, G. F. Joplin, and T. R. Fraser, "Florid diabetic retinopathy and its response to treatment by photocoagulation or pituitary ablation," *Diabetes*, vol. 25, no. 2, pp. 104–110, 1976.

- [51] W. J. Ramsay, R. C. Ramsay, R. L. Purple, and W. H. Knobloch, "Involutional diabetic retinopathy," *American Journal of Ophthalmology*, vol. 84, no. 6, pp. 851–858, 1977.
- [52] M. C. White, E. M. Kohner, J. C. Pickup, and H. Keen, "Reversal of diabetic retinopathy by continuous subcutaneous insulin infusion: a case report," *The British Journal of Ophthalmology*, vol. 65, no. 5, pp. 307–311, 1981.
- [53] K. Takahashi, S. Kishi, K. Muraoka, and K. Shimizu, "Reperfusion of occluded capillary beds in diabetic retinopathy," *American Journal of Ophthalmology*, vol. 126, no. 6, pp. 791–797, 1998.
- [54] A. Levin, I. Rusu, A. Orlin et al., "Retinal reperfusion in diabetic retinopathy following treatment with anti-VEGF intravitreal injections," *Clinical Ophthalmology*, vol. Volume 11, pp. 193–200, 2017.
- [55] S. Bonnin, B. Dupas, C. Lavia et al., "Anti-vascular endothelial growth factor therapy can improve diabetic retinopathy score without change in retinal perfusion," *Retina*, vol. 39, no. 3, pp. 426–434, 2019.
- [56] A. Shimouchi, A. Ishibazawa, S. Ishiko et al., "A proposed classification of intraretinal microvascular abnormalities in diabetic retinopathy following panretinal photocoagulation," *Investigative Ophthalmology & Visual Science*, vol. 61, no. 3, p. 34, 2020.
- [57] T. E. de Carlo, M. A. Bonini Filho, C. R. Baumal et al., "Evaluation of preretinal neovascularization in proliferative diabetic retinopathy using optical coherence tomography angiography," *Ophthalmic Surgery, Lasers & Imaging Retina*, vol. 47, no. 2, pp. 115–119, 2016.
- [58] A. Ishibazawa, T. Nagaoka, H. Yokota et al., "Characteristics of retinal neovascularization in proliferative diabetic retinopathy imaged by optical coherence tomography angiography," *Investigative Ophthalmology & Visual Science*, vol. 57, no. 14, pp. 6247–6255, 2016.
- [59] T. Hirano, K. Hoshiyama, K. Hirabayashi et al., "Vitreoretinal interface slab in OCT angiography for detecting diabetic retinal neovascularization," *Ophthalmology Retina*, vol. 4, no. 6, pp. 588–594, 2020.
- [60] K. Ghasemi Falavarjani, A. Habibi, P. Anvari et al., "Effect of segmentation error correction on optical coherence tomography angiography measurements in healthy subjects and diabetic macular oedema," *The British Journal of Ophthalmology*, vol. 104, no. 2, pp. 162–166, 2020.
- [61] R. F. Spaide, J. G. Fujimoto, and N. K. Waheed, "Image artifacts in optical coherence tomography angiography," *Retina*, vol. 35, no. 11, pp. 2163–2180, 2015.
- [62] J. F. Russell, H. W. Flynn Jr., J. Sridhar et al., "Distribution of diabetic neovascularization on ultra-widefield fluorescein angiography and on simulated widefield OCT angiography," *American Journal of Ophthalmology*, vol. 207, pp. 110–120, 2019.
- [63] H. Khalid, R. Schwartz, L. Nicholson et al., "Widefield optical coherence tomography angiography for early detection and objective evaluation of proliferative diabetic retinopathy," *The British Journal of Ophthalmology*, p. bjophthalmol-2019-315365, 2020.
- [64] Q. S. You, Y. Guo, J. Wang et al., "Detection of clinically unsuspected retinal neovascularization with wide-field optical coherence tomography angiography," *Retina*, vol. 40, no. 5, pp. 891–897, 2020.
- [65] L. P. Aiello, I. Odia, A. R. Glassman et al., "Comparison of early treatment diabetic retinopathy study standard 7-field imaging with ultrawide-field imaging for determining severity of diabetic retinopathy," *JAMA Ophthalmol*, vol. 137, no. 1, pp. 65–73, 2019.
- [66] P. S. Silva, J. D. Cavallerano, N. M. N. Haddad et al., "Comparison of nondiabetic retinal findings identified with nonmydriatic fundus photography vs ultrawide field imaging in an ocular telehealth program," *JAMA Ophthalmol*, vol. 134, no. 3, pp. 330–334, 2016.
- [67] P. S. Silva, H. el-Rami, R. Barham et al., "Hemorrhage and/or microaneurysm severity and count in ultrawide field images and early treatment diabetic retinopathy study photography," *Ophthalmology*, vol. 124, no. 7, pp. 970–976, 2017.
- [68] J. F. Russell, Y. Shi, J. W. Hinkle et al., "Longitudinal wide-field swept-source OCT angiography of neovascularization in proliferative diabetic retinopathy after panretinal photocoagulation," *Ophthalmol Retina*, vol. 3, no. 4, pp. 350–361, 2019.
- [69] R. Schwartz, H. Khalid, S. Sivaprasad et al., "Objective evaluation of proliferative diabetic retinopathy using OCT," *Ophthalmology Retina*, vol. 4, no. 2, pp. 164–174, 2020.

Research Article

Influence of Metabolic Parameters and Treatment Method on OCT Angiography Results in Children with Type 1 Diabetes

Marta Wysocka-Mincewicz ¹, Marta Baszyńska-Wilk ¹, Joanna Gołębowska ^{2,3},
Andrzej Olechowski ², Aleksandra Byczyńska ¹, Wojciech Hautz ²,
and Mieczysław Szalecki ^{1,4}

¹Department of Endocrinology and Diabetology, The Children's Memorial Health Institute, Warsaw, Poland

²Department of Ophthalmology, The Children's Memorial Health Institute, Warsaw, Poland

³Lazarski University, Faculty of Medicine, Warsaw, Poland

⁴Collegium Medicum, Jan Kochanowski University, Kielce, Poland

Correspondence should be addressed to Marta Wysocka-Mincewicz; syndykarka@wp.pl

Received 31 July 2020; Accepted 26 October 2020; Published 18 November 2020

Academic Editor: Irini Chatziralli

Copyright © 2020 Marta Wysocka-Mincewicz et al. This is an open access article distributed under the Creative Commons Attribution License, which permits unrestricted use, distribution, and reproduction in any medium, provided the original work is properly cited.

Aim. To evaluate the influence of metabolic parameters and the treatment method in children with type 1 diabetes (T1D) on the optical coherence tomography angiography (OCTA) results as early markers of diabetic retinopathy (DR). **Material and Methods.** This prospective study enrolled 175 consecutive children with T1D. OCTA was performed using AngioVue (Avanti, Optovue). Whole superficial capillary vessel density (wsVD), fovea superficial vessel density (fsVD), parafovea superficial vessel density (psVD), whole deep vessel density (wdVD), fovea deep vessel density (fdVD), parafovea deep vessel density (pdVD), foveal thickness (FT), parafoveal thickness (PFT), and foveal avascular zone (FAZ) in superficial plexus were evaluated and analyzed in relation to individual characteristics, i.e., sex, weight, height, body mass index (BMI), and metabolic factors: current and mean value of glycated hemoglobin A1c (HbA1c). Furthermore, the analysis concerned the diabetes duration, age at the T1D onset, and type of treatment—multiple daily insulin injections (MDI) or continuous subcutaneous insulin infusion (CSII). **Results.** In the study group, we did not identify any patient with DR in fundus ophthalmoscopy. Age at the onset of diabetes correlated negatively with FAZ ($r = -0.17$, $p < 0.05$). The higher level of HbA1c corresponded to a decrease of wsVD ($r = -0.13$, $p < 0.05$). We found significantly lower fsVD ($32.25 \pm .1$ vs. $33.98 \pm .1$, $p < 0.01$), wdVD ($57.87 \pm .1$ vs. $58.64 \pm .9$, $p < 0.01$), and pdVD ($60.60 \pm .2$ vs. $61.49 \pm .1$, $p < 0.01$) and larger FAZ area ($0.25 \pm .1$ vs. $0.23 \pm .1$, $p < 0.05$) in the CSII vs. MDI group. **Conclusion.** The metabolic parameters, age of the onset of diabetes, and treatment method affected the OCTA results in children with T1D. Further studies and observation of these young patients are needed to determine if these findings are important for early detection of DR or predictive of future DR severity.

1. Introduction

Type 1 diabetes (T1D) is the third most common chronic disease in children. Diabetic retinopathy (DR) is the most common microvascular complication of diabetes, and it develops in most patients with long-standing T1D [1]. However, in pediatric population, DR is very rare. The pubertal status and the prepubertal duration of diabetes influence the risk

of developing DR, as children under the age of 10 have minimal risk, and no cases of proliferative DR in the first decade of life were noted [2, 3]. New imaging technologies would be useful in the early identification of retinal structural and functional changes, before DR is clinically detectable. Optical coherence tomography angiography (OCTA) is a new, noninvasive tool, based on the detection and measurement of intravascular erythrocyte movement [4]. OCTA enables

reproducible, quantitative assessment of the retinal microcirculation and seems to be an effective method in the detection of early microcirculation disorders. The aim of the study was to assess the influence of metabolic parameters and the treatment method on OCTA results in children with T1D.

2. Material and Methods

2.1. Patients. This prospective, observational study enrolled 175 consecutive Caucasian children with T1D remaining under control of the Department of Endocrinology and Diabetology of The Children's Memorial Health Institute, which met criteria and agreed to study participation. The study was approved by the Bioethics Committee of The Children's Memorial Health Institute in Warsaw and followed the tenets of the Declaration of Helsinki. Written informed consent was obtained from the patient's legal guardian and from patients > 16 years old after an explanation of the nature of the noninvasive study. The inclusion criteria were a diagnosis of T1D based on the International Society for Pediatric and Adolescent Diabetes (ISPAD) criteria and insulin treatment (not in full remission). In the study, 25 children have newly recognized T1D (from 2 weeks up to a year after the diagnosis). The exclusion criteria were the history of prematurity, other concomitant retinal pathologies, such as hereditary retinal dystrophies, vitreoretinal diseases, myopia or hypermetropia (more than 6 diopters), and history of uveitis.

Metabolic control was measured by the current glycated hemoglobin A1c level (HbA1c) and the mean value for the whole T1D duration (minimum 4 tests per year), the amount of insulin per kilogram of the weight, the mean total daily insulin (taken from the pump memory or profile led in hospital), and the dose of insulin for breakfast (as one of the markers connected with insulin resistance). In the study, the weight, the height, body mass index (BMI), BMI Z-score, the age at onset, and the T1D duration were evaluated.

The BMI Z-score was calculated using the LMS method based on the Box-Cox transformation [5, 6].

$$Z\text{-score}(x) = \frac{(X/M)^L - 1}{LxS}, \quad (1)$$

where X is a measured anthropometric parameter (e.g., height and BMI), M is the median of the value, L is the power of the Box-Cox' transformacy, and S is a variability coefficient. L , M , and S values were taken from the reference tables for the chosen anthropometric parameters for the determined age and sex (by Kułaga et al.) [7, 8]. We checked the effect of the presence of diabetic ketoacidosis (DKA) at the time of the T1D onset. The next part of the analysis concerned the type of treatment—multiple daily insulin injections (MDI) or continuous subcutaneous insulin infusion (CSII) at the moment of taking the OCTA images. The MDI group included 81 children (the mean diabetes duration 3.38 ± 3.0 years) treated by pens in the basal-bolus functionally scheme, when the mean dose of the insulin analogue is calculated dependently on the amount of food and correction, or children with strict doses for the main meals. The CSII group consisted of 87 children treated with an insulin

pump for more than a year (the mean duration of CSII 3.74 ± 1.9 years, the mean duration of T1D 5.47 ± 3.3 years), but not all of them strictly followed the recommendations of the diabetes care team (strict doses per meal, not weighed meals) (Table 1).

2.2. Database. OCTA was performed using a commercially available RTVue XR Avanti with AngioVue (Optovue, Fremont, CA, USA) with $3 \text{ mm} \times 3 \text{ mm}$ images of macula, centered on the foveola. Each OCTA en face image contains 304×304 pixels created from the intersection of the 304 vertical and the 304 horizontal B-scans. AngioVue automatically segments the area into four layers, including superficial capillary plexus layer (SP), deep capillary plexus layer (DP), outer retinal layer, and choriocapillaris. The SP en face image was segmental with an inner boundary at $3 \mu\text{m}$ beneath the internal limiting membrane and outer boundary set at $15 \mu\text{m}$, beneath the inner plexiform layer, whereas the deep capillary plexus en face image was segmented with an inner boundary at $15 \mu\text{m}$ beneath the inner plexiform layer and an outer boundary at $70 \mu\text{m}$ beneath the inner plexiform layer. Integrated automated algorithms provided by the machine software were used to quantify the foveal avascular zone (FAZ) (mm^2) and macular vascular density (%). FAZ area was automatically calculated for superficial plexus; capillary vascular density in the macular and paramacular region was measured both in superficial and deep plexuses. Vessel density is calculated as the percentage area occupied by following blood vessels in the selecting region, which enables the quantitative assessment of microvasculature. The whole superficial capillary vessel density (wsVD), fovea superficial vessel density (fsVD), parafovea superficial vessel density (psVD), whole deep vessel density (wdVD), fovea deep vessel density (fdVD), and parafovea deep vessel density (pdVD) were taken into analysis. Foveal thickness (FT) (μm) and parafoveal thickness (PFT) (μm) data were obtained from retinal maps, using the same device. All subjects were dilated with 1% tropicamide eye drops before examination. The scans for each eye were captured; then, the best one in quality (with a signal strength index > 60) was considered for analysis. Two trained OCTA readers reviewed all images independently to ensure correct segmentation and identify poor quality scans, with motion artifacts or blurred images, where data were insufficient for proper analysis. The data of both eyes of patients were taken into all analysis independently, because of intraeye differences and metabolic parameters influenced on both eyes. After exclusion of eyes with poor quality scans, 330 eyes (from 168 patients) were taken to the final analysis.

2.3. Statistical Analysis. The data was described by mean, median, standard deviation, and minimum and maximum values. Values with normal distribution (which was checked using the Shapiro-Wilks test) were analyzed by Pearson correlation, but those which were not normal in distribution were analyzed by Spearman rank R correlations. The differences between the two groups were tested by the unpaired Student t -test or Mann-Whitney U test as appropriate. A

TABLE 1: The characteristics of the studied patients.

Investigative trait	Mean	SD	Median	Min	Max
Age (years)	12.74	±3.7	13.00	4.50	18.00
Diabetes duration (years)	5.48	±3.7	4.46	0.02	15.33
Age at onset (years)	8.30	±3.8	7.98	1.46	17.04
Weight (kg)	47.70	±18.6	46.00	16.50	97.00
Height (cm)	155.40	±19.5	159.99	106.00	181.50
BMI (kg/m ²)	18.94	±4.3	17.90	11.99	32.56
HbA1c current (%)	8.3	±1.8	7.9	5.8	14.0
HbA1c mean (%)	7.8	±1.2	7.7	6.0	12.0

SD = standard deviation; BMI = body mass index; HbA1c = glycated hemoglobin A1c.

level $p < 0.05$ was recognized as statistically significant. The tests were done using the Statistica 6.0 StatSoft Company.

3. Results

The characteristics of the study population are summarized in Table 1.

In the study group, we did not identify any patient with DR in fundus ophthalmoscopy.

We did not find any significant correlation between the T1D duration and the OCTA parameters. Age at the onset of T1D correlated significantly positively with FT ($r = 0.12$, $p < 0.05$) and negatively with FAZ ($r = -0.17$, $p < 0.05$).

Mean HbA1c correlated negatively with wsVD ($r = -0.13$, $p < 0.05$). HbA1c current and mean correlated with FT ($r = -0.19$, $p \leq 0.01$ and $r = -0.18$, $p < 0.02$, respectively) and PFT ($r = -0.28$, $p \leq 0.01$ and $r = -0.26$, $p \leq 0.01$, respectively) (Figures 1–4).

The weight and the height influenced on FT ($r = 0.13$, $p = 0.05$ and $r = 0.13$, $p < 0.05$, respectively), however, no correlation between BMI or BMI Z-score and FT were found.

The influence of DKA at the onset of T1D measured by pH correlated with FT and PFT ($r = 0.18$, $p = 0.02$ and $r = 0.20$, $p < 0.01$, respectively), psVD ($r = 0.18$, $p < 0.05$), and fdVD ($r = 0.20$, $p < 0.02$).

When dividing the group by sex (83 girls, 86 boys), none of the parameters such T1D duration, age at T1D onset, weight, height, BMI Z-score, and current and mean HbA1c were statistically different. The groups were statistically different in OCTA parameters: FT (girls 250.40 ± 17.9 vs. boys 260.20 ± 19.2 , $p < 0.01$), PFT (314.97 ± 17.1 vs. 321.25 ± 15.3 , $p < 0.01$), fsVD (32.39 ± 5.1 vs. 33.87 ± 5.2 , $p < 0.05$, respectively), fdVD (31.52 ± 6.1 vs. 33.43 ± 5.6 , $p < 0.01$, respectively), and pdVD (61.30 ± 2.2 vs. 60.70 ± 2.2 , $p < 0.03$, respectively).

Statistically significant correlations were found between the duration of CSII treatment and FT ($r = 0.19$, $p < 0.01$), FAZ ($r = -0.17$, $p < 0.05$), fsVD ($r = 0.20$, $p < 0.01$). The dose of insulin per day positively correlated only with FT ($r = 0.12$, $p < 0.05$). There were no significant correlations between the OCTA parameters and the amount of basal insulin or the amount of insulin per breakfast.

After dividing the groups by the type of treatment (MDI = 81 or CSII = 87), we recorded the differences

between the groups regarding the T1D duration, age at T1D onset, weight, height, and mean HbA1c (Table 2). These groups were statistically different in FAZ, fsVD, wdVD, and pdVD but not in FT and PFT.

4. Discussion

Nowadays, we do not observe clinical signs of diabetic retinopathy in pediatric population, as in this study group was not any child with this complication. Similarly, among 370 children with DM1 enrolled in the study of Geloneck et al., no patient was diagnosed with DR [9]. Probably, this results from better metabolic control effect, more physiological treatment using CSII by means of an insulin pump, more frequent use of continuous glucose monitoring, and more active and aggressive treatment based on monitoring trends. However, the analysis from the United Kingdom demonstrated that 9.5% of children under 12 years old had signs of background DR [10]. Our study also included children with poor metabolic control, but none of them had any signs of DR (neither in funduscopy nor on fundus color photography), even after 14 years of T1D duration. We performed OCTA to analyze possible early structural and/or functional dependencies with clinical parameters in pediatric population. Early DR is clinically diagnosed by observing microaneurysms using funduscopy. Preclinical DR may be accompanied by initial vascular abnormalities of the capillaries before the occurrence of microaneurysms.

Pediatric patients are the most important population of T1D, because of long life duration of this disease and its influence on all tissues. We detected weak but very significant negative correlations between the OCTA parameters and the parameters of diabetic metabolic control. In our previous studies, we did not observe such dependencies possibly because of smaller homogeneity of the study group [11].

Analyzing the groups undergoing different methods of treatment, we showed significantly lower fsVD, wdVD, and pdVD and a larger FAZ area in the CSII group. These results were completely surprising because we expected better retinal perfusion in children on CSII therapy, which is a more physiological type of treatment. But this group had longer T1D duration and an earlier T1D onset, which could partly justify these findings; however, T1D duration did not correlate with any OCTA parameters, and age at T1D onset

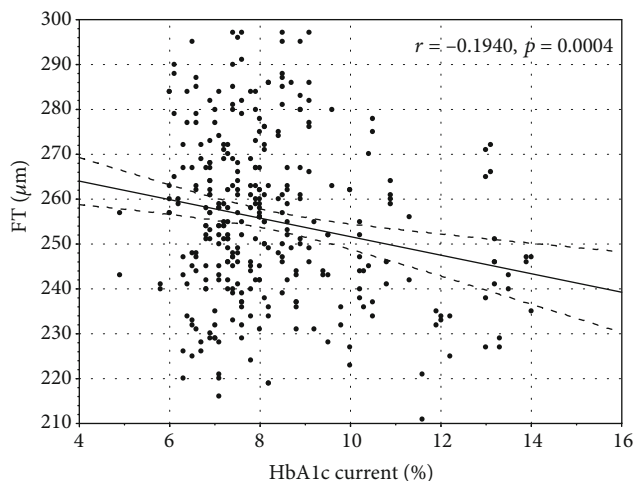


FIGURE 1: The correlation between current glycated hemoglobin A1c and foveal thickness.

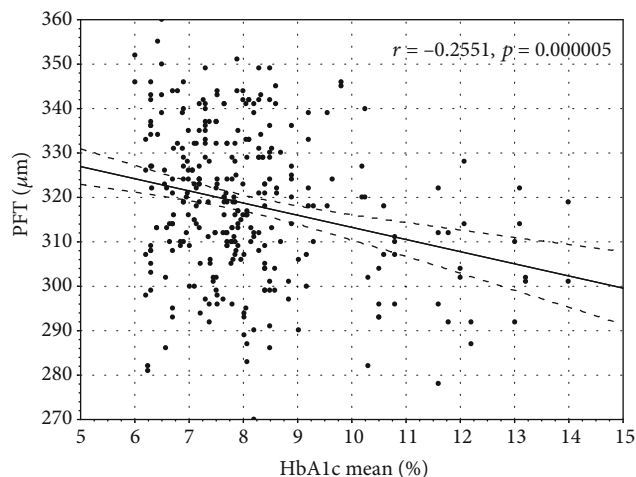


FIGURE 4: The correlation between mean average glycated hemoglobin A1c and parafoveal thickness.

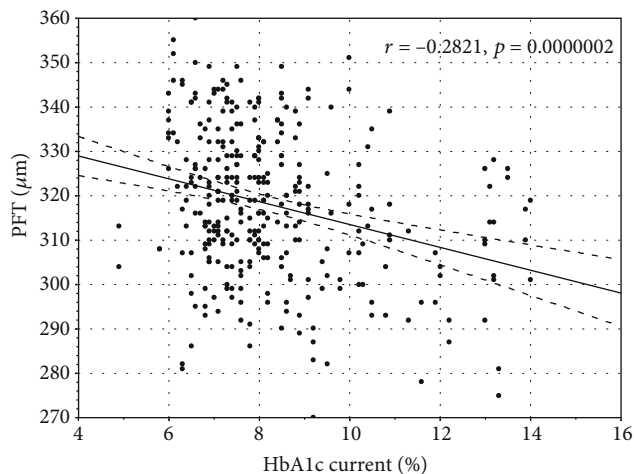


FIGURE 2: The correlation between current glycated hemoglobin A1c and parafoveal thickness.

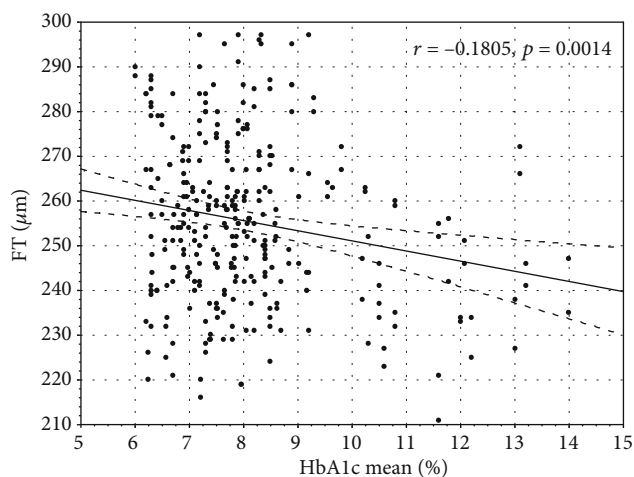


FIGURE 3: The correlation between mean average glycated hemoglobin A1c and foveal thickness.

correlated only with FAZ and FT. These groups differed in many demographic and metabolic parameters, but the same variables had no influence on the OCTA data in the other analyses and correlations. The FAZ area is considered as one of the most important parameters in OCTA, which could help evaluate the risk of developing DR in diabetic patients without any retinal changes on clinical examination. To avoid the effect of axial length and age on FAZ, baseline characteristics were similar between the study groups; the groups were comparable in terms of age, gender, and refraction. Other authors have reported the same approach to minimize FAZ variability in their studies [12, 13].

In the study of Nistrata-Ortiz et al., the FAZ parameters were increased proportionally to the diabetes duration [14], which was not reflected in our analysis, similarly as in other authors' research [15]. Statistically larger FAZ in diabetic patients was noted by the other authors too [15–17], but not in our previous study [6] and Tam et al. [18].

When we analyzed the differences between girls and boys, the FAZ area was smaller in boys, but this difference was not statistically significant, which Nistrata-Ortiz et al. observed [19]. They revealed the smaller mean FAZ surface area in boys similarly in the diabetic and control groups, both in superficial and deep capillary plexuses. In our study, we detected significantly higher central foveal and parafoveal thickness in the group of boys. These results could confirm the physiological differences between the genders, regardless of T1D.

Another significant factor is the age at the onset of T1D. In our study, this parameter negatively correlated with FAZ. This is contrary to the research by Onoe et al., where the larger FAZ area was associated with the older onset age [20] or to the study of Mameli et al., in which the correlation was not statistically significant [21]. Nevertheless, the number of participants in the aforementioned studies was remarkably smaller in comparison with our analysis.

In our study, mean HbA1c correlated negatively with wsVD. Wang et al. revealed that for every 1-point increase in HbA1c, the hazard for DR increased by 20% among youths

TABLE 2: Comparison of the groups treated by MDI or CSII.

	MDI, $n = 81$ Mean \pm SD	CSII, $n = 87$ Mean \pm SD	p level
Age (years)	12.69 \pm 3.8	12.91 \pm 3.5	$p = 0.58$
Age at T1D onset (years)	9.10 \pm 4.0	7.40 \pm 3.5	$p < 0.01$
Diabetes duration (years)	3.40 \pm 3.3	5.40 \pm 3.4	$p \leq 0.01$
Weight (kg)	45.40 \pm 17.3	49.50 \pm 19.4	$p < 0.05$
Height (cm)	152.80 \pm 19.1	157.50 \pm 19.7	$p < 0.05$
Mean HbA1c (%)	8.6 \pm 1.8	7.7 \pm 1.1	$p \leq 0.01$
FT	255.20 \pm 19.0	255.40 \pm 19.0	$p = 0.90$
PFT	317.60 \pm 17.0	318.80 \pm 15.0	$p = 0.50$
FAZ	0.23 \pm 0.1	0.25 \pm 0.1	$p < 0.05$
wsVD	51.50 \pm 3.0	51.10 \pm 2.7	$p = 0.30$
fsVD	33.98 \pm 5.1	32.25 \pm 5.1	$p < 0.01$
psVD	53.04 \pm 3.4	52.70 \pm 2.9	$p = 0.40$
wdVD	58.64 \pm 1.9	57.87 \pm 2.1	$p < 0.01$
fdVD	33.08 \pm 5.6	31.85 \pm 6.2	$p = 0.09$
pdVD	61.49 \pm 2.1	60.60 \pm 2.2	$p < 0.01$

MDI = multiple daily insulin injections; CSII = continuous subcutaneous insulin infusion; T1D = type 1 diabetes; HbA1c = glycated hemoglobin A1c; wsVD = whole superficial capillary vessel density; fsVD = fovea superficial vessel density; psVD = parafovea superficial vessel density; wdVD = whole deep vessel density; fdVD = fovea deep vessel density; pdVD = parafovea deep vessel density; FAZ = foveal avascular zone.

with T1D (hazard ratio (HR) = 1.20; 95% confidence interval (CI) 1.06-1.35) [22]. Conversely, several studies indicate the lack of correlation between mean HbA1c and retinal vessel density in patients with T1D [17, 23]. Due to the discordance in literature, the authors suggest a greater focus on new parameters in clinical practice, i.e., “time in range” (described as the percentage of time when a patient has a blood glucose level in the target range) [17]. The value of this parameter has already been proven in type 2 diabetes [24]. We have to remember that such a parameter describes a short period of the patient’s life—only this time when we have a monitoring memory. In the near future when almost the whole population will be subject to monitoring systems, this factor may play a crucial role in the process of unification and analysis of the same parameters.

In our study, we also performed the analysis of the parameters regarding the onset of T1D. DKA measured by pH at the moment of the diagnosis correlated with psVD, fdVD, FT, and PFT. To our knowledge, this is the first report on such dependence. In the literature, we found one study which analyzed the DKA status and its influence on the OCT parameters (OCT performed at the onset of T1D). Jeziorny et al. reported no significant difference in the retinal nerve fiber layer (RNFL) in OCT between DKA and non-DKA patients [25]. Currently, uncertainty remains with regard to the relationship between the severity of DKA at the moment of the diagnosis and the risk of DR. In one study of 230 patients with childhood-onset T1D, the authors (after 20 years of observation) did not confirm such a correlation [26].

5. Conclusion

To our knowledge, this is the biggest analysis of diabetic children, using OCT angiography, which considered the influence of many possible metabolic, demographic, and treatment parameters. In our study, we found significant correlations between, e.g., HbA1c, DKA, age at the onset of T1D, the treatment method, and the OCTA results in children with T1D. The detected correlations were predominantly weak, but statistically significant. All the children participated in the study had no changes suggested DR; probably in children, there is a strong capacity for autoregulation, and because of that, our correlations were so weak. Further studies are needed to detect the most important parameters for early detection of DR.

Data Availability

Due to the nature of this research, participants of this study did not agree for their data to be shared publicly, so supporting data is not available.

Conflicts of Interest

The authors have no conflicts of interest relevant to this article to disclose.

References

- [1] A. Girach, D. Manner, and M. Porta, “Diabetic microvascular complications: can patients at risk be identified? A review,” *International Journal of Clinical Practice*, vol. 60, no. 11, pp. 1471–1483, 2006.
- [2] R. W. Holl, G. E. Lang, M. Grabert, E. Heinze, G. K. Lang, and K. M. Debatin, “Diabetic retinopathy in pediatric patients with type-1 diabetes: effect of diabetes duration, prepubertal and pubertal onset of diabetes, and metabolic control,” *The Journal of Pediatrics*, vol. 132, no. 5, pp. 790–794, 1998.
- [3] Y. H. Cho, M. E. Craig, and K. C. Donaghue, “Puberty as an accelerator for diabetes complications,” *Pediatric Diabetes*, vol. 15, no. 1, pp. 18–26, 2014.
- [4] Y. Jia, O. Tan, J. Tokayer et al., “Split-spectrum amplitude-decorrelation angiography with optical coherence tomography,” *Optics Express*, vol. 20, no. 4, pp. 4710–4725, 2012.
- [5] T. J. Cole, “Growth references and standards,” in *Human Growth and Development*, N. Cameron, Ed., p. 386, Academic Press, San Diego, 2006.
- [6] T. J. Cole and P. J. Green, “Smoothing reference centile curves: the lms method and penalized likelihood,” *Statistics in Medicine*, vol. 11, no. 10, pp. 1305–1319, 1992.
- [7] Z. Kułaga, M. Litwin, M. Tkaczyk et al., “Polish 2010 growth references for school-aged children and adolescents,” *European Journal of Pediatrics*, vol. 170, no. 5, pp. 599–609, 2011.
- [8] Z. Kułaga, A. Grajda, B. Gurzkowska et al., “Polish 2012 growth references for preschool children,” *European Journal of Pediatrics*, vol. 172, no. 6, pp. 753–761, 2013.
- [9] M. M. Geloneck, B. J. Forbes, J. Shaffer, G.-s. Ying, and G. Binenbaum, “Ocular complications in children with diabetes mellitus,” *Ophthalmology*, vol. 122, no. 12, pp. 2457–2464, 2015.

- [10] A. Hamid, H. M. Wharton, A. Mills, J. M. Gibson, M. Clarke, and P. M. Dodson, "Diagnosis of retinopathy in children younger than 12 years of age: implications for the diabetic eye screening guidelines in the UK," *Eye (London, England)*, vol. 30, no. 7, pp. 949–951, 2016.
- [11] J. Gołębiowska, A. Olechowski, M. Wysocka-Mincewicz et al., "Optical coherence tomography angiography vessel density in children with type 1 diabetes," *PLoS One*, vol. 12, no. 10, article e0186479, 2017.
- [12] W. A. Samara, A. Shahlaee, M. K. Adam et al., "Quantification of diabetic macular ischemia using optical coherence tomography angiography and its relationship with visual acuity," *Ophthalmology*, vol. 124, no. 2, pp. 235–244, 2017.
- [13] M. Abdelshafy and A. Abdelshafy, "Correlations between optical coherence tomography angiography parameters and the visual acuity in patients with diabetic retinopathy," *Clinical Ophthalmology*, vol. 14, pp. 1107–1115, 2020.
- [14] M. Niestrata-Ortiz, P. Fichna, W. Stankiewicz, and M. Stopa, "Enlargement of the foveal avascular zone detected by optical coherence tomography angiography in diabetic children without diabetic retinopathy," *Graefe's Archive for Clinical and Experimental Ophthalmology*, vol. 257, no. 4, pp. 689–697, 2019.
- [15] N. Takase, M. Nozaki, A. Kato, H. Ozeki, M. Yoshida, and Y. Ogura, "Enlargement of foveal avascular zone in diabetic EYES evaluated by en face optical coherence tomography angiography," *Retina*, vol. 35, no. 11, pp. 2377–2383, 2015.
- [16] G. Dimitrova, E. Chihara, H. Takahashi, H. Amano, and K. Okazaki, "Quantitative retinal optical coherence tomography angiography in patients with diabetes without diabetic retinopathy," *Investigative Ophthalmology & Visual Science*, vol. 58, no. 1, pp. 190–196, 2017.
- [17] T. E. de Carlo, A. T. Chin, M. A. Bonini Filho et al., "Detection of microvascular changes in eyes of patients with diabetes but NOT clinical diabetic RETINOPATHY using optical coherence tomography angiography," *Retina*, vol. 35, no. 11, pp. 2364–2370, 2015.
- [18] J. Tam, K. P. Dhamdhere, P. Tiruveedhula et al., "Subclinical capillary changes in non-proliferative diabetic retinopathy," *Optometry and Vision Science*, vol. 89, no. 5, pp. E692–E703, 2012.
- [19] M. Niestrata-Ortiz, P. Fichna, W. Stankiewicz, and M. Stopa, "Sex-related variations of retinal and choroidal thickness and foveal avascular zone in healthy and diabetic children assessed by optical coherence tomography imaging," *Ophthalmologica*, vol. 241, no. 3, pp. 173–178, 2019.
- [20] H. Onoe, Y. Kitagawa, H. Shimada, A. Shinojima, M. Aoki, and T. Urakami, "Foveal avascular zone area analysis in juvenile-onset type 1 diabetes using optical coherence tomography angiography," *Japanese Journal of Ophthalmology*, vol. 64, no. 3, pp. 271–277, 2020.
- [21] C. Marni, A. Invernizzi, A. Bolchini et al., "Analysis of retinal perfusion in children, adolescents, and young adults with type 1 diabetes using optical coherence tomography angiography," *Journal Diabetes Research*, vol. 2019, article 5410672, pp. 1–8, 2019.
- [22] S. Y. Wang, C. A. Andrews, W. H. Herman, T. W. Gardner, and J. D. Stein, "Incidence and risk factors for developing diabetic retinopathy among youths with type 1 or type 2 diabetes throughout the United States," *Ophthalmology*, vol. 124, no. 4, pp. 424–430, 2017.
- [23] R. Sacconi, M. Casaluci, E. Borrelli et al., "Multimodal imaging assessment of vascular and neurodegenerative retinal alterations in type 1 diabetic patients without fundoscopic signs of diabetic retinopathy," *Journal of Clinical Medicine*, vol. 8, no. 9, p. 1409, 2019.
- [24] J. Lu, X. Ma, J. Zhou et al., "Association of time in range, as assessed by continuous glucose monitoring, with diabetic retinopathy in type 2 diabetes," *Diabetes Care*, vol. 41, no. 11, pp. 2370–2376, 2018.
- [25] K. Jeziorny, A. Niwald, A. Moll et al., "Measurement of corneal thickness, optic nerve sheath diameter and retinal nerve fiber layer as potential new non-invasive methods in assessing a risk of cerebral edema in type 1 diabetes in children," *Acta Diabetologica*, vol. 55, no. 12, pp. 1295–1301, 2018.
- [26] S. Salardi, M. Porta, G. Maltoni et al., "Ketoacidosis at diagnosis in childhood-onset diabetes and the risk of retinopathy 20years later," *Journal of Diabetes and its Complications*, vol. 30, no. 1, pp. 55–60, 2016.

Research Article

Quantitative Analysis of Retinal Microvascular Perfusion and Novel Biomarkers of the Treatment Response in Diabetic Macular Edema

Young Gun Park¹ and Young-Hoon Park² 

¹Department of Ophthalmology and Visual Science, Seoul St. Mary's Hospital, College of Medicine, The Catholic University of Korea, Seoul, Republic of Korea

²Catholic Institute for Visual Science, College of Medicine, The Catholic University of Korea, Seoul, Republic of Korea

Correspondence should be addressed to Young-Hoon Park; parkyh@catholic.ac.kr

Received 5 August 2020; Revised 27 October 2020; Accepted 2 November 2020; Published 17 November 2020

Academic Editor: Irini Chatziralli

Copyright © 2020 Young Gun Park and Young-Hoon Park. This is an open access article distributed under the Creative Commons Attribution License, which permits unrestricted use, distribution, and reproduction in any medium, provided the original work is properly cited.

Purpose. We aimed to assess the changes of retinal microvascular parameters using optical coherence tomography angiography (OCTA) between diabetic macular edema (DME) and controls. We assessed the changes between the baseline microvascular parameters and final treatment response in patients with DME, initially treated with intravitreal dexamethasone (DEX) implant followed by anti-vascular endothelial growth factor (VEGF) injections on an as-needed basis. **Methods.** This retrospective study included 90 DME patients and 24 healthy control subjects. All subjects had their best-corrected visual acuity (BCVA) and central macular thickness (CMT) measured at baseline and after 12 months. Vessel density (VD) in the superficial capillary plexus (SCP) and deep capillary plexus (DCP) and the deep/superficial flow ratio at baseline were analyzed. A subgroup analysis was used to compare the treatment response. A poor-response group was defined by five or more retreatments at 12 months. **Results.** BCVA and CMT showed a significant improvement at 12 months (all $p < 0.001$). The VD in the whole and parafoveal areas of the DCP was significantly reduced in DME patients compared to that in controls (all $p < 0.05$). The DCP/SCP flow ratio was also significantly reduced in the DME group (1.08 ± 0.03 vs. 1.05 ± 0.02 , $p = 0.001$). In the subgroup analysis, the VD in the foveal and whole DCP areas was significantly lower in the poor-response group than that in the good-response group ($p = 0.043$ and $p = 0.048$, respectively). The DCP/SCP flow ratio was also significantly lower in the poor-response group ($p = 0.011$). **Conclusion.** DME correlated with significant retinal microvascular impairment in the DCP. A decreased DCP/SCP flow ratio was observed in patients with DME that exhibited a poor treatment response. Retinal microvascular parameters could predict the treatment response in DME and help optimize clinical outcomes.

1. Introduction

Diabetic macular edema (DME), macular thickening due to diabetic retinopathy (DR), can present at any stage of this disease. It is caused by a blood-retinal barrier defect that leads to vascular leakage and fluid accumulation [1]. This process is the outcome of the expression of inflammatory factors, including vascular endothelial growth factor (VEGF), intercellular adhesion molecule-1, interleukin-6, and monocyte

chemotactic protein-1, and leukostasis [2, 3]. Because DME can cause vision loss in severe cases, it is becoming an important public health issue [4].

Many different treatment options for DME have been developed, including anti-VEGF agents and corticosteroids [5, 6]. Intravitreal injection of anti-VEGF agents is a standard treatment for DME approved by the United States Food and Drug Administration [5]. However, this treatment poses a heavy financial burden on patients because of the numerous

required injections during the year. On the other hand, intravitreal dexamethasone (DEX) implants (0.7 mg) (Ozurdex, Allergan, Inc., Irvine, CA, USA) consist of a biodegradable copolymer that slowly releases steroids over a period of approximately 4–6 months [7].

Recently, with the increased use of optical coherence tomography (OCT) and OCT angiography (OCTA), several studies have reported various imaging biomarkers and their association with the treatment response in DME [8, 9]. OCTA allows the acquisition of images of the retinal microvasculature with good reproducibility and repeatability in a safe, rapid, and noninvasive manner. However, OCTA studies on the foveal microvascular impairment in DME are limited compared with those using OCT. Previous OCTA studies have only reported on the changes in the foveal avascular zone and the impairment of foveal microcirculation in eyes with DR [10, 11].

Based on these results, we aimed to evaluate the changes in retinal microvascular parameters between DME patients and healthy controls. We assessed the differences between the baseline microvascular parameters and final treatment response in DME patients, initially treated with intravitreal DEX implant followed by anti-VEGF injections on an as-needed basis.

2. Materials and Methods

2.1. Ethical Considerations. All procedures were conducted in accordance with the Declaration of Helsinki and its later amendments. The study was approved by the Ethics Committee of Seoul St. Mary's Hospital and the Catholic University of Korea. The requirement for informed patient consent was waived due to the retrospective design of the study.

2.2. Study Design and Subjects. This study was a retrospective review of consecutive patients who attended the Department of Ophthalmology of Seoul St. Mary's Hospital between January 2017 and January 2019. The study included patients with a diagnosis of diabetes mellitus and DME, who received a DEX implant injection and were followed up for at least 12 months. The healthy control group included healthy patients with no posterior segment abnormalities or systemic comorbidities who attended medical checkups.

The exclusion criteria for patients with DME were as follows: (1) any other ocular disease that may affect ocular circulation (e.g., glaucoma, age-related macular degeneration, and refractive error > 5 diopters); (2) intraocular pressure > 25 mmHg; (3) severe media opacity (e.g., lens opacity due to cataract or thick asteroid hyalosis); (4) macular edema due to any other condition (such as retinal vessel obstruction or macular ischemia); and (5) history of retinal treatment, including laser, intravitreal injections, and other subtenon steroid injections, within 6 months before baseline evaluation.

All patients and controls had their best-corrected visual acuity (BCVA) measured initially and then underwent standardized dilated fundus examinations, including measurements by swept-source OCT and OCTA imaging (DRI OCT Triton; Topcon, Tokyo, Japan). In all patients, reevalua-

tion after treatment was scheduled (as per usual clinical practice) 2 months after DEX implantation or 1 month after intravitreal anti-VEGF agent injection.

2.3. Treatment Protocol. The initial DEX implant (0.7 mg) was injected into the vitreous cavity using standard protocols. After the first DEX implant injection, patients received a second treatment with anti-VEGF agents (Avastin®; Genentech, Inc., San Francisco, CA) on an as-needed basis—pro re nata (PRN) dosing the regimen. The retreatment criterion was defined as central macular thickness (CMT) > 300 μm .

Patients were classified into two groups according to their treatment response: good-response group, comprising patients who received 4 or fewer treatments, and poor-response group, comprising patients who received more than 5 treatments over 12 months from the initial treatment.

2.4. OCT Measurements. Swept-source OCT (DRI OCT Triton; Topcon) is a high-quality fundus imaging technique that relies on active eye tracking. The OCT images were generated using the horizontal OCT cross section (25 lines spaced 240 μm apart). CMT was measured using swept-source OCT (DRI OCT, Topcon, Japan). DME was defined as a CMT > 300 μm .

2.5. OCTA Imaging and Analysis. OCTA was performed using the same device (DRI OCT Triton; Topcon). This device has an A-scan rate of 70,000 scans/s with an 840 nm wavelength light source and a 45 nm bandwidth. Patients with low-quality images (signal strength index < 50) were excluded. OCTA images of the superficial capillary plexus (SCP), deep capillary plexus (DCP), and the choriocapillaris network were generated and segmented automatically by the built-in software (IMAGEnet 6, version 1.25). SCP was delineated by 2.6 μm below the internal limiting membrane to 15.6 μm below the junction, between the inner plexiform and the inner nuclear layers; DCP was delineated by 15.6 μm below the inner plexiform and the inner nuclear layers to 70.2 μm below them. Large intraretinal cysts in DME are often involved in multilayers and lead to inaccurate segmentation errors. For eyes with incorrect segmentation, we manually adjusted the offset value of the inner and outer borders for the DCP so that the DCP slab was segmented from just below the inner plexiform layer to just below the outer plexiform layer. Vessel density was defined as the percentage area occupied by vessels in a circular region centered on the center of the foveal avascular zone. Whole en face, foveal, and parafoveal vessel density of the SCP and DCP within 1 and 3 mm inner and outer circles was measured using computer software. We calculated the flow ratio as the ratio of the vessel density in the DCP to that in the SCP (flow ratio = DCP vessel density/SCP vessel density) and determined the average values [12].

2.6. Statistical Analysis. Shapiro-Wilk test was used to assess the normality of data. A repeated measures ANOVA was used for the determination of the changes in visual acuity and in foveal thickness into the study patients. Unpaired *t*-tests were used for between-group comparisons. Correlations between OCT parameters and the number of

retreatments were assessed using Pearson's correlation test. Univariate and multivariate logistic regression models were used to identify the potential factors associated with retreatment. The receiver operating characteristic (ROC) curve and the area under the curve were used to assess the predictability of the DCP/SCP ratio for good treatment response in DME. p values < 0.05 were considered statistically significant. All analyses were performed using commercial software (SPSS version 22.0; IBM, Armonk, NY, USA).

3. Results

3.1. Patients' Characteristics. In total, 90 eyes of 90 patients (38 women and 52 men) with DME treated with DEX implant injection and 25 eyes of 25 age-matched control subjects were included. The baseline clinical and demographic characteristics of all study subjects are shown in Table 1.

3.2. Clinical and OCT Parameters. The mean BCVA significantly improved from 0.45 ± 0.22 LogMAR at baseline to 0.38 ± 0.15 LogMAR after 12 months of treatment ($p < 0.001$). Moreover, the mean CMT significantly reduced from $508.07 \pm 99.78 \mu\text{m}$ at baseline to $277.04 \pm 65.23 \mu\text{m}$ ($p < 0.001$) after 12 months of treatment. (Figure 1) The average time from intravitreal DEX injection to anti-VEGF was 4.33 ± 1.13 months (range 3-8). The total number of injections was 4.79 ± 1.35 .

3.3. OCTA Parameters. Table 2 shows the SCP and DCP vessel density—whole, foveal, and parafoveal (superior/inferior/nasal/temporal)—in all patients. A statistically significant difference was observed between the DME and control groups in the microvascular parameters (Figure 2). In particular, the retinal vessel density in the whole and parafoveal areas of the DCP was significantly reduced in patients with DME compared with that in controls (all $p < 0.05$). In the SCP, only the whole retinal vessel density was significantly reduced in patients with DME ($p = 0.026$). The DCP/SCP flow ratio was also significantly reduced in the DME group (1.08 ± 0.03 vs. 1.05 ± 0.02 , $p = 0.001$).

3.4. Correlation Analysis. Among the OCTA parameters, the whole area vessel density in the DCP and the DCP/SCP flow ratio correlated significantly with the number of injections received ($p = 0.015$, $r = -0.415$ and $p = 0.025$, $r = -0.336$, respectively).

In the multivariate linear regression analyses for identifying factors related to the number of injections received, only the glycated hemoglobin level among the clinical parameters and the DCP/SCP flow ratio among the OCTA parameters showed a significant association ($\beta = -0.36$, $p = 0.047$ and $\beta = -1.003$, $p = 0.017$, respectively).

3.5. Subgroup Analysis. There were 26 eyes in the good-response group and 64 eyes in the poor-response group. The foveal and whole vessel density in the DCP was significantly lower in the poor-response group than in the good-response group ($p = 0.043$ and $p = 0.048$, respectively) (Figure 1). Moreover, the DCP/SCP flow ratio was significantly lower in the poor-response group ($p = 0.011$)

TABLE 1: Baseline characteristics of the diabetic macular edema study population.

Characteristics	
Age	59.85 \pm 9.04
Sex (M:F)	52:38
DM duration (yr)	13.46 \pm 7.32
HbA1c	7.14 \pm 0.66
DR grade	
Mild	0
Moderate	3
Severe NPDR	48
PDR	39
Hx of photocoagulation	62
No. of treatment-naïve patients	8 (8.9%)
BCVA (LogMAR)	0.45 \pm 0.22
Phakic eyes	33 (37%)
Central macular thickness (μm)	508.07 \pm 99.78

Data are presented as means \pm standard deviation, numbers, or numbers (percentages). DM: diabetes mellitus; HbA1c: glycated hemoglobin; DR: diabetic retinopathy; NPDR: nonproliferative diabetic retinopathy; PDR: proliferative diabetic retinopathy; Hx: history; BCVA: best-corrected visual acuity; LogMAR: logarithm of the minimum angle of resolution.

(Table 3). The ROC curve of the DCP/SCP flow ratio as a biomarker to predict poor treatment response is shown in Figure 3. The area under the curve was 0.702. No significant differences were observed between the two groups in the SCP vessel density and the DCP parafoveal vessel density.

3.6. Side Effects. No injection-related complications were observed. Four eyes developed ocular hypertension and were treated with antihypertensive drops. Two of the phakic eyes (6%) underwent cataract surgery due to the progression of lens opacity.

4. Discussion

In this study, we evaluated the OCTA microvascular parameters after a single intravitreal DEX implant injection followed by anti-VEGF therapy on a PRN basis and investigated their correlation with the number of injections received. DME was associated with significant retinal microvascular impairment in the DCP. There was a significant BCVA improvement and CMT reduction 12 months after the initial treatment. In patients with DME who had poor treatment response, there was a decreased DCP/SCP flow ratio.

We demonstrated that intravitreal DEX implant injection as initial therapy combined with anti-VEGF therapy on a PRN basis is effective for treating DME. In our study, we classified patients in the two response groups based on the number of treatments received. Busch et al. reported the outcomes of continued anti-VEGF therapy compared to switching DEX implant in eyes with DME in a real-world setting. At

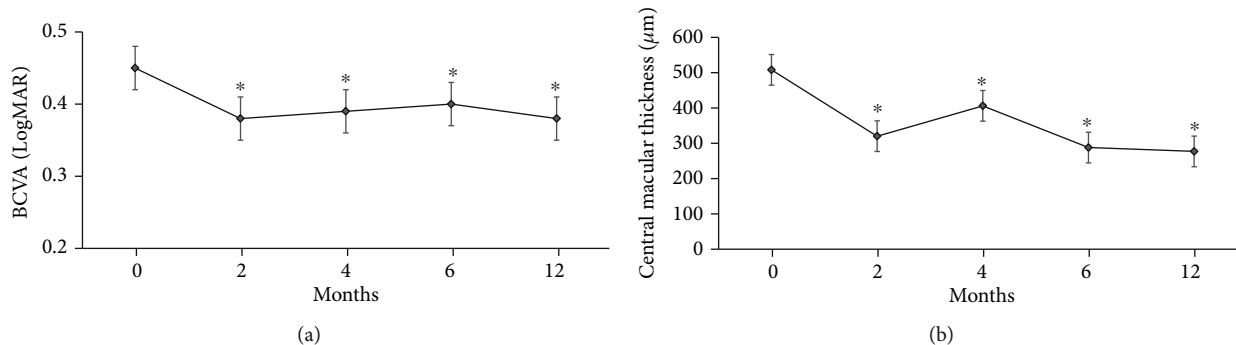


FIGURE 1: (a, b) Best-corrected visual acuity (BCVA) and central macular thickness (CMT) improved significantly compared to baseline during the observation period. * $p < 0.001$; repeated measures ANOVA.

TABLE 2: Vessel density in patients with DME and controls.

Characteristics	DME	Control	p value
<i>Superficial capillary plexus</i>			
Whole vessel density	44.58 \pm 3.19	46.04 \pm 2.29	0.026*
Foveal vessel density	15.34 \pm 5.45	15.23 \pm 3.31	0.583
Parafoveal vessel density			
Superior	46.65 \pm 4.95	48.7 \pm 4.54	0.067
Inferior	45.72 \pm 5.27	47.40 \pm 5.73	0.167
Temporal	44.01 \pm 4.60	45.74 \pm 3.31	0.102
Nasal	41.94 \pm 5.27	43.32 \pm 3.94	0.243
<i>Deep capillary plexus</i>			
Whole vessel density	46.21 \pm 3.01	49.55 \pm 3.01	0.001*
Foveal vessel density	14.46 \pm 5.66	14.50 \pm 2.74	0.389
Parafoveal vessel density			
Superior	48.26 \pm 5.10	52.51 \pm 4.64	0.001*
Inferior	47.33 \pm 4.94	50.86 \pm 5.78	0.01*
Temporal	45.42 \pm 4.17	48.46 \pm 3.81	0.002*
Nasal	43.83 \pm 4.94	46.38 \pm 4.15	0.016*
DCP/SCP ratio	1.05 \pm 0.02	1.08 \pm 0.03	0.001*

Data are presented as means \pm standard deviation. DME: diabetic macular edema; DCP: deep capillary plexus; SCP: superficial capillary plexus.

12 months, mean anti-VEGF injections were 4.2 ± 2.4 except for the 3 loading injections. Therefore, we selected five treatments as the cutoff value [13, 14].

The pathophysiology of DME is complex and multifactorial; currently considered to be a chronic, low-grade inflammatory disorder [15]. It is associated with various vascular, neural, and glial cell components in the retina. Chronic hyperglycemia induces activation of the retinal glial cells that secrete VEGF and proinflammatory cytokines, leading to disruption in the blood-retinal barrier. Two widely used therapeutic strategies are the intravitreal steroid and intravitreal anti-VEGF injections [16–18].

Anti-VEGF agents, including ranibizumab, aflibercept, and bevacizumab, have been widely used for the treatment of DME for decades because of their convenience. However, the frequent injections due to the short duration of effect

and the associated costs may be a heavy burden on the patients. In real-life settings, the treat-and-extend or PRN regimens have become popular as they decrease the treatment burden [18, 19].

DEX implants have demonstrated efficacy in the treatment of persistent DME, resistant to anti-VEGF treatment. Additionally, their effect is longer than that of anti-VEGF agents and six times stronger than that of triamcinolone acetate [20, 21]. Several studies have reported on the use of intravitreal DEX as initial therapy in patients with DME [22–24].

In the present study, we compared the degree of microvascular damage in relation to the treatment response and the DCP/SCP flow ratio was found to represent a response index. The vessel density in the whole area in the DCP and the DCP/SCP flow ratio correlated significantly with the number of injections. Furthermore, the DCP/SCP flow ratio was the only OCTA parameter significantly related to the number of injections in the multivariate linear regression analyses. Considering that the vessel density in OCTA demonstrates personal variations, the DCP/SCP flow ratio is remarkable. Yeung et al. reported that the DCP/SCP flow ratio in patients with branch retinal vein occlusion was associated with the treatment response ($p = 0.015$) and suggested that this ratio can represent the relative damage of the DCP to that of the SCP in BRVO [12]. We wondered that the hypothesis that the capillary loss in the DCP is more prominent than that in the SCP in DR may be relatively acceptable. Instead of absolute values in the individual layer of the capillary plexus, the ratio of the vessel density in the DCP to that in the SCP may be more meaningful.

In a previous study, Moon et al. reported that the DCP loss was more prominent in DME eyes than in non-DME eyes [25, 26]. This trend was observed in anti-VEGF nonresponders compared with anti-VEGF responders. Altered vessel density in the DCP may imply a preference for this part of the retinal vascular system in the pathogenesis of DR or DME, as retinal venules originate from the deep retinal vascular layers. The earlier alterations in the deep vascular layer probably demonstrate retinal venular widening, damage to the capillary endings, and microaneurysms. It may also influence the breakdown of the blood-retinal barrier and the presence of DME [27–29].

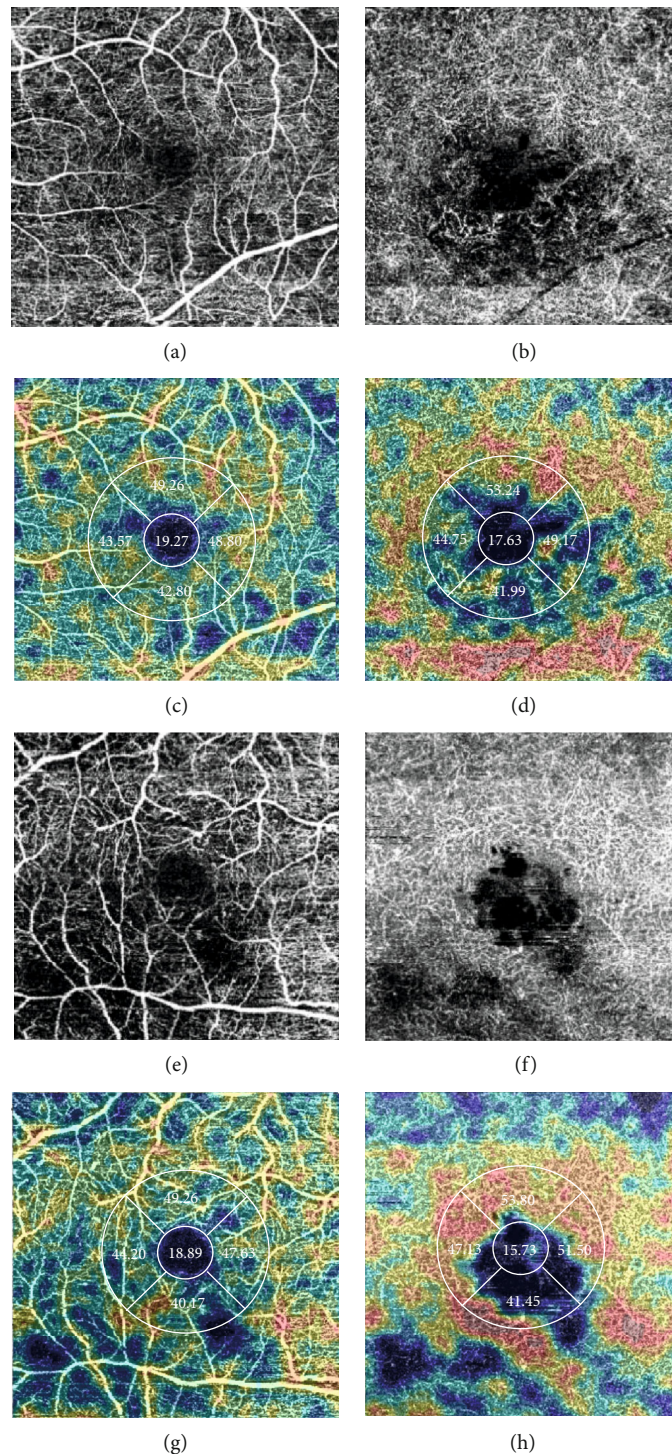


FIGURE 2: Representative samples of the microvascular parameters relative to the treatment response: (a–d) the parafoveal vessel density in the SCP and DCP (good-response group); (e–h) the parafoveal vessel density in the SCP and DCP (poor-response group).

In addition, we compared the two groups based on the number of treatment injections. The foveal and whole vessel density in the DCP and the DCP/SCP flow ratio were significantly lower in the poor-response group than in the good-response group. The underlying mechanism of the association between the low vessel density in the DCP and treatment inefficacy remains to be clearly defined. One possibility is excessive fluid flux from the

vessels to the tissue because of the breakdown of the blood-retinal barrier caused by damage to the capillary endothelial tight junctions or various inflammatory cytokines [30, 31]. The other suggestion is that the DCP might play a part in the removal of excess fluid from the retina. The smaller vessel density in the DCP could lead to fluid accumulation in the retina and would reduce fluid absorption [32, 33].

TABLE 3: Clinical characteristics according to the DME treatment response.

Characteristics	Good-response group	Poor-response group	<i>p</i> value
Superficial capillary plexus			
Whole vessel density	44.80 ± 2.71	44.49 ± 3.34	0.41
Foveal vessel density	13.76 ± 4.81	15.98 ± 5.52	0.063
Parafoveal vessel density			
Superior	47.74 ± 5.23	46.2 ± 4.73	0.219
Inferior	45.99 ± 4.62	45.61 ± 5.47	0.725
Temporal	42.91 ± 4.42	44.46 ± 4.56	0.192
Nasal	42.58 ± 3.23	41.67 ± 5.13	0.51
Deep capillary plexus			
Whole vessel density	47.13 ± 2.12	45.83 ± 3.20	0.043*
Foveal vessel density	13.08 ± 5.39	15.03 ± 5.62	0.048*
Parafoveal vessel density			
Superior	49.5 ± 4.95	47.66 ± 5.01	0.094
Inferior	48.44 ± 4.41	46.87 ± 5.72	0.31
Temporal	44.89 ± 3.85	45.64 ± 4.24	0.504
Nasal	45.45 ± 3.35	43.17 ± 5.28	0.081
DCP/SCP ratio	1.05 ± 0.02	1.02 ± 0.03	0.011*
Number of injections	3.46 ± 0.49	5.47 ± 0.9	0.03*

Data are presented as means ± standard deviation. DME: diabetic macular edema; DCP: deep capillary plexus; SCP: superficial capillary plexus.

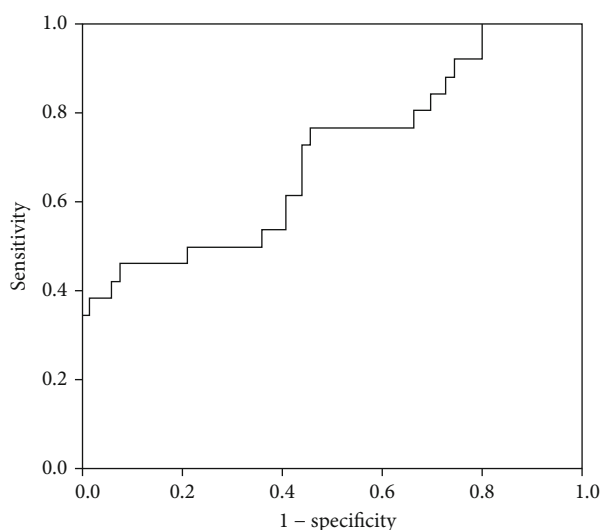


FIGURE 3: The ROC curve of the DCP/SCP flow ratio for predicting the treatment response. The area under the ROC curve was 0.703. ROC: receiver operating characteristics; DCP: deep capillary plexus; SCP: superficial capillary plexus.

To reduce ineffective repeated injections, it is important to screen for treatment-resistant DME in baseline examinations [14, 34]. However, it is difficult to directly compare the result of various treatment regimens. Ebnetter et al. reported a comparison between a PRN and a treat-and-extend regimen in managing DME with intravitreal ranibizumab [35]. The mean number of injections was significantly different between the groups (PRN group: 5.9 ± 1.8 ;

treat-and-extend group: 8.9 ± 2.0 ; $p < 0.001$). The VA of both groups showed similar gains (8.3 ± 6.7 vs. 9.3 ± 8.9 , $p = 0.3$). In considering the duration of DEX implants, the number of retreatments in our study is not inferior to these results (3.46 ± 0.49 vs. 5.47 ± 0.9).

The most remarkable finding in our study was that the number of retreatments was related to the DCP/SCP flow ratio. Although several studies have evaluated the hard exudate or the microstructure with OCT to identify variables predicting the treatment response, we focused on the retinal microvascular changes evaluated with OCTA at baseline. In general, retinal vessel density was significantly reduced in patients with DME compared with that in controls. Compared with the SCP, vessel density rarefaction was prominent in the DCP, with the telangiectatic appearance of the retinal vessels. If the damage in the DCP is more severe than that in the SCP (in other words, considering the DCP/SCP ratio), the treatment response may be poor. Further studies are needed to identify predictors of the response to DME therapies and determine individualized therapeutic strategies according to the patients' features.

Our study has several limitations. First, the limited number of evaluated eyes led to low statistical power. Second, a selection bias may exist due to the retrospective study design. Third, most patients had a previous history of treatment and it may affect the outcomes. Fourth, the OCTA image artifacts can interfere with an accurate assessment of the actual status of the retinal microvasculatures. Projection artifacts might affect the visualization of the deep layer, and bias of segmentation error in cystoid macular edema may occur despite our best efforts to minimize such an effect. Last, it will be useful to observe the OCTA parameter changes, before and after the

12-month treatment. However, it is difficult to consistently examine OCTA during follow-up periods in real-life practice. Regardless, this report provides a framework for further research.

5. Conclusions

The results of our study suggested that the OCTA retinal microvascular parameters at baseline influence the treatment outcomes in DME. Furthermore, decreased DCP/SCP flow ratio was observed in patients with DME who manifested poor treatment response. These parameters could represent predictors of the treatment response and would help to optimize the clinical outcomes.

Data Availability

The data used to support the findings of this study are available from the corresponding author upon request.

Conflicts of Interest

The authors have no conflict of interest with regard to this manuscript.

Acknowledgments

The authors wish to acknowledge the financial support of the Catholic Medical Center Research Foundation made in the program year of 2019.

References

- [1] N. Bhagat, R. A. Grigorian, A. Tutela, and M. A. Zarbin, "Diabetic macular edema: pathogenesis and treatment," *Survey of Ophthalmology*, vol. 54, no. 1, pp. 1–32, 2009.
- [2] H. Funatsu, H. Noma, T. Mimura, S. Eguchi, and S. Hori, "Association of vitreous inflammatory factors with diabetic macular edema," *Ophthalmology*, vol. 116, no. 1, pp. 73–79, 2009.
- [3] P. Brito, J. Costa, N. Gomes, S. Costa, J. Correia-Pinto, and R. Silva, "Serological inflammatory factors as biomarkers for anatomic response in diabetic macular edema treated with anti-VEGF," *Journal of Diabetes and its Complications*, vol. 32, no. 7, pp. 643–649, 2018.
- [4] D. A. Antonetti, R. Klein, and T. W. Gardner, "Diabetic retinopathy," *The New England Journal of Medicine*, vol. 366, no. 13, pp. 1227–1239, 2012.
- [5] L. Zhang, W. Wang, Y. Gao, J. Lan, and L. Xie, "The Efficacy and Safety of Current Treatments in Diabetic Macular Edema: A Systematic Review and Network Meta-Analysis," *PLOS ONE*, vol. 11, no. 7, p. e0159553, 2016.
- [6] U. Schmidt-Erfurth, J. Garcia-Arumi, F. Bandello et al., "Guidelines for the management of diabetic macular edema by the European Society of Retina Specialists (EURETINA)," *Ophthalmologica*, vol. 237, no. 4, pp. 185–222, 2017.
- [7] Y. He, X.-j. Ren, B.-j. Hu, W.-C. Lam, and X.-r. Li, "A meta-analysis of the effect of a dexamethasone intravitreal implant versus intravitreal anti-vascular endothelial growth factor treatment for diabetic macular edema," *BMC Ophthalmology*, vol. 18, no. 1, p. 121, 2018.
- [8] G. Jian, X. Y. Jing, L. Yang, and L. Lun, "Quantitative Analysis of Foveal Microvascular Differences in Diabetic Macular Edema with and without Subfoveal Neuroretinal Detachment," *Journal Diabetes Research*, vol. 2020, article 2582690, pp. 1–7, 2020.
- [9] S. Vujosevic, C. Toma, E. Villani et al., "Diabetic macular edema with neuroretinal detachment: OCT and OCT-angiography biomarkers of treatment response to anti-VEGF and steroids," *Acta Diabetologica*, vol. 57, no. 3, pp. 287–296, 2020.
- [10] F. J. Freiberg, M. Pfau, J. Wons, M. A. Wirth, M. D. Becker, and S. Michels, "Optical coherence tomography angiography of the foveal avascular zone in diabetic retinopathy," *Graefes Archive for Clinical and Experimental Ophthalmology*, vol. 254, no. 6, pp. 1051–1058, 2016.
- [11] L. Liu, Jian Gao, W. Bao et al., "Analysis of Foveal Microvascular Abnormalities in Diabetic Retinopathy Using Optical Coherence Tomography Angiography with Projection Artifact Removal," *Journal of Ophthalmology*, vol. 2018, Article ID 3926745, 9 pages, 2018.
- [12] L. Yeung, W. C. Wu, L. H. Chuang, N. K. Wang, and C. C. Lai, "Novel optical coherence tomography angiography biomarker in branch retinal vein occlusion macular edema," *Retina*, vol. 39, no. 10, pp. 1906–1916, 2019.
- [13] C. Busch, for the International Retina Group, S. Fraser-Bell et al., "Real-world outcomes of non-responding diabetic macular edema treated with continued anti-VEGF therapy versus early switch to dexamethasone implant: 2-year results," *Acta Diabetologica*, vol. 56, no. 12, pp. 1341–1350, 2019.
- [14] C. Busch, For the International Retina Group, D. Zur et al., "Shall we stay, or shall we switch? Continued anti-VEGF therapy versus early switch to dexamethasone implant in refractory diabetic macular edema," *Acta Diabetologica*, vol. 55, no. 8, pp. 789–796, 2018.
- [15] N. Cheung, P. Mitchell, and T. Y. Wong, "Diabetic retinopathy," *Lancet*, vol. 376, no. 9735, pp. 124–136, 2010.
- [16] D. V. Do, Q. D. Nguyen, A. A. Khwaja et al., "Ranibizumab for Edema of the Macula in Diabetes Study," *JAMA Ophthalmology*, vol. 131, no. 2, pp. 139–145, 2013.
- [17] U. Schmidt-Erfurth, G. E. Lang, F. G. Holz et al., "Three-year outcomes of individualized ranibizumab treatment in patients with diabetic macular edema: the RESTORE extension study," *Ophthalmology*, vol. 121, no. 5, pp. 1045–1053, 2014.
- [18] C. Prunte, F. Fajnkuchen, S. Mahmood et al., "Ranibizumab 0.5 mg treat-and-extend regimen for diabetic macular oedema: the RETAIN study," *British Journal of Ophthalmology*, vol. 100, no. 6, pp. 787–795, 2016.
- [19] Y. J. Sepah, M. A. Sadiq, D. Boyer et al., "Twenty-four-month outcomes of the ranibizumab for edema of the macula in diabetes - protocol 3 with high dose (READ-3) study," *Ophthalmology*, vol. 123, no. 12, pp. 2581–2587, 2016.
- [20] D. S. Boyer, Y. H. Yoon, Belfort R Jr et al., "Three-year, randomized, sham-controlled trial of dexamethasone intravitreal implant in patients with diabetic macular edema," *Ophthalmology*, vol. 121, no. 10, pp. 1904–1914, 2014.
- [21] D. Zur, M. Igllicki, and A. Loewenstein, "The role of steroids in the management of diabetic macular edema," *Ophthalmic Research*, vol. 62, no. 4, pp. 231–236, 2019.
- [22] S. K. Mahapatra and S. Kumari, "Long-term results of a single injection of intravitreal dexamethasone as initial therapy in

- diabetic macular edema,” *Indian Journal of Ophthalmology*, vol. 68, no. 3, pp. 490–493, 2020.
- [23] G. W. Blankenship, “Evaluation of a single intravitreal injection of dexamethasone phosphate in vitrectomy surgery for diabetic retinopathy complications,” *Graefe’s Archive for Clinical and Experimental Ophthalmology*, vol. 229, no. 1, pp. 62–65, 1991.
- [24] M. Igllicki, C. Busch, D. Zur et al., “Dexamethasone implant for diabetic macular edema in naive compared with refractory eyes,” *Retina*, vol. 39, no. 1, pp. 44–51, 2019.
- [25] S. A. Agemy, N. K. Sripsema, C. M. Shah et al., “Retinal vascular perfusion density mapping using optical coherence tomography angiography in normals and diabetic retinopathy patients,” *Retina*, vol. 35, no. 11, pp. 2353–2363, 2015.
- [26] B. G. Moon, T. Um, J. Lee, and Y. H. Yoon, “Correlation between deep capillary plexus perfusion and long-term photoreceptor recovery after diabetic macular edema treatment,” *Ophthalmol Retina*, vol. 2, no. 3, pp. 235–243, 2018.
- [27] K. Sambhav, K. K. Abu-Amero, and K. V. Chalam, “Deep capillary macular perfusion indices obtained with OCT angiography correlate with degree of nonproliferative diabetic retinopathy,” *European Journal of Ophthalmology*, vol. 27, no. 6, pp. 716–729, 2017.
- [28] R. F. Spaide, “Retinal vascular cystoid macular edema: review and new theory,” *Retina*, vol. 36, no. 10, pp. 1823–1842, 2016.
- [29] T. Mathis, T. Lereuil, A. Abukashabah et al., “Long-term follow-up of diabetic macular edema treated with dexamethasone implant: a real-life study,” *Acta Diabetologica*, vol. 57, no. 12, pp. 1413–1421, 2020.
- [30] J. K. Sun, M. M. Lin, J. Lammer et al., “Disorganization of the retinal inner layers as a predictor of visual acuity in eyes with center-involved diabetic macular edema,” *JAMA Ophthalmol*, vol. 132, no. 11, pp. 1309–1316, 2014.
- [31] A. Das, P. G. McGuire, and S. Rangasamy, “Diabetic macular edema: pathophysiology and novel therapeutic targets,” *Ophthalmology*, vol. 122, no. 7, pp. 1375–1394, 2015.
- [32] A. Couturier, V. Mané, S. Bonnin et al., “CAPILLARY PLEXUS ANOMALIES IN DIABETIC RETINOPATHY ON OPTICAL COHERENCE TOMOGRAPHY ANGIOGRAPHY,” *Retina*, vol. 35, no. 11, pp. 2384–2391, 2015.
- [33] R. Lazic, M. Lukic, I. Boras et al., “Treatment of anti-vascular endothelial growth factor-resistant diabetic macular edema with dexamethasone intravitreal implant,” *Retina*, vol. 34, no. 4, pp. 719–724, 2014.
- [34] G. Demir, A. Ozkaya, E. Yuksel et al., “Early and late switch from ranibizumab to an Intravitreal dexamethasone implant in patients with diabetic macular edema in the event of a poor anatomical response,” *Clinical Drug Investigation*, vol. 40, no. 2, pp. 119–128, 2020.
- [35] A. Ebnetter, D. Waldmeier, D. C. Zysset-Burri, S. Wolf, and M. S. Zinkernagel, “Comparison of two individualized treatment regimens with ranibizumab for diabetic macular edema,” *Graefe’s Archive for Clinical and Experimental Ophthalmology*, vol. 255, no. 3, pp. 549–555, 2017.

Review Article

The Role of SGLT2 Inhibitor on the Treatment of Diabetic Retinopathy

Wenjun Sha,¹ Song Wen,² Lin Chen,¹ Bilin Xu,¹ Tao Lei ¹ and Ligang Zhou ²

¹Department of Endocrinology and Metabolism, Putuo Hospital, Shanghai University of Traditional Chinese Medicine, Shanghai 200062, China

²Department of Endocrinology, Shanghai Pudong Hospital, Fudan University, Shanghai 201399, China

Correspondence should be addressed to Tao Lei; leitao5899@126.com and Ligang Zhou; zhouligang@yahoo.com

Received 6 August 2020; Revised 16 October 2020; Accepted 23 October 2020; Published 12 November 2020

Academic Editor: Dominika Pohlmann

Copyright © 2020 Wenjun Sha et al. This is an open access article distributed under the Creative Commons Attribution License, which permits unrestricted use, distribution, and reproduction in any medium, provided the original work is properly cited.

Diabetic retinopathy (DR) is one of the most serious complications of diabetic microangiopathy. DR has an early onset and is not easy to detect. When visual impairment occurs, the optimal period for therapy is often missed. Therefore, the prevention and treatment of DR should start from the early stage of diabetes. Sodium-dependent glucose transporter 2 inhibitor (SGLT2i) is a new antidiabetic drug which is mainly used in clinical practice to control blood glucose of patients with type 2 diabetes prone to develop chronic heart failure. Recent studies have found that SGLT2 is also expressed in the human retina. Now, the prevention and treatment of diabetic retinopathy with SGLT2i while reducing blood sugar has become a new research field. Hence, this article reviewed the recent therapeutic and research progress of SGLT2 in the treatment of diabetic retinopathy.

1. Introduction

Diabetes is a group of metabolic diseases characterized by hyperglycemia and microvascular and macrovascular complications caused by insulin secretion defect and/or its biological function disorder [1–3]. According to the International Diabetes Federation (IDF), there were 425 million people with diabetes aged 20–79 worldwide in 2017, and the number will increase to 629 million at the middle of this century [4]. Diabetic retinopathy (DR) is one of the most common and serious microvascular complications in diabetes. Studies demonstrate that the incidence of DR increases with the course of diabetes.

An epidemiological survey in 2011 showed that the incidence of DR is about 25% of 5 years after the diagnosis of diabetes, 60% after 10 years of it, and up to 75%~80% after 15 years of it [5]. At the same time, DR is also the main cause of visual impairment and irreversible blindness in middle-aged and elderly people. According to the data published by the World Health Organization in 2002, DR worldwide caused about 4.8% of the 37 million cases of blindness [6].

2. The Classification of Diabetic Retinopathy

The classification of DR development is related to the abnormalities of retinal microvascular system, including increased blood retinal barrier permeability, decreased vascular endothelial cells and pericytes, thickened vascular basement membrane, capillary occlusion, retinal neurons, and glial abnormalities. Therefore, DR is currently divided into non-proliferative diabetic retinopathy (NPDR) and proliferative diabetic retinopathy (PDR).

2.1. Nonproliferative Diabetic Retinopathy (NPDR). Nonproliferative diabetic retinopathy (NPDR) occurs in the early stage of DR. The main pathophysiological basis is high glucose-induced retinal degeneration, including loss of capillary pericytes, thickening of the basement membrane, thinning of the blood vessel layer and destruction of the blood-retinal barrier, changes in the broken line leading to retinal hemorrhage and arteriole tumors, and microvascular abnormalities in the retina and cotton wool spots (fluffy white plaques on the retina caused by local swelling of the

retinal nerve fiber layer) [7]. However, in the NPDR stage, patients are usually asymptomatic and have normal vision. When visual impairment occurs, the best period of treatment is often missed [8]. Therefore, it is necessary to prevent the occurrence of DR in the early stage of diabetes.

2.2. Proliferative Diabetic Retinopathy (PDR). Studies have found that the prevalence of PDR is close to 50% after 25 years of diabetes diagnosis, and most patients with type 1 diabetes (T1DM) will develop PDR after about 10 years [9]. At the PDR stage, the new blood vessels in the eye are continuously generated and often accompanied by the oozing and hyperplasia of the eye tissue, which can destroy the normal structure and function of the eye and ultimately lead to the visual impairment of the patient [10]. Compared with NPDR, PDR is more harmful to eyesight and could cause severe vision loss or even complete blindness.

3. The Mechanism for Diabetic Retinopathy

The pathogenesis of DR is complex, and the mechanism has not yet been fully elucidated. The pathological mechanism hypotheses currently proposed mainly include the theory of chronic inflammation, retinal hemodynamic changes, oxidative stress, gene polymorphism, and neurodegenerative changes (Figure 1).

3.1. Inflammation. Chronic hyperglycemia leads to oxidative damage of retinal capillary wall and vascular occlusion by activating various metabolic pathways. In the early stage of hyperglycemia, transcription factors are activated to elevate proinflammatory factors, triggering the activation of microglia cells and resulting in low-grade inflammation on the retina [11]. Secondly, the increase of icAM-1 expression in retinal endothelial cells and the accumulation of white blood cells around the retinal capillary walls will cause the retina to produce low-grade inflammation through the release of cytokines, chemokines, proinflammatory factors, and proangiogenic growth factors [12].

This low-grade inflammation destroys the tight junctions between endothelial cells by pericyte injury [13], increasing the permeability of blood vessels, exuding serum and weakening the vascular wall barrier, destroying the retinal blood barrier (BRB), and causing edema in the retina. Because of edema, the extracellular hydrostatic pressure increases, causing the capillary network to collapse and increase occlusion, leading to increased retinal ischemia, glycosylation, thickening of the endothelial basement membrane, development of vascular malformations, and formation of microaneurysms [11].

3.2. Oxidative Stress and Free Radicals. There are a large number of polyunsaturated fatty acids on the retina, which makes it particularly sensitive to oxidative stress [14]. In the process of glucose oxidation, nonenzymatic saccharification of proteins occurs and reactive oxygen species (ROS) is produced. Hyperglycemia leads to an increase in the synthesis of ROS in the retina, which acts as a coiniciating factor to activate four classical molecular pathways [15], namely, abnormal polyol pathway, inositol metabolism pathway, accumulation of protein nonenzymatic glycosylation end

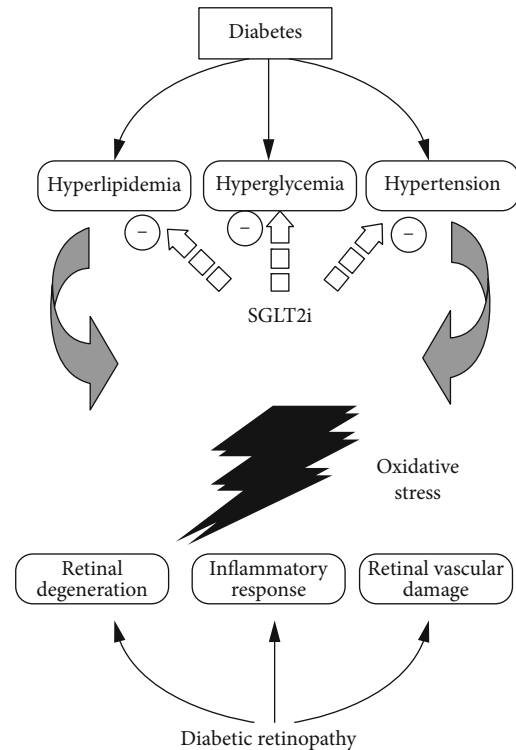


FIGURE 1: The proposed mechanism of SGLT2 inhibitor (SGLT2i) against diabetic retinopathy, in which SGLT2i improves hyperlipidemia, hyperglycemia, and hypertension.

products [16], and protein kinase C (PKC) activates [17] and acts on the angiotensin-converting enzyme system [18]. The activation of each pathway further promotes the generation of ROS with positive feedback, which enhances oxidation and damages the blood-retinal barrier structure, which ultimately leads to the occurrence of DR.

4. The Treatment of New Diabetic Drug SGLT2 Inhibitor on the DR Treatment

In 1835, Petersen extracted Phlorizin, the nonselective sodium-dependent glucose transporters (SGLT) inhibitor from apple roots [19]. In further animal models, it was found to increase urine glucose excretion and reduce hyperglycemia. However, Phlorizin is prone to cause adverse reactions of the digestive tract and has low utilization efficiency, so it is not used in the treatment of diabetes [20]. Modern studies have found that SGLT2 belongs to the superfamily of sodium-glucose cotransporters. It is a low-affinity, high-efficiency transporter. It is not only distributed in the proximal convoluted tubules S1 and S2 in the kidney but also in the lens and the retina [21]. SGLT2 provides protection for the subtle nutrient metabolism of the eye [22]. Based on this, sodium-glucose transport synergistic protein 2 inhibitor (SGLT2i) is independent of hypoglycemic effect and also has DR protective effect.

4.1. Improvement of Factors of Diabetic Pathogenesis. There are many risk factors affecting the occurrence of DR,

including poor blood sugar control, hypertension, and hyperlipidemia. Improving these influence factors can effectively delay the progress of DR [23].

4.1.1. Control of Hyperglycemia. It is known that the microvascular complications of type 2 diabetes (T2DM) are related to hyperglycemia. UKPDS has shown that a 1% reduction in HbA1c can reduce the risk of microvascular complications by 37% [24]. For every 1 mmol/L decrease in blood glucose level, the risk of DR will decrease by 21% [25]. In the “Diagnostic Standards for Diabetes Medicine” issued by the American Diabetes Association (ADA) in 2020, the new hypoglycemic drug SGLT2i is recommended as a first-line drug in the patients with chronic heart failure. In the first week of treatment, it can reduce fasting blood glucose by about 1.5 mmol/L and effectively reduce HbA1c by about 1.5%, which is equivalent to the efficacy of metformin 2000 mg per day. Due to its multiple benefits in addition to hypoglycemic effect, SGLT2i could also be administrated in appropriate diabetic patients [26].

4.1.2. Control of Hypertension. In T2DM patients with hypertension, strict control of blood pressure can delay the progression of DR and the deterioration of visual acuity [27]. Studies have confirmed that for every 10 mmHg drop in systolic blood pressure (SBP), the risk of diabetic microvascular complications can be reduced by 13%, and strict blood pressure control can reduce the risk of blindness in DR by 47% [28]. Elevated 24-hour SBP is independently associated with higher wall-to-lumen ratio (WLR) in retinal arterioles [29]. A clinical study involving 311 centers in 16 countries has confirmed that SGLT2i has a significant antihypertensive effect, which can reduce SBP by 11.9 mmHg on average. SGLT2i combined with other common hypertension drugs can achieve more satisfactory antihypertensive effect [30]. At present, some scholars believe that the antihypertensive mechanism of SGLT2i should be related to the osmotic diuresis caused by glucose excretion [31]. Some other scholars also believe that its antihypertensive effect is related to the inhibitory effect on the renin-angiotensin-aldosterone system when promoting urine excretion. Dapagliflozin improves muscle insulin sensitivity but enhances endogenous glucose production [32, 33]. Clinical studies found that BP parameters were lower than baseline 6 weeks after Dapagliflozin treatment. Therefore, Dapagliflozin may prevent retinal wall remodeling by lowering BP [34].

4.1.3. Control of Hyperlipidemia. Dyslipidemia also promotes the development of DR. The hard exudation of DR is the exudate of lipid and protein that occurs in the plexiform layer of the retina. It has been found that the severity of hard exudation of DR is positively correlated with triglyceride (TG), low-density lipoprotein (LDL), and total cholesterol (TC) levels and negatively correlated with high-density lipoprotein (HDL) levels [35]. Blood lipid control can improve the function of retinal vascular endothelial cells, reduce inflammation and leakage of fundus microvessels, and thus delay the development of DR [36]. The effect of SGLT2i on blood lipids is multifold. It can be observed that total cholesterol increa-

se/no change, triacylglycerol decrease/no change, and LDL-C and high-density lipoprotein cholesterol (HDL-C) increase by 5%~10%, but LDL-C/HDL-C ratio is not affected [37]. In addition, small and dense LDL-C was reduced by 20%~30% after SGLT2i treatment [38].

4.2. Protection of Blood-Retinal Barrier. DR is characterized by the destruction of the blood-retinal barrier (BRB) and leakage of retinal vascular. Normal retina has two layers, an inner and outer BRB. There are two types of BRBs in the normal retina. The inner barrier is composed of zonula occludens between retinal capillary endothelial cells and pericytes; and the outer barrier is composed of retinal pigment epithelium (RPE) layer and the small closed zone between them. Hyperglycemia, ischemia, hypoxia, oxidative stress, inflammation, and inflammatory factors are the main predisposing factors for the destruction of BRB caused by diabetes [39]. The destruction of the inner BRB caused by DR is the main cause of vascular leakage.

SGLT2 acts as a glucose sensor in the retinal microvasculature. Excessive entry of Na⁺-dependent glucose can cause intracellular swelling of pericytes [40] and lead to loss of contractile function, death of pericytes, and overperfusion of the retina. The overexpression of the extracellular matrix (such as fibronectin, collagen IV, and laminin) is associated with the thickening of the basement membrane, subsequent microvascular occlusion, and insufficient retinal perfusion [41]. This change in retinal hemodynamics can lead to multiple downstream triggers of DR. SGLT2 inhibitors have been shown to reduce pericyte swelling and extracellular matrix overexpression [42]. Early suppression of hemodynamic changes in DR is of great significance for the development of effective DR treatments [43].

Takakura and others have shown the effect of iplegliflozin on the diabetic retina of spontaneously diabetic Torii obese rats. In this study, diabetic rats treated with iplegliflozin showed a decrease in the oscillating potential on the electroretinogram, the outer nuclear layer of the neural retina was irregular, and iplegliflozin inhibited the progression of lens cataract formation [44].

4.3. Protection of the Fundus Capillaries. Arteriole remodeling is a factor leading to the progression of diabetic retinopathy [45]. In PDR, the basement membrane of retinal capillaries thickens, pericytes gradually disappear, microangiomas form, endothelial cells proliferate, luminal occlusion, and finally new blood vessels form. Many increases in WLR and cross-sectional area are characteristic of vascular hypertrophy [46]. Multiple clinical and animal studies have shown that the occurrence and development of DR are related to the increase of WLR and cross-sectional area of arteriolar walls. Grunwald et al. found that in patients with type 1 diabetes and background retinopathy with poor blood glucose control, retinal total volume blood flow was 23% higher than normal [47]. Patel et al. found that compared with patients without diabetes, diabetic patients with signs of diabetic retinopathy had higher blood flow and larger blood vessel diameter [48]. This increased blood flow may cause vascular damage by

increasing shear stress, leading to endothelial dysfunction, basement membrane disruption, and extracellular matrix remodeling [49].

A prospective, single-center, placebo-controlled, double-blind, randomised crossover phase IIIb study evaluated the effects of dapagliflozin on the retinal microvasculature, showing that compared with the placebo group, dagrazine treatment group did not increase the retinal wall-cavity ratio and reduced retinal capillary flow, suggesting that dagrazine could prevent vascular hyperemia [50]. In addition, the treatment seemed to prevent structural changes in retinal arterioles. This may be due in part to the drug's ability to reduce glucose resulting in reduced blood flow, reduced subcutaneous fibrin deposition, altered smooth muscle cells, and prevented arteriolar wall thickening [51].

4.4. Protection of the Optic Nerve. The optic nerve is a special somatosensory nerve, which is very sensitive to ischemia and hypoxia. The optic nerve is made up of ganglion cell axons. The surface of its nerve fibers has only myelin sheath and no nerve membrane. Once it undergoes apoptosis, it is difficult to regenerate. The progressive apoptosis of optic nerve cells is the main cause of irreversible damage to visual function. There are roughly three most important mechanisms for neurodegeneration in patients with DR: accumulation of extracellular glutamate, oxidative stress, and reduction of neuroprotective factors synthesized by the retina [52].

Recent findings indicate that there is a correlation between SGLT2 expression and the sympathetic nervous system. Hyperfunction of the sympathetic nervous system (SNS) is a feature of obesity and T2DM [53]. We showed for the first time that norepinephrine, the main neurotransmitter of SNS, upregulates the expression of SGLT2 protein in human proximal renal tubular cells [54]. In addition, high-fat diet-fed mice treated with dapagliflozin showed decreased tissue norepinephrine content and tyrosine hydroxylase expression in both heart and kidney tissues, indicating SGLT2 inhibitors in our animal model. It has significant sympathetic inhibition [55]. So far, limited studies have studied the autonomic nervous system associated with DR, and these studies have shown that DR is associated with early autonomic dysfunction in patients with T1D and T2D [56]. The balance between sympathetic and parasympathetic effects determines the normal function of the autonomic nervous system. We have generated new data highlighting that in a mouse model of neuropathic hypertension with substantially activated SNS, nerve damage in the outer layer of the retina is obvious, which is DR. Therefore, SGLT2i may also reduce harmful retinal changes that may be supported by SNS overactivation.

To sum up, SGLT2i has been widely used in the clinical treatment of diabetes. However, the data on their efficacy in diabetic complications, especially in the treatment of DR, were mainly derived from animal experiments. These animal experimental data and conclusions allow us to see the great clinical application potential of SGLT2i in the treatment of DR. It is believed that with more clinical studies on SGLT2i, clinical data on the efficacy of DR will be more abundant.

Conflicts of Interest

The authors declare no conflict of interest.

Authors' Contributions

Wenjun Sha and Song Wen contributed equally to this work.

Acknowledgments

This work was supported by the National Natural Science Foundation of China (81774083, 81704027, and 81370932), Key Subject Construction Project of Shanghai Municipal Health and Family Planning Commission (ZK2019B16), Special Department Fund of the Pudong New Area Health Planning Commission (WZzk2017-03), Integrative Medicine Special Fund of Shanghai Municipal Health Planning Committee (ZHYY-ZXYJHZX-2-201712), Shanghai Municipal Health and Family Planning Commission (201840345), Outstanding Leaders Training Program of Pudong Health Bureau of Shanghai (PWRI2014-06), Outstanding Clinical Discipline Project of Shanghai Pudong (PWYgy-2018-08), Natural Science Foundation of China (21675034), and Shanghai Natural Science Foundation (19ZR1447500).

References

- [1] American Diabetes Association, "2. Classification and diagnosis of diabetes: standards of medical care in diabetes-2019," *Diabetes Care*, vol. 42, Supplement 1, pp. S13–s28, 2019.
- [2] M. Gong, S. Wen, T. Nguyen, C. Wang, J. Jin, and L. Zhou, "Converging relationships of obesity and hyperuricemia with special reference to metabolic disorders and plausible therapeutic implications," *Diabetes, Metabolic Syndrome and Obesity: Targets and Therapy*, vol. 13, pp. 943–962, 2020.
- [3] S. Wen, C. Wang, M. Gong, and L. Zhou, "An overview of energy and metabolic regulation," *Science China Life Sciences*, vol. 62, no. 6, pp. 771–790, 2019.
- [4] T. Y. Wong and C. Sabanayagam, "The war on diabetic retinopathy," *Asia-Pacific Journal of Ophthalmology*, vol. 8, no. 6, pp. 448–456, 2019.
- [5] G. P. Giuliari, "Diabetic retinopathy: current and new treatment options," *Current Diabetes Reviews*, vol. 8, no. 1, pp. 32–41, 2012.
- [6] D. S. W. Ting, G. C. M. Cheung, and T. Y. Wong, "Diabetic retinopathy: global prevalence, major risk factors, screening practices and public health challenges: a review," *Clinical & Experimental Ophthalmology*, vol. 44, no. 4, pp. 260–277, 2016.
- [7] R. P. Homme, M. Singh, A. Majumder et al., "Remodeling of retinal architecture in diabetic retinopathy: disruption of ocular physiology and visual functions by inflammatory gene products and pyroptosis," *Frontiers in Physiology*, vol. 9, p. 1268, 2018.
- [8] P. H. Scanlon, S. J. Aldington, and I. M. Stratton, "Epidemiological issues in diabetic retinopathy," *Middle East African Journal of Ophthalmology*, vol. 20, no. 4, pp. 293–300, 2013.
- [9] D. P. Hainsworth, I. Bebu, L. P. Aiello et al., "Risk factors for retinopathy in type 1 diabetes: the DCCT/EDIC study," *Diabetes Care*, vol. 42, no. 5, pp. 875–882, 2019.
- [10] K. Kaku, S. Inoue, O. Matsuoka et al., "Efficacy and safety of dapagliflozin as a monotherapy for type 2 diabetes mellitus

- in Japanese patients with inadequate glycaemic control: a phase II multicentre, randomized, double-blind, placebo-controlled trial," *Diabetes, Obesity & Metabolism*, vol. 15, no. 5, pp. 432–440, 2013.
- [11] F. Semeraro, F. Morescalchi, A. Cancarini, A. Russo, S. Rezzola, and C. Costagliola, "Diabetic retinopathy, a vascular and inflammatory disease: therapeutic implications," *Diabetes & Metabolism*, vol. 45, no. 6, pp. 517–527, 2019.
- [12] M. Mesquida, F. Drawnel, and S. Fauser, "The role of inflammation in diabetic eye disease," *Seminars in Immunopathology*, vol. 41, no. 4, pp. 427–445, 2019.
- [13] B. G. Spencer, J. J. Estevez, E. Liu, J. E. Craig, and J. W. Finnie, "Pericytes, inflammation, and diabetic retinopathy," *Inflammopharmacology*, vol. 28, no. 3, pp. 697–709, 2020.
- [14] O. M. Ighodaro, "Molecular pathways associated with oxidative stress in diabetes mellitus," *Biomedicine & Pharmacotherapy*, vol. 108, pp. 656–662, 2018.
- [15] M. Benlarbi-Ben Khedher, K. Hajri, A. Dellaa et al., "Astaxanthin inhibits aldose reductase activity in *Psammomys obesus*, a model of type 2 diabetes and diabetic retinopathy," *Food Science & Nutrition*, vol. 7, no. 12, pp. 3979–3985, 2019.
- [16] M. Mishra, A. J. Duraisamy, S. Bhattacharjee, and R. A. Kowluru, "Adaptor protein p66Shc: a link between cytosolic and mitochondrial dysfunction in the development of diabetic retinopathy," *Antioxidants & Redox Signaling*, vol. 30, no. 13, pp. 1621–1634, 2019.
- [17] H. L. Deissler and G. E. Lang, "The protein kinase C inhibitor: ruboxistaurin," *Developments in Ophthalmology*, vol. 55, pp. 295–301, 2016.
- [18] S. Luo, C. Shi, F. Wang, and Z. Wu, "Association between the angiotensin-converting enzyme (ACE) genetic polymorphism and diabetic retinopathy—a meta-analysis comprising 10,168 subjects," *International Journal of Environmental Research and Public Health*, vol. 13, no. 11, article 1142, 2016.
- [19] J. R. L. Ehrenkranz, N. G. Lewis, C. Ronald Kahn, and J. Roth, "Phlorizin: a review," *Diabetes/Metabolism Research and Reviews*, vol. 21, no. 1, pp. 31–38, 2005.
- [20] M. Uldry and B. Thorens, "The SLC2 family of facilitated hexose and polyol transporters," *Pflügers Archiv*, vol. 447, no. 5, pp. 480–489, 2004.
- [21] T. Yakovleva, V. Sokolov, L. Chu et al., "Comparison of the urinary glucose excretion contributions of SGLT2 and SGLT1: a quantitative systems pharmacology analysis in healthy individuals and patients with type 2 diabetes treated with SGLT2 inhibitors," *Diabetes, Obesity & Metabolism*, vol. 21, no. 12, pp. 2684–2693, 2019.
- [22] M. May, T. Framke, B. Junker, C. Framme, A. Pielen, and C. Schindler, "How and why SGLT2 inhibitors should be explored as potential treatment option in diabetic retinopathy: clinical concept and methodology," *Therapeutic Advances in Endocrinology and Metabolism*, vol. 10, article 2042018819891886, 2019.
- [23] J. Dziuba, P. Alperin, J. Racketa et al., "Modeling effects of SGLT-2 inhibitor dapagliflozin treatment versus standard diabetes therapy on cardiovascular and microvascular outcomes," *Diabetes, Obesity & Metabolism*, vol. 16, no. 7, pp. 628–635, 2014.
- [24] I. M. Stratton, A. I. Adler, H. A. Neil et al., "Association of glycaemia with macrovascular and microvascular complications of type 2 diabetes (UKPDS 35): prospective observational study," *BMJ*, vol. 321, no. 7258, pp. 405–412, 2000.
- [25] N. K. Wang, C. C. Lai, J. P. Wang et al., "Risk factors associated with the development of retinopathy 10 yr after the diagnosis of juvenile-onset type 1 diabetes in Taiwan: a cohort study from the CGJDES," *Pediatric Diabetes*, vol. 17, no. 6, pp. 407–416, 2016.
- [26] American Diabetes Association, "1. Improving care and promoting health in populations: standards of medical care in diabetes-2020," *Diabetes Care*, vol. 43, Supplement 1, pp. S7–s13, 2020.
- [27] UK Prospective Diabetes Study Group, "Tight blood pressure control and risk of macrovascular and microvascular complications in type 2 diabetes: UKPDS 38," *BMJ*, vol. 317, no. 7160, pp. 703–713, 1998.
- [28] S. Wang, L. Xu, J. B. Jonas et al., "Major eye diseases and risk factors associated with systemic hypertension in an adult Chinese population," *Ophthalmology*, vol. 116, no. 12, pp. 2373–2380, 2009.
- [29] M. Salvetti, C. Agabiti Rosei, A. Paini et al., "Relationship of wall-to-lumen ratio of retinal arterioles with clinic and 24-hour blood pressure," *Hypertension*, vol. 63, no. 5, pp. 1110–1115, 2014.
- [30] A. Merovci, C. Solis-Herrera, G. Daniele et al., "Dapagliflozin improves muscle insulin sensitivity but enhances endogenous glucose production," *The Journal of Clinical Investigation*, vol. 124, no. 2, pp. 509–514, 2014.
- [31] B. Peene and K. Benhalima, "Sodium glucose transporter protein 2 inhibitors: focusing on the kidney to treat type 2 diabetes," *Therapeutic Advances in Endocrinology and Metabolism*, vol. 5, no. 5, pp. 124–136, 2014.
- [32] S. J. Shin, S. Chung, S. J. Kim et al., "Effect of sodium-glucose co-transporter 2 inhibitor, dapagliflozin, on renal renin-angiotensin system in an animal model of type 2 diabetes," *PLoS One*, vol. 11, no. 11, article e0165703, 2016.
- [33] B. Wang, F. Wang, Y. Zhang et al., "Effects of RAS inhibitors on diabetic retinopathy: a systematic review and meta-analysis," *The Lancet Diabetes and Endocrinology*, vol. 3, no. 4, pp. 263–274, 2015.
- [34] E. G. Dorsey-Treviño, B. M. Contreras-Garza, J. G. González-González et al., "Systematic review and meta-analysis of the effect of SGLT-2 inhibitors on microvascular outcomes in patients with type 2 diabetes: a review protocol," *BMJ Open*, vol. 8, no. 6, article e020692, 2018.
- [35] H. Y. Zhang, J. Y. Wang, G. S. Ying, L. P. Shen, and Z. Zhang, "Serum lipids and other risk factors for diabetic retinopathy in Chinese type 2 diabetic patients," *Journal of Zhejiang University Science B*, vol. 14, no. 5, pp. 392–399, 2013.
- [36] J. Li, J. J. Wang, D. Chen et al., "Systemic administration of HMG-CoA reductase inhibitor protects the blood-retinal barrier and ameliorates retinal inflammation in type 2 diabetes," *Experimental Eye Research*, vol. 89, no. 1, pp. 71–78, 2009.
- [37] S. Filippas-Ntekouan, V. Tsimihodimos, T. Filippatos, T. Dimitriou, and M. Elisaf, "SGLT-2 inhibitors: pharmacokinetic characteristics and effects on lipids," *Expert Opinion on Drug Metabolism & Toxicology*, vol. 14, no. 11, pp. 1113–1121, 2018.
- [38] E. Ferrannini, "Sodium-glucose co-transporters and their inhibition: clinical physiology," *Cell Metabolism*, vol. 26, no. 1, pp. 27–38, 2017.
- [39] D. H. Jo, J. H. Yun, C. S. Cho, J. H. Kim, J. H. Kim, and C. H. Cho, "Interaction between microglia and retinal pigment epithelial cells determines the integrity of outer blood-retinal

- barrier in diabetic retinopathy," *Glia*, vol. 67, no. 2, pp. 321–331, 2019.
- [40] M. Wakisaka, M. Yoshinari, S. Nakamura et al., "Suppression of sodium-dependent glucose uptake by captopril improves high-glucose-induced morphological and functional changes of cultured bovine retinal pericytes," *Microvascular Research*, vol. 58, no. 3, pp. 215–223, 1999.
- [41] S. Roy, E. Bae, S. Amin, and D. Kim, "Extracellular matrix, gap junctions, and retinal vascular homeostasis in diabetic retinopathy," *Experimental Eye Research*, vol. 133, pp. 58–68, 2015.
- [42] H. Yoshizumi, T. Ejima, T. Nagao, and M. Wakisaka, "Recovery from diabetic macular edema in a diabetic patient after minimal dose of a sodium glucose co-transporter 2 inhibitor," *Am J Case Rep*, vol. 19, pp. 462–466, 2018.
- [43] Y. Y. Chen, T. T. Wu, C. Y. Ho et al., "Dapagliflozin prevents NOX- and SGLT2-dependent oxidative stress in lens cells exposed to fructose-induced diabetes mellitus," *International Journal of Molecular Sciences*, vol. 20, no. 18, article 4357, 2019.
- [44] S. Takakura, T. Toyoshi, Y. Hayashizaki, and T. Takasu, "Effect of ipragliflozin, an SGLT2 inhibitor, on progression of diabetic microvascular complications in spontaneously diabetic Torii fatty rats," *Life Sciences*, vol. 147, pp. 125–131, 2016.
- [45] C. Ott, A. Jumar, K. Striepe et al., "A randomised study of the impact of the SGLT2 inhibitor dapagliflozin on microvascular and macrovascular circulation," *Cardiovascular Diabetology*, vol. 16, no. 1, p. 26, 2017.
- [46] A. Jumar, C. Ott, I. Kistner et al., "Early signs of end-organ damage in retinal arterioles in patients with type 2 diabetes compared to hypertensive patients," *Microcirculation*, vol. 23, no. 6, pp. 447–455, 2016.
- [47] J. E. Grunwald, J. DuPont, and C. E. Riva, "Retinal haemodynamics in patients with early diabetes mellitus," *The British Journal of Ophthalmology*, vol. 80, no. 4, pp. 327–331, 1996.
- [48] V. Patel, S. Rassam, R. Newsom, J. Wiek, and E. Kohner, "Retinal blood flow in diabetic retinopathy," *BMJ*, vol. 305, no. 6855, pp. 678–683, 1992.
- [49] O. Simó-Servat, R. Simó, and C. Hernández, "Circulating biomarkers of diabetic retinopathy: an overview based on pathophysiology," *Journal Diabetes Research*, vol. 2016, article 5263798, pp. 1–13, 2016.
- [50] J. Green, A. Yurdagul Jr., M. C. McInnis, P. Albert, and A. W. Orr, "Flow patterns regulate hyperglycemia-induced subendothelial matrix remodeling during early atherogenesis," *Atherosclerosis*, vol. 232, no. 2, pp. 277–284, 2014.
- [51] P. Lacolley, V. Regnault, A. Nicoletti, Z. Li, and J. B. Michel, "The vascular smooth muscle cell in arterial pathology: a cell that can take on multiple roles," *Cardiovascular Research*, vol. 95, no. 2, pp. 194–204, 2012.
- [52] R. Simó, C. Hernández, and C. Hernández, "Neurodegeneration in the diabetic eye: new insights and therapeutic perspectives," *Trends in Endocrinology and Metabolism*, vol. 25, no. 1, pp. 23–33, 2014.
- [53] N. E. Straznicky, M. T. Grima, N. Eikelis et al., "The effects of weight loss versus weight loss maintenance on sympathetic nervous system activity and metabolic syndrome components," *The Journal of Clinical Endocrinology and Metabolism*, vol. 96, no. 3, pp. E503–E508, 2011.
- [54] A. A. Thorp and M. P. Schlaich, "Relevance of sympathetic nervous system activation in obesity and metabolic syndrome," *Journal Diabetes Research*, vol. 2015, article 341583, pp. 1–11, 2015.
- [55] V. B. Matthews, R. H. Elliot, C. Rudnicka, J. Hricova, L. Herat, and M. P. Schlaich, "Role of the sympathetic nervous system in regulation of the sodium glucose cotransporter 2," *Journal of Hypertension*, vol. 35, no. 10, pp. 2059–2068, 2017.
- [56] L. Y. Herat, V. B. Matthews, P. E. Rakoczy, R. Carnagarin, and M. Schlaich, "Focusing on sodium glucose cotransporter-2 and the sympathetic nervous system: potential impact in diabetic retinopathy," *International Journal of Endocrinology*, vol. 2018, Article ID 9254126, 8 pages, 2018.